



**IJCER**

ONLINE PEER REVIEWED JOURNAL

International Journal of Computational  
Engineering research

2013

# International Journal of Computational Engineering Research(IJCER)

Volume 3, Issue 11,  
November, 2013

I

J

C

E

R

# Editorial Board

## Editor-In-Chief

### **Prof. Chetan Sharma**

Specialization: Electronics Engineering, India  
Qualification: Ph.d, Nanotechnology, IIT Delhi, India

## Editorial Committees

### **DR.Qais Faryadi**

Qualification: PhD Computer Science  
Affiliation: USIM(Islamic Science University of Malaysia)

### **Dr. Lingyan Cao**

Qualification: Ph.D. Applied Mathematics in Finance  
Affiliation: University of Maryland College Park,MD, US

### **Dr. A.V.L.N.S.H. HARIHARAN**

Qualification: Phd Chemistry  
Affiliation: GITAM UNIVERSITY, VISAKHAPATNAM, India

### **DR. MD. MUSTAFIZUR RAHMAN**

Qualification: Phd Mechanical and Materials Engineering  
Affiliation: University Kebangsaan Malaysia (UKM)

### **Dr. S. Morteza Bayareh**

Qualificatio: Phd Mechanical Engineering, IUT  
Affiliation: Islamic Azad University, Lamerd Branch  
Daneshjoo Square, Lamerd, Fars, Iran

### **Dr. Zahéra Mekkioui**

Qualification: Phd Electronics  
Affiliation: University of Tlemcen, Algeria

### **Dr. Yilun Shang**

Qualification: Postdoctoral Fellow Computer Science  
Affiliation: University of Texas at San Antonio, TX 78249

### **Lugen M.Zake Sheet**

Qualification: Phd, Department of Mathematics  
Affiliation: University of Mosul, Iraq

### **Mohamed Abdellatif**

Qualification: PhD Intelligence Technology  
Affiliation: Graduate School of Natural Science and Technology

**Meisam Mahdavi**

Qualification: Phd Electrical and Computer Engineering

Affiliation: University of Tehran, North Kargar st. (across the ninth lane), Tehran, Iran

**Dr. Ahmed Nabih Zaki Rashed**

Qualification: Ph. D Electronic Engineering

Affiliation: Menoufia University, Egypt

**Dr. José M. Merigó Lindahl**

Qualification: Phd Business Administration

Affiliation: Department of Business Administration, University of Barcelona, Spain

**Dr. Mohamed Shokry Nayle**

Qualification: Phd, Engineering

Affiliation: faculty of engineering Tanta University Egypt

## CONTENTS :

S.No	Title Name	Page No.
<b>Version I</b>		
1.	Appm: A Narrative Data Embedding Method Using Adaptive Pixel Pair Matching <b>P.Ramesh Babu, Y.Chitti Babu, Dr.P.Harini</b>	01-06
2.	SPURGEAR <b>T.Shoba Rani, T.Dada Khalandar</b>	07-12
3.	Stress Analysis of Splice Joint of the Aircraft Bottom Wing Skin by Finite Element Method <b>A.Rukesh Reddy, P. Ramesh, B. Siddeswara rao</b>	13-17
4.	Identification Of Eligible Customer Requirements <b>Pavel MIKUŠ</b>	18-22
5.	Cloud Information Accountability Framework for Auditing the Data Usage in Cloud Environment <b>D.Dhivya, S.Chinnadurai</b>	23-27
6.	Mobile Phone Based Multi-Devices Secured Control System <b>Elsanosy Mohamed Elamin , AbdirasoulJabar Alzubaidi</b>	28-32
7.	Determination Gamma Width and Transition Strength Of Gamma Rays from $^{48}\text{Ti}(\text{n}, \gamma)^{49}\text{Ti}$ Reaction <b>Nguyen An Son, Pham Dinh Khang, Nguyen Duc Hoa, Nguyen Xuan Hai, Dang Lanh</b>	33-37
8.	Offline Signature Recognition Using Maximally Stable Extremely Regions (Mser) <b>Mohammad B. Abdulkareem , Santosh Gaikwad , Bharti Gawali</b>	38-44
9	The Effect Of Water Solubles On The Hygroscopicity Of Urban Aerosols <b>B. I. Tijjani</b>	45-60
10	Efficient Solution of Constraint Satisfaction Problems by Equivalent Transformation <b>Hiroshi Mabuchi</b>	61-70

11	Experimental Analysis & Designing of fabrication Method Of Shear Fatigue Strength Of Glass Fiber Epoxy And Chapstan E-Glass Epoxy Laminates <b>Pns Srinivas, Movva Mounika, M.Rajya Lakshmi</b>	71-83
----	--	-------

### Version II

1.	An Evaluation of Software Development Methodology Adoption by Software Developer in Sri Lanka <b>C.D. Manawadu, Md Gapar Md Johar, S.S.N. Perera</b>	01-11
2.	Harmonic Filter Design for Hvdc Lines Using Matlab <b>P.Kumar , P.Prakash</b>	12-19
3.	Adsorption Capacity Of Nicotine From Tobacco Products By Different Adsorbents <b>Zamzam Basher , A.K.Gupta ,Amit Chattrre</b>	20-22
4.	An Automated Image Segmentation Scheme for Iris Recognition <b>Dr. G. Saravana Kumar, J. Munikrishnan, Manimaraboopathy</b>	23-30
5.	DWDM Link with Multiple Backward Pumped Raman Amplification <b>Awab Fakih, Santosh Jagtap, Shraddha Panbude</b>	31-40
6.	Fingerprint Recognition Using Genetic Algorithm and Neural Network <b>Purneet Kaur , Jaspreet Kaur</b>	41-46
7.	Content Based Medical Image Retrieval – Performance Comparison of Various Methods <b>Harishchandra Hebbar, Niranjana U C, Sumanth Mushigeri</b>	47-57

### Version III

1	Direct Method for Finding an Optimal Solution for Fuzzy Transportation Problem <b>A.Srinivasan , G. Geetharamani</b>	01-07
2.	Polynomials having no Zero in a Given Region <b>M. H. Gulzar</b>	08-12
3.	Simple Domestic Air Conditioning by using the Ice Thermal Storage Capacity <b>Mohammed Hadi Ali</b>	13-20
4.	Design of A network Data Security Circuit <b>Nuha Abdelmageed Tawfig Khalil, Abdelrasoul Jabar Alzubaidi</b>	21-24

5.	Key pad Based Online Examination System <b>S.G.Pardeshi, K.S.Jadhav</b>	25-29
6.	Connectedness of e-Service Quality, e-Satisfaction and e-Loyalty. A Configuration Analysis with QDA Software <b>Nanis Susanti, Surachman, Djumilah Hadiwidjojo, Fatchur Rohman</b>	30-38
7.	Estimation of Stress- Strength Reliability model using finite mixture of exponential distributions <b>K.Sandhya, T.S.Umamaheswari</b>	39-46

# Appm: A Narrative Data Embedding Method Using Adaptive Pixel Pair Matching

P.Ramesh Babu<sup>1</sup> Y.Chitti Babu<sup>2</sup> Dr.P.Harini<sup>3</sup>

<sup>1</sup> II Year M.Tech, St. Ann's College Of Engineering And Technology,  
Chirala, Prakasam(Dt), Andhra Pradesh, India

<sup>2</sup> Associate Professor , Dept Of CSE , St.Anns's College Of Engineering & Technology,  
Chirala, Prakasam(Dt), Andhra Pradesh, India

<sup>3</sup> Professor And HOD Dept Of CSE , St.Anns's College Of Engineering & Technology,  
Chirala, Prakasam(Dt), Andhra Pradesh, India

## ABSTRACT

Here We Proposed A New Data-Hiding Method Based On Pixel Pair Matching (PPM). In This Paper The Basic Idea Of PPM Is To Use The Values Of Pixel Pair As A Reference Coordinate, And Coordinate Search In The Neighborhood Used To Set Of This Pixel Pair According To A Given Message Digit. The Pixel Pair Is Then Replaced By The Searched Coordinate To Conceal The Digit.(EMD)Exploitedmodificationdirection(EMD) And Diamond Encoding (DE) Are Two Data-Hiding Methods Proposed Recently Based On PPM. Then The Maximum Capacity Of EMD Is 1.161 Bpp And DE Extends The Payload Of EMD By Embedding Digits In A Larger Notational System.This Is The Proposed Method Offers Lower Distortion Than DE By Having High Compact Neighborhood Sets And It Will Also Accepting Embedded Digits In Any Representative System. Then It Will Be Compared With The (OPAP)Optimal Pixel Adjustment Process Method, Then This Method Always Has Lower Distortion For Various Payloads. Experimental Results Reveal That The Proposed Method Does Not Only Provides Performance Better Than Those Of OPAP And DE, But Also Is Secure Under The Detection Of Some Well-Known Steganalysis Techniques.

**INDEX TERMS:** (ADPPM)Adaptive Pixel Pair Matching,(DE) Diamond Encoding , Exploiting Modification Direction (EMD), Least Significant Bit (LSB), Optimal Pixel Adjustment Process (OPAP), Pixel Pair Matching (PPM).

## I. INTRODUCTION

In digital image processing, while processing images here we need to follow certain criteria. Combining data into a carrier for conveying secret messages that should be confidentially is the technique of data hiding [1], [2]. After embedding, pixels of cover images will be modified and deformation occurs. The distortion caused by data embedding is called the embedding distortion [3]. A good data-hiding method must be capable of evading visual and statistical detection [4] while providing an adjustable payload [5]. Many approaches of information hiding have been proposed for diverse applications, such as patent protection, top secret transmission, tampering exposure, and figure authentication. large amount well-known data hiding format is the least significant bits (LSBs) replacement process. This process embeds fixed-length covert bits into the least significant bits of pixels by directly replacing the LSBs of cover picture with the secret message bits. Although this process is simple, it generally effects noticeable deformation when the number of embedded bits for each pixel exceeds three. Several methods have been proposed to decrease the distortion induced by LSBs replacement. Another approach of improving LSBs scheme is to decrease the amount of alterations required to be introduced into the cover image for data hiding when the numeral of secret bits is significantly less than that of available cover pixels. The method proposed by Tseng et al. [6] can cover up as many as  $\log_2(mn+1)$  bits of data in a binary image block sized  $m \times n$  by changing, at most, two bits in the block. Matrix encoding, on the other hand, uses less than one change of the least significant bit in average to embed  $w$  bits into  $2w - 1$  cover pixels. Diamond Encoding(DE)method is the extension of the exploiting modification direction (EMD) embedding scheme [2]. The main idea of the EMD embedding scheme is that each  $(2n + 1)$ -ary notational secret digit is carried by  $n$  cover pixels, and only one pixel worth increases or decreases by 1 at most. For each block of  $n$  cover pixels, there are  $2n$  possible states of only one pixel value plus 1 or minus 1. The  $2n$  states of alteration plus the case in which no pixel is modified form  $(2n + 1)$  different cases.

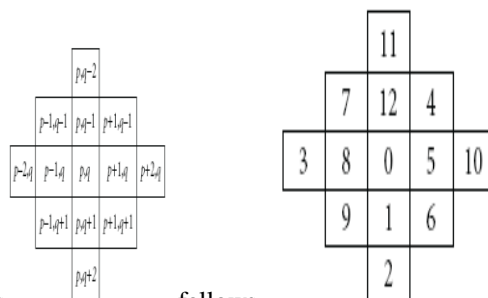
Therefore, the  $(2n + 1)$ -ary notational secret digit is embedded into the cover pixels by changing the state. Before the data embedding method, the pre-process can convert the secret data into sequences of digits with  $(2n + 1)$ -ary notational representation

## II .RELATED WORK

OPAP effectively reduces the image distortion compared with the traditional LSB method. DE enhances the payload of EMD by embedding digits in a  $B$ -ary notational system. These two methods offer a high payload while preserving an acceptable stego image quality. In this section, OPAP and DE will be briefly reviewed. The OPAP method proposed by Chan *et al.* in 2004 greatly improved the image distortion problem resulting from LSB replacement.

### Diamond Encoding (DE)

The EMD scheme embeds  $(2n + 1)$ -ary digit into  $n$  cover pixels, but the diamond encoding scheme can conceal  $(2k^2 + 2k + 1)$ -ary digit into a cover pixel pair where  $k$  is the embedding parameter. The detail of this scheme is



described as

follows.

$$f(x, y) = ((2k + 1) \times x + y) \bmod (2k^2 + 2k + 1)$$

$$k = 2, (x, y) = (0, 0)$$

$$f(x, y) = (5 \times x + y) \bmod (13)$$

$$f(0, 0) = (5 \times 0 + 0) \bmod (13) = 0$$

$$f(1, 0) = (5 \times 1 + 0) \bmod (13) = 5$$

$$f(2, 0) = (5 \times 2 + 0) \bmod (13) = 10$$

$$f(0, 1) = (5 \times 0 + 1) \bmod (13) = 1$$

$$f(0, 2) = (5 \times 0 + 2) \bmod (13) = 2$$

⋮

$$f(0, -1) = (5 \times 0 + (-1)) \bmod (13) = 12$$

Assume that  $a, b, p,$  and  $q$  are pixel values, and  $k$  is a positive integer. The neighborhood set  $S_k(p, q)$  represents the set that contains all the vectors  $(a, b)$  with the distance to vector  $(p, q)$  smaller than  $k$ , and  $S_k(p, q)$  is defined as the above. Let the absolute value  $|S_k|$  denote the number of elements of the set  $S_k$ , and each member in  $S_k$  is called neighboring vector of  $(p, q)$ . We calculate the value of  $|S_k|$  to obtain the embedding base and embedded base with a parameter  $k$ . Diamond encoding method uses a diamond function  $f$  to compute the diamond characteristic value (DCV) in embedding and extraction procedures. The DCV of two pixel values  $p$  and  $q$  can be defined as above: where  $l$  is the absolute value of  $S_k$ . The DCV have two important properties: the DCV of the vector  $(p, q)$  is the member of  $S_k$  belongs to  $\{0, 1, 2, \dots, l-1\}$  and any two DCVs of vectors in  $S_k(p, q)$  are distinct. Assume that  $E_k$  represents the embedded digit and  $E_k$  belongs to  $\{0, 1, 2, \dots, l-1\}$ . For secret data embedding, we replace the DCV of the vector  $(p, q)$  with the embedded secret digit. Therefore, the modulus distance between  $f(p, q)$  and  $S_k$  is  $dk = f(p, q) - E_k \bmod l$ . For each  $k$ , we can design a distance pattern  $D_k$  to search which neighboring pixel owns the modulus distance  $dk$ . Then, the vector  $(p, q)$  is replaced with the neighboring vector  $(p', q')$  by  $dk$ . The vector  $(p', q')$  is the member of  $S_k(p, q)$  and the DCV of  $(p', q')$  equals to the embedded secret digit  $E_k$ . The vector  $(p', q')$  can extract the correct secret digit by above formulas. The diamond encoding scheme promises that the distortion of vector  $(p, q)$  is no more than  $k$  after embedding a secret digit  $E_k$ . Therefore, this minimal distortion scheme can be employed to embed large amount of data.

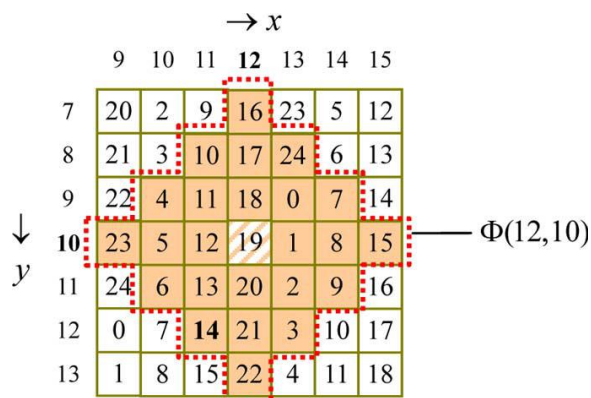


Fig. 1. Neighborhood set for  $\omega(12,10)$  for  $k=3$ .

**III. PROCEDURE AND ALGORITHM:**

**ADAPTIVE PIXEL PAIR MATCHING (APPM)**

The basic idea of the PPM-based data-hiding method is to use pixel pair  $(x,y)$  as the coordinate and through a coordinate  $(x_1,y_1)$ , surrounded by a predefined locality set  $\omega(x,y)$  such that  $f(x,y)=S_b$ , where  $f$  is the drawing out function and  $S_b$  is the message digit in a  $b$ -ary notational structure to be covered. Data embedding is done by replacing  $(x,y)$  with  $(x_1,y_1)$ . For a PPM-based process, suppose a digit  $S_b$  is to be covered. The range of  $S_b$  is between 0 and  $B-1$ , and a coordinate  $(x_1,y_1) \in \omega(x,y)$  has to be found such that  $f(x_1,y_1)=S_b$ . Therefore, the range  $f(x,y)$  of must be integers between 0 and  $B-1$ , and each integer must occur at least once. In addition, to reduce the distortion, the number of coordinates in  $\omega(x,y)$  should be as small as possible.

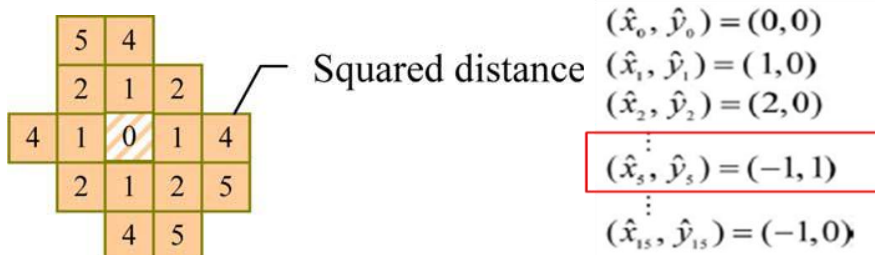


Fig: Neighborhood set  $\omega_{16}(0,0)$  and  $f(x,y)$ , where  $0 \leq i < B-1$ .

The best PPM method shall satisfy the following three requirements:

- 1) There are exactly  $B$  coordinates in  $\omega(x,y)$ .
- 2) The values of extraction function in these coordinates are mutually exclusive.
- 3) The design of  $\omega(x,y)$  and  $f(x,y)$  should be capable of embedding digits in any notational structure so that the best  $B$  can be selected to achieve junior embedding deformation.

DE is a data-hiding method based on PPM. DE greatly enhances the payload of EMD though preserving acceptable stego image quality. but, there are several problems. First, the payload of DE is determined by the selected notational structure, which is restricted by the bound; therefore, the notational system cannot be arbitrarily selected. For example, when is 1, 2, and 3, then digits in a 5-ary, 13-ary, and 25-ary notational structure are used to surround data, respectively. However, embedding digits in a 4-ary or 16-ary (i.e., 2 bits per pixel) notational system are not supported in DE. Second,  $\omega(x,y)$  in DE is defined by a diamond shape, which may lead to some unnecessary distortion when  $k > 2$ . In fact, there exists  $\omega(x,y)$  a better other than diamond shape resulting in a smaller embedding deformation. The wished-for method not only allows concealing digits in any notational structure, but also provides the same or even smaller embedding deformation than DE for various payloads.

**Embedding Procedure:**

Consider the cover image is of size  $M \times M$ , then each of R, G, B channels will be of size  $M \times M$ .  $S$  is the message bits to be concealed for each channel image and the size of  $S$  is  $|S|$ . First we calculate the minimum  $B$  such that all the message bits can be embedded. Then, message digits are sequentially concealed into pairs of pixels.

- [1] First minimum  $B$  satisfying  $|M \times M / 2| \geq |SB|$ , and convert  $S$  into a list of digits with a  $B$ -ary notational system  $sB$ .
- [2] The discrete optimization problem is solved to find  $cB$  and  $\emptyset B(x, y)$ .
- [3] In the region defined by  $\emptyset B(x, y)$ , record the coordinate  $(x', y')$  such that  $f(x', y') = i, 0 \leq i \leq B-1$ .
- [4] Construct a nonrepeating random embedding sequence  $Q$  using a key  $Kr$ .
- [5] To embed a message digit  $sB$ , two pixels  $(x, y)$  in the cover image are selected according to the embedding sequence  $Q$ , and calculate the modulus distance between  $sB$  and  $f(x, y)$ , then replace  $(x, y)$  with  $(x + x', y + y')$  [7].
- [6] Repeat step 5, until all the message bits are embedded To avoid any distortion because of replacing pixels right under each other in different layers, the regions  $\emptyset(x, y)$  for each layer are taken distinct subsets.

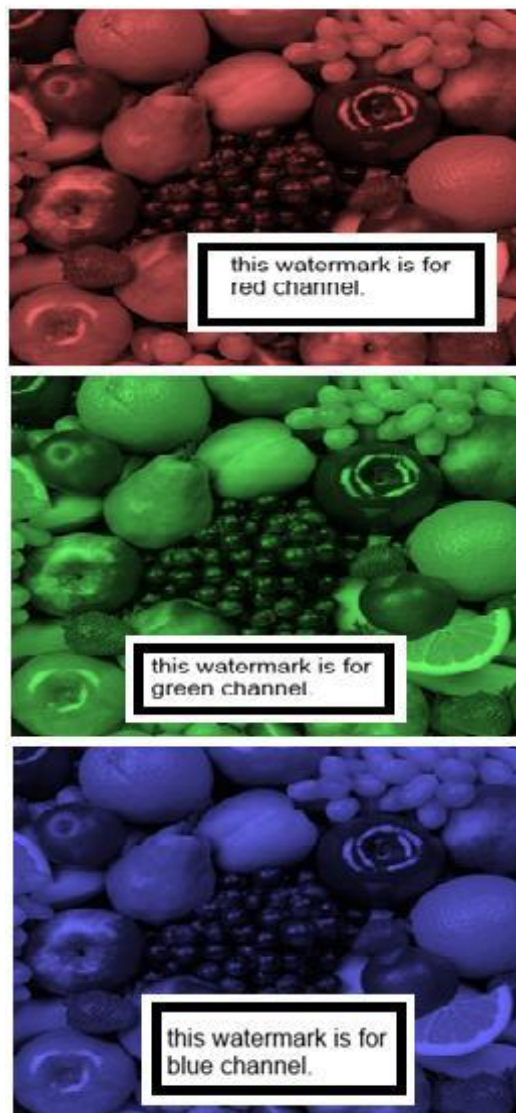


Figure 1. Embedding respective watermarks for different Channel Images

**. Extraction Procedure:**

To extract the embedded message digits, pixel pairs are scanned in the same order as in the embedding procedure. The embedded message digits are the values of extraction function of the scanned pixel pairs.

1. The watermarked image is split into respective R, G, B layers and each is considered as a Channel Image.
2. Construct the embedding sequence Q using a key Kr.
3. Select two pixels (x', y') according to the embedding sequence Q.
4. Calculate f(x', y'), the result is the embedded digit.
5. Repeat Steps 2 and 3 until all the message digits are extracted.
6. Finally, the message bits can be obtained by converting the extracted message digits into a binary bit stream.

**IV. EXPERIMENTS AND EVALUTION**

**Performance**

To evaluate the performance of the proposed scheme, a high definition image is taken. The simulation is run using MATLAB. First, LSB, DE, APPM and EAPPM are evaluated for Mean Square Error (MSE) with different payloads. Table 1 presents the obtained MSEs. It is observed that APPM outperforms APPM, DE and LSB.

Table2 presents the maximum payload supported by the four embedding methods at an MSE of 0.092. EAPPM is able to support 300% more than APPM. As the data is embedded in all the three layers, for EAPPM, the payload support will be more than 3 times that of APPM.

Max Payload supported with MSE at 0.092	
LSB	0.025431
DE	0.025431
APPM	0.114441
EAPPM	0.772476

Table1. MSE Comparison

Payload (bpp)	LSB	DE	APPM	EAPPM
0.025431	0.168676	0.143649	0.094927	
0.076294	0.168676	0.143649	0.094927	0.091497
0.114441	0.164326	0.143727	0.091771	0.095604
0.157671	0.168766	0.143901	0.094807	0.091497
0.203451	0.168973	0.143826	0.094971	0.091497
0.257492	0.169243	0.144003	0.095374	0.091497

Table2. Max Payload support Comparison

## V. CONCLUSION

proposed a simple and efficient data embedding process based on PPM. Two pixels are scanned as an embedding element and a specially designed neighbourhood set is employed to insert message digits with a smallest notational structure. APPM allows users to select digits in any notational structure for data embedding, and thus achieves an enhanced image quality. The proposed process not only resolves the low-payload trouble in EMD, but also offers smaller MSE compared with OPAP and DE. Moreover, because APPM produces no artifacts in stego images and the steganalysis results are comparable to those of the cover images, it offers a secure communication below variable embedding Capacity.

## REFERENCES

- [1] J. Fridrich, *Steganography in Digital Media: Principles, Algorithms, and Applications*. Cambridge, U.K.: Cambridge Univ. Press, 2009.
- [2] N. Provos and P. Honeyman, "Hide and seek: An Introduction to steganography," *IEEE Security Privacy*, vol. 3, no. 3, pp. 32–44, May/June 2003.
- [3] A. Cheddad, J. Condell, K. Curran, and P. McKeivitt, "Digital image steganography: Survey and analysis of current methods," *Signal Process.*, vol. 90, pp. 727–752, 2010.
- [4] T. Filler, J. Judas, and J. Fridrich, "Minimizing embedding impact in steganography using trellis-coded quantization," in *Proc. SPIE, Media Forensics and Security*, 2010, vol. 7541, DOI: 10.1117/12.838002.
- [5] S. Lyu and H. Farid, "Steganalysis using higher-order image statistics," *IEEE Trans. Inf. Forensics Security*, vol. 1, no. 1, pp. 111–119, Mar. 2006.
- [6] Y.-C. Tseng, Y.-Y. Chen, and H.-K. Pan, "A secure data hiding scheme for binary images," *IEEE Transactions on Communications*, vol. 50, no. 8, pp. 1227–1231, 2002.
- [7] W. Zhang, X. Zhang, and S. Wang, "A double layered plus-minus one data embedding scheme," *IEEE Signal Process. Lett.*, vol. 14, no. 11, pp. 848–851, Nov. 2007.

## AUTHORS:



**Dr. P. Harini** is presently working as a professor and HOD, Dept of Computer Science and Engineering, in St. Ann's College of Engineering and Technology, Chirala. She obtained Ph.D in distributed and Mobile Computing from JNTUA, Ananthapur. She Guided Many UG and PG Students. She has More than 15 Years of Excellence in Teaching and 2 Years of Industry Experience. She published more than 20 International Journals and 25 Research Oriented Papers in Various Areas. She was awarded **Certificate of Merit** by JNTUK, Kakinada on the University Formation Day on 21 - August - 2012. . from JNTUK, Kakinada.



**Y. Chitti babu** is presently working as an Associate professor, Dept of Computer Science and Engineering, in St. Ann's College of Engineering and Technology, Chirala. He Guided Many UG and PG Students. He has More than 10 Years of Teaching Experience. He published more than 5 International Journals and 7 Research Oriented Papers in Various Areas.



**P. Ramesh babu** is presently Studying the M.Tech (CSE) in St. Ann's College Of Engineering and Technology, Chirala affiliated to Jawaharlal Nehru Technological University, Kakinada.

# SPURGEAR

<sup>1</sup>, T.Shoba Rani, <sup>2</sup>, T.Dada Khalandar

<sup>1</sup>M.Tech (ME), INTL- Anantapur (Dt), Affiliated to JNTUA University, Andhra Pradesh, INDIA.

<sup>2</sup> Assistant Professor, Department of ME, INTELL ENGG. COLLEGE Anantapur (Dt), Affiliated to JNTUA University, Andhra Pradesh, INDIA.

## ABSTRACT

The creep nature of metallic spur gear results in the deficiency because of the deformation of teeth when pressure angle of 20 acting on it. At the replacing points of tooth between driving and driven the disturbances such as in-avoidable random noise, elastic deformation and manufacturing error, alignment error in assembly all these together causes the high level of gear vibration and noise and leads to loss in efficiency. The main motto is to reduce the deformation of teeth, by replacing the metallic cast iron gear with Nylon gear and proved that the deformation of Nylon gear is less compared to metallic and polycarbonate. Since the deformation is less the loss in efficiency is also less compared to metallic gear.

**KEYWORDS:** Gear, Spur gear, nylon spur gear.

## I. INTRODUCTION

The spur gear is simplest type of gear manufactured and is generally used for transmission of rotary motion between parallel shafts. The spur gear is the first choice option for gears except when high speeds, loads, and ratios direct towards other options. Other gear types may also be preferred to provide more silent low-vibration operation. A single spur gear is generally selected to have a ratio range of between 1:1 and 1:6 with a pitch line velocity up to 25 m/s. The spur gear has an operating efficiency of 98-99%. The pinion is made from a harder material than the wheel. A gear pair should be selected to have the highest number of teeth consistent with a suitable safety margin in strength and wear. The minimum number of teeth on a gear with a normal pressure angle of 20 degrees is 18. Mild steel is a poor material for gears as it has poor resistance to surface loading. The carbon content for unhardened gears is generally 0.4% (min) with 0.55% (min) carbon for the pinions. Dissimilar materials should be used for the meshing gears - this particularly applies to alloy steels. Alloy steels have superior fatigue properties compared to carbon steels for comparable strengths. For extremely high gear loading case hardened steels are used the surface hardening method employed should be such to provide sufficient case depth for the final grinding process used.

### SPUR GEAR STRENGTH AND DURABILITY CALCULATIONS:

Designing spur gears is normally done in accordance with standards the two most popular series are listed under standards below:

**Bending :** The basic bending stress for gear teeth is obtained by using the Lewis formula  $\sigma = F_t / ( b_a \cdot m \cdot Y )$  where  $F_t$  = Tangential force on tooth,  $\sigma$  = Tooth Bending stress (MPa)  $b_a$  = Face width (mm),  $Y$  = Lewis Form Factor,  $m$  = Module (mm),  $v$  Where  $y = Y/\pi$  and  $p$  = circular pitch. When a gear wheel is rotating the gear teeth come into contact with some degree of impact. To allow for this a velocity factor ( $K_v$ ) is introduced into the equation. This is given by the Barth equation.

$$\text{For cut or milled gears} \quad K_v = \frac{6,1 + V}{6,1}$$

$$\text{For cast iron , cast gears} \quad K_v = \frac{3,05 + V}{3,05}$$

$$\text{For hobbed or shaped gears} \quad K_v = \frac{3,56 + \sqrt{V}}{3,56}$$

$$\text{For shaved or ground gears} \quad K_v = \sqrt{\frac{5,56 + \sqrt{V}}{5,56}}$$

The Lewis formula is thus modified as follows :

$$\sigma = K_v \cdot F_t / ( b_a \cdot m \cdot Y )$$

Through advancements in plastic resins and manufacturing techniques plastic gears today can be utilized in a multitude of crucial applications, from transmitting amounts of torque to accurate positioning of critical components in medical devices. Plastic offers many benefits, including design flexibility and significant cost savings. Plastic gears possess many advantages over those made of metal. Plastic gears are lighter, quieter, retain an inherent lubricity and are corrosion resistant. They can be produced in a variety of types, including bevel gears, offset bevel gears, spiral bevel gears, helical gears, metric gears, metric spur gears, plastic worm gears and more. Cams, lugs, ribs, webs, shafts and holes can be moulded into plastic gears in one integral design in a single operation, opening the door to significantly lower production costs.

#### SPECIFICATION OF EXISTING CAST IRON GEAR:

The typical chemical composition of the cast iron material : Carbon - 2.5 to 3.7%, Silicon - 1.0 to 3.0%, Manganese - 0.5 to 1.0%, Phosphorus - 0.1 to 0.9% and Sulphur - 0.07 to 0.10%.

#### SPECIFICATIONS OF NYLON AND POLYCARBONATE PLASTIC MATERIALS:

Chemical composition of Nylon:

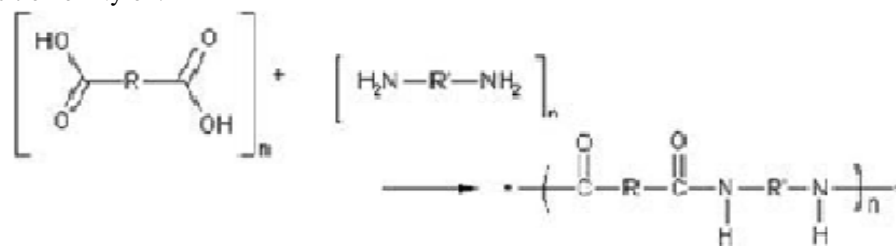


Fig 1.1 Chemical Composition Of Nylon

Its properties are determined by the R and R' groups in the monomers. In nylon 6, 6, R' = 6C and R = 4C alkanes, but one also has to include the two carboxyl carbons in the di acid to get the number it donates to the chain. The majorities of nylons tends to be semi-crystalline and are generally very tough materials with good thermal and chemical resistance. The different types give a wide range of properties with specific gravity, melting point and moisture content tending to reduce as the nylon number increases. Nylons can be used in high temperature environments. Heat stabilized systems allow sustained performance at temperatures up to 185°C.

#### Chemical composition of Polycarbonate:

The main polycarbonate material is produced by the reaction of bisphenol A and phosgene COCl<sub>2</sub>. The overall reaction can be written as follows:

Polycarbonates received their name because they are polymers containing carbonate groups ( $-O-(C=O)-O-$ ). Most polycarbonates are derived from rigid monomers. A balance of useful features include temperature resistance and impact resistance.

#### MATERIAL PROPERTIES OF CAST IRON, NYLON AND POLYCARBONATE:

Material property	Cast Iron	Nylon	polycarbonate
Young's modulus	1.65e5	2.1e5	2.75e5
Poissons Ratio	0.25	0.39	0.38
Density (kg/mm)	7.2e-6	1.13e-6	1.1e-6
Co-efficient of friction	1.1	0.15-0.25	0.31
Ultimate Tensile strength	320-350	55-83	55-70

#### MODELING

The modeling of Spur gear using ANSYS Finite Element Analysis for cast iron, Nylon and polycarbonate are shown as follows:

Displacement pattern of Cast Iron gear:

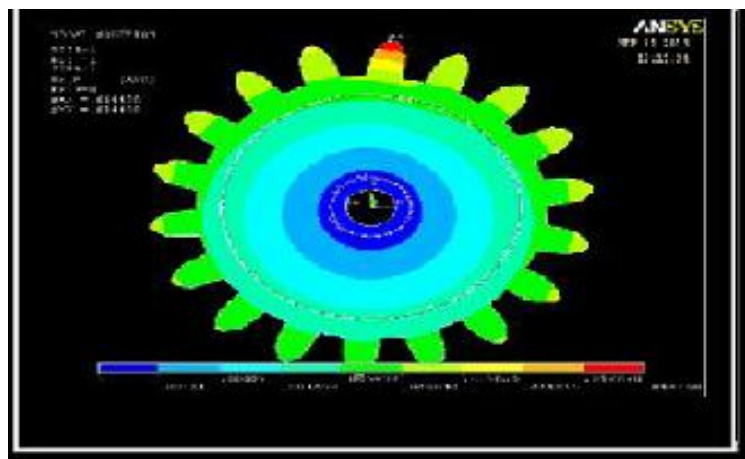


Fig 2.1 Displacement pattern of Cast Iron gear

Displacement pattern of Nylon:

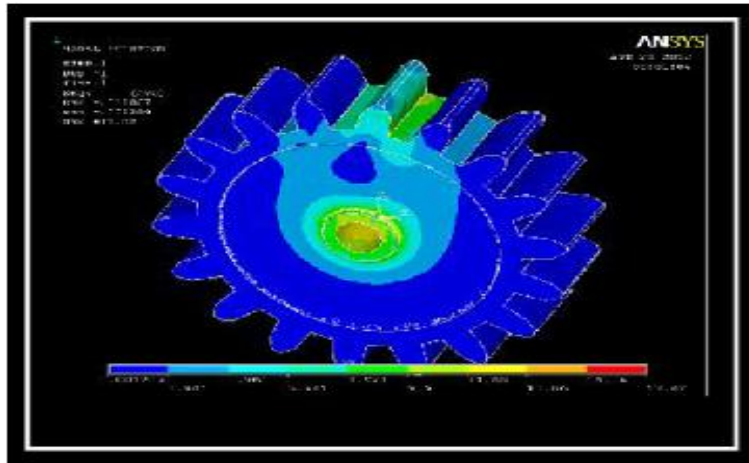


Fig 2.2 Displacement pattern of Nylon gear

Stress Distribution of Cast Iron

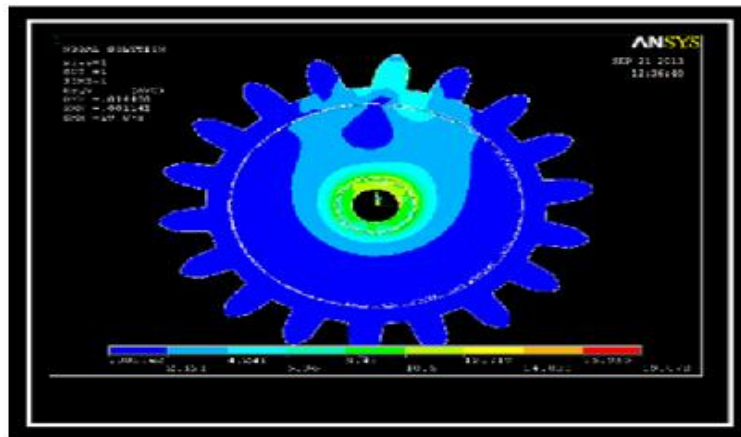


Fig 2.3 Stress Distribution of Cast Iron gear

Stress Distribution Of PolyCarbonate

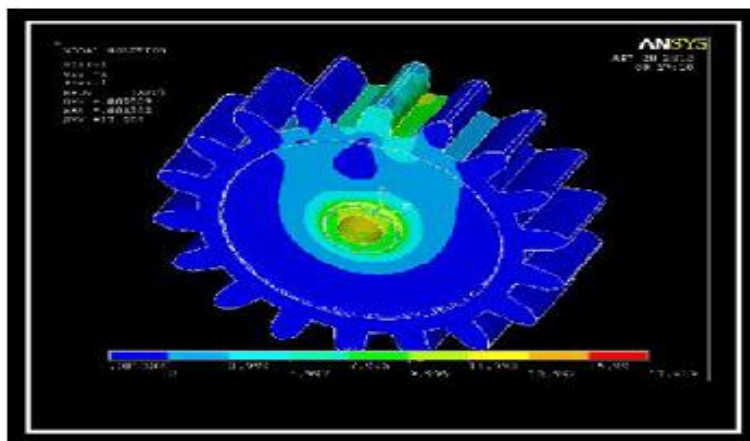


Fig 2.4 Stress Distribution of Polycarbonate gear

## Stress Distribution OF Nylon Spur GEAR

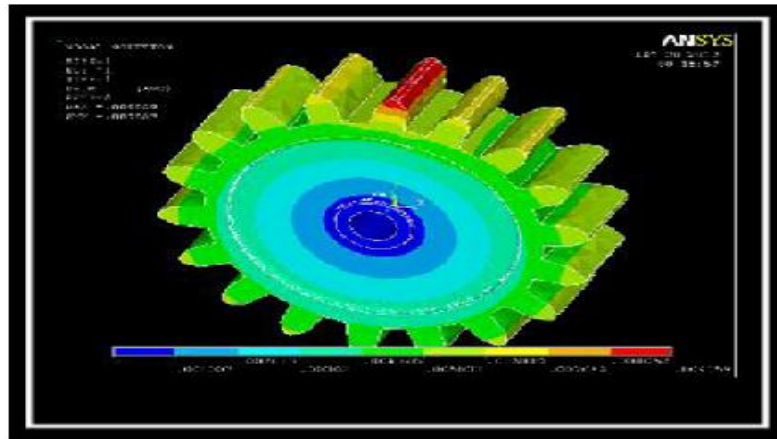


Fig 2.5 Stress Distribution of Nylon gear

**II. RESULTS**

From the static analysis , the deflections and Vonmises stress and strain values for the cast iron, Nylon and polycarbonate are obtained as following

## FOR CAST IRON SPUR GEAR

Pressure (N/mm <sup>2</sup> )	Vonmises Stress (N/mm <sup>2</sup> )	Deflection (mm)	Strain
1	3.832	0.002905	2.21e-4
2	7.665	0.005811	4.41e-4
3	11.497	0.008716	6.62e-4
4	15.33	0.011622	8.82e-4
5	19.078	0.014488	1.14e-3

Tab 4.1 Analysis for Cast Iron spur gear

## FOR NYLON SPUR GEAR

For Nylon Spur gear: Pressure (N/mm <sup>2</sup> )	Vonmises Stress (N/mm <sup>2</sup> )	Deflection (mm)	Strain
1	3.582	0.002381	2.19e-4
2	7.163	0.004762	4.37e-4
3	10.745	0.007143	6.56e-4
4	14.327	0.009524	8.74e-4
5	17.82	0.011867	1.29e-3

Tab 4.2 Analysis for Nylon spur gear  
FOR POLYCARBONATE SPUR GEAR

Pressure (N/mm <sup>2</sup> )	Vonmisse Stress (N/mm <sup>2</sup> )	Deflection (mm)	Strain
1	3.615	0.001817	2.20e-4
2	7.863	0.003635	4.45e-4
3	10.846	0.005452	6.61e-4
4	14.462	0.007274	8.82e-4
5	17.989	0.009059	1.38e-3

Tab 4.3 Analysis for Polycarbonate spur gear

### III. CONCLUSION

Since the deflections are less the efficiency of nylon spur gear is more than the cast iron spur gear, results in less noise and long life, The metallic gear results in more deflection compared to nylon and polycarbonate, the cost price and life of nylon is also good. When we replace the metallic spur gear with nylon gear there would be better results we can find in the automobile, robotic and in medical fields where the need of nylon gear is there.

### REFERENCES

- [1] Ali Raad Hassan, 'Transient Stress Analysis in Medium Modules Spur Gear Tooth by Using of Mode Super Position Technique', International Conference of Mechanical Engineering, Tokyo, Japan, 27-29 May 2009, World Academy of Science, Engineering and Technology, Volume53,2009,pp.49-56 .
- [2] ANSYS (2004), Release 9.0, SAS IP, ANSYS Inc. U.S.A.,([www.ansys.com](http://www.ansys.com)).
- [3] Boresi A.P. and Schmidt R.J. (2003), 'Advanced Mechanics of Materials', Sixth edition, John Wiley & Sons (ASIA) Pte. Ltd., Singapore, pp. 589-624.
- [4] Colbourne J.R. (1987), 'The Geometry of Involute Gears', SpringerVerlag, New York.
- [5] Harris T.A. (1966), 'Rolling Bearing Analysis, London', New York, Sidney, Wiley.
- [6] Johnson K.L. (1985), 'Contact Mechanics', Press Syndicate of the University of Cambridge, London, New York, Melbourne.
- [7] Lynwander Peter (1983), 'Gear Drive Systems', American Lohmann Corporation, Hillside, New Jersey.

## Stress Analysis of Splice Joint of the Aircraft Bottom Wing Skin by Finite Element Method

<sup>1</sup>A.Rukesh Reddy, <sup>2</sup>P. Ramesh, <sup>3</sup>B. Siddeswara rao

<sup>1</sup> (Department of Mechanical Engineering, Sri Venkateswara college of engineering and technology, Chittoor-517002

<sup>2,3</sup> (Department of Mechanical Engineering, Siddhartha college of engineering and technology, Puttur- 517583

### ABSTRACT:

*This paper investigates the maximum stress concentrated part of the splice joint of an aircraft bottom wing skin due to tensile loading. Wings are the aerofoils attached to each side of the fuselage to produce lift force. Joints are inevitable in any large structure like an aircraft wing. Splicing is normally used to retain a clean aerodynamic surface of the skin for most of the aircraft structure. This analysis considers the wing box with a bottom skin splice joint. The wing box comprises of two spar beams, three ribs, stiffeners covered with skin plate. In this paper the chord-wise splicing of wing skin is considered for a detailed analysis. The splicing is multi row riveted joint under the action of tensile in plane load due to wing bending. The stress analysis of the joint is carried out to compute the stresses at rivet holes due to By-pass load, bearing load and secondary bending. The splice is optimized to minimize the rivet hole local stress. A finite element analysis is carried out to evaluate the stresses. Analyses were performed by MSC PATRAN and NASTRAN software.*

**KEYWORDS:** stress analysis, splice joint, wing skin and rivet holes.

### 1. INTRODUCTION

The ideal flight vehicle structure would be the single complete unit of the same material involving one manufacturing operation. Unfortunately this cannot be achieved in practical because the every portion of aircraft structure involves numerous numbers of parts and the unavailability of material for required span. So joints are inevitable in any large structure like an airframe. Splicing is normally used to retain a clean aerodynamic surface of the skin for all structural components. The wings are the most important lift-producing part of the aircraft. Wings vary in design depending upon the aircraft type and its purpose. The wing box has two crucial joints, the skin splice joint & spar splice joint. Top and bottom skins of inboard and outboard portions are joined together by means of skin splicing. Front and rear spars of inboard and outboard are joined together by means of spar splicing. The spars resist much of the bending moment in the wing and the skins resist the shear force.

In this paper the chord-wise splicing of wing skin will be considered for a detailed analysis. The splicing is a multi-row riveted joint under the action of tensile in plane load due to wing bending. The basic knowledge about the loads acting on aircraft is necessary to understand the wing bending.

The Loads acting on the aircraft structure are,

1. Weight
2. Lift
3. Drag
4. Thrust

#### Weight

Weight is a force that is always directed toward the center of the earth. The magnitude of the weight depends on the mass of all the airplane parts, plus the amount of fuel, plus any payload on board

#### Lift

To overcome the weight force, airplanes generate an opposing force called lift. Lift is generated by the motion of the airplane through the air and is an aerodynamic force. "Aero" stands for the air, and "dynamic" denotes motion. Lift is directed perpendicular to the flight direction.

**Drag.**

As the airplane moves through the air, there is another aerodynamic force present. The air resists the motion of the aircraft and the resistance force is called drag.

**Thrust.**

To overcome drag, airplanes use a propulsion system to generate a force called thrust.[2]

**Wing and Wing Box:** Wing is the important structural unit of an aircraft and it is going to bend during flying due to lift load acting in it. Hence bottom wing skin subjected to tensile load and top wing skin is under compression [4]. The largest forces on the wings occur when the plane is airborne. Since the wings must then support the whole weight of the aircraft the steady stresses are high, and with the wings bending upwards, so that the upper surfaces are in compression and the underside in tension. Due to this tension force the maximum tensile stress concentration will be found on the joints of bottom wing skin of the aircraft. This paper is focused on the middle part of the wing with riveted splice joint at the bottom skin, which is called wing box. The wing box comprises of two numbers of spar beams (C-section), three numbers of ribs (I-section), four numbers of L-shaped stiffeners at top of ribs and four numbers of rectangular shaped stiffeners at bottom of ribs. The top and bottom portions of the wing box are covered with the thin sheet which is called wing skin. The top skin is designed as the integrated part with wing box structure. The bottom skin is designed in two pieces and they have joined by the splice plate. Here the bottom flange of the middle rib is considered as the splice plate of the joint. The bottom skin and splice plate is joined by rivets. The wing box is completely unsymmetrical in its all axes. The dimensions of the wing box parts have been finalised by the aerodynamic calculations which involve the computational fluid dynamics procedure. the aerodynamic calculations provide the thicknesses of spar beams (3 mm), ribs (2 mm), skin (1.5 mm) and stiffeners (4 mm).

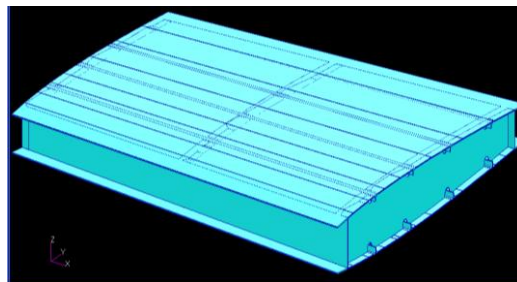


Figure 1(a): CAD model of Wing box (CATIA V5R19)

**II. EXPERIMENTAL DETAILS**

**2.1 Stress Analysis Using Finite Element Analysis Software.**

The IGES model was imported from the CATIA V5R19 into the Finite Element Analysis software MSC-PATRAN for geometry extraction. The components of wing box such as spar beams, ribs, stiffeners and skin are meshed separately. Quadratic and triangular elements have been used in this model, due to their lower stiffness properties. The beam elements were used for rivet connections. Near the stiffener cut-out region the fine mesh has been done and the coarse mesh has been done for the rest of the portions of wing box. The material properties, loads and boundary conditions were applied to the meshed wing box to ascertain the stress distribution at wing box.

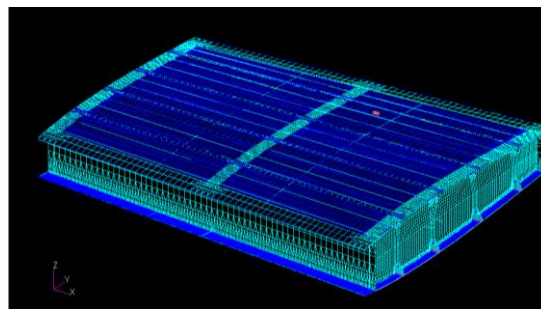


Figure 2(a) Meshed model of wing box

## 2.2 Finite Element Analysis Software's.

- PATRAN pre-processing and Post processing
- NASTRAN solver

## 2.3 Load Calculations.

All-up weight of the aircraft considered for the analysis is 2000 kg.

(4-seater aircraft)

- Weight of the aircraft = 2000 kg.
- Design load factor considered = 3g.
- Total load acting on the aircraft =  $2000 \times 3$   
Total load = 6000kg
- Factor of safety considered = 1.5
- The design load =  $6000 \times 1.5$   
Design load = 9000kg

Lift load experienced by both fuselage and wing.

- Lift load on the wing = 80% of total load =  $0.8 \times 9000$
- Lift load on the wing = 7200kg
- Load acting on each wing =  $7200/2$   
= 3600 Kg

The total span of the wing and the wing box (portion shown in dark line) dimensions with resultant load are shown in figure 2(b)

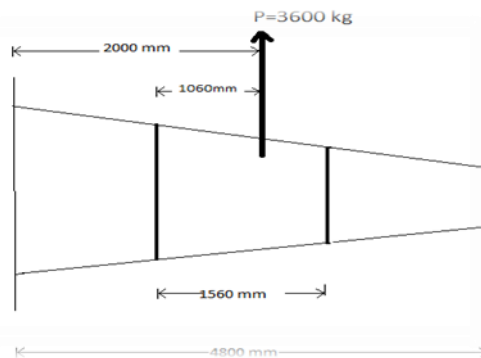


Figure 2(b) Wing box dimensions with load.

The resultant load is acting at a distance of 2000 mm (from aerodynamic calculations) from the root of the wing.

- The maximum B.M at the wing root =  $3600 \times 2000 = 7.2 \times 10^6$  kg-mm
- The B.M at the root of the wing box =  $3600 \times 1060 = 3.392 \times 10^6$  kg-mm
- The load at tip of the wing box =  $3.392 \times 10^6 / 1560 = 2174$  kg
- This 2174 kg load is converted into uniformly distributed load (1.03 kg/mm as UDL) and applied at tip side of wing box in bending direction of wing.

## 2.4 Loads and Boundary Conditions.

Uniformly distributed load of 1.03 kg/mm was applied at tip side of the wing box and other end is fixed which is called the root side of the wing box. A two dimensional linear static stress analysis is carried out using finite element analysis software MSC PATRAN and MSC NASTRAN. Mesh independent stress magnitudes are obtained through iterative mesh refinement process. Aluminum 2024-T351 alloy properties are given to the Pre-processor material properties. Load corresponding to the maximum lift load on the wing is considered to be applied on the wing box

## III. RESULTS AND DISCUSSION

The loads and boundary conditions applied to the wing box are shown in figure 3(a).

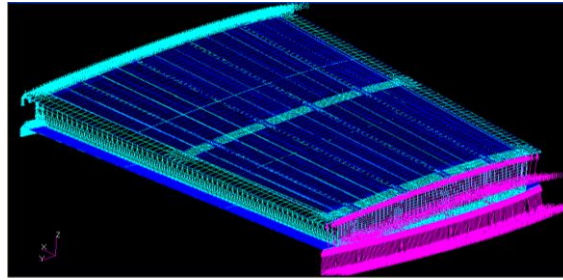


Figure 3(a) wing box loading conditions

The stress distribution for the given loads have been observed and that reveals the stress is distributed uniformly but maximum stresses are developed near the rivet joint portion of the bottom skin splice joint. The maximum stress concentrated portion of the wing box i.e. splice joint of the bottom wing skin is shown in below figure 3(b)



Figure 3(b) maximum stress concentration at bottom skin splice joint

Figure 3(b) shows the maximum stress near the small riveted circular holes by applying load 1.03 kg/mm, the maximum stress is  $\sigma_{max} = 25.2 \text{ kg/mm}^2$ . the figure 3(c) and figure 3(d) shows the maximum stress in red colour.

Figure 3(c) maximum stress near splice joint rivet hole

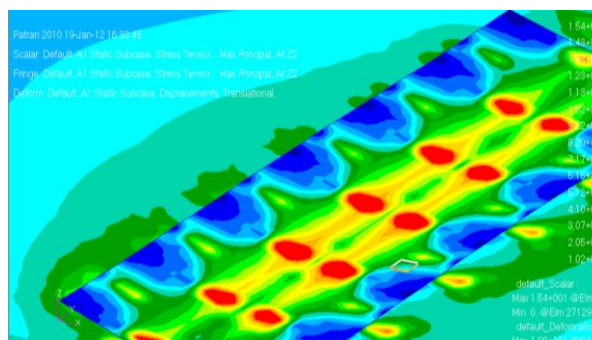
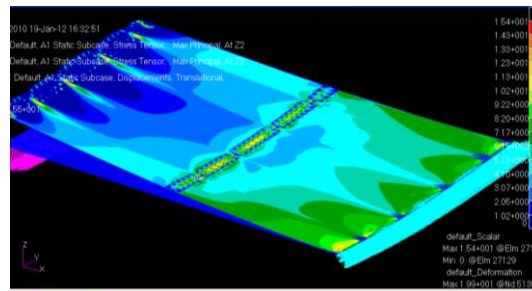


Figure 3(d) maximum stress at rivet holes of the splice plate

From the figure 3(a), 3(b) and 3(c) it was observed that maximum stress of the wing box is concentrated near the rivet hole locations of the splice joint of the bottom wing skin. And these will be fatigue critical locations in the aircraft bottom wing skin.

#### **IV. CONCLUSIONS:**

- The maximum stress concentrated part of the bottom wing skin splice joint has been identified for the stress analysis
- Finite element method approach is used for the stress analysis
- Loads and boundary conditions are accurately simulated to obtain the response of the wing box similar to the response of the parent structure at this location.
- Maximum stress of  $\sigma_{\max} = 25.2 \text{ kg/mm}^2$  is obtained near one of the rivet hole location of the bottom wing skin splice joint.
- The highest tensile stress location will be the location of fatigue crack initiation spot in the wiring box. So using these results we can go for the fatigue life to crack initiation calculations.

#### **REFERENCES**

- [1] Fawaz, S. A. and BörjeAndersson. "Accurate Stress Intensity Factor Solutions for UnsymmetricCornerCracks at a Hole". Proc. of the Fourth Joint NASA Conference on Aging Aircraft, vol 15 (2000),pp 135-139
- [2] C.S. Kusko, J.N. Dupont, A.R. Marder, "Influence of stress ratio on fatigue crack propagation behavior of stainless steel welds". Welding Journal, vol 19,(2004), pp 122-130,
- [3] N. Ranganathan, H. Aldroe, F. Lacroix, F. Chalon, R. Leroy, A. Tougui. "Fatigue crack initiation at a notch". International Journal of Fatigue, vol 33, (2011), pp 492-499.
- [4] Newman, J.C. "A crack opening stress equation for fatigue crack growth". International Journal of Fracture, vol 24(2003), pp 131-135.
- [5] Lance Proctor et al, local analysis of fastener holes using the linear gap technology using MSC/NASTRAN, Presented at MSC Aerospace Users' Conference, 2000, pp1-24.
- [6] A.M.Brown, Simulating fretting contact in single lap splices, International Journal of Fatigue, 2009, pp 375-384.
- [7] M.R. Urban, Analysis of the fatigue life of riveted sheet metal helicopter airframe joints, International journal of fatigue, 2003, pp 1013-1026.
- [8] Gresnigt AM, Steenhuis CM. Stiffness of lap joints with preloaded bolts, Proceedings of the NATO ARW, 2000.
- [9] Brombolich LJ. Elastic-plastic analysis of stresses near fastener holes. AIAA 11th Aerospace Sciences Meeting, 1973. [AIAA no. 72-252].
- [10] S.G.S. Raman, V.M. Radhakrishnan, "On cyclic stress-strain behaviour and low cycle fatigue life," Materials and Design, 2002, Vol.23, pp.249- 254.
- [11] RamzyzanRamly et al, Design and Analysis for Development of a Wing Box Static Test Rig, International conference on science and social research, December 2010, pp 113-117.
- [12] Huth H. Influence of fastener flexibility on the prediction of load transfer and fatigue life for multiple-row joints. In: Potter JM, editor. Fatigue in mechanically fastened composite and metallic joints, ASTM STP 927. 1986. p. 221-50.
- [13] Szolwinski MP, Farris TN. Linking riveting process parameters to the fatigue performance of riveted aircraft structures. AIAA-99-1339, 1999.

# Identification Of Eligible Customer Requirements

Pavel MIKUŠ

Catholic University In Ružomberok Faculty Of Education

## ABSTRACT

The paper deals with the changes which must be made by the company for customer satisfaction. The mission of the company is meeting customer requirements, which can be understood as the perception and understanding of his expectations. Making changes is based on a thorough analysis of options of organization and customer requirements. There are many methods by which it is possible to identify the eligible customer's requirements to improve the quality of service or product. The paper deals with a relatively new and simple method BDI - band diagram of interest (band diagram of interest) that is used for the comparison of customer satisfaction, perceptions of the importance of a particular factor as well as perception of the importance of individual perception and the possibility of his influence.

**KEY WORDS:** customer satisfaction, build loyalty, band diagram, analysis of customer requirements.

## II. PREFACE

The satisfaction of customer's needs is the fundamental function, which is performed by enterprise. At the same time it is fulfilling the nature of its existence, which comes out from its mission. The term customer satisfaction can be understood as the perception and understanding of customers' expectations which were met or exceeded by supplier's activities.

## III. CUSTOMER'S SATISFACTION

Evaluation of customer satisfaction is therefore a self-assessment of how customers perceive the value of the product and its properties offered for their use. Addressing the customer may not have a favorable response to all customers because every customer recognizes the value and prefer their own product characteristics. Therefore, customer requirements must be considered from a complex viewpoint. Satisfaction of customer needs is psychic interactive process between the enterprise and customers. The result of this relationship is the customer's satisfaction based on their requirements and needs, as well as on business opportunities. Customer creates own requirements based on their own experiences after using a product or service. A satisfied customer comes and buys again, so customer satisfaction is one of the fundamental pillars of long-term business success.

Satisfied customer is at the time when the needs and expectations are fulfilled continuously during the whole life-time of the product. If service supplier did not fulfill the expectations then the chance is given to competitors. It is very important to have the bunch of regular customers. Satisfied customer comes and again requests the product, which satisfied their needs. Short-term goal of marketing activities is to achieve the sales success. With the satisfied customers the direction of the marketing is focused on long-term customer's satisfaction during which customer does not accept the competitor's offers. Customer satisfaction after the purchase of a product depends on what the real value of the product is due to their expectations. "Customer satisfaction depends on their feelings - of pleasure or disappointment resulting from comparing the performance of consumer with the expected performance." <sup>1</sup> If actual performance is lagging behind expectations, the customer is dissatisfied. Conversely, if actual performance exceeds our expectations, the customer is satisfied and is happy with product or provided service. "All those involved in the management systems must perceive needs and expectations of customer requirements..." <sup>2</sup> Building customer loyalty; customer decisions are influenced by many subjective factors that are not always completely rational, by economic choice. One of these

<sup>1</sup> KOTLER P.: *Marketing Management*. GRADA PUBLISHING, Praha, 1998, str.49.

<sup>2</sup> BUDAL P. – FILO, M.: *Manažment operácií*. Vydavateľstvo Michala Vaška, Prešov, 2008, str. 14.

factors is customer loyalty to their supplier for occasional purchases. If the concept of loyalty for measuring customer satisfaction is particularly important, it must be examined in some depth. Customer loyalty is the cornerstone of successful service, loyalty affects employees and contractors. It also produces incomes that encourage loyalty of shareholders. Gains may be caused either by lower prices as a means of obtaining a first contract or particular market position, or possibly as preparation for launching a new service on the market, both are associated with exploring of the requirements and desires of a new customer. "Keeping existing customers is less costly than acquiring new, because the costs of keeping loyal customers make up only 20% of the cost of acquiring new"<sup>3</sup>. Evaluation of customer satisfaction; before the enterprise comes to detailed evaluation of customer satisfaction with the appropriate tools and in respect of the planned changes, firstly it must come to usage of the possibility of feedback, which is the most trusted way to get opinions and evaluations of a particular product. This is the creation of additional contacts with customers with the aim to gain easy and quick evaluation of its product. Some companies use direct contact with customers and make a telephone survey of satisfaction with a particular product or service. Others add a short questionnaire to a new product which is available for answering to the customer after some time of usage and customer is to send it to the company. These events are usually associated with the competition events. There is a popular way of using the Internet, where the customer logs on to the web address of the manufacturer and evaluate the product and as bonus they receive a bonus such as extended period of the warranty period, or permanent collection of information on new products, with the possibility of granting discounts. This creates a certain interest groups of people who are connected by the same product. Setting consumer advisers, consumer clubs, may then also serve as a tool for feedback to the opening of qualitative information on the causes of dissatisfaction. For the customer perception as well as other relations with customers special critical experiences, events, complaints and claims are evaluated at the various points of contact. "The aim is to actively create conditions for satisfaction of enterprise and of customer as well. Procedures focused on performance through benchmarking, testing, mostly links to the regular referral of the facts to verify compliance with technical or objective characteristics of the product. These procedures should therefore be eligible for the special screening of objective, measurable factors.

#### **IV. BDI – THE METHOD FOR THE ANALYSING OF CUSTOMER NEEDS AND OPPORTUNITIES OF ENTERPRISE**

Making changes is based on a thorough analysis of enterprise opportunities and customer requirements. There are many methods by which it is possible to identify the eligible customer's requirements to improve the quality of service or product. Very simple method BDI - band diagram of interest (band diagram of interest) that is used to compare client satisfaction, the importance of the perception of a particular factor as well as the importance perceived from the side of enterprise and the possibility of its influence. It does not require a different statistical analysis and evaluation of questionnaires or the knowledge of the statistical apparatus. Therefore, the usage is wider. It takes into consideration the compliance rate of legitimate customer requirements and their satisfaction against the organization opportunities to fulfill these requirements. The statistical support is not excluded and analysis of results using statistical methods. The method can be applied as an action, therefore, for immediate detection of dependence on a phenomenon perceived in the organization. It is practical, easily manageable and illustrative when at look the final quadrant provides meaningful value for further action of manager in implementing the change in the company. It is easy to define the different quadrants and their importance which is already known in advance. Therefore, this is a method for the analysis and definition of required changes from the side of the consumer, customer, and for improvement business processes. Why changes? Easy answer, the changes are moving the world. For example, current period is characteristic by world economic crisis. It is the change, which with unforeseeable and with huge measure touched all areas of social and industrial life not only in Slovakia, but got the whole world measure. The starting point from this situation is the activation of the change processes, which will probably lead to wished – better state comparing with today. It of course expects to make a trough analysis and future requests. By the means of BDI method – band diagram of interest, it is quite easy to find out the customer's requests and perception of their importance considered by customer. Perception of customer's request can be inadequate; therefore, they are corrected by view of perception of possibilities from the side of enterprise. BDI is the method of compromise of eligible client's requests and view of the significance, resp. importance and possibilities from the view of enterprise. Importance of perception of customer's requests is then reviewed by stating the significance and importance from the side of enterprise. The enterprise features here as the regulator of competence of requests and the possibilities of its fulfillment. The factors of satisfaction are necessary to state in line with the increase of quality of company activities, which leads to customer satisfaction. It is the process of changes,

---

<sup>3</sup> REICHELDT, F. – SASSER, W.: *Služby cesta k úspechu*. Praha, Victoria Publishing 1993, str. 39

which are to satisfy the customer's needs based on their legitimate requests, possibilities and performance of the enterprise.

**Basic relation;** it is based on the customer's requests and realted premises to fulfill these requests.

**Usage;** By analyzing of customer's satisfaction in manufacturing as well as in nonmanufacturing area, detection of request of potential customer's, purchasers and consumers.

The procedure of BDI application; the procedure represents the group of steps, which are necessary to make from the side of the enterprise in order to detect the needs of customers:

1. to state the factors (elements) of satisfaction
2. to find its importance from the view of customer
3. to define the importance from the view of enterprise
4. to state the quadrant of legitimate requests
5. to create contrastive matrix rate of significance factors of satisfaction with the rate of importance and options from the side of organization and their rate of importance.
6. to define the meaning of particular quadrants
7. to state the tolerance of ideal state
8. intersection of quadrants and their characteristics
9. to state the procedure in order to transform the satisfaction to the zone according to the options.

Principles: - customer orientation

- Focusing on results
- Stability of objectives and their adaptation to customer
- Management according to satisfaction factors
- Constant changes leading to quality
- Revealing of new possibilities of the potential usage
- Responsibility for customers and their needs

Recalling BDI value; it is possible to consider the recalling value as the consequential graphical processing and stating of recalling value of particular quadrants. From the intersections of BDI1 and BDI2 it is possible to state the objectives which must be done in order to get the customer's satisfaction to quadrant of satisfaction.

Major feature; the major feature of BDI method is consistent respect of client with the objective of satisfaction of their legitimate requests bound to potential and possibilities of organization.

Using this method it is possible to reduce the risks which arise from:

- Building of the management system
- Development of product and its construction
- Satisfaction of client's needs in given services
- In preparation of new technologies
- In preparation of changes and their implementation either proactively or exceptionally reactively.

**Contribution of BDI:**

- Structural approach to improvement of company activities in favor of customer
- Self valuation based on factors and potential
- Straight confrontation of customer's requests and company possibilities
- Regular valuation of organization trends
- Preconditions to better master the process of proactive changes
- The innovations must be focused on weak points
- Wide usage
- Support to initiative and teamwork
- Sound of feedback

**Consecutive contributions:**

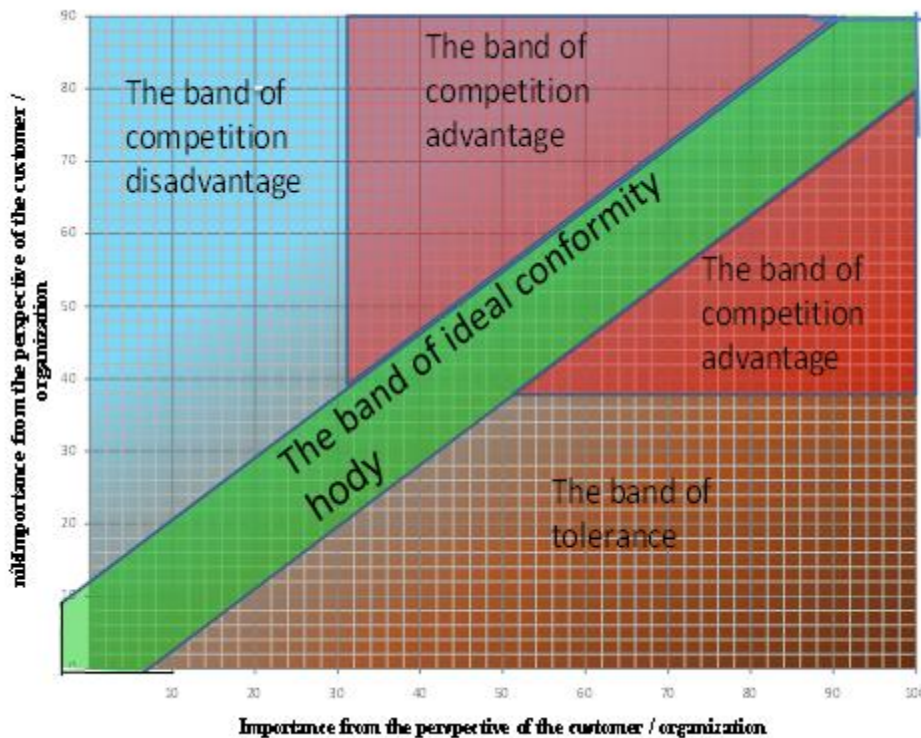
- Focusing on customer,
- Image improvement
- Improvement of quality of process changes

Using the BDI method (band diagram of interest) - it is possible to analyze all chosen factors.

The profile of customer's satisfaction describes the relation between the importance of particular parameters and customer's satisfaction with these parameters. This ideal zone is possible to name as balanced zone, which is created by interval +/-10 up to 15% from balance axis.

The same is valid for BDI from the view of enterprise as well. The company makes the comparison of importance of guessed factors with its possibilities in consideration of sources, human potential, finances, technical and technological possibilities to make with the legitimate customer's needs. This net graph was created being based on assumption: amount incurred by enterprise are put on to legitimate customer's satisfaction and it is equal to importance from the side of customer, i.e. ideal zone. The profile of customer's satisfaction describes the relation between the importance of particular parameters and customer's satisfaction with these parameters.

## V. BAND DIAGRAM OF INTEREST



Picture: band diagram as graphical BDI interpretation

It is necessary to divide the diagram to several zones (quadrants):

The band of competition advantage; it is possible to perceive in 3 levels

- a) Customer – relatively high satisfaction, over 50% importance of particular factors
- b) Organization – options are used for satisfaction of customer, the importance of guessed factor is relatively high and in line with customer perception
- c) Mixed – it is possible to state relatively high rate of conformity of perception of guessed factors from the view of customer as well as organization. The rate of conformity and importance is then considered as the competition advantage, supported by the favor of customers.

The band of ideal conformity; represents the same view of both subjects on factors perception in 3 levels:

- a) Customer – satisfaction is perceived in conformity with importance of particular factors
  - b) Organization – the rate of importance of particular factors is measured to its possibilities
  - c) Mixed – the same perception of importance defined in customer's satisfaction as response to possibilities of organization
1. Margin of tolerance; customer satisfaction and the possibility of organizing are more than 15%, but given the relatively low level perception of the importance of both entities it is possible, factors that occur in this zone, identified as less important and it is not necessary to pay attention to them.

2. Band of a competitive disadvantage; attention to the high level of attention,
  - a) Customer - shows low satisfaction with the service provided, to which attaches high importance, and expresses their dissatisfaction,
  - b) Organizations - low potential of organization to affect the factor, but also it perceives it as very important for meeting the needs of customers
  - c) The common and very important is that the factors which are found in this band, represent a threat of losing a customer to the organization. It is therefore a band of problems which are to be addressed urgently.

Ideally, the company moves when the satisfaction and importance are in balance. This area can be described as an ideal and an equilibrium zone is formed by an interval of +/- 5 up to 10% from the equilibrium axis. Strategic disadvantages are lower than the percentage expression of the limit value and satisfaction rating is in an ideal area. Limited value of satisfaction is set by the desired value of satisfaction and depends on the objectives of the company, its market position but also the maturity of its customer portfolio and over time may change its value. Strategic benefits are the percentage expressing of the ratio of satisfaction and importance of a limit value satisfaction boarded by ideal area bounded from above, but also from the bottom. Customer orientation is now a fundamental vision of all advanced business and satisfied customer is the main objective. For business success is therefore very important to correctly identify the requirements and expectations of its customers, to monitor and manage their level of satisfaction. Enterprises that have a balanced set of strategic evaluation criteria and their tracking system are more powerful and successful than their competitors. The implementation of process changes for customers means to take into account several factors that affect customer decision making and hence the success and profitability of the company on a diverse and rapidly changing market. The customer is in many enterprises motivating factor, but also an indicator of success, but not the only measure of business efficiency.

## VI. CONCLUSION

Processing results in such proposed chart will bring a structured overview of research results, but also a practical tool for managers in the planning process changes and operational decisions. No company is interested in providing low quality products or services. Many times, there is the difference between what it considered as important for business as a quality product and customer perception in terms of importance. To eliminate this gap it is valuable to systematically measure the needs of customers based on specified criteria and using the results of these surveys to determine the further strategy of the company.

## BIBLIOGRAPHY

- [1] BUDAJ, P. – FIEO, M.: *Manažment operácií*. Vydavateľstvo Michala Vaška, Prešov, 2008.
- [2] DROPPA, M.: *Riadenie ľudských zdrojov*. Edičné stredisko Pedagogickej fakulty Katolíckej univerzity. Ružomberok, 2008.
- [3] KOTLER P.: *Marketing Management*. GRADA PUBLISHING, Praha, 1998.
- [4] MIKUŠ, P.: *Manažment zmien-konkurencieschonosť organizácie*. VERBUM – vydavateľstvo Katolíckej univerzity, Ružomberok, 2010.
- [5] MIKUŠ, P.: *Teória procesu zmeny a jeho riadenie*. Edičné stredisko PF, Ružomberok. Akcentprint Prešov, 2008. ISBN 978-80-8084-287-1.
- [6] MIKUŠ, P.- DROPPA, M.: *Manažment inováčnej zmeny*. Studia Scientifica Facultatis Pedagogicae Ružomberok, Katolícka univerzita, 2005.
- [7] REICHELDT, F. – SASSER, W.: *Služby cesta k úspechu*. Praha, Victoria Publishing 1993.

# Cloud Information Accountability Framework for Auditing the Data Usage in Cloud Environment

D.Dhivya<sup>1</sup>, S.CHINNADURAI<sup>2</sup>

1,M.E.(Cse), Srinivasan Engg College,Perambalur,Tamilnadu,India.

2,Ap/Cse, Srinivasan Engg College,Perambalur,Tamilnadu,India.

## ABSTRACT:

Cloud computing enables highly scalable services to be easily consumed over the Internet on an as-needed basis. A major feature of the cloud services is that users' data are usually processed remotely in unknown machines that users do not own or operate. While enjoying the convenience brought by this new emerging technology, users' fears of losing control of their own data (particularly, financial and health data) can become a significant barrier to the wide adoption of cloud services. To address this problem, in this paper, a novel highly decentralized information accountability framework to keep track of the actual usage of the users' data in the cloud. In particular, an object-centered approach that enables enclosing our logging mechanism together with users' data and policies. Leverage the JAR programmable capabilities to both create a dynamic and traveling object, and to ensure that any access to users' data will trigger authentication and automated logging local to the JARs. To strengthen user's control, provide distributed auditing mechanisms. Extensive experimental studies that demonstrate the efficiency and effectiveness of the proposed approaches.

**KEYWORDS:** Cloud computing, accountability, data sharing

## I. INTRODUCTION

Cloud computing presents a new way to supplement the current consumption and delivery model for IT services based on the Internet, by providing for dynamically scalable and often virtualized resources as a service over the Internet. To date, there are a number of notable commercial and individual cloud computing services. Details of the services provided are abstracted from the users who no longer need to be experts of technology infrastructure. Moreover, users may not know the machines which actually process and host their data. While enjoying the convenience brought by this new technology, users also start worrying about losing control of their own data. The data processed on clouds are often out sourced, leading to a number of issues related to accountability, including the handling of personally identifiable information. Such fears are becoming significant barrier to the wide adoption of cloud services. Conventional access control approaches developed for closed domains such as databases and operating systems, or approaches using a centralized server in distributed environments, are not suitable due to the following features characterizing cloud environments. CIA framework provides end-to-end accountability in a highly distributed fashion. One of the maintaining lightweight and powerful accountability that combines aspects of access control, usage control and authentication. Two distinct modes for auditing: push mode and pull mode. The push mode refers to logs being periodically sent to the data owner or stakeholder while the pull mode refers to an alternative approach whereby the user can retrieve the logs as needed. First, Integrated integrity checks and oblivious hashing (OH) technique to our system in order to strengthen the dependability of our system in case of compromised JRE. Updated the log records structure to provide additional guarantees of integrity and authenticity. Second the security analysis to cover more possible attack scenarios. Third, the results of new experiments and provide a thorough evaluation of the system performance. Fourth, detailed discussion on related works to prepare readers with a better understanding of background knowledge. Finally, improved the presentation by adding more examples and illustration graphs.

## II. RELATED WORK

### 2.1. Cloud Privacy and Security

Cloud computing has raised a range of important privacy and security issues. Such issues are due to the fact that, in the cloud, users' data and applications reside—at least for a certain amount of time—on the cloud Cluster. Concerns arise since in the cloud it is not always clear to Individuals

why their personal information is requested or it will be used or passed on to other parties. Their basic idea is that the user's private data are sent to the cloud in an encrypted form, and the processing is done on encrypted data. The output of the processing is deobfuscated by the privacy manager to reveal the correct result. The author's present layered architecture for addressing the end-to-end trust management and accountability problem in federated systems. The authors' focus is very different from ours, in that they mainly leverage trust relationships for accountability, along with authentication and anomaly detection. Further, their solution requires third-party services to complete the monitoring and focuses on lower level monitoring of system resources. The authors propose the usage of policies attached to the data and present logic for accountability data in distributed settings. Crispo and Ruffo proposed an interesting approach related to accountability in case of delegation. It is mainly focused on resource consumption and on tracking of sub jobs processed at multiple computing nodes, rather than access control.

### 2.2. Self-Defending Objects

Self-defending objects are an extension of the object-oriented programming paradigm, where software objects that offer sensitive functions or hold sensitive data are responsible for protecting those functions/data. Similarly, extend the concepts of object-oriented programming. The key difference in our implementations is that the authors still rely on a centralized database to maintain the access records, while the items being protected are held as separate files. Provided a Java-based approach to prevent privacy leakage from indexing, which could be integrated with the CIA framework proposed in this work since they build on related architectures.

### 2.3. Proof-Carrying Authentication

The PCA includes a high order logic language that allows quantification over predicates, and focuses on access control for web services. While related to ours to the extent that it helps maintaining safe, high-performance, mobile code, the PCA's goal is highly different from our research, as it focuses on validating code, rather than monitoring content. Another work is by Mont et al. who proposed an approach for strongly coupling content with access control, using Identity-Based Encryption (IBE). We also leverage IBE techniques, but in a very different way. We do not rely on IBE to bind the content with the rules. Instead, we use it to provide strong guarantees for the encrypted content and the log files, such as protection against chosen plaintext and cipher text attacks.

## III. SYSTEM MODEL

### 3.1. Data Owner Configuration Phase

In this module every data owner must register their details in the cloud server. And Cloud server establishes the public key and private key access policy using IBE scheme. Finally the cloud server distributes the secret key to the data owner. Cloud server stores the data owner details in the data store as an entity (it is key object model). It is persistence storage

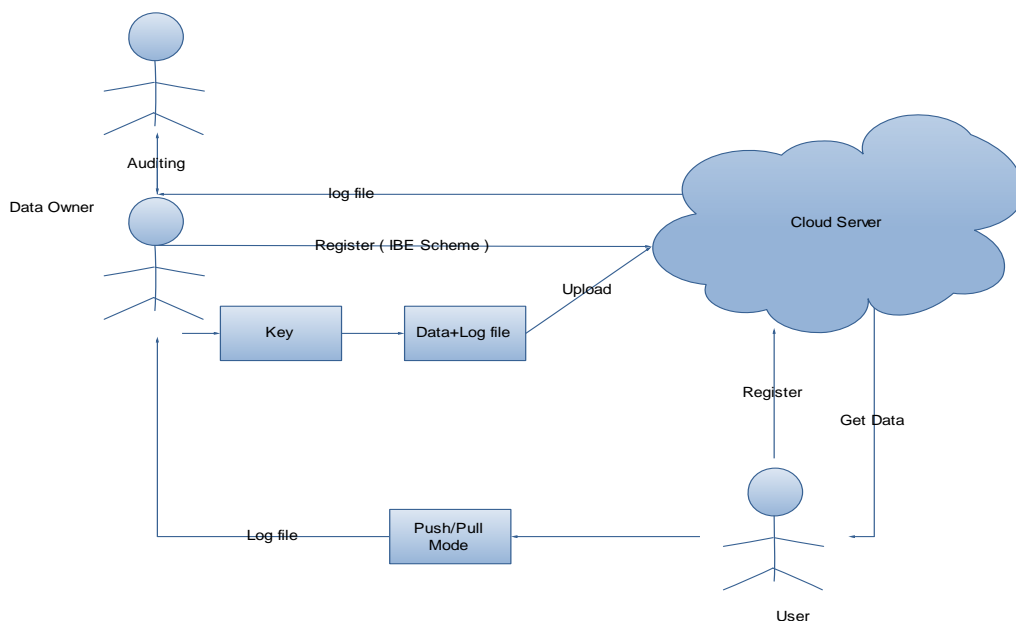


Fig 1: Overview architecture

**3.2. Data Uploading in Cloud Server.**

After configuration process completed data owner create the log file (it contain configuration details) and encrypt it using the secret key established by the cloud server to the particular data owner. Then load the owner data into encrypted log file. The owner data and log file is bounded or coupled together.

**3.3. User Configuration Phase**

In this module every user must register their details and account details in the cloud server. And Cloud server establishes the public key and private key access policy using IBE scheme. Finally the cloud server distributes the secret key to the user. Cloud server stores the user details in the data store as a entity (it is key object model). When the user request to get the data from the cloud server, the user get data with log file. This log file store the user session details and finally this log file send to data owner.

**3.4. Auditing Phase.**

In this module log harmonizer is used to perform the auditing work. This is maintained in the data owner. Data owner gets the log file information from the cloud server and user separately and decrypts the log files using the secret keys of data owner, and passes decrypted log files into the log harmonizer. Finally auditing process is conducted.

**IV. EXPERIMENTAL RESULT**

This experiment the time taken to create a log file and then measure the overhead in the system. With respect to time, the overhead can occur at three points: during the authentication, during encryption of a log record, and during the merging of the logs.

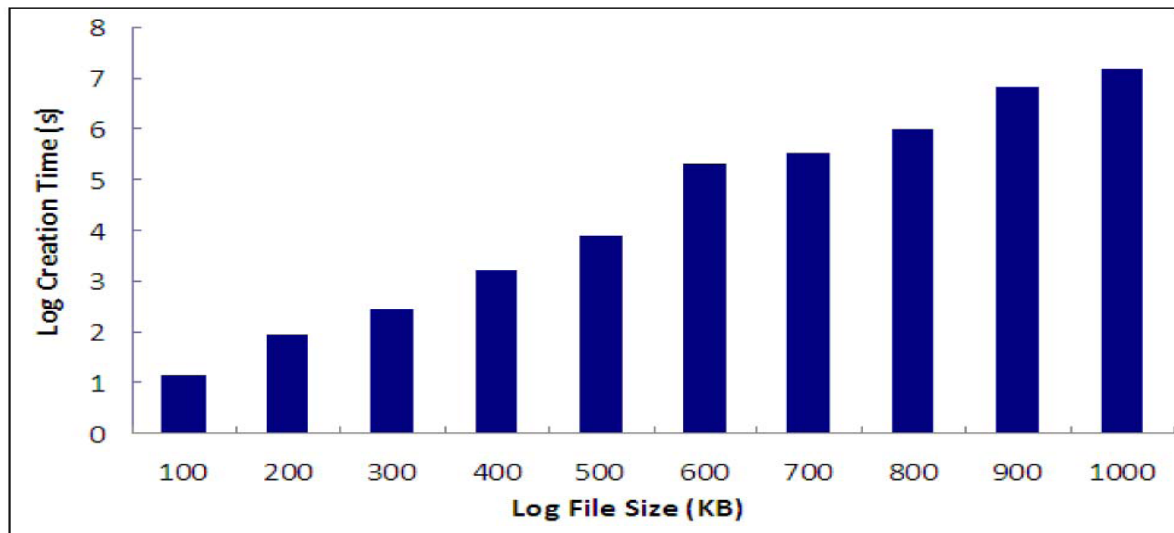


Fig 2: This result shows that time to create log files of different sizes.

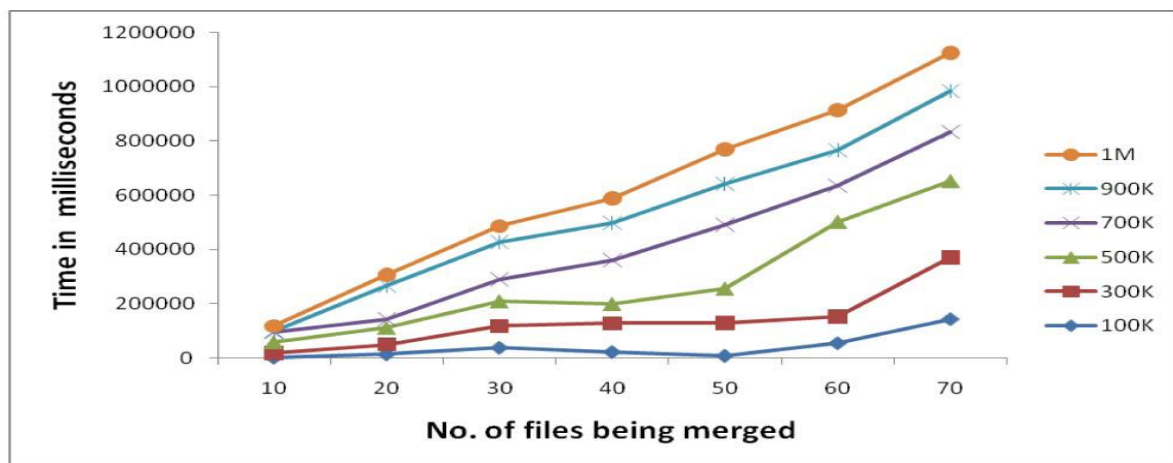


Fig 3: This result shows that time to merge log files

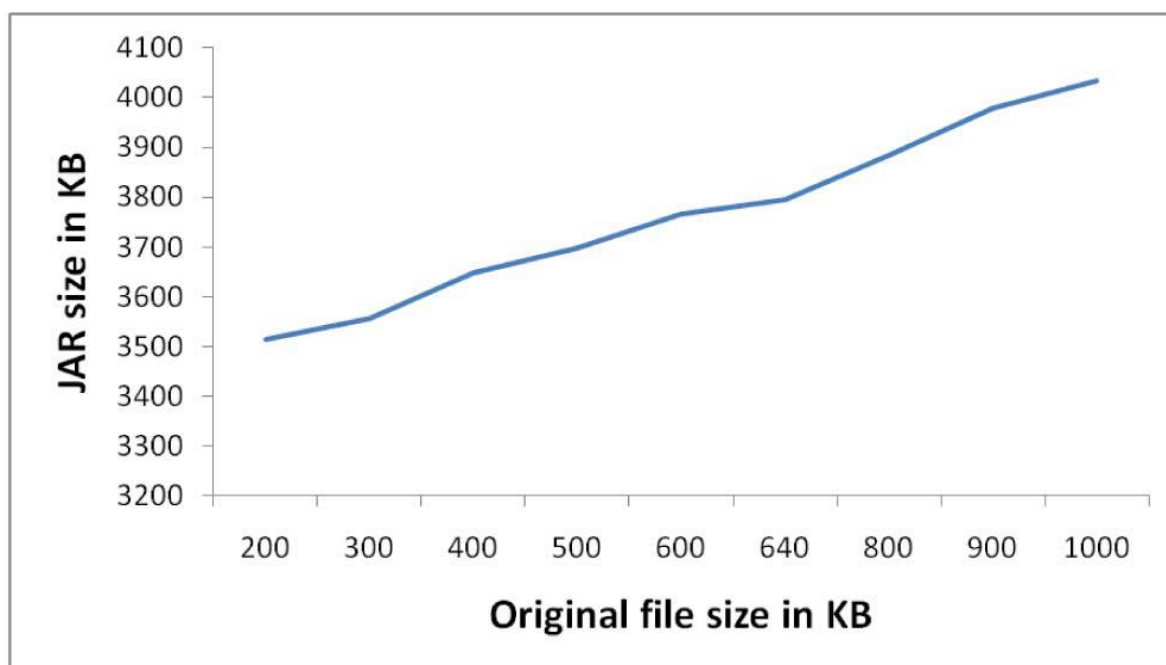


Fig 4: This result shows that size of the logger component.

## V. CONCLUSION

Innovative approaches for automatically logging any access to the data in the cloud together with an auditing mechanism. The data owner to not only audit his content but also enforce strong back-end protection if needed. Moreover, one of the main features of our work is that it enables the data owner to audit even those copies of its data that were made without his knowledge. In future plan to refine our approach to verify the integrity of the JRE and the authentication of JARs. For example, investigate whether it is possible to leverage the notion of a secure JVM being developed by IBM. This research is aimed at providing software tamper resistance to Java applications. Design a comprehensive and more generic object-oriented approach to facilitate autonomous protection of traveling content. To support a variety of security policies, like indexing policies for text files, usage control for executables, and generic accountability and provenance controls.

## ACKNOWLEDGEMENTS

This work was presented in part at the IEEE International Conference on Communications (ICC), 2012. This work was done in part of in our institution and support of all staff members.

## REFERENCES

- [1] B. Chun and A.C. Bavier, "Decentralized Trust Management and Accountability in Federated Systems," Proc. Ann. Hawaii Int'l Conf. System Sciences (HICSS), 2004.
- [2] R. Corin, S. Etalle, J.I. den Hartog, G. Lenzini, and I. Staicu, "A Logic for Auditing Accountability in Decentralized Systems," Proc. IFIP TC1 WG1.7 Workshop Formal Aspects in Security and Trust, pp. 187-201, 2005.
- [3] J.W. Holford, W.J. Caelli, and A.W. Rhodes, "Using Self-Defending Objects to Develop Security Aware Applications in Java," Proc. 27th Australasian Conf. Computer Science, vol. 26, pp. 341-349, 2004.
- [4] P.T. Jaeger, J. Lin, and J.M. Grimes, "Cloud Computing and Information Policy: Computing in a Policy Cloud?," J. Information Technology and Politics, vol. 5, no. 3, pp. 269-283, 2009.
- [5] J. Park and R. Sandhu, "Towards Usage Control Models: Beyond Traditional Access Control," SACMAT '02: Proc. Seventh ACM Symp. Access Control Models and Technologies, pp. 57-64, 2002.
- [6] A. Pletschner, M. Hilty, and D. Basin, "Distributed Usage Control," Comm. ACM, vol. 49, no. 9, pp. 39-44, Sept. 2006.
- [7] Sumitha Sundareswaran, Anna C. Squicciarini, "Ensuring Distributed Accountability for Data Sharing in the Cloud," IEEE Transactions on Dependable and secure computing, Vol 9. No.4, July/Aug 2012.
- [8] S. Sundareswaran, A. Squicciarini, D. Lin, and S. Huang, "Promoting Distributed Accountability in the Cloud," Proc. IEEE Int'l Conf. Cloud Computing, 2011.
- [9] D.J. Weitzner, H. Abelson, T. Berners-Lee, J. Feigenbaum, J. Hendler, and G.J. Sussman, "Information Accountability," Comm. ACM, vol. 51, no. 6, pp. 82-87, 2008.
- [10] Q. Wang, C. Wang, J. Li, K. Ren, and W. Lou, "Enabling Public Verifiability and Data Dynamics for Storage Security in Cloud Computing," Proc. European Conf. Research in Computer Security (ESORICS), pp. 355-370, 2009.
- [11] M. Xu, X. Jiang, R. Sandhu, and X. Zhang, "Towards a VMBased Usage Control Framework for OS Kernel Integrity Protection," SACMAT '07: Proc. 12th ACM Symp. Access Control Models and Technologies, pp. 71-80, 2007.

### **AUTHORS PROFILE**



**D. Dhivya received** the B.E Degree computer science and engineering and now she is an M.E student in the Department of Computer Science & Engineering, Srinivasan Engineering College – Dhanalakshmi Srinivasan Group of Institutions, Perambalur, TN, India.

Her research interest includes Network Security and Cloud Computing.

**S. Chinnadurai** is working as Assistant Professor/CSE, Srinivasan Engineering College – Dhanalakshmi Srinivasan Group of Institutions, Perambalur, TN, India.

His research interest includes pervasive computing, Wireless Networks and Image Processing.

# Mobile Phone Based Multi-Devices Secured Control System

Elsanosy Mohamed Elamin<sup>1</sup>, AbdirasoulJabar Alzubaidi<sup>2</sup>

<sup>1</sup>Engineering Researches & Industrial Technology, Sudan academy of Sciences,

<sup>2</sup>Electronics Engineering School, Sudan University of Science and Technology

## ABSTRACT

*In this paper, the integration or merge of technologies is presented to aid in reducing men-hands within the system as a total cost reduction especially in the industrial sectors as well as developing systems to comply with a running requirements instead of reengineering. The controlling system is regarded as a flexible tool to develop a way of traditional controlling technique. The structure of system is divided into three different functional parts which are: cellular mobile network, PC, and interface circuits to show, clarify, and make ease of the controlling signal transition from the user to the controlled devices. In addition, for well-designed process, interface circuits are utilized to enhance and boost the controlling signal. PC is the heart of the controlling process due to the reside program that decode and manipulate the incoming controlling signal from user to assist in making appropriate decision. The integration of technologies include both cellular mobile network and PC. Utilization of this integration or merge cause to accelerate decision making, and reduce men hand within the system as a total cost minimization.*

**KEYWORDS:** Controlling Signal, mobile network, DTMF, interface circuit, controlled devices

## I. INTRODUCTION

The rapid growth and deployment of the technologies drive users to exploit them in many different applications to facilitate and promote the systems management as well as reducing the overall cast. This paper introduce the merge of these technologies to show the advantages of such integration. To accomplish such integration, systems are designed to perform the different tasks according to the required functions that were well-specified. This work is parting into certain manner to facilitate the transmission of controlling signal. In contrast to the previous studies [1],the paper is used PC instead of microcontroller to increase the span of user mobility, strengthen the security process so as to enhance the control process to be performed by an authorized users, and add more interface circuits to make used of more interfaced devices as flexibility feature.In this work, a remote secured control devices is presented to control motor, valve, lever, and siren. These devices are only an example to prove that the controlling signal can be originated in the transmitter and passed through the system to the controlled devices such as home appliances. The remote control of multi-devices is carried out through the cellular mobile telephones and PC. The cellular mobile telecommunication technology introduces both the transmitter and receiver where the transmitter is used by the user or the controller and the receiver unit is reside with the controlled devices.

## II. SYSTEM STRUCTURE

The system components is structured in two principal categories to assist in maintaining, interfacing more devices, testing, and modification:

- Hardware
- Software

The hardware of the system revealed the performance mechanism of each part as well as to smooth the track of the controlling signal. It grouped into four phases as shown in fig. 1: controlling signal generator and receiver, processing unit, interface circuit, controlled devices. The system is integrated from the services point of view. The integration of system is due to the state transition flow of the control signal to achieve appropriate control process. Accordingly, the hardware implementation of the system is structured properly to make a route of the control signal from the user through the system to the controlled devices directly and smoothly.

### III. HARDWARE

#### 1. The Controlling Signal

The cellular mobile network represents the source of controlling signal that should be received by the controlled devices. It partially consists of the physical equipment, such as the radio transceiver, digital signal processors, and air interface as well as signaling scheme (dual tone multi-frequency, DTMF). The DTMF signal is the sum of two tones, one from a low group (697-941Hz) and one from a high group (1209-1477Hz) with each group containing four individual tones to allow for 12 unique combinations [10].

#### 2. MT8870 Receiver

It is an integrated IC characterized with low power consumption, adjustable acquisition and release time, power down and inhibit mode, single 5v power supply, and dial tone suppression. It consists of band split filter and decoder functions with few external passive components to achieve design flexibility. External low cost 3.58 MHz color burst crystal is used to synchronize the information transmission and to provide a power down option which, when enabled, drops consumption to less than 0.5 mW[11].The DTMF receiver is defined generally into three functional stages. First, the interface stage, is carried out through (RC) passive components to block dc components control signal gain. Second, the integrated DTMF receiver itself where the transmitting system signals can be processed as state transition flow for each specific signal delivered through the interface stage. Third, the output control logic[5]:

#### 3. The Processing Unit

The exploitation of computers in this work made most of the operational and maintenance aspects of the system easy, feasible, and flexible. The PC program software is well-interfaced with the user and controlled devices. The predefined process that aid in making an appropriate decision of the controlled devices is done in turbo C++ language for both easy concepts and applications.

#### 4. The Interface Circuits

The interface circuits are used to boost signal transition in between different phases. Here, DB25 male connector, HD 74LS373, and ULN2803A are used. The DB-25 male connector is used for device control and communication through software program.It consist of data, control, and status lines to be used as input/output buses. these lines are connected to relevant registers as stated in table 2.[7].To boost the signal level to drive the devices, the ULN2803A is used. The HD74LS373 is 8-bit register features totem-pole three-states output designed specifically for driving highly capacitive or relatively low-impedance loads. The ULN2803A is designed for general purpose applications with a current limit circuits. It consist of eight Darlington transistors with common emitters and internal suppression diodes for inductive loads. Each Darlington features a peak load current rating of about 500mA and can resist at least 95V in the off state[9].

Table 1: Parallelport address

Register	LPT1	LPT2
Data register(base address0)	0x378	0x278
Status register(base address+1)	0x379	0x279
Control register(base address+2)	0x37a	0x27a

#### 5. The load

The controlled devices can be any low current devices such as zener diode for TTL circuits, relays, solenoids, stepper motors, magnetic print hammers, multiplexed LED and incandescent displays, and heaters[7]. In this case: dc motor, valve, lever, and siren circuit are used.

### IV. The Design Concepts

For more simplification, both fig. 1 and table 2 are clarifying the concepts of design and the flow of the logical control signal sequences in between the user and devices via a communication channel. To fulfill such process, two mobile phones are used to transmit and receive data according to the network requirements.

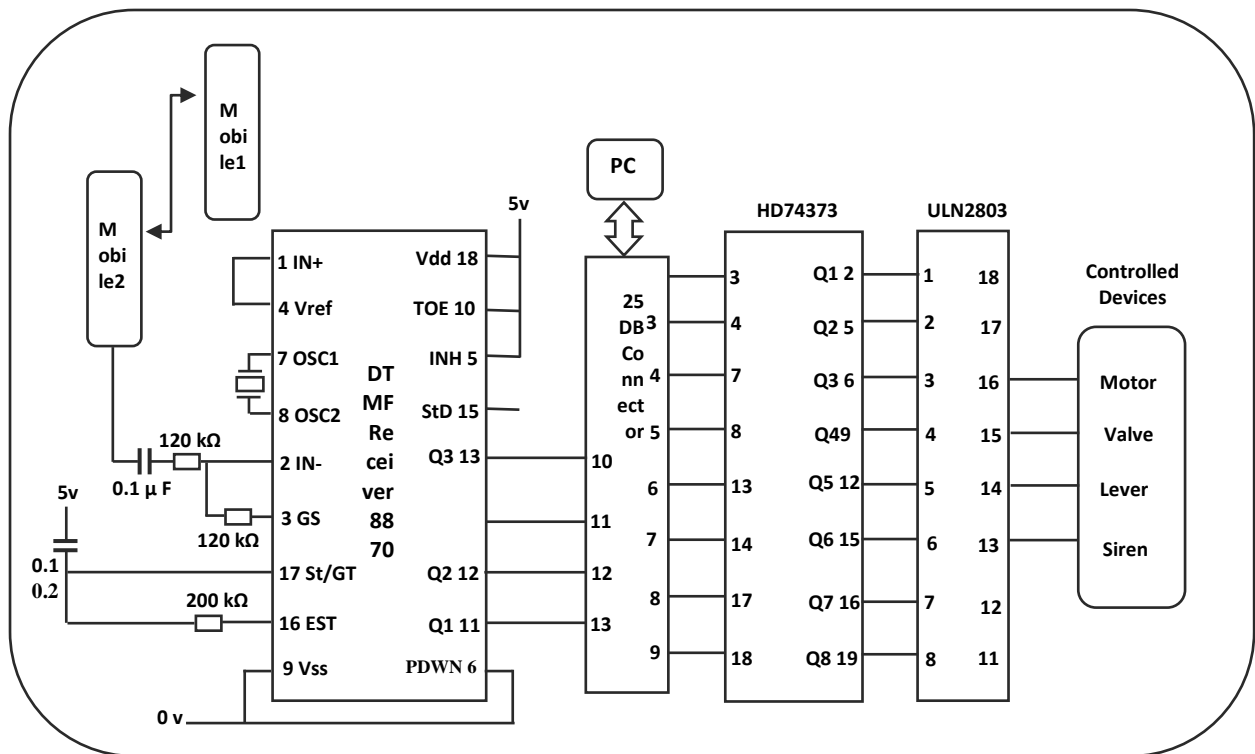


Figure 1 The pins configuration of mobile phone based multi-devices secured control system

**1. The Cellular Mobile Network**

In this circuit, the controlling signal is sent by the cellular mobile phone no.1 to the cellular mobile phone no.2 which is located together with the DTMF controller circuit[12],[2].Through this process, the mobile phone network performed all the security issues such as authentication, confidentiality, anonymity, and integrity[6],[3].The output of the cellular mobile phone no.2 is then directed via a coupling capacitor to the DTMF decoder circuit

Table 2: The pins configurations of the system structure components

Keypad	8870		DB25		74373		2803		Controlled Devices
out	In	out	In	out	In	out	in	out	
0	2	11	13	2	3	2	1	18	Motor
1	3	12	12	3	4	5	2	17	Valve
2	-	13	11	4	7	6	3	16	Lever
3	-	14	10	5	8	9	4	15	Siren
4	-	-	-	6	13	12	5	14	-
5	-	-	-	7	14	15	6	13	-
6	-	-	-	8	17	16	7	12	-
7	-	-	-	9	18	19	8	11	-
8	-	-	-	-	-	-	-	-	-
9	-	-	-	-	-	-	-	-	-

**2. MT8870 DTMF Receiver**

In the first stage of the DTMF receiver, the incoming controlling signal that comes from far distant mobile station no.1 up to the mobile station no.2 represents the input conditions to the integrated MT8870 DTMF receiver through the RC adjustable gain circuit to set the signal according to the application requirements. Such a function is done inside the MT8870 by the buffer circuit which is represented by operational amplifier providing a unity gain and buffer the other input components from incoming into the DTMF receiver circuit. Then, the buffer circuit followed by the band pass filter which is minimize the incoming signal bandwidth.

This filter is succeeded by splitting circuit to feed high and low pass filters to drive a digital detect circuit through high gain comparators which are limiting the signal to prevent detection of unwanted low level signal. The digital detection circuit consist of digital counting technique to determine the frequencies of the incoming signal and to verify that the incoming signal components correspond to standard DTMF frequencies[11]. So, a valid DTMF signal decoded to yield the output combinations as  $Q_1$  – to -  $Q_4$ . [13].

The scenario that the system has to carry out sequentially depends upon the controlling signal that sent from user. The controlling signal is a combination of just decimal numbers:

- The operating software has to first put all the controlled devices in an idle state when starting.
- The Turbo C++ received only the correct password and initialized the system
- Reading the received signal from the user through the mobile phone no.1 as an output of the MT8870 DTMF at the relevant address of the parallel communication port.
- Reacting to the incoming signal as appropriate decision to drive specific device.
- Showing the device states as indicator of control process actions to reflect that the functions are performed in specific and well manner according to the codes.

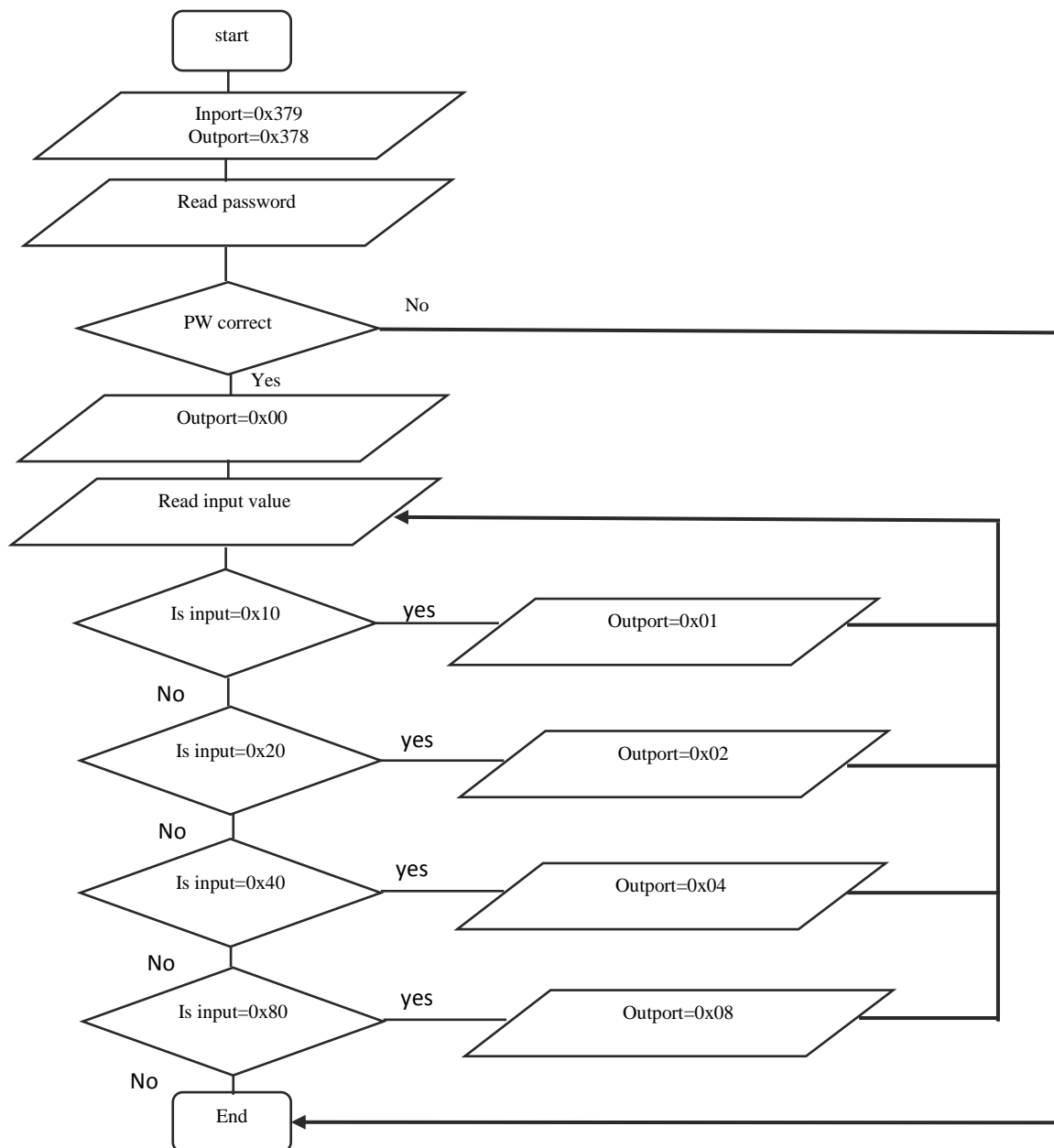


Figure 2the program flow chart

## V. RESULTS AND DISCUSSION

The system is carried out perfectly according to the codes and resulted in good performance as stated before. But, there are several constrains that affect the operation of the system negatively. These constrains are due to the network performance which is affected by other uncontrollable parameters. These constrains are:

- The network diverge mostly due to the environmental conditions.
  - Handoff process as the user moving to high densely populated area when in progress.
- The aforementioned constrains may tend to completely loss, block or drop the controlling signal.

## VI. CONCLUSION

In this paper, the mobile phone based multi-devices secured control system is presented. The control process is carried out securely and easily via both cellular mobile phones and PC. The exploit of technologies due to their rapid deployment and low cost, help in facilitating the controlling way or techniques as well as introducing many different advantages over traditional techniques. So, the transition of controlling signal through both cellular mobile network and PC to the controlled devices serve as developing tool to the security feature and enhance documentation, mentainance, and interfacing more devices to the system. Generally, the integration of technologies in this work is regarded as a flexible platform to the development.

## REFERENCES

- [1] Das, C. K. ;Sanullah M. ; Sarower, H. M. G.; Hassan, and M. M. (2008), Development of a cell phone based remote control system: an effective switching system for controlling home and office appliances, International Journal of Electrical and Computer Sciences IJECS Vol. 9 No. 10
- [2] Johnnes, A. (2006), Investigation issues in mobile network in security, Modern Applied Science, Vol.2 No. 6 (2:6)
- [3] Ja'afar, A. S.; Soufian, Y.; Mohamed, N. (2006), Analysis and enhancement of authentication algorithm in mobilenetworks
- [4] Khiyal, M. S.; Khan A. ; Shehzadi, E. (2008), SMS based wireless home appliance control system for automating appliances and security, Issues in Informing Science and Information Technology, Vol. 6
- [5] MITEL (1995), ISO-CMOS MT8870D/MT8870D-1 Integrated DTMF receiver, Datasheet.
- [6] Praphul C. (2005), Bulletproof wireless security, Elsevier Inc. (144:152)
- [7] Renesas Technology Corp. (2005), HD74LS373 Octal D-Type Transparent latches, Rev.2.11 (1:3)
- [8] Svein Y. W. (2003), Forsics and GSM mobile telephone system, International Journal of Digital Evidence, Spring 2003, Vol.2 Issue 1 (1:4)
- [9] TEXAS Instruments Incorp. (2012), ULN2803A Darlington transistor Array. Datasheet.
- [10] Yuvus, E.; Hassan, H. B.; Serkan, I.; Duygu, K. (2007), Safe and secure PIC based remote control application for intelligent home, IJCSNS International Journal of Computer Science and Network Security, Vol.7 No. 5 (179:181)
- [11] ZarlinkSemiconductor Inc. (2001), Application of the 8870 integrated DTMF receiver, Datasheet.
- [12] Ali, I. G. (2006), Security in wireless cellular networks (1:6), www.cse.wustl.edu.celluular\_security
- [13] Clare Inc. (2001), M-8870 DTMF Receiver, Datasheet.

## Determination Gamma Width and Transition Strength Of Gamma Rays from $^{48}\text{Ti}(n_{th}, 2 \text{ gamma})^{49}\text{Ti}$ Reaction

Nguyen An Son<sup>1</sup>, Pham Dinh Khang<sup>2</sup>, Nguyen Duc Hoa<sup>1</sup>,  
Nguyen Xuan Hai<sup>3</sup>, Dang Lanh<sup>3</sup>

<sup>1</sup>University of Dalat, 01 Phu Dong Thien Vuong, Dalat, Lamdong, Vietnam

<sup>2</sup>Nuclear Training Center, 140 Nguyen Tuan, Hanoi, Vietnam

<sup>3</sup>Nuclear Research Institute, 01 Nguyen Tu Luc, Dalat, Vietnam

### ABSTRACT

The experiment was setup on the 3<sup>rd</sup> horizontal channel of Dalat nuclear reactor. The sample was activated by thermal neutron which is about  $10^6$  neutron/cm<sup>2</sup>/s. The gamma-gamma system is used to collect experimental data. The Summation of Amplitude Coincidence Pulses method (SACP) treats the experimental data. In this paper, the gamma cascades based on  $^{48}\text{Ti}(n_{th}, 2 \text{ gamma})^{49}\text{Ti}$  reaction. Event – event coincidence method got relative intensity, gamma ray energy directly, and the gamma cascades collected directly as well. Since then, the transition probabilities and some intermediate quantum characteristics are splitted and determined. The single particle model is applied to treat the results. The advantage of this method is that it allows determining a pair of the transitions and the intermediate levels directly. The branching ratios of such gamma transitions are used to calculate the partial gamma width, the total gamma width, lifetime of level. Besides, the transition strengths have been calculated for gamma transitions.

**KEY WORDS:** Gamma cascade; Gamma width; Transition strength; Lifetime; Level; Spin and parity

### I. INTRODUCTION

The  $^{49}\text{Ti}$  nucleus, with two protons and one neutron hole outside the doubly magic  $^{48}\text{Ca}$ , constitutes a very good test for shell-model calculations. The studies of gamma decay of  $^{49}\text{Ti}$  have been previously published in many works based on two ways: on accelerator and on reactor. The results on  $^{50}\text{V}(t, \alpha)^{49}\text{Ti}$ ,  $^{50}\text{Ti}(d, t)^{49}\text{Ti}$ ,  $^{48}\text{Ca}(\alpha, 3n)^{49}\text{Ti}$  [6, 10] showed spin and parity of  $^{49}\text{Ti}$  ground state is  $7/2^-$  and compound state is  $1/2^+$ . Those results provided 0÷5 MeV energy arrange. Activation of  $^{48}\text{Ti}$  by neutron is the method which is usually to do on the nuclear reactor. Those previously studies showed gamma rays, levels... more than research on accelerator [4, 7, 8]. The same results in two ways of study are agreed with spin and parity of  $^{49}\text{Ti}$  at compound state and ground state. Almost previous works used a Multi Channel Analysis (MCA) system to get experimental data that could not determine gamma cascade energy, intensity of a pair of gamma cascades which were determined by Ritz algorithms. The lifetime of these levels: 1381 keV (<5ps), 1585 keV (<11ps) and 1762 keV (<14 ps) were determined [2], but high levels were incomplete.

In this experiment, to get experimental data by gamma-gamma coincidence system which treats by SACP method therefore it reduced background effectively.

### II. THEORY

The intensity of gamma cascade is a function which depends on gamma width level:

$$I_{\gamma\gamma} = \sum \frac{\Gamma_{\lambda i} \times \Gamma_{if}}{\Gamma_i \times \Gamma_{\lambda}} \quad (1)$$

where  $\Gamma_{\lambda i}$  and  $\Gamma_{if}$  are the partial widths of the transitions connecting the levels  $\lambda \rightarrow i \rightarrow f$ ;  $\Gamma_i$  and  $\Gamma_{\lambda}$  are the total width levels of the decaying states  $\lambda$  and  $i$ , respectively.

In this experiment, the relative intensity of gamma cascade transfer was calculated:

$$I_i^{\gamma\gamma} = \frac{S_i^{\gamma\gamma}}{\sum_i S_i^{\gamma\gamma}} \quad (2)$$

$S_i^n$  is the calibrated area of  $i^{\text{th}}$  peak in the cascade transfer.

If  $J^\pi$  is spin and parity of the ground state of nucleus, the spin and the parity of the compound nuclear as capturing neutron (s wave neutron capture) are ability  $J^\pi \pm 1/2$ . Because the lifetime of nuclei at excited states is very short, gamma radiations emitted from compound nuclei are usually electric dipole (E1), magnetic dipole (M1), electric quadruple (E2) or a mixture of M1 + E2. Selection rules for the multiple order of radiation are identified by:

$$|J_i - J_f| \leq L \leq J_i + J_f \quad (3)$$

here, L is multiple order,  $J_i$  is the spin of the initial state,  $J_f$  is the spin of the final state.

When the electromagnetic transfer, the parity is conservative:

$$\pi_i \pi_f \pi_\gamma = 1 \quad (4)$$

$\pi_i$  is the parity of initial level,  $\pi_f$  is the parity of final level  $\pi_\gamma$  is the parity of gamma ray.

For electric transfer:

$$\pi_\gamma = (-1)^L \quad (5)$$

For magnetic transfer:

$$\pi_\gamma = (-1)^{L+1} \quad (6)$$

The total gamma width ( $\Gamma_\gamma$ ) of an excited state of a certain mean lifetime ( $\tau_m$ ) is given by:

$$\Gamma_\gamma = \frac{\hbar}{\tau_m} = \frac{\hbar \times \ln 2}{t_{1/2}} \quad (7)$$

where  $\hbar$  is the Dirac constant =  $0.658212 \times 10^{-15}$  eV.s and  $t_{1/2}$  is lifetime of level.

If two or more  $\gamma$ -rays de-excited from the same state, then the partial gamma width of  $i^{\text{th}}$  gamma transition ( $\Gamma_{\gamma i}$ ) is:

$$\Gamma_{\gamma i} = \Gamma_\gamma \times B_{\gamma i} \quad (8)$$

where  $B_{\gamma i}$  is the branching ratio of  $i^{\text{th}}$  gamma ray, and it is obtained from the following equation:

$$B_{\gamma i} = \frac{I_{\gamma \gamma i}}{I_{\text{tot}}} \times 100\% \quad (9)$$

here,  $I_{\gamma \gamma i}$  is the intensity of  $i^{\text{th}}$  gamma transition and  $I_{\text{tot}}$  is the total intensity.

From the total gamma width, we can calculate the transition strengths of E1, M1 and E2.

Components of the gamma rays are defined by the following [5]:

$$\left| \frac{\Gamma(E, M(L))}{\Gamma_{\gamma w u}(E, M(L))} \right|^2 = \frac{\Gamma(E, M(L))}{\Gamma_{\gamma w u}(E, M(L))} \quad (10)$$

where,  $\Gamma(E, M(L))$  is the partial gamma width of electric transfer, magnetic transfer, L is multiple orders. In Weisskopf units can be obtained from the following relations in equations:

$$\Gamma_{\gamma w u}(E1) = 6.7492 \times 10^{-11} A^{2/3} E_\gamma^3 \quad (11)$$

$$\Gamma_{\gamma w u}(E2) = 4.7925 \times 10^{-23} A^{4/3} E_\gamma^5 \quad (12)$$

$$\Gamma_{\gamma w u}(M1) = 2.0734 \times 10^{-11} E_\gamma^3 \quad (13)$$

where, A represents the mass number of the nucleus and  $E_\gamma$  is the energy of the gamma transitions in keV units.

### III. EXPERIMENT AND METHOD

Experimental sample is natural titan. The isotope ratio of the titan samples and thermal neutron capture cross sections are:  $^{46}\text{Ti}$  (8.25%; 0.600 barn),  $^{47}\text{Ti}$  (7.44%; 1.600 barn),  $^{48}\text{Ti}$  (73.72%; 7.900 barn),  $^{49}\text{Ti}$  (5.41%; 1.900 barn) and  $^{50}\text{Ti}$  (5.18%; 0.179 barn), respectively [1]. The neutron beam, sample and detector were set up for maximum efficiency of gamma detection. In this experiment the sample is set at  $45^\circ$  from neutron beam, two detectors are placed opposite ( $180^\circ$ ) with each other. The thermal neutron flux at sample position was about  $10^6$  n/cm<sup>2</sup>/s. Cadmium coefficient is 900 (1 mm in thickness).

The experimental system was a gamma – gamma coincidence spectrometer with the event-event counting method, as shown in Fig. 1. The operating principle was briefly described as follows: The signals from two detectors were amplified and shaped by the amplifiers (Amp. 7072A), that convert the output signals from the amplifiers to digital signals when the conditions of 7811R interfacing part are satisfied. Timing signals from the two detectors were amplified and shaped by Timing Filter amplifiers (TFA 474). The output signals from

TFA 474 went through the Constant Fraction Discriminators (CFD 584). There were two output signals from the CFDs, one was directly sent to Start input and the other was delayed before coming to Stop input of TAC 566. The linear output signal of TAC went to the input of ADC 8713, and the valid convert used for control of three coincidence gates of ADCs. ADC 8713 was used for the timing channel while two other ADCs 7072 were used for the energy channels.

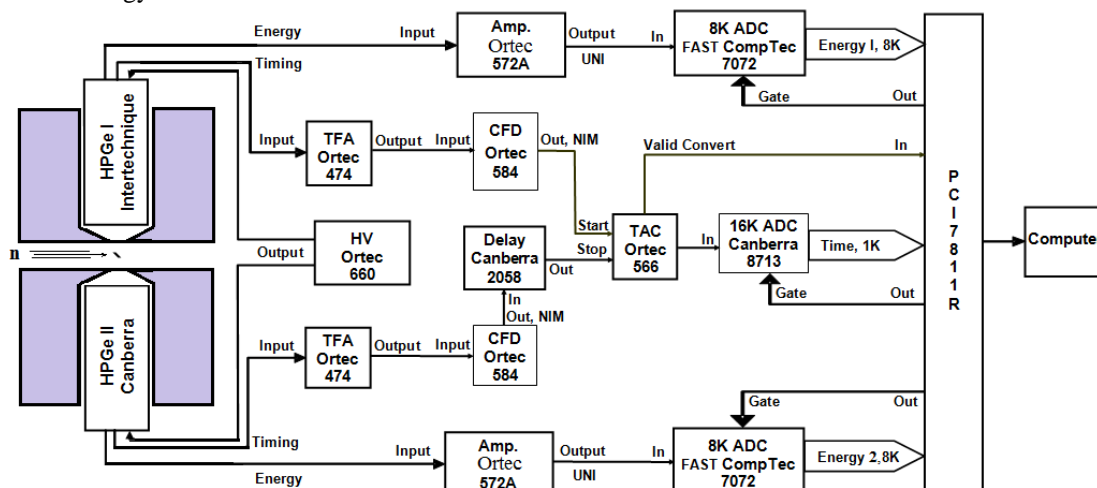


Fig. 1. The experimental system for gamma-gamma coincidence measurement [9]

#### IV. RESULTS AND DISCUSSION

##### Energy, relative intensity, spin, the intermediate level of two-step cascade transfer

The time for titan sample measurement was about 300 hours. The numbers of event – event coincidence are about  $30 \times 10^6$  events, the statistic counts of sum peak at  $B_n$  ( $B_n$ : neutron binding energy) are about 12000. Table 1 showed information of sum peaks, Fig. 2 is a part of sum spectrum of  $^{49}\text{Ti}$ .

Table 1. The information of sum peaks

No	Sum peak energy (keV)	Final level (keV)	Spin and parity of final level
1	8142.50	0	7/2
2	6761.08	1381.42	3/2
3	6419.04	1723.46	3/2
4	3260.38	0	7/2
5	3175.64	0	7/2

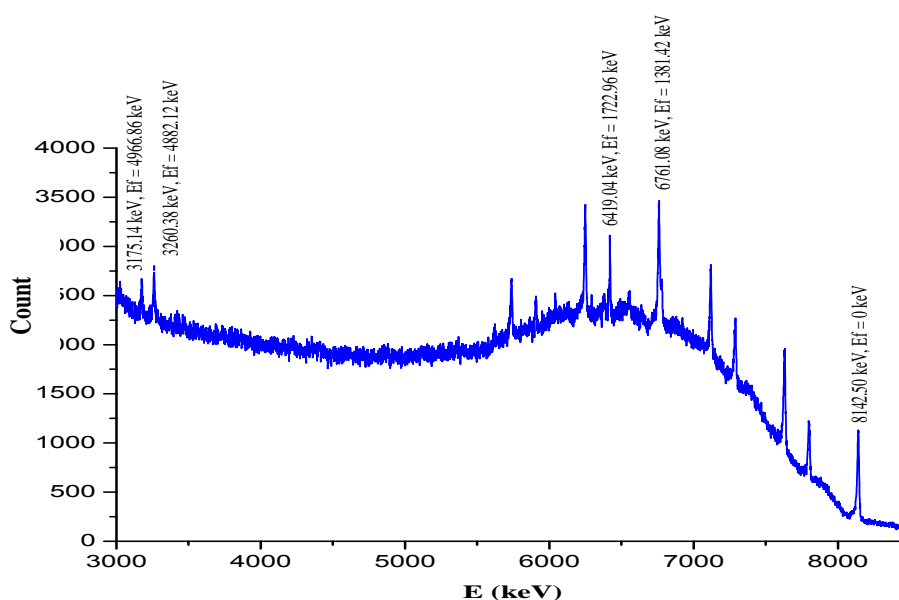


Fig. 2. A part of sum spectrum

**Table 2.** Some experimental data obtained from the  $^{48}\text{Ti}(n, 2\gamma)^{49}\text{Ti}$  reaction

$E_{\gamma 1}(\text{keV})$	$E_L(\text{keV})$	$E_{\gamma 2}(\text{keV})$	$I_{\gamma}(\Delta I_{\gamma}) (\%)$
<b>E1+E2 = 8142.50 keV, <math>E_f = 0</math> keV</b>			
6761.08(101)	1381.42	1381.42(070)	46.300(269)
6556.06(079)	1586.44	1585.44(083)	5.919(312)
<b>E1+E2 = 6761.08 keV, <math>E_f = 1381.42</math> keV</b>			
6419.04(078)	1723.46	341.29(050)	4.145(437)
4966.86(098)	3175.64	1793.47(089)	2.703(213)
4713.83(122)	3428.67	2046.50(092)	0.494(104)
4353.78(133)	3788.72	2405.54(105)	0.468(231)
3920.73(164)	4221.77	2839.60(121)	1.561(311)
3026.62(135)	5115.88	3733.71(156)	2.626(376)
<b>E1+E2 = 6419.04 keV, <math>E_f = 1723.46</math> keV</b>			
3920.73(164)	4221.77	2498.55(113)	0.999(102)
3475.68(164)	4666.82	2943.61(132)	2.175(78)
3026.62(135)	5115.88	3389.66(154)	1.045(94)
<b>E1+E2 = 3260.38 keV, <math>E_f = 0</math> keV</b>			
1498.43(077)	1761.95	1761.46(071)	10.203(167)
1674.45(054)	1585.93	1585.44(083)	2.292(134)
<b>E1 + E2 = 3175.64 keV, <math>E_f = 0</math> keV</b>			
1793.47(089)	1381.67	1381.42(070)	7.324(209)

Note: E1 (keV) is the energy of primary gamma rays; E2 (keV) is the energy of the secondary gamma rays;  $E_L$  (keV) is the energy of the intermediate level;  $I_{\gamma}$  (%) and  $\Delta I_{\gamma}$  (%) is intensity and intensity error of cascade gamma transfer.

**Gamma width and transition strength**

From the experimental data of gamma intensity and electromagnetic transfer selection, the lifetime level, width level and gamma transition strength were calculated for some levels of  $^{49}\text{Ti}$  nucleus at compound state as capturing neutron. The result showed on the table 3.

**Table 3.** The lifetime, width level, spin and transition strength of some level

Level (keV)	$t_{1/2}$ (s)	$\Gamma_{\gamma i}$ (eV)	$E_{\gamma}$ (keV)	$J_i^{\pi} \rightarrow J_f^{\pi}$	$J_i^{\pi} \rightarrow J_f^{\pi}$ [3]	Transition Strength		
						$ M(E(1)) ^2$	$ M(M(1)) ^2$	$ M(E(2)) ^2$
8142.50	4.89599E-16	1.34	6761.08	$1/2^+ \rightarrow 3/2^-$	$1/2^+ \rightarrow 3/2^-$	1.48	---	---
			6556.06	$1/2^+ \rightarrow 3/2^-$	$1/2^+ \rightarrow 3/2^-$	11.62	---	---
			6419.04	$1/2^+ \rightarrow 1/2^-$	$1/2^+ \rightarrow 1/2^-$	16.39	---	---
			4966.86	$1/2^+ \rightarrow 1/2^-$	$1/2^+ \rightarrow 1/2^-$	24.99	---	---
			3920.73	$1/2^+ \rightarrow 1/2^-$	$1/2^+ \rightarrow 1/2^-$	27.02	---	---
			3475.68	$1/2^+ \rightarrow 1/2^-$	$1/2^+ \rightarrow 1/2^-$	1.48	---	---
			3026.62	$1/2^+ \rightarrow 1/2^-$	$1/2^+ \rightarrow 1/2^-$	0.06	---	---
			4713.83	$1/2^+ \rightarrow 1/2^+$	$1/2^+ \rightarrow 3/2^-$	---	14.92	---
			4353.78	$1/2^+ \rightarrow 1/2^+$	$1/2^+ \rightarrow 3/2^-$	---	20.40	---

5115.38	6.67683E-16	0.99	3733.71	$1/2^- \rightarrow 3/2^-$	$1/2^- \rightarrow 3/2^-$	---	1.40	---
			3389.66	$1/2^- \rightarrow 3/2^-$	$1/2^- \rightarrow 3/2^-$	---	3.52	---
4221.27	1.64314E-15	1.60	2839.60	$1/2^- \rightarrow 3/2^-$	$1/2^- \rightarrow 3/2^-$	---	1.64	---
			2498.55	$1/2^- \rightarrow 3/2^-$	$1/2^- \rightarrow 3/2^-$	---	2.56	---
3260.08	8.65394E-15	0.08	1674.45	$1/2^- \rightarrow 3/2^-$	$1/2^- \rightarrow 3/2^-$	---	5.51	---
			1498.43	$1/2^- \rightarrow 3/2^-$	$1/2^- \rightarrow 5/2^-$	---	1.27	---

In this result, spin and parity of some levels are different from LANL [3]. Especially, two gamma rays: 4713.83 keV and 4353.78 keV emitted from  $B_n$  to intermediate level, they are not electronic dipole, and they must be magnetic dipole. The results used to calculate the single particle model of nuclei which compares to experimental data. Thus, we conclude that  $^{49}\text{Ti}$  nucleus can be explained by the single particle model. A comparison of ratio between theoretical result with experimental result is about 12 times (for electronic dipole), while the ratio between theoretical result with experimental result is about 1.3 times (for magnetic dipole).

## V. CONCLUSIONS

By the empirical study of the cascade transfers of  $^{49}\text{Ti}$  nucleus from  $^{48}\text{Ti}(n, 2\gamma)^{49}\text{Ti}$  reaction, we measured 14 pairs of cascade transfer and arranged into nuclear scheme; in addition, the relative intensities of the transfers were presented. Using the rules of calculation of spin and parity, the possible spin and parity were calculated for experimental levels. The spins, the parities were updated for unsuitable levels. The results also showed lifetime level, width level and gamma transition strength of some levels.

## REFERENCES

- [1] Chart of the nuclides. 7th edition, 2006.
- [2] D. C. S. WHITE, W. J. McDONALD, D. A. HUTCHEON and G. C. NEILSON, Pulsed beam lifetime measurements in  $^{64}\text{Cu}$ ,  $^{59}\text{Ni}$ ,  $^{65}\text{Zn}$ ,  $^{45,47,49}\text{Ti}$  and  $^{47,49,50,51}\text{V}$ , Nuclear Physics A260 (1976) 189-212.
- [3] <http://www-nds.iaea.org/pgaa/PGAAdatabase/LANL/isotopic/22Ti26>
- [4] J.F.A.G. P.M. Endt, Investigation of the  $^{48}\text{Ti}(n,\gamma)^{49}\text{Ti}$  reaction, Nuclear Physics A407 (1983) 60-76.
- [5] J. M. Blatt and V. F. Weisskopf, Theoretical Nuclear Physics. John Wiley and Sons, Newyork (1952).
- [6] M. Berhar, A. Filevich. G. Garcia Bermudez, Ma. . J. Mariscotti and E. Ventura, High spin states in  $^{49}\text{Ti}$  and the empirical model, Nuclear Physics A366 (1981) 61-67.
- [7] P. Carlos, J. Matuszek, A. Audias, B. P. Maier, H. Nifenecker, G. Perrin et R. Sammama, Capture radiative de neutrons thermiques dans  $^{48}\text{Ti}$ , Nuclear Physics A107 (1968) 436-448.
- [8] P. Fettweis and M. Saidane, The level scheme of  $^{48}\text{Ti}$  and  $^{49}\text{Ti}$  as studied by the neutron capture  $\gamma$  ray spectra, Nuclear Physics A139 (1969) 113 - 131.
- [9] Pham Dinh Khang, V.H. Tan, N.X. Hai, N.N. Dien, Gamma-gamma coincidence spectrometer setup for neutron activation analysis and nuclear structure studies. Nucl. Instr. and Meth. (2011) A634, 47-51.
- [10] S. Asgaard Andersen, Ole Hansen and L. Vistisen, A spectroscopic study of  $^{49}\text{Ti}$ , Nuclear Physics A125 (1969) 65-79.

# Offline Signature Recognition Using Maximally Stable Extremely Regions (Mser)

Mohammad B. Abdulkareem<sup>1</sup>, Santosh Gaikwad<sup>2</sup>, Bharti Gawali<sup>\*</sup>

<sup>1,2</sup> Research Fellow, \*Professor

Department of computer science and information Technology,  
Dr. Babasaheb Ambedkar Marathwada University, Aurangabad (M.S),  
Aurangabad, Maharashtra, India.

## ABSTRACT:

This paper describes an approach for signature is an offline environment based on Maximally Stable Extremely Regions (MSER) features. MSER features are the parts of the image where local binarization is stable over a large range of thresholds. We discuss a system designed using geometric and MSER based feature which provides efficient recognition for offline signature.

**KEYWORDS:** Signatures, Centroid, FAR, FRR, MSER, TAR, TRR.

## I. INTRODUCTION

Biometrics refers to methods for uniquely recognize humans, based one or more intrinsic physical or behavioral traits. Handwritten Signature is an example of a behavioral feature and the term which has come to general acceptance for this class of biometrics is 'behavior metrics'. Signatures stand as the most accepted form of personal identification for bank transactions, credit card and most of the other routine billing systems [1]. Signature has been a distinguishing feature for person identification through ages. Even today an increasing number of transactions, especially financial, are being authorized via signature, hence methods of automatic signature verification must be developed if authenticity is to be verified on a regular basis. Approaches to signature verification fall into two categories according to the acquisition of the data: On-line and Off-line. On-line data records the motion of the stylus while the signature is produced, and includes location, and possibly velocity, acceleration and pen pressure, as functions of time [2].

An off-line or a Static Signature Verification (SSV) System takes in the scanned image of the signatures and extracts certain features for initial steps of processing before it is given as input to the verification system [3]. Online systems use information captured during acquisition. These dynamic characteristics are specific to each individual and sufficiently stable. Off-line data is a 2-D image of the signature. Processing Off-line is complex due to the absence of stable dynamic characteristics. Difficulty also lies in the fact that it is hard to segment signature strokes due to highly stylish and unconventional writing styles. The non-repetitive nature of variation of the signatures, because of age, illness, geographic location and perhaps to some extent the emotional state of the person, accentuates the problem. A robust system has to be designed which should not only be able to consider these factors but also detect various types of forgeries [4, 5]. The system should neither be too sensitive nor too coarse. It should have an acceptable trade-off between a low False Acceptance Rate (FAR) and a low False Rejection Rate (FRR). The rest of the paper is organized as preprocessing is described in section 2. Offline signature database is described in section 3. Section 4 is explains the extraction of parameters. Section 5 deals with implementation details and simulation of results followed by conclusion.

## II. PREPROCESSING

Preprocessing involves removing noise, smoothing, skeletonization, space standardization and normalization.

### 2.1 Noise Removal

The goal of noise removal is to eliminate the noise. The Imperfection in the scanner intensity of light, scratches on the camera scanner lens introduces noises in the scanned signature images. For this noise reduction filtering function is used to remove the noises in the image. The Gaussian filter is used for the noise removal. Since Gaussian function is symmetric, smoothing is performed equally in all directions, and the edges in an image will not be biased in particular direction. The signature before and after removal of noise are as shown in the Figure 1 (A) and (B) respectively.

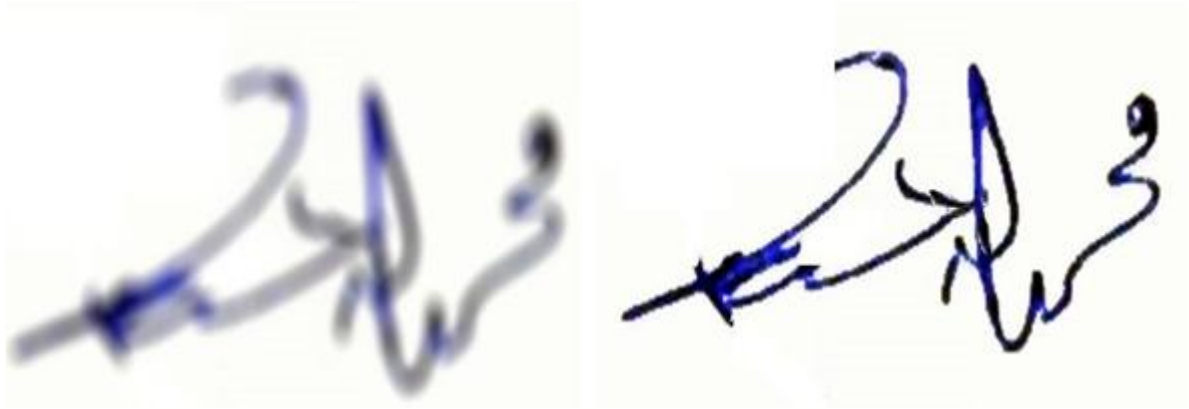


Figure 1. (A) Noisy signature Image (B) Preprocessed Image

## 2.2 Smoothing

The edge feature demonstrates the border line of the image, in this research the figure 2 (A) described the edge feature of the image which demonstrates the border point of the image. For the preprocessing we concentrated toward special domain image enhancement such as histogram, on the basis of this histogram behavior we understand the nature of signature as noisy or not. The figure 2(B) describes the histogram feature of signature image.

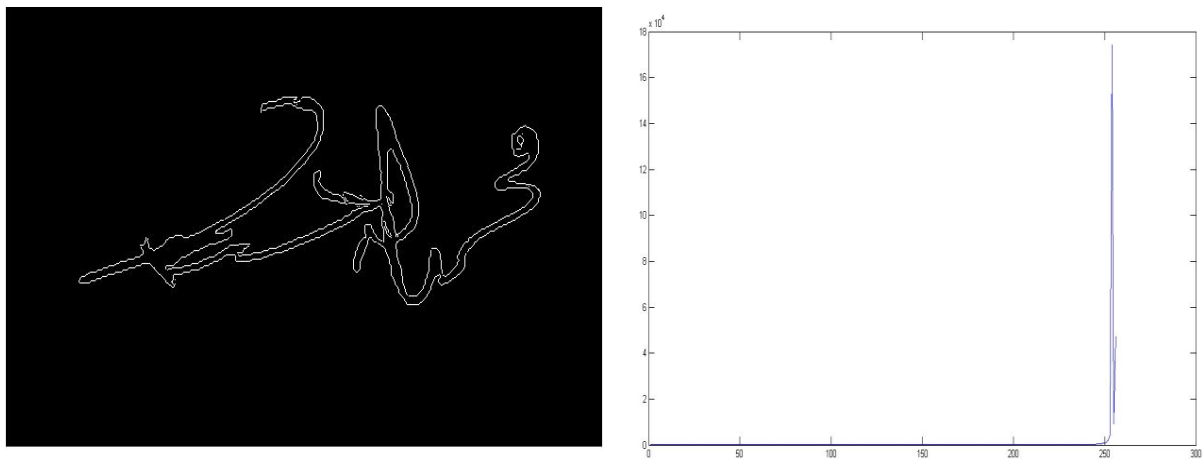


Figure 2. (A) Edge feature of the signature (B) Histogram of the signature

## 2.3 Skeletonization

A simplified version of the skeletonization technique described by Lam and Suen (1991) is used. The simplified algorithm used here consists of following three steps:

Step 1: Mark all the points of the signature that are candidate for removing black pixel.

Step 2: Examine one by one all of them, following the contour line of the signature image, and remove these as their removal will not cause a break in the resulting pattern.

Step 3: If at least one point was deleted go again to step 1 and repeat the process once more.

## 2.4 Standardization and normalization.

It is supposed that the features of the process of signing originate from the intrinsic properties of human neuromuscular system which produces the aforementioned rapid movements. Knowing that this system is constituted by a very large number of neurons and muscle, fibers is possible to declare based on the central limit theorem that a rapid and habitual movement velocity profile tends toward a delta-log normal equation [7]. This statement explains stability of the characteristics of the signature. Thus, the signature can be treated as an output of a system obscured in a certain time interval necessary to make the signature. This system models the person making the signature [6]. Normally any person while putting his signature uses an arbitrary baseline. The positional information of the signature is normalized by calculating an angle  $\theta$  about the centroid  $(x, y)$  such that rotating the signature by  $\theta$  brings it back to a uniform baseline. The size normalization in the offline signature recognition is very important because it create a common platform for image comparison. In this paper the database as scanned image files in jpg format with standard size of  $200 \times 100$  pixels.

The choice of features depends on the parameters by which the classification needs to be done. The relevant features used by the classification are listed below

- i) Centroid: This feature gives the row and column of the centre of mass in the logical matrix.
- ii) Length and Width: Length and width of the signature in the  $200 \times 100$  pixels image box. This involves finding the best fit rectangular box for the signature and calculating the actual length and width of this rectangle in pixels. The size normalization using the best fit image is described in figure 3.

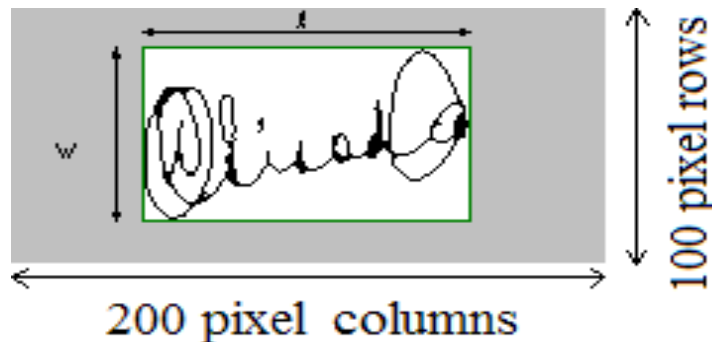


Figure 3. The best fit image box.

### III. DATABASE DESIGN

This research contributed towards the creation of offline signature database. The signatures are collected using either black or blue ink, on a white A4 sheet of a paper, with forty signatures per page from thirty four volunteer. Using MF4350D scanner the scanner the four signatures are digitized, with 300-dpi resolution in 256 grey levels. The volunteer selected are from students of Department of Computer science and Information Technology, Dr. Babasaheb Ambedkar Marathwada University. The 16 subject are from 20-25 age group and 18 subjects are in the 25-30 age group. The total size of dataset is 1360. The signatures are stored in the offline database is scanned image files in jpg format with standard size of  $200 \times 100$  pixels. The basic preprocessing operations include the spatial alignment of the image, followed by binarization, which converts the image files into logical matrices and finally a skeletonization process that extracts the thin path or contour of the signature.

### IV. FEATURE EXTRACTION

The choice of a powerful set of feature is crucial in signature recognition systems. The features used must be suitable for the application and for the applied classifier. In this system, maximally Stable Extremely Region (MSER) features are used such as grid features and global features. The global features provide information about specific cases concerning the structure of the signature grid feature. This method of extracting a comprehensive number of corresponding image elements contributes to the wide-baseline matching, and it has led to better stereo matching and object recognition algorithms. The original algorithm is proposed by Mates [9] is in the number of pixels. It proceeds by first sorting the pixels by intensity. This would take time, using BINSORT. After sorting, pixels are marked in the image, and the list of growing and merging connected components and their areas is maintained using the union-find algorithm. This would take time. In practice these steps are very fast. During this process, the area of each connected component as a function of intensity is stored producing a data structure. A merge of two components is viewed as termination of existence of the smaller component and an insertion of all pixels of the smaller component into the larger one. In the extremely regions, the 'maximally stable' ones are those corresponding to thresholds where the relative area change as a function of relative change of threshold is at a local minimum, i.e. the MSER are the parts of the image where local binarization is stable over a large range of thresholds[8][10].

The component tree is the set of all connected components of the thresholds of the image, ordered by inclusion. Efficient (quasi-linear whatever the range of the weights) algorithms for computing it do exist [11]. Thus this structure offers an easy way for implementing MSER [12]. The steps for MSER feature extraction are as follows [13].

- Sweep threshold of intensity from black to white, performing a simple luminance Thresholding of the image
- Extraction of the connected components ("External Regions")
- Find a threshold when an extremely region is "Maximally Stable", i.e. local minimum of the relative growth of its square.

- Approximation of a region with an ellipse.
- Creation of feature vector of region description.

The border (corner) point of the signature play an important role for the identification of signature match area, the figure 4 (A) described the corner point detection of the signature. The Extracted MSER feature of signature is described in figure 4 (B).

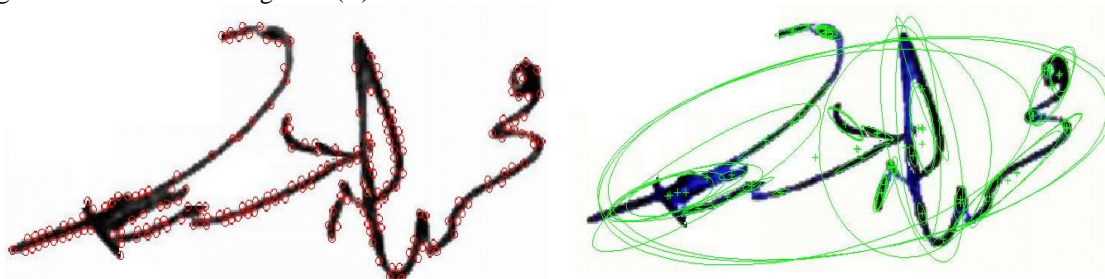


Figure 4. (A) The corner point detection of signature recognition (B) Extracted feature of signature using MSER

### V. EXPERIMENTAL RESULT

The Centroid function is calculated in preprocessing because of fully understanding the descriptor which is based on centroid distance function. The position of the centroid, the center of gravity, is fixed in relation to the shape. The shape in this particular context is a binary image. The centroid can be calculated by taking the average of all the points that are defined inside a shape. Under the assumption that our shape is simply connected, we can compute the centroid simply by using only the boundary points. The centroid is having unique values which are arises as Mean X and Mean Y. The length and width are also responsible for morphological feature in the matching of the signature. The detail Numerical results of Centroid X, Centroid Y, Height and width are discussed in table 1.

Table 1. The centroid of the test sample

Sr. No	Sample	Centroid X	Centroid Y	Height	Width
1	Signature 1	111	100	199	231
2	Signature 2	282.506	124.997	249	564
3	Signature 3	166.5	102.5	204	332
4	Signature 4	62.5	42.5	84	124
5	Signature 5	40	33	65	79
6	Signature 6	53.5	34.5	68	106
7	Signature 7	49.5	32.5	64	89
8	Signature 8	168	81.5	162	335
9	Signature 9	121	100	199	241
10	Signature 10	219	128.5	256	437

We are extracted the feature using MSER technique. The graphical representation of Extracted feature of signature using MSER is presented in figure 5.

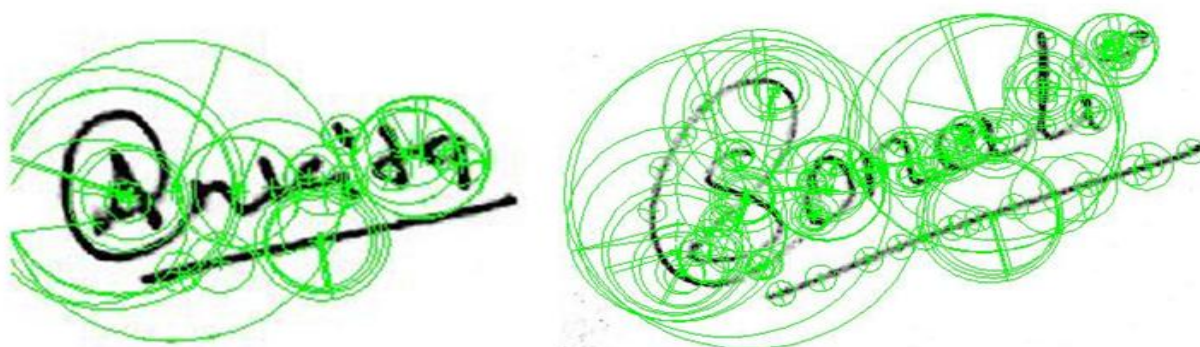


Figure 5. Graphical representation of extracted feature using MSER

The MSER feature is the combination of the centroid, Axes location, orientation as well as pixel list point, so detail MSER feature set are described in table 2.

Table 2. The Extracted MSER Feature of signature

Feature	Centroid		Axes		Orientation	Pixel point	
	Min	Max	Min	Max		Min	Max
1	123.41	545.61	5.7696	8.7965	-1.2460	120	548
2	175.15	416.37	416.56	79.21	-1.2054	134	429
3	173.94	416.37	22.67	79.21	-1.3972	132	431
4	162.17	232.28	30.84	90.05	0.2338	101	256
5	159.62	232.97	30.98	118.71	0.2535	81	258
6	214.41	224.30	6.5997	26.77	0.2153	210	237
7	190.94	243.29	3.7177	31.4282	0.1891	178	246
8	224.02	244.08	6.9389	18.4363	0.2714	221	253
9	219.79	233.36	7.1262	99.3435	0.3355	176	256
10	169.80	229.51	29.9482	147.67	0.2892	80	259

Figure 6 [A] is represents the graphical match point of two different signatures on the basis of MSER feature. The graphical representation of match point of two different signature is describes in figure 6 [B].

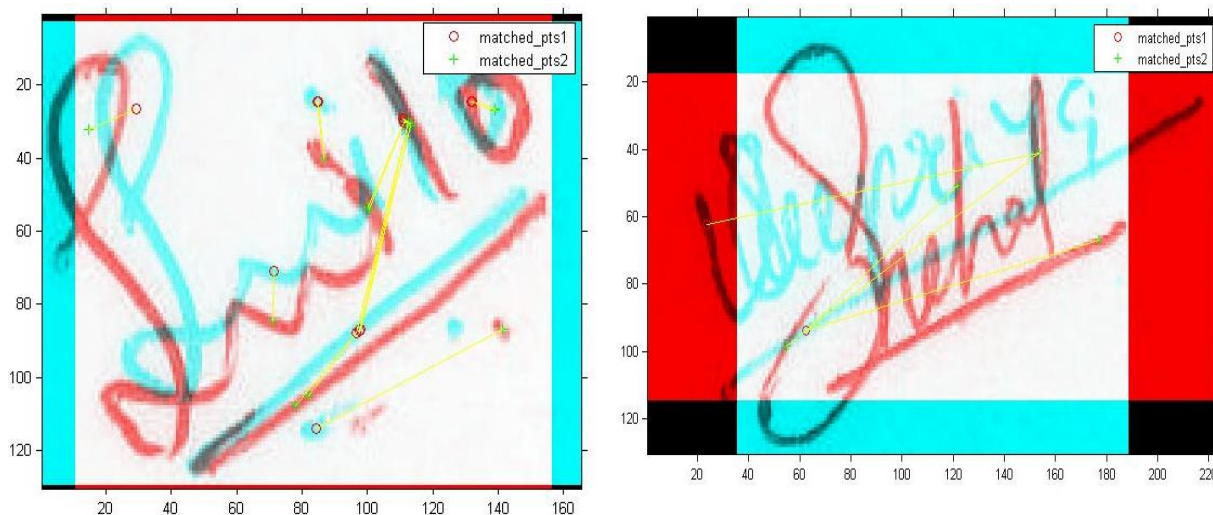


Figure 6. The graphical representation of matching of two [A] same signature [B] Different signatures

The match point such as location, scale and orientation of single signature is described in table 3.

Table 3. The Match Feature of signature

Match point	Location		Scale	Orientation
	Min	Max		
1	190.94	243.29	1.600	1.7280
2	169.80	229.51	8.2667	1.8837
3	1.8540	258.73	2.1333	2.0377
4	163.77	292.35	1.6000	2.2402
5	163.77	292.35	1.6000	2.2402
6	153.66	303.32	1.8867	2.3237
7	153.66	303.32	1.8867	2.3237
8	292.52	274.05	1.600	1.7948
9	200.01	355.60	2	1.9420
10	200.01	355.60	2	1.9420

Table 4. Template of signature for Training the system

Sr. No	Sample	Mean	Std
1	Subject 1	246.8304	23.7681
2	Subject 2	240.4696	34.3885
3	Subject 3	238.6819	22.1952
4	Subject 4	246.7398	19.153
5	Subject 5	249.4727	14.059
6	Subject 6	250.3945	18.7765
7	Subject 7	243.2835	16.9837
8	Subject 8	241.8306	25.5672
9	Subject 9	243.9682	22.0494
10	Subject 10	239.3624	27.3068

#### 4.1 Performance parameters

Performance Analysis of the system includes an evaluation of all possible errors – False Acceptance and False Rejection give a fairly good idea of the efficiency for verification. The True Acceptance Rate (TAR) and the True Rejection Rate (TRR) are the correct-classification rates.

##### a) False Acceptance Rate(FAR)

The false acceptance rate, or FAR, is the measure of the probability likelihood that the system will incorrectly accept an access attempt by an unauthorized user. A system's FAR typically is stated as the ratio of the number of false acceptances divided by the number of identification attempts.

##### b) False Rejection Rate (FRR)

The false rejection rate (FRR), is the measure of the likelihood that the system will incorrectly reject an access attempt by an authorized user. A system's FRR typically is stated as the ratio of the number of false rejections divided by the number of identification attempts.

##### c) True Acceptance Rate (TAR)

True Acceptance Rate (TAR) measures representation of the degree that the system is able to correctly match the information from the same person. Researcher of the current era is attempting to maximize this measure.

##### d) True Rejection Rate (TRR)

True Rejection Rate (TRR) represents the frequency of cases when information from one person is correctly not matched to any records in a database because, in fact, that person is not in the database. Researcher is attempting to maximize this measure.

The detail of False Acceptance rate and false rejection rate with appropriate matching are described in table 5. The False Acceptance Rate and False rejection Rate counts for different individuals (40 samples each) are presented in Table 5.

Total accuracy is calculated by following formula:

$$\text{Accuracy} = 100 - (\text{FAR} + \text{FRR}) / 2$$

The system result is compare to available statistics performance in the literature, in that the author got the highest accuracy as when FAR is 5.24 and FRR is 4.0 . The results are slightly improves as compare to other results. The system performance is the compare with the other system available in literature for offline signature recognition. The proposed research attempted best accuracy as compared to reported result in literature [14, 15, 16, 17, 18, and 19].

Table 5. False acceptance rate and false rejection rate for the system

Test signature	No. of toke passed	FRR (%)	FAR (%)	Accuracy
Subject 1	40	5	7.5	87.5
Subject 2	40	7.5	0	80
Subject 3	40	2.5	10	87.5
Subject 4	40	5	2.5	90
Subject 5	40	5	7.5	87.5
Subject 6	40	2.5	7.5	90
Subject 7	40	7.5	10	82.5
Subject 8	40	2.5	2.5	95
Subject 9	40	2.5	10	92.5
Subject 10	40	0	5	95
Average	40	4	5.25	95.374

## VI. CONCLUSION

Signature is a behavioral biometric used to authenticate a person in day to day life. The paper gives in depth review of offline signature recognition systems. The performance metrics of typical systems are compared along with their feature extraction mechanisms. We have discussed the offline signature recognition on the basis of maximally stable extremely regions (MSER) feature extraction. The MSER is the most robust and dynamic feature extraction technique in the computer vision. The system is has reported accuracy of 95.371% where FAR is 5.25 % and FRR are 4 %, which is higher than individual performance metrics.

## REFERENCES

- [1] Rasha Abbas, Department of Computer Science, RMIT, Master's thesis, "A prototype System for offline signature verification using multilayered feed forward neural networks", 1996
- [2] Plamondon.R., Brault J.J., "A Complexity Measure of Handwritten curves: Modeling of Dynamic Signature Forgery", IEEE Trans. on Systems, Man and Cybernetics, Vol. 23, No.2, 1993, pp. 400-413.
- [3] Stephane Armand, Michael Blumenstein and Vallipuram Muthukkumarasamy, "Off-line Signature Verification based on the Modified Direction Feature", 2006, International Joint Conference on Neural Networks, pages 684-691.
- [4] Ostu N., "A Threshold Selection Method from Gray Level Histogram", IEEE Trans. on Systems, Man and Cybernetics, SMC-8, 1978, pp. 62-66.
- [5] Gonzalez R.C., Woods E., "Digital Image Processing", Addison-Wesley, 1993.
- [6] Luan Ling Lee, "Neural Approaches for Human Signature Verification", Proceedings of the Third International Conference on Document Analysis and Recognition, 1995
- [7] Hong Pan and Liang-Zheng Xia, "Efficient Object Recognition Using Boundary Representation and Wavelet Neural Network", 2001 4th International Conference On ASIC.
- [8] J. Matas, O. Chum, M. Urban and T. Pajdla. "Robust wide baseline stereo from maximally stable extremely regions." Proc. of British Machine Vision Conference, pages 384-396, 2002.
- [9] Salembier, Philippe; A. Oliver as and L. Garrison (1998), "Anti-extensive Connected Operators for Image and Sequence Processing". IEEE Transactions on Image Processing 7 (4): 555-570.
- [10] K. Mikolajczyk, T. Tuytelaars, C. Schmidt, A. Fisherman, T. Kadir and L. Van Gool, "A Comparison of Affine Region Detectors"; International Journal of Computer Vision, Volume 65, Numbers 1-2 / November, 2005, pp 43-72
- [11] L. Najman and M. Couprie, "Building the component tree in quasi-linear time", IEEE Transaction on Image Processing, Volume 15, Numbers 11 , 2006, pp 3531-3539
- [12] Denser, M. and Bishop, H., " Efficient Maximally Stable Extremely Region (MSER) Tracking", CVPR, 2006.
- [13] MSER Feature [online]. [http://en.wikipedia.org/wiki/Maximally\\_stable\\_extremal\\_regions#cite\\_note-matas-1](http://en.wikipedia.org/wiki/Maximally_stable_extremal_regions#cite_note-matas-1) viewed 2/9/2013
- [14] V A Bharadi, H B Kekre "Off-Line Signature Recognition Systems", ©2010 International Journal of Computer Applications (0975 - 8887) Volume 1 – No. 27.
- [15] S. Lee and J. C. Pan, "Off-line tracing and representation of Signatures," IEEE Trans. Syst., Man and Cyber. vol. 22, no. 4, pp. 755-771, July/August 1992.
- [16] S. Chen and S. Srihari, "Use of Exterior Contours and Shape Features in Off-line Signature Verification", Proceedings of the 2005 Eight International Conference on Document Analysis and Recognition (ICDAR'05), 1520-5263/05
- [17] H. Batsakis, N. Papadakos, "A new signature verification technique based on a two-stage neural network classifier", Engineering Applications of Artificial Intelligence 14 (2001) 95±103, 0952-1976/01
- [18] M. K camera, S. Shorthair, "Offline Signature Verification and Identification Using Distance Statistics", International Journal of Pattern Recognition and Artificial Intelligence Vol. 18, No. 7 (2004) 1339-1360, World Scientific Publishing Company.
- [19] Y. Xuhua, F. Takashi, K. Obata, Y. Uchikawa, "Constructing a High Performance Signature Verification System Using a GA Method", IEEE Conf. ANNES, 20-23 Nov. 1995, PP: 170 - 173, 10.1109/ANNES.1995.499465

# The Effect of Water Solubles on the Hygroscopicity of Urban Aerosols

B. I. Tijjani

Department of Physics, Bayero University, Kano. NIGERIA.

## ABSTRACT

*In this paper, the author extracted some microphysical and optical properties of urban aerosols from OPAC by varying the concentrations of water soluble at the spectral range of 0.25 $\mu$ m to 2.5 $\mu$ m and eight relative humidities (RHs) (0, 50, 70, 80, 90, 95, 98, and 99%). The microphysical properties extracted were diameters, volume mix ratio, number mix ratio, mass mix ratio and refractive indices while the optical properties are optical depth and asymmetric parameters all as a function of RHs. Using the microphysical properties, hygroscopic growth factors of the mixtures and their effective refractive indices were determined while using optical depth we determined its relation with RHs, the enhancement parameters and Angstrom parameters. The hygroscopic growths and enhancement parameters were then parameterized using some models to determine their relationship with RHs. The data fitted the models very well. The angstrom coefficients show that the mixtures have bi-modal type of distribution with the dominance of fine mode particles and the mode sizes increase with the increase in water soluble concentrations and RH. The relation of optical depth with RH shows improvement with the increase in water soluble but decreases with the increase in wavelengths. The asymmetric parameters show that hygroscopic growth enhances forward scattering at smaller wavelengths.*

**KEYWORDS:** *microphysical properties, optical properties, hygroscopic growth, enhancement parameters, Angstrom coefficients, spectral range, water soluble.*

## I. INTRODUCTION

The ambient relative humidity changes the phase and microphysical and optical properties of hygroscopic atmospheric aerosols such as sulfates, nitrates and chlorides. These aerosols contribute the largest to the mass budget of fine atmospheric particles on a global basis [1-3]. These inorganic salt aerosols are hygroscopic by nature, thus their size, phase and subsequently the optical properties would be strongly influenced by their concentration and the ambient relative humidity (RH). As the ambient relative humidity (RH) changes, hygroscopic atmospheric aerosols undergo phase transformation, droplet growth, and evaporation. Phase transformation from a solid particle to a saline droplet usually occurs spontaneously when the RH reaches a level called the deliquescence humidity. Its value is specific to the chemical composition of the aerosol particle [4,5]. Since aerosols are far from being a single component, the question is how changes in relative humidity and changes in their concentrations influence the properties of natural aerosol mixtures, which can contain both soluble and insoluble components. Also most atmospheric aerosols are externally mixed with respect to hygroscopicity, and consist of more and less hygroscopic sub-fractions [6]. The ratio between these fractions as well as their content of soluble material determines the hygroscopic growth of the overall aerosol. In the natural environment the changes observed at a given wavelength are signs that measuring conditions have changed. These changes can be related either to an increase in RH or to a change in the aerosol concentration, though most often, both factors are present. Optical measurements at one single wavelength will not resolve the question whether the observed changes are caused only by the increased humidity or whether the additional aerosol particles have contributed to the changes. To be able to retrieve more accurate information about the aerosol mixtures, spectral measurements are needed.

The more spectral information available, the greater are the chances of getting a more realistic idea of the aerosol composition. To model droplet growth, information about water activity and density as a function of solute concentration is needed. The chemical and physical characteristics of aerosols are diverse and attempting to encompass such variability within a hygroscopic model is complex. By taking up water, particles grow in size

and experience modifications to their refractive indices, which change their ability to interact with solar radiation. An aerosol may exist in a solid or liquid state or a combination of the two over a wide range of ambient conditions both in the sub and super saturated humid environment [7-10]. Thus, where possible, the ability to couple the chemical and physical characteristics to the equilibrium phase of the aerosol is the ultimate aim of any hygroscopic modeling approach. The cloud droplets and water in deliquesced aerosol particles provide an aqueous medium for chemical reactions, which can lead to a change in the chemical composition of the particles [11-15]. Additionally, depending on the chemical and physical compositions, aerosol hygroscopic growth with increasing relative humidity (RH) may lead to dramatic changes in its mass concentration, size distribution and corresponding optical properties, which could enhance the cooling effect of aerosols in the atmosphere by directly scattering more light radiation [16-20], or change cloud microphysical properties [21] by serving as cloud condensation nuclei (CCN) [22]. Particle hygroscopicity may vary as a function of time, place, and particle size [6,23,24]. Previous studies reported that different types of aerosol particles usually have distinct hygroscopic growth properties [25-27]. Hand and Malm [28] indicated that the scattering coefficients of  $(\text{NH}_4)_2\text{SO}_4$  and  $(\text{NH}_4)\text{HSO}_4$  aerosols could be enhanced by a factor of three when relative humidity is over 85%. Dust particles, dominant in coarse mode, are mostly insoluble [29], but they could also be hygroscopic when coated by sulfate or other soluble inorganic aerosols during transportation [30,31].

The hygroscopicity, are currently modeled in global climate models (GCMs), mostly to better predict the scattering properties and size distribution under varying humidity conditions [32]. Measured and modeled enhancement factors have been described in several previous studies, including studies on urban [33,34]. Jeong et al. [35] demonstrated an exponential dependence of the aerosol optical thickness on relative humidity. A strong correlation of spectral aerosol optical thickness with precipitable water, especially for continental air masses, was shown by Rapti [36]. A weaker dependence was observed for air masses of maritime origin. In this paper some microphysical and optical properties of urban aerosols were extracted from OPAC at the spectral wavelength of 0.25 to 2.50 $\mu\text{m}$ , at relative humidities of 0, 50, 70, 80, 90, 95, 98 and 99% and varying the concentrations of water soluble. The microphysical properties extracted are diameters of the aerosols, number mix ratios, volume mix ratio, mass mix ratio and refractive indices. They were used to determine the hygroscopic and the effective refractive indices. The optical properties extracted are optical depth and asymmetric parameters. The optical depth was used to determine the angstrom parameters using power law and enhancement parameters. The angstrom coefficients are used determine the particles' type and the type mode size distributions. One and two parameter models were used to determine the relationship between the enhancement parameter and hygroscopic growth with RH. The asymmetric parameters are used to determine the effects of hygroscopic growth and concentration of water soluble on forward scattering. The relationship between optical depth and RH was also determined as done by Jeong et al. [35] and Rapti[36].

## II. METHODOLOGY

The models extracted from OPAC are given in table 1.

Table 1 Compositions of aerosols types [37].

Components	Model A ( $N_i, \text{cm}^{-3}$ )	Model B ( $N_i, \text{cm}^{-3}$ )	Model C ( $N_i, \text{cm}^{-3}$ )
Insoluble	1.50	1.50	1.50
water soluble	15,000.00	25,000.00	35,000.00
Soot	130,000.00	130,000.00	130,000.00
<b>Total</b>	<b>145,001.50</b>	<b>155,001.50</b>	<b>165,001.50</b>

Where ( $N_i, \text{cm}^{-3}$ ) is the number of particles  $\text{cm}^{-3}$ , water soluble components, consist of scattering aerosols, that are hygroscopic in nature, such as sulfates and nitrates present in anthropogenic pollution, while water insoluble and soot are not soluble in water and therefore the particles are assumed not to grow with increasing relative humidity.

The aerosol's hygroscopic growth factor  $gf(\text{RH})$ , [6,20] is defined as:

$$gf(\text{RH}) = \frac{D(\text{RH})}{D(\text{RH}=0)} \quad (1)$$

where RH is taken for seven values 50%, 70%, 80%, 90%, 95%, 98% and 99%. But since natural aerosols consist of mixtures of both the soluble and insoluble components, and more and less hygroscopic sub fractions, so information on the hygroscopicity modes was merged into an "over-all" hygroscopic growth factor of the mixture,  $gf_{\text{mix}}(\text{RH})$ , representative for the entire particle population as:

$$gf_{\text{mix}}(\text{RH}) = (\sum_k x_k gf_k^3)^{1/3} \quad (2)$$

where the summation is performed over all compounds present in the particles and  $x_k$  represent their respective volume fractions, using the Zdanovskii-Stokes-Robinson relation [38-41]. Solute-solute interactions are neglected in this model and volume additivity is also assumed. The model assumes spherical particles, ideal mixing (i.e. no volume change upon mixing) and independent water uptake of the organic and inorganic components.

Equation (2) was also computed using the  $x_k$  as the corresponding number fractions [42,43].

We finally proposed the  $x_k$  to represent the mass mix ratio of the individual particles though since mass and volume are proportional, but this will enable us to see the effect of hygroscopic growth on the density of the mixture.

The RH dependence of  $gf_{mix}(RH)$  can be parameterized in a good approximation by a one-parameter equation[44] as:

$$gf_{mix}(a_w) = \left(1 + \kappa \frac{a_w}{1-a_w}\right)^{\frac{1}{3}} \quad (3)$$

Here,  $a_w$  is the water activity, which can be replaced by the relative humidity RH, if the Kelvin effect is negligible, as for particles with sizes more relevant for light scattering and absorption. Particle hygroscopicity is a measure that scales the volume of water associated with a unit volume of dry particle [44] and depends on the molar volume and the activity coefficients of the dissolved compounds [45]. The coefficient  $\kappa$  is a simple measure of the particle's hygroscopicity and captures all solute properties (Raoult effect), that is it is for the ensemble of the particle which can be defined in terms of the sum of its components. The  $\kappa$  values derived for particles of a given composition may vary, depending upon the size, the concentration and RH it is derived at. The following sub-divisions at 85% RH were made by Liu et al., [46]; as: nearly-hydrophobic particles (NH):  $\kappa \leq 0.10$  ( $gf_{mix} \leq 1.21$ ), less-hygroscopic particles (LH):  $\kappa = 0.10-0.20$  ( $gf_{mix} = 1.21-1.37$ ); more-hygroscopic particles (MH):  $\kappa > 0.20$  ( $gf_{mix} > 1.37$ ).

The humidograms of the ambient aerosols obtained in various atmospheric conditions showed that  $gf_{mix}(RH)$  could as well be fitted well with a  $\gamma$ -law [47-51] as

$$gf_{mix}(RH) = \left(1 - \frac{RH}{100}\right)^{\gamma} \quad (4)$$

The bulk hygroscopicity factor B under sub saturation RH conditions was determined using the relation:

$$B = (1 - gf_{mix}^2) \ln a_w \quad (5)$$

where  $a_w$  is the water activity, which can be replaced by the RH as explained before. The equation can be described as the rate of absorption of water of the bulk mixture as the RH increases.

The impact of hygroscopic growth on the aerosol optical depth is usually described by the enhancement factor  $f_r(RH, \lambda)$ :

$$f_r(RH, \lambda) = \frac{\tau(RH, \lambda)}{\tau(RH=0, \lambda)} \quad (6)$$

where RH is taken for seven values 50%, 70%, 80%, 90%, 95%, 98% and 99%.

In general the relationship between  $f_r(RH, \lambda)$  and RH is nonlinear [35]. In this paper we determine the empirical relations between the enhancement parameter and RH [52] as:

$$f_r(RH, \lambda) = \frac{\tau(RH, \lambda)}{\tau(RH_{ref}, \lambda)} = \left(\frac{100 - RH_{ref}}{100 - RH_{high}}\right)^{\gamma} \quad (7)$$

where in our study  $RH_{ref}$  was 0%, and  $RH_{high}$  was taken for seven values 50%, 70%, 80%, 90%, 95%, 98% and 99%. The  $\gamma$  known as the humidification factor represents the dependence of aerosol optical properties on RH, which results from changes in the particle size and refractive index upon humidification. The use of  $\gamma$  has the advantage of describing the hygroscopic behavior of aerosols in a linear manner over a broad range of RH values; it also implies that particles are deliquesced [53], a reasonable assumption for this data set due to the high ambient relative humidity during the field studies. The  $\gamma$  parameter is dimensionless, and it increases with increasing particle water uptake. From previous studies, typical values of  $\gamma$  for ambient aerosol ranged between 0.1 and 1.5 [53-55].

Two parameters empirical relation was also used [35,56] as:

$$f_r(RH, \lambda) = a \left(1 - \frac{RH(\%)}{100}\right)^b \quad (8)$$

Equations (7) and (8) were determined at wavelengths 0.25, 0.45, 0.55, 0.70, 1.25, and 2.50  $\mu\text{m}$ .

To determine the effect of particles mode distributions as a result of change in RH and water soluble, the Angstrom exponent was determined using the spectral behavior of the aerosol optical depth, with the wavelength of light ( $\lambda$ ) was expressed as inverse power law [57]:

$$\tau(\lambda) = \beta \lambda^{-\alpha} \quad (9)$$

The Angstrom exponent was obtained as a coefficient of the following regression,

$$\ln\tau(\lambda) = -a\ln(\lambda) + \ln\beta \tag{10}$$

However equation (10) was determined as non-linear (that is the Angstrom exponent itself varies with wavelength), and a more precise empirical relationship between the optical depth and wavelength was obtained with a 2nd-order polynomial [58-68] as:

$$\ln\tau(\lambda) = \alpha_2(\ln\lambda)^2 + \alpha_1\ln\lambda + \ln\beta \tag{11}$$

We then proposed the cubic relation to determine the type of mode distribution as:

$$\ln\tau(\lambda) = \ln\beta + \alpha_1\ln\lambda + \alpha_2(\ln\lambda)^2 + \alpha_3(\ln\lambda)^3 \tag{12}$$

where  $\beta, \alpha, \alpha_1, \alpha_2, \alpha_3$  are constants that were determined using regression analysis with SPSS16.0 for windows. Equations (10), (11) and (12) were evaluated at eight RHs for the corresponding change in water soluble concentrations.

We also determined an exponential dependence of the aerosol optical thickness on relative humidity as done by Jeong et al. [35] as:

$$\tau(RH) = A e^{B(RH/100)} \tag{13}$$

where A and B are constants determined using regression analysis with SPSS 16.0 for windows. The relationship was determined at 0.25 $\mu$ m, 1.25 $\mu$ m and 2.50 $\mu$ m.

We finally determined the effect of hygroscopic growth and the change in the concentration of water soluble on the effective refractive indices of the mixed aerosols using the formula [69]:

$$\frac{\epsilon_{eff} - \epsilon_0}{\epsilon_{eff} + 2\epsilon_0} = \sum_{i=1}^3 f_i \frac{\epsilon_i - \epsilon_0}{\epsilon_i + 2\epsilon_0} \tag{14}$$

where  $f_i$  and  $\epsilon_i$  are the volume fraction and dielectric constant of the  $i^{th}$  component and  $\epsilon_0$  is the dielectric constant of the host material.

The relation between dielectrics and refractive indices is

$$m_i = \sqrt{\epsilon_i} \tag{15}$$

For the case of Lorentz-Lorentz [70,71], the host material is taken to be vacuum,  $\epsilon_0 = 1$ .

The computation of equations (14) and (15) was done using the complex functions of Microsoft Excel 2010.

### III. RESULTS AND DISCUSSIONS

Table 2a: the growth factors of the aerosols using number mix ratio (equation 2) and Bulk hygroscopicity factor (equation 5) for Model A.

RH(%)	50	70	80	90	95	98	99
gf <sub>mix</sub> (RH)	1.0297	1.0470	1.0649	1.1063	1.1661	1.0538	1.3660
B	0.0635	0.0527	0.0463	0.0373	0.0301	0.0034	0.0156

Table 2b: the growth factors of the aerosols using number mix ratio (equation 2) and Bulk hygroscopicity factor (equation 5) for Model B.

RH(%)	50	70	80	90	95	98	99
gf <sub>mix</sub> (RH)	1.0456	1.0716	1.0980	1.1578	1.2416	1.3863	1.5061
B	0.0992	0.0822	0.0722	0.0582	0.0469	0.0336	0.0243

Table 2c: the growth factors of the aerosols using number mix ratio (equation 2) and Bulk hygroscopicity factor (equation 5) for Model C.

RH(%)	50	70	80	90	95	98	99
gf <sub>mix</sub> (RH)	1.0592	1.0923	1.1255	1.1995	1.3010	1.4719	1.6106
B	0.1305	0.1082	0.0950	0.0765	0.0617	0.0442	0.0319

Tables 2a, 2b and 2c show that there is an increase in both gf<sub>mix</sub>(RH) and B with the increase in the concentrations of water soluble. It can also be observed the hygroscopic growth has caused increased in gf<sub>mix</sub>(RH) but decrease in B.

The data from tables 2a, 2b and 2c were applied for the parametrisations of equations (3) and (4). The results obtained are as follows:

The results of the parameterizations by one parameter of equations (3) and (4) for Model A are:

$$k = 0.0175, R^2 = 0.9470 \quad \text{using equation (3)}$$

$$\gamma = -0.0588, R^2 = 0.9731 \quad \text{using equation (4)}$$

The results of the parameterizations by one parameter of equations (3) and (4) for Model B are:

$$k = 0.0272, R^2 = 0.9470 \quad \text{using equation (3)}$$

$$\gamma = -0.0798, R^2 = 0.9834 \quad \text{using equation (4)}$$

The results of the parameterizations by one parameter of equations (3) and (4) for Model C are:

$k=0.0358, R^2=0.9470$  using equation (3)

$\gamma=-0.0949, R^2=0.9891$  using equation (4)

From the observations of  $R^2$  it can be seen that the data fitted the equations very well (equations 3 and 4). It can also be observed that hygroscopicity of the mixtures ( $k$ ) and  $\gamma$  using  $\gamma$ -law, all increase with the increase in the concentrations of water solubles.

Table 3a: the growth factors of the aerosols using volume mix ratio (equation 2) and Bulk hygroscopicity factor (equation 5) for Model A.

RH(%)	50	70	80	90	95	98	99
$gf_{mix}(RH)$	1.1190	1.2019	1.2886	1.4822	1.7346	2.1242	2.4162
B	0.2781	0.2626	0.2544	0.2377	0.2164	0.1734	0.1317

Table 3b: the growth factors of the aerosols using volume mix ratio (equation 2) and Bulk hygroscopicity factor (equation 5) for Model B.

RH(%)	50	70	80	90	95	98	99
$gf_{mix}(RH)$	1.1482	1.2415	1.3348	1.5344	1.7862	2.1689	2.4550
B	0.3561	0.3259	0.3075	0.2753	0.2410	0.1859	0.1387

Table 3c: the growth factors of the aerosols using volume mix ratio (equation 2) and Bulk hygroscopicity factor (equation 5) for Model C.

RH(%)	50	70	80	90	95	98	99
$gf_{mix}(RH)$	1.1657	1.2638	1.3597	1.5607	1.8111	2.1895	2.4725
B	0.4048	0.3633	0.3377	0.2952	0.2534	0.1919	0.1419

Tables 3a, 3b and 3c show that there is an increase in both  $gf_{mix}(RH)$  and B with the increase in the concentrations of water soluble. It can also be observed the hygroscopic growth has caused increased in  $gf_{mix}(RH)$  but decrease in B.

The data from tables 3a, 3b and 3c were applied for the parametrizations of equations (3) and (4). The results obtained are as follows:

The results of the parameterizations by one parameter of equations (3) and (4) for Model A are:

$k=0.1441, R^2=0.9729$  using equation (3)

$\gamma=-0.1857, R^2=0.9966$  using equation (4)

The results of the parameterizations by one parameter of equations (3) and (4) for Model B are:

$k=0.1530, R^2=0.9658$  using equation (3)

$\gamma=-0.1936, R^2=0.9993$  using equation (4)

The results of the parameterizations by one parameter of equations (3) and (4) for Model C are:

$k=0.1572, R^2=0.9618$  using equation (3)

$\gamma=-0.1975, R^2=0.9997$  using equation (4)

From the observations of  $R^2$  it can be seen that the data fitted the equations very well (equations 3 and 4). It can also be observed that hygroscopicity of the mixtures ( $k$ ) and  $\gamma$  using  $\gamma$ -law, all increase with the increase in the concentrations of water solubles.

Table 4a: the growth factors of the aerosols using mass mix ratio (equation 2) and Bulk hygroscopicity factor (equation 5) for Model A.

RH(%)	50	70	80	90	95	98	99
$gf_{mix}(RH)$	1.1086	1.1816	1.2590	1.4364	1.6785	2.0657	2.3614
B	0.2512	0.2317	0.2221	0.2069	0.1913	0.1579	0.1223

Table 4b: the growth factors of the aerosols using mass mix ratio (equation 2) and Bulk hygroscopicity factor (equation 5) for Model B.

RH(%)	50	70	80	90	95	98	99
$gf_{mix}(RH)$	1.1383	1.2233	1.3098	1.4988	1.7457	2.1294	2.4191
B	0.3291	0.2963	0.2783	0.2494	0.2216	0.1749	0.1322

Table 4c: the growth factors of the aerosols using mass mix ratio (equation 2) and Bulk hygroscopicity factor (equation 5) for Model C.

RH(%)	50	70	80	90	95	98	99
gf <sub>mix</sub> (RH)	1.1567	1.2480	1.3386	1.5321	1.7794	2.1597	2.4458
B	0.3796	0.3366	0.3121	0.2735	0.2377	0.1833	0.1370

Tables 4a, 4b and 4c show that there is an increase in both gf<sub>mix</sub>(RH) and B with the increase in the concentrations of water soluble. It can also be observed the hygroscopic growth has caused increased in gf<sub>mix</sub>(RH) but decrease in B.

The data from tables 4a, 4b and 4c were applied for the parametrisations of equations (3) and (4). The results obtained are as follows:

The results of the parameterizations by one parameter of equations (3) and (4) for Model A are:

$k=0.1328, R^2=0.9777$  using equation (3)

$\gamma=-0.1776, R^2=0.9939$  using equation (4)

The results of the parameterizations by one parameter of equations (3) and (4) for Model B are:

$k=0.1451, R^2=0.9701$  using equation (3)

$\gamma=-0.1879, R^2=0.9983$  using equation (4)

The results of the parameterizations by one parameter of equations (3) and (4) for Model C are:

$k=0.1511, R^2=0.9655$  using equation (3)

$\gamma=-0.1930, R^2=0.9994$  using equation (4)

From the observations of  $R^2$  it can be seen that the data fitted the equations very well (equations 3 and 4). It can also be observed that hygroscopicity of the mixtures (k) and  $\gamma$  using  $\gamma$ -law, all increase with the increase in the concentrations of water solubles, though the  $\gamma$ -law shows inverse power laws.

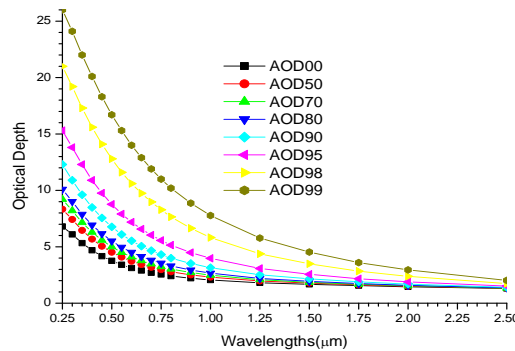


Figure 1a: A graph of optical depth against wavelengths for Model A.

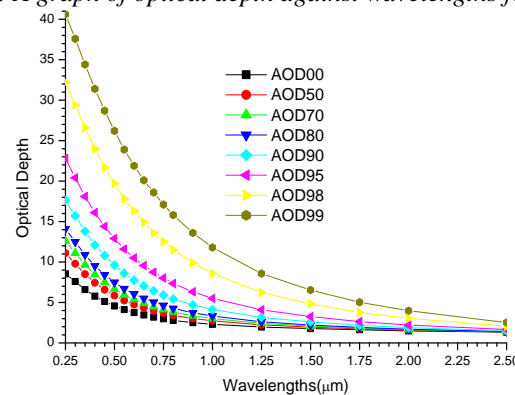


Figure 1b: A graph of optical depth against wavelengths for Model B.

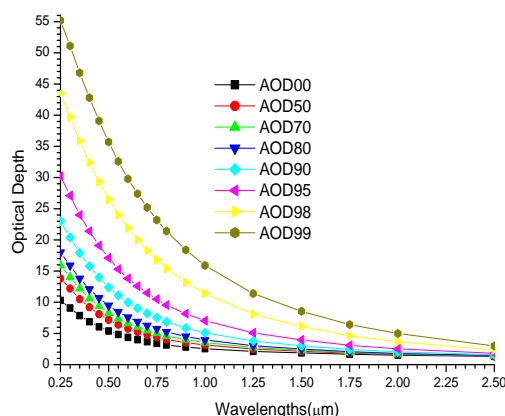


Figure 1c: A graph of optical depth against wavelengths for Model C.

From figures 1a, 1b and 1c, it can be observe that the optical depth follows a relatively smooth decrease with wavelength for all RHs and can be approximated with power law wavelength dependence. It is evident from the figures that there is relatively strong wavelength dependence of optical depth at shorter wavelengths that gradually decreases towards longer wavelengths irrespective of the RH and concentrations, attributing to the dominance of fine over coarse particles. The presence of a higher concentration of the fine-mode particles which are selective scatters enhance the irradiance scattering in shorter wavelength only while the coarse-mode particles provide similar contributions to the AOD at both wavelengths [72]. This also shows that hygroscopic growth has more effect on fine particles than coarse particles. The relation of optical depth with RH and water soluble concentrations are such that at the deliquescence point (90 to 99%) this growth with higher humidities increases substantially, making this process strongly nonlinear with relative humidity and the increase in the concentrations of water soluble [25,73].

The data that were used in plotting figures 1a, 1b and 1c were applied to equation (13), at the wavelengths of 0.25, 1.25 and 2.50μm. The results obtained are as follows:

The exponential relations (13) between optical depth and RHs for *Model A* are:

At  $\lambda=0.25\mu\text{m}$ ,  $A=5.4740$ ,  $B=1.1185$ ,  $R^2= 0.6577$

At  $\lambda=1.25 \mu$ ,  $A=1.4583$ ,  $B=0.8678$ ,  $R^2= 0.5022$

At  $\lambda=2.50 \mu$ ,  $A=1.2070$ ,  $B=0.2858$ ,  $R^2= 0.3862$

The relation between optical depth and RHs using equation (13) for *Model B* are:

At  $\lambda=0.25\mu$ ,  $A=6.7084$ ,  $B=1.3187$ ,  $R^2= 0.6856$

At  $\lambda=1.25 \mu$ ,  $A=1.5039$ ,  $B=1.1344$ ,  $R^2= 0.5360$

At  $\lambda=2.50 \mu$ ,  $A=1.1794$ ,  $B=0.4350$ ,  $R^2= 0.4124$

The relation between optical depth and RHs for *Model C* using equation (13) are:

At  $\lambda=0.25\mu$ ,  $A=7.9690$ ,  $B=1.4323$ ,  $R^2= 0.6984$

At  $\lambda=1.25 \mu$ ,  $A=1.5640$ ,  $B=1.3222$ ,  $R^2= 0.5602$

At  $\lambda=2.50 \mu$ ,  $A=1.1593$ ,  $B=0.5580$ ,  $R^2=0.4273$

The relation between optical depth and RH shows decrease in  $R^2$  and the exponent B with the increase in wavelength but both increase with the increase in the concentrations of water solubles. This shows that the relation is better for fine particles.

Table 5a the results of the Angstrom coefficients for Model A using equations (10), (11) and (12) at the respective relative humidities using regression analysis with SPSS16 for windows.

RH (%)	Linear equ(10)		Quadratic equ(11)			Cubic equ(12)			
	R2	$\alpha$	R2	$\alpha1$	$\alpha2$	R2	$\alpha1$	$\alpha2$	$\alpha3$
0	0.9757	0.7485	0.9963	-0.6745	0.1610	0.9976	-0.7206	0.2136	0.0689
50	0.9861	0.8388	0.9967	-0.7796	0.1289	0.9986	-0.8417	0.1997	0.0929
70	0.9904	0.8819	0.9968	-0.8335	0.1054	0.9990	-0.9024	0.1840	0.1031
80	0.9936	0.9205	0.9970	-0.8839	0.0796	0.9993	-0.9576	0.1637	0.1102
90	0.9972	0.9909	0.9974	-0.9826	0.0182	0.9997	-1.0615	0.1082	0.1180
95	0.9963	1.0584	0.9981	-1.0887	-0.0661	0.9999	-1.1637	0.0194	0.1120
98	0.9862	1.1164	0.9992	-1.2035	-0.1897	1.0000	-1.2544	-0.1317	0.0760
99	0.9747	1.1283	0.9998	-1.2515	-0.2682	0.9999	-1.2773	-0.2387	0.0386

Table 5b the results of the Angstrom coefficients for Model B using equations (10), (11) and (12) at the respective relative humidities using regression analysis with SPSS16 for windows.

RH (%)	Linear equ(10)		Quadratic equ(11)			Cubic equ(12)			
	R2	$\alpha$	R2	$\alpha_1$	$\alpha_2$	R2	$\alpha_1$	$\alpha_2$	$\alpha_3$
0	0.9849	0.8527	0.9965	-0.7899	0.1367	0.9985	-0.8549	0.2109	0.0973
50	0.9932	0.9635	0.9968	-0.9239	0.0863	0.9993	-1.0042	0.1779	0.1201
70	0.9958	1.0128	0.9971	-0.9885	0.0530	0.9996	-1.0732	0.1497	0.1267
80	0.9972	1.0545	0.9973	-1.0460	0.0186	0.9997	-1.1327	0.1176	0.1297
90	0.9967	1.1249	0.9979	-1.1514	-0.0577	0.9999	-1.2346	0.0372	0.1244
95	0.9914	1.1831	0.9988	-1.2528	-0.1518	1.0000	-1.3204	-0.0747	0.1011
98	0.9771	1.2168	0.9997	-1.3428	-0.2743	1.0000	-1.3733	-0.2395	0.0456
99	0.9644	1.2088	0.9999	-1.3666	-0.3436	0.9999	-1.3688	-0.3411	0.0033

Table 5c the results of the Angstrom coefficients for Model C using equations (10), (11) and (12) at the respective relative humidities using regression analysis with SPSS16 for windows.

RH (%)	Linear equ(10)		Quadratic equ(11)			Cubic equ(12)			
	R2	$\alpha$	R2	$\alpha_1$	$\alpha_2$	R2	$\alpha_1$	$\alpha_2$	$\alpha_3$
0	0.9901	0.9353	0.9965	-0.8840	0.1117	0.9990	-0.9621	0.2009	0.1168
50	0.9961	1.0558	0.9970	-1.0340	0.0474	0.9996	-1.1240	0.1501	0.1346
70	0.9973	1.1064	0.9973	-1.1026	0.0081	0.9998	-1.1944	0.1128	0.1372
80	0.9973	1.1477	0.9976	-1.1621	-0.0314	0.9999	-1.2524	0.0717	0.1351
90	0.9944	1.2130	0.9984	-1.2654	-0.1141	1.0000	-1.3451	-0.0231	0.1193
95	0.9868	1.2599	0.9993	-1.3563	-0.2098	1.0000	-1.4127	-0.1454	0.0844
98	0.9711	1.2735	0.9999	-1.4229	-0.3252	1.0000	-1.4371	-0.3090	0.0212
99	0.9584	1.2519	0.9998	-1.4293	-0.3860	0.9999	-1.4153	-0.4020	-0.0209

First, from tables 5a, 5b and 5c, it can be observed that at each table there is an increase in  $\alpha$  with the increase in RH and water solubles, except tables 5b and 5c where  $\alpha$  decreased at 99% RH, and this shows that increase in the concentration of water soluble has lowered the delinquent point of the mixtures. This increase in  $\alpha$  signifies the increase in mode size distribution of the particles. The decrease in  $\alpha_2$  at the positive part (the decrease in the curvature) and becoming more negative in the negative part (the increase in the curvature) with the increase in RH and water solubles, reflects the increase in the concentrations of small particles as a result of nucleation, accumulation and sedimentation. The cubic part signifies the type of mode distributions as bi-modal with the dominance of fine mode particles.

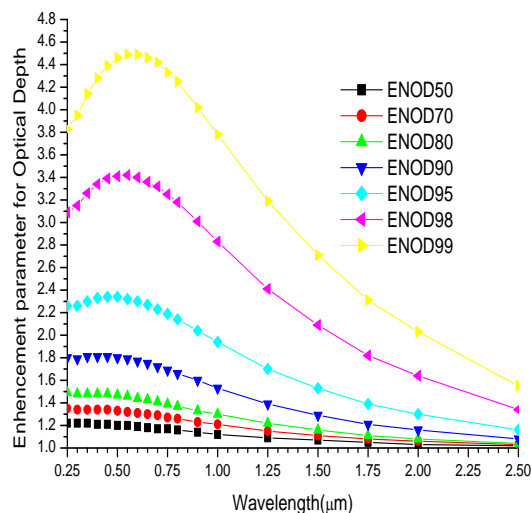


Figure 2a: A graph of enhancement parameter for optical depth against wavelengths for Model A

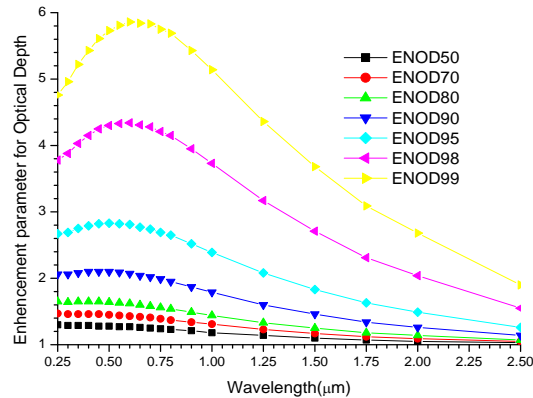


Figure 2b: A graph of enhancement parameter for optical depth against wavelengths for Model B.

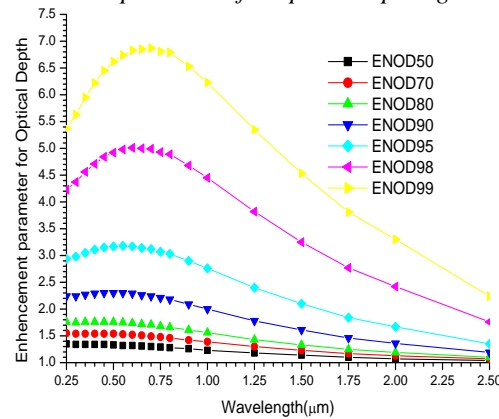


Figure 2c: A graph of enhancement parameter for optical depth against wavelengths for Model C

Figures 2a, 2b and 2c show that the enhancement factors increase both with the increase in RH and concentrations of water soluble in almost non-linear form. The most interesting phenomena is the visible range window (0.4 - 0.7  $\mu\text{m}$ ) and the near-infrared (0.7-1.0) where the enhancement is higher with both the increase in RH and the concentrations of water soluble. This shows that at this window the increase in the concentrations of water soluble can cause decrease in cloud cover, and/or reflective aerosol, this can cause decrease in global albedo, can result in the increase in energy input into Earth/Atmosphere system and finally can cause warming effect. That is it allows most solar radiation through to the surface and enables solar radiation to “deliver” the bulk of its energy to the surface (for use in climate processes)

The data that were used in plotting figures 2a, 2b and 2c were applied for the parametrisations of equations (7) and (8), at the wavelengths of 0.25, 0.45, 0.55, 0.70, 1.25 and 2.50 $\mu\text{m}$ . The results obtained are as follows: The results of the fitted curves of equations (7) and (8) for *Model A* are presented as follows;

For a single parameter using equation (7).

At  $\lambda=0.25\mu$ ,  $\gamma=0.2809$ ,  $R^2=0.9974$

At  $\lambda=0.45\mu$ ,  $\gamma=0.3002$ ,  $R^2=0.9925$

At  $\lambda=0.55\mu$ ,  $\gamma=0.9925$ ,  $R^2=0.9898$

At  $\lambda=0.70\mu$ ,  $\gamma=0.2922$ ,  $R^2=0.9849$

At  $\lambda=1.25\mu$ ,  $\gamma=0.2113$ ,  $R^2=0.9575$

At  $\lambda=2.50\mu$ ,  $\gamma=0.0701$ ,  $R^2=0.8914$

For two parameters using equation (8).

At  $\lambda=0.25\mu$ ,  $a=1.2062$ ,  $b=-0.2985$ ,  $R^2=0.9940$

At  $\lambda=0.45\mu$ ,  $a=1.4255$ ,  $b=-0.3377$ ,  $R^2=0.9895$

At  $\lambda=0.55\mu$ ,  $a=1.5132$ ,  $b=-0.3460$ ,  $R^2=0.9873$

At  $\lambda=0.70\mu$ ,  $a=1.6466$ ,  $b=-0.3462$ ,  $R^2=0.9834$

At  $\lambda=1.25\mu$ ,  $a=2.1526$ ,  $b=-0.2781$ ,  $R^2=0.9619$

At  $\lambda=2.50\mu$ ,  $a=2.8743$ ,  $b=-0.1048$ ,  $R^2=0.9078$

The results of the fitted curves of equations (7) and (8) for *Model B* are presented as follows;

For a single parameter using equation (7).

- At  $\lambda=0.25\mu$ ,  $\gamma=0.9899$ ,  $R^2=0.9883$
- At  $\lambda=0.45\mu$ ,  $\gamma=1.1033$ ,  $R^2=0.9851$
- At  $\lambda=0.55\mu$ ,  $\gamma=1.1248$ ,  $R^2=0.9826$
- At  $\lambda=0.70\mu$ ,  $\gamma=1.1132$ ,  $R^2=0.9797$
- At  $\lambda=1.25\mu$ ,  $\gamma=0.8462$ ,  $R^2=0.9777$
- At  $\lambda=2.50\mu$ ,  $\gamma=0.4501$ ,  $R^2=0.9192$

For two parameters using equation (8).

- At  $\lambda=0.25\mu$ ,  $a=0.6800$ ,  $b=-0.8832$ ,  $R^2=0.9550$
- At  $\lambda=0.45\mu$ ,  $a=0.9693$ ,  $b=-1.0926$ ,  $R^2=0.9361$
- At  $\lambda=0.55\mu$ ,  $a=1.0495$ ,  $b=-1.1421$ ,  $R^2=0.9294$
- At  $\lambda=0.70\mu$ ,  $a=1.1000$ ,  $b=-1.1474$ ,  $R^2=0.9214$
- At  $\lambda=1.25\mu$ ,  $a=0.8195$ ,  $b=-0.7966$ ,  $R^2=0.9012$
- At  $\lambda=2.50\mu$ ,  $a=0.0279$ ,  $b=-0.2122$ ,  $R^2=0.8794$

The results of the fitted curves of equations (7) and (8) for *Model Care* presented as follows;

For a single parameter using equation (7).

- At  $\lambda=0.25\mu$ ,  $\gamma=1.1004$ ,  $R^2=0.9896$
- At  $\lambda=0.45\mu$ ,  $\gamma=1.2472$ ,  $R^2=0.9835$
- At  $\lambda=0.55\mu$ ,  $\gamma=1.2822$ ,  $R^2=0.9799$
- At  $\lambda=0.70\mu$ ,  $\gamma=1.2857$ ,  $R^2=0.9759$
- At  $\lambda=1.25\mu$ ,  $\gamma=1.0045$ ,  $R^2=0.9744$
- At  $\lambda=2.50\mu$ ,  $\gamma=0.5018$ ,  $R^2=0.9424$

For two parameters using equation (8);

- At  $\lambda=0.25\mu$ ,  $a=0.7975$ ,  $b=-1.0276$ ,  $R^2=0.9549$
- At  $\lambda=0.45\mu$ ,  $a=1.1158$ ,  $b=-1.2916$ ,  $R^2=0.9362$
- At  $\lambda=0.55\mu$ ,  $a=1.2100$ ,  $b=-1.3637$ ,  $R^2=0.9294$
- At  $\lambda=0.70\mu$ ,  $a=1.2842$ ,  $b=-1.3950$ ,  $R^2=0.9214$
- At  $\lambda=1.25\mu$ ,  $a=1.0923$ ,  $b=-1.0331$ ,  $R^2=0.9013$
- At  $\lambda=2.50\mu$ ,  $a=0.1013$ ,  $b=-0.2922$ ,  $R^2=0.8797$

For both the one and two parameters models, the values of the exponents increase with the increase in the construction of water soluble, and they increased most at the solar spectral window (0.40 to 0.70 $\mu$ m). These signified increase in water uptake with the increase in the concentrations of water soluble.

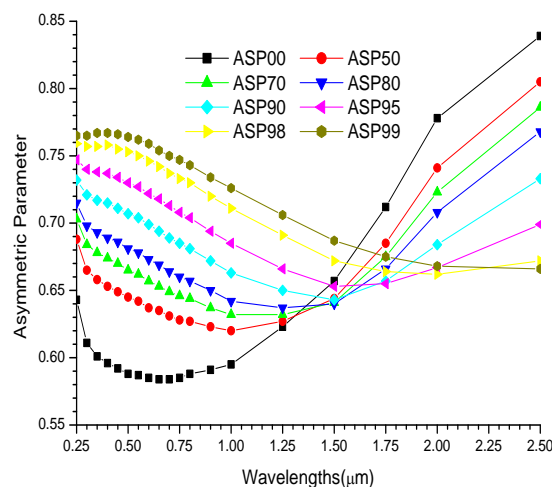


Figure 3a: A graph of Asymmetric parameter against wavelengths for *Model A*

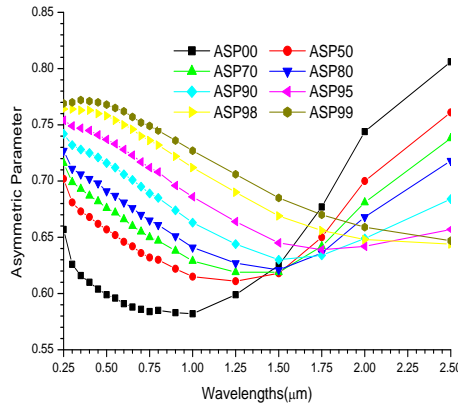


Figure 3b: A graph of Asymmetric parameter against wavelengths for Model B.

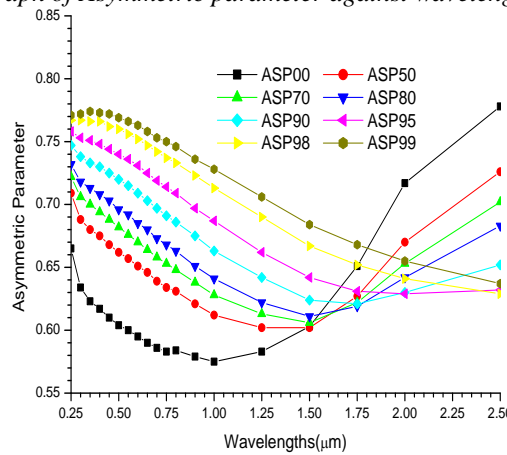


Figure 3c: A graph of Asymmetric parameter against wavelengths for Model C

Figures 3a, 3b and 3c show a slight increase in the asymmetric parameters with the increase in the concentration of water soluble. The increase with the increase in RH is faster at the solar spectral window. This shows that smaller particles enhance forward scattering with the increase in RH and water solubles.

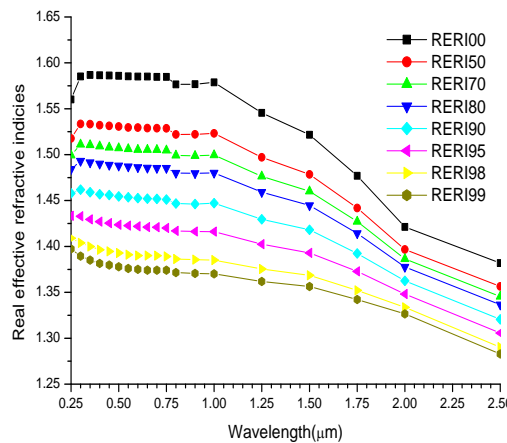


Figure 4a: A plot of real effective refractive indices against wavelength using volume mix ratio for Model A.

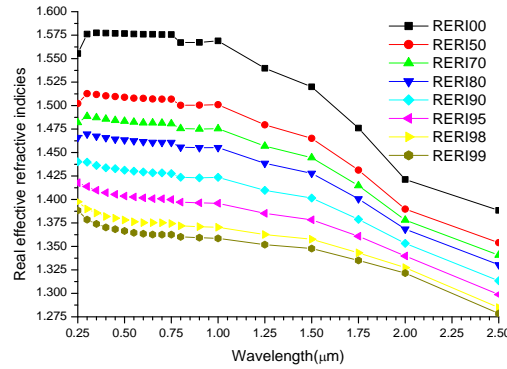


Figure 4b: A plot of real effective refractive indices against wavelength using volume mix ratio for Model B.

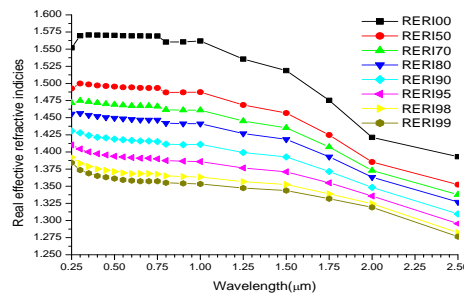


Figure 4c: A plot of real effective refractive indices against wavelength using volume mix ratio for Model C.

Figures 4a, 4b and 4c show decrease in the real effective refractive indices with increase in RH and water soluble. This signifies the reason why scattering increases with the increase in RH and water soluble. The linear relation decreases with the increase in wavelength.

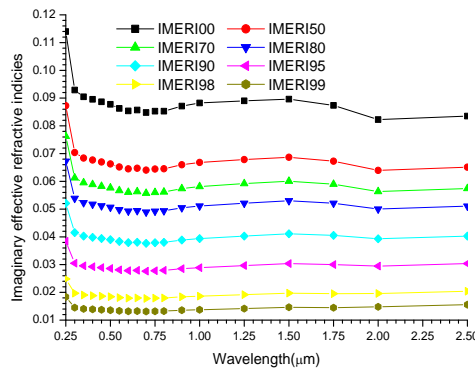


Figure 5a: A plot of imaginary effective refractive indices against wavelength using volume mix ratio for Model A.

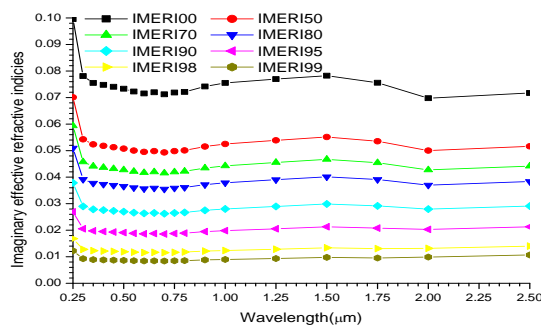


Figure 5b: A plot of imaginary effective refractive indices against wavelength using volume mix ratio for Model B.

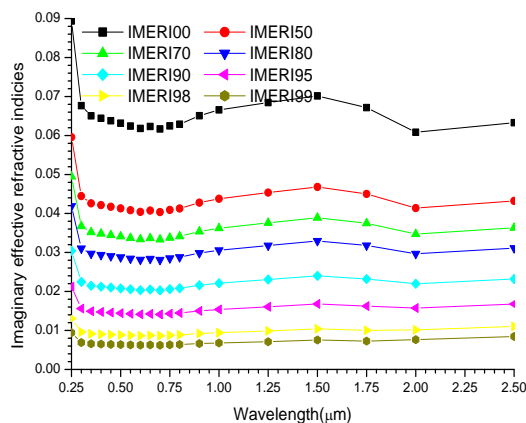


Figure 5c: A plot of imaginary effective refractive indices against wavelength using volume mix ratio for Model C.

Figures 5a, 5b and 5c show a slight decrease with the increase in RH and water soluble. This signifies decrease in absorption. It becomes more linear and constant with the increase in RH.

#### IV. CONCLUSIONS

In this paper we investigated the influence of relative humidity and soot on the microphysical and optical properties of atmospheric aerosol mixtures. The principal conclusions are:

- [1] From the three  $gf_{\text{mix}}(\text{RH})$  it can be concluded that the higher values are observed using volume and mass mix ratios because of the high density of water soluble. This is in line with what Sheridan et al. [74] found, on the basis of analysis of in situ data collected at SGP in 1999, that aerosols containing higher fractions of smaller particles show larger hygroscopic growth factors. From our results despite soot being having the least size and higher in fractions, it shows that using volume mix and mass mix ratios, shows that the mixture is more hygroscopic. However, still in their studies, they also showed that aerosols containing higher fractions of more strongly absorbing particles exhibit lower hygroscopic growth factors, in our own case it shows that using number mix ratio. The importance of determining  $gf_{\text{mix}}(\text{RH})$  as a function of RH and volume fractions, mass fractions and number fractions, and enhancement parameters as a function of RH and wavelengths can be potentially important because it can be used for efficiently representing aerosols-water interactions in global models.
- [2] Equation (3) with mass mix ratios has higher  $R^2$  while equation (4) has higher values of  $R^2$  using volume mix ratio. But since volume mix ratios gave higher values of  $gf_{\text{mix}}(\text{RH})$ ,  $k$  and  $\gamma$ , and the values of  $R^2$  are greater than 95%, it can be concluded that just as the optical effects of atmospheric aerosols are more closely related to their volume than their number [75,76], we discovered that the microphysical properties are also more closely related to their volume followed by mass. The increase in the values of  $gf_{\text{mix}}(\text{RH})$ ,  $k$  and  $\gamma$  with the increase in soot and water soluble concentration show that they increase hygroscopicity of aerosols.
- [3] Changes in RH and soot and water soluble concentrations modified the optical properties not only of hygroscopic aerosol mixtures but also of mixtures containing non-hygroscopic aerosols like black carbon. As a result of wetting the hydroscopic particles grow, thereby changing the effective radius of the aerosol mixture and subsequently the aerosol extinction or aerosol optical thickness[77]. The changes are more substantial especially at the delinquent points where the hygroscopic growth factor, optical parameters and enhancement parameters increase so substantial that the process become strongly nonlinear with relative humidity [25,73,77]. This effect is observed at different wavelengths, but for higher RH, the increase in AOT values is more evident at smaller wavelengths than longer wavelengths.
- [4] The observed variations in Angstrom coefficients can be explained by changes in the effective radius of a mixture resulting from changes in RH and/or soot and water soluble concentrations: the larger the number of small aerosol particles, the smaller the effective radius and the larger the Angstrom coefficient. As a consequence of non-uniform increase in the optical depth with the increase in RH, the Ångström coefficient also becomes a function of RH, though at the delinquent points it decreases with the increase in RHs. This is because at the delinquent conditions the hygroscopic aerosols particles grow and this is what makes the Angstrom coefficients to decrease. However, the change in Angstrom coefficient due to variation in RH is more than that caused by differences in soot concentrations.

- [5] The effect of RHs on asymmetric parameter shows that for smaller particles the hygroscopic growth increase forward scattering while for coarse particle it decreases forward scattering. It shows that increase in RH increases forward scattering because particle growth enhances forward diffraction Liou,[78]for smaller particles while in larger particles it causes increase in the backward scattering. It also shows that the mixture is internally mixed for smaller particles because of the increase in forward scattering as a result of the hygroscopic growth [79].
- [6] These hygroscopic growth behaviors also reveal an immense potential of light scattering enhancement in the forward direction at high humidities and the potential for being highly effective cloud condensation nuclei for smaller particles.
- [7] Finally, the data fitted our models very and can be used to extrapolate the hygroscopic growth and enhancements parameters at any RH. The values of R2 from the models show that Kelvin effects can be neglected.

## REFERENCES

- [1] IPCC (2007). Climate Change 2007: The Scientific Basis. In Solomon, S., Ding, Y., Griggs, D.G., Noguer, M., Vanderlinden, P.G., Dai, X., Maskell, K. and Johnson, C.A. (Eds). Contribution of Working Group I to the Fourth Assessment Report of the Intergovernmental Panel on Climate Change. Cambridge University Press. Cambridge.
- [2] Li, W.F, Bai, Z.P., Liu, A.X., Chen, J. and Chen, L. (2009). Characteristics of Major PM<sub>2.5</sub> Components during Winter in Tianjin, China. *Aerosol Air Qual. Res.* 9: 105–119.
- [3] Shen, Z.X., Cao, J.J, Tong, Z., Liu, S.X., Reddy, L.S.S., Han, Y.M, Zhang, T. and Zhou, J. (2009). Chemical Characteristics of Submicron Particles in Winter in Xi'an. *Aerosol Air Qual. Res.* 9: 80–93.
- [4] Orr Jr. C., Hurd F. K., Corbett W. J., 1958, Aerosol size and relative humidity, *J. Colloid Sci.*, 13, 472–482.
- [5] Tang I. N., (1976), Phase transformation and growth of aerosol particles composed of mixed salts, *J. Aerosol Sci.*, 7, 361–371.
- [6] Swietlicki, E., Hansson, H.-C., Hameri, K., Svenningsson, B., Massling, A., et al.:(2008) Hygroscopic properties of submicrometer atmospheric aerosol particles measured with H-TDMA instruments in various environments – a review, *Tellus B*, 60(3), 432–469.
- [7] Corrigan, C. E. and Novakov, T.: Cloud condensation nucleus activity of organic compounds: a laboratory study, *Atmos. Environ.*, 33 (17), 2661–2668, 1999.
- [8] Pitchford, M. L. and McMurry, P. H.: Relationship between Measured Water-Vapor Growth and Chemistry of Atmospheric Aerosol for Grand-Canyon, Arizona, in Winter 1990, *Atmos. Environ.*, 28 (5), 827–839, 1994.
- [9] Shulman, M. L., Jacobson, M. C., Charlson, R. J., Synovec, R. E., and Young, T. E.: Dissolution behavior and surface tension effects of organic compounds in nucleating cloud droplets (vol. 23, p. 277, 1996), *Geophys. Res. Lett.*, 23 (5), 603–603, 1996.
- [10] Swietlicki, E., Zhou, J. C., Berg, O. H., Martinsson, B. G., Frank, G., Cederfelt, S. I., Dusek, U., Berner, A., Birmili, W., Wiedensohler, A., Yuskiewicz, B., and Bower, K. N.: A closure study of sub-micrometer aerosol particle hygroscopic behaviour, *Atmos. Res.*, 50 (3-4), 205–240, 1999.
- [11] Hegg, D. A.: The importance of liquid phase oxidation of SO<sub>2</sub> in the atmosphere, *J. Geophys. Res.*, 90, 3773–3779, doi:10.1029/JD090iD02p03773, 1985.
- [12] Blando, J. D. and Turpin, B. J.: Secondary organic aerosol formation in cloud and fog droplets: a literature evaluation of plausibility, *Atmos. Environ.*, 34, 1623–1632, doi:10.1016/S1352-2310(99)00392-1, 2000.
- [13] El Haddad, I., Yao Liu, Nieto-Gligorovski, L., Michaud, V., Temime-Roussel, B., Quivet, E., Marchand, N., Sellegri, K., and Monod, A.: In-cloud processes of methacrolein under simulated conditions – Part 2: Formation of secondary organic aerosol, *Atmos. Chem. Phys.*, 9, 5107–5117, doi:10.5194/acp-9-5107-2009, 2009.
- [14] Bateman, A. P., Nizkorodov, S. A., Laskin, J., and Laskin, A.: Photolytic processing of secondary organic aerosols dissolved in cloud droplets, *Phys. Chem. Chem. Phys.*, 13, 12199–12212, doi:10.1039/c1cp20526a, 2011.
- [15] Ervens, B., Turpin, B. J., and Weber, R. J.: Secondary organic aerosol formation in cloud droplets and aqueous particles (aqSOA): a review of laboratory, field and model studies, *Atmos. Chem. Phys.*, 11, 11069–11102, doi:10.5194/acp-11-11069-2011, 2011.
- [16] Ogren, J. A. and Charlson R. J.: Implications for models and measurements of chemical inhomogeneities among cloud droplets, *Tellus*, 44B, 489–504, 1992.
- [17] Carrico, C. M., Rood, M. J., and Ogren, J. A.: Aerosol light scattering properties at Cape Grim, Tasmania, during the First Aerosol Characterization Experiment (ACE 1), *J. Geophys. Res.*, 103(D13), 16565–16574, 1998.
- [18] Carrico, C. M., Rood, M. J., Ogren, J. A., et al.: Aerosol Optical properties at Sagres, Portugal during ACE-2, *Tellus B*, 52(2), 694–715, 2000.
- [19] Kotchenruther, R. A., Hobbs, P. V., and Hegg, D. A.: Humidification factors for atmospheric aerosols off the mid-Atlantic coast of the United States, *J. Geophys. Res.*, 104(D2), 2239–2252, 1999.
- [20] Randles, C. A., Russell L. M. and Ramaswamy V. (2004) Hygroscopic and optical properties of organic sea salt aerosol and consequences for climate forcing, *Geophysical Research Letters*, Vol. 31, L16108, doi:10.1029/2004GL020628.
- [21] Crumeyrolle, S., Gomes, L., Tulet, P., Matsuki, A., Schwarzenboeck, A., and Crahan, K.: Increase of the aerosol hygroscopicity by cloud processing in a mesoscale convective system: a case study from the AMMA campaign, *Atmos. Chem. Phys.*, 8, 6907–6924, 2008, <http://www.atmos-chem-phys.net/8/6907/2008/>.
- [22] Houghton, J. T., Ding, Y., Griggs, D. J., et al.: IPCC, 2001: Climate Change 2001: The Scientific Basis. Contribution of Working Group I to the Third Assessment Report of the Intergovernmental Panel on Climate Change, Cambridge University Press, Cambridge, 2001.
- [23] McMurry, P. and Stolzenburg, M.: On the sensitivity of particle size to relative humidity for Los Angeles aerosols, *Atmos. Environ.*, 23, 497–507, 1989.
- [24] Cocker, D., Whitlock, N., Flagan, R., and Seinfeld, J. H.: Hygroscopic properties of Pasadena, California aerosol, *Aerosol Sci. Technol.*, 35, 2, 637–647, 2001.
- [25] Tang I.N., (1996) Chemical and size effects of hygroscopic aerosols on light scattering coefficient, *J. Geophys. Res.*, 101(D14), 19245–19250.
- [26] Cruz, C. N. and Pandis, S. N.: Deliquescence and Hygroscopic Growth of Mixed Inorganic–Organic Atmospheric Aerosol, *Environ. Sci. Technol.*, 34(20), 4313–4319, 2000.
- [27] Kim, J., Yoon, S. C., Jefferson, A., et al.: Aerosol hygroscopic properties during Asian dust, pollution, and biomass burning episodes at Gosan, Korea in April 2001, *Atmos. Environ.*, 40(8), 1550–1560, 2006.

- [28] Hand, J. L. and Malm, W. C.: Review of the IMPROVE Equation for Estimating Ambient Light Extinction Coefficients-Final Report, 47, 2006.
- [29] Li-Jones, X., Maring, H. B., and Prospero, J. M.: Effect of relative humidity on light scattering by mineral dust aerosol as measured in the marine boundary layer over the tropical Atlantic Ocean, *J. Geophys. Res.*, 103(D23), 31113-31121, 1998.
- [30] Perry, K. D., Cliff, S. S., and Jimenez-Cruz, M. P.: Evidence for hygroscopic mineral dust particles from the Intercontinental Transport and Chemical Transformation Experiment, *J. Geophys. Res.*, 109, D23S28, doi:10.1029/2004JD004979, 2004.
- [31] Shi, Z., Zhang, D., Hayashi, M., et al.(2007): Influences of sulfate and nitrate on the hygroscopic behaviour of coarse dust particles, *Atmos. Environ.*, 42(4), 822–827.
- [32] Randall, D. A., Wood, R. A., Bony, S., Colman, R., Fichefet, T., Fyfe, J., Kattsov, V., Pitman, A., Shukla, J., Srinivasan, J., Stouffer, R. J., Sumi, A., and Taylor, K. E.: Contribution of Working Group I to the Fourth Assessment Report of the Intergovernmental Panel on Climate Change – Climate Models and their Evaluation, Cambridge University Press, Cambridge, United Kingdom and New York, 589–662, 2007.
- [33] Yan, P., Pan, X. L., Tang, J., Zhou, X. J., Zhang, R. J., and Zeng, L. M.: Hygroscopic growth of aerosol scattering coefficient: a comparative analysis between urban and suburban sites at winter in Beijing, *Particuology*, 7, 52–60, 2009.
- [34] Fitzgerald, J. W., Hoppel, W. A., and Vietti, M. A.: The size and scattering coefficient of urban aerosol particles at Washington, DC as a function of relative humidity, *J. Atmos. Sci.*, 39, 1838–1852, 1982.
- [35] Jeong M. J, Li Z., Andrews E., Tsay S. C., (2007) Effect of aerosol humidification on the column aerosol optical thickness over the Atmospheric Radiation Measurement Southern Great Plains site, *J. Geophys. Res.*, 112, D10202, doi:10.1029/2006JD007176.
- [36] Rapti A.S., (2005) Spectral optical atmospheric thickness dependence on the specific humidity in the presence of continental and marine air masses, *Atmos. Res.*, 78(1–2),13–32.
- [37] Hess M., Koepke P., and Schult I (May 1998), *Optical Properties of Aerosols and Clouds: The Software Package OPAC*, *Bulletin of the American Met. Soc.* 79, 5, p831-844.
- [38] Sjogren, S., Gysel, M., Weingartner, E., Baltensperger, U., Cubison, M. J., Coe, H., Zardini, A. A., Marcolli, C., Krieger, U. K., and Peter, T.: Hygroscopic growth and water uptake kinetics of two-phase aerosol particles consisting of ammonium sulfate, adipic and humic acid mixtures, *J. Aerosol Sci.*, 38, 157–171, doi:10.1016/j.jaerosci.2006.11.005, 2007.
- [39] Stokes, R. H. and Robinson, R. A.: Interactions in aqueous nonelectrolyte solutions. I. Solute-solvent equilibria, *J. Phys. Chem.*, 70, 2126–2130, 1966.
- [40] Meyer, N. K., Duplissy, J., Gysel, M., Metzger, A., Dommen, J., Weingartner, E., Alfarra, M. R., Prevot, A. S. H., Fletcher, C., Good, N., McFiggans, G., Jonsson, A. M., Hallquist, M., Baltensperger, U., and Ristovski, Z. D.: Analysis of the hygroscopic and volatile properties of ammonium sulphate seeded and unseeded SOA particles, *Atmos. Chem. Phys.*, 9, 721–732, doi:10.5194/acp-9-721-2009, 2009.
- [41] Stock M., Y. F. Cheng, W. Birmili, A. Massling, B. Wehner, T. Muller, S. Leinert, N. Kalivitis, N. Mihalopoulos, and A. Wiedensohler, Hygroscopic properties of atmospheric aerosol particles over the Eastern Mediterranean: implications for regional direct radiative forcing under clean and polluted conditions, *Atmos. Chem. Phys.*, 11, 4251–4271, 2011 [www.atmos-chem-phys.net/11/4251/2011/](http://www.atmos-chem-phys.net/11/4251/2011/) doi:10.5194/acp-11-4251-2011
- [42] Duplissy J., P. F. DeCarlo, J. Dommen, M. R. Alfarra, A. Metzger, I. Barnpadimos, A. S. H. Prevot, E. Weingartner, T. Tritscher, M. Gysel, A. C. Aiken, J. L. Jimenez, M. R. Canagaratna, D. R. Worsnop, D. R. Collins, J. Tomlinson, and U. Baltensperger, (2011) Relating hygroscopicity and composition of organic aerosol particulate matter *Atmos. Chem. Phys.*, 11, 1155–1165, [www.atmos-chem-phys.net/11/1155/2011/](http://www.atmos-chem-phys.net/11/1155/2011/) doi:10.5194/acp-11-1155-2011.
- [43] Meier J., B. Wehner, A. Massling, W. Birmili, A. Nowak, T. Gnauk, E. Brüggemann, H. Herrmann, H. Min, and A. (2009) Wiedensohler Hygroscopic growth of urban aerosol particles in Beijing (China) during wintertime: a comparison of three experimental methods, *Atmos. Chem. Phys.*, 9, 6865–6880, [www.atmos-chem-phys.net/9/6865/2009](http://www.atmos-chem-phys.net/9/6865/2009).
- [44] Petters, M. D. and Kreidenweis, S. M. (2007). A single parameter representation of hygroscopic growth and cloud condensation nucleus activity. *Atmos. Chem. Phys.* 7(8): 1961–1971.
- [45] Christensen, S. I. and Petters, M. D. (2012). The role of temperature in cloud droplet activation. *J. Phys. Chem. A* 116(39): 9706–9717.
- [46] Liu P. F., Zhao C. S., Gobel T., Hallbauer E., Nowak A., Ran L., Xu W. Y., Deng Z. Z., Ma N., Mildnerberger K., Henning S., Stratmann F., and Wiedensohler A. (2011) Hygroscopic properties of aerosol particles at high relative humidity and their diurnal variations in the North China Plain, *Atmos. Chem. Phys. Discuss.*, 11, 2991–3040
- [47] Swietlicki, E., Zhou, J., Covert, D. S., Hameri, K., Busch, B., Vakeva, M., Dusek, U., Berg, O. H., Wiedensohler, A., Aalto, P., Makela, J., Martinsson, B. G., Papaspiropoulos, G., Mentes, B., Frank, G., and Stratmann, F.: Hygroscopic properties of aerosol particles in the northeastern Atlantic during ACE-2, *Tellus*, 52B, 201–227, 2000.
- [48] Birmili, W., Nowak, A., Schwirn, K., Lehmann, K. et al. (2004) A new method to accurately relate dry and humidified number size distributions of atmospheric aerosols. *Journal of Aerosol Science* 1, 15–16, Abstracts of EAC, Budapest 2004.
- [49] Kasten, F.: Visibility forecast in the phase of pre-condensation, *Tellus*, XXI, 5, 631–635, 1969.
- [50] Gysel, M., McFiggans, G. B., and Coe, H.: Inversion of tandem differential mobility analyser (TDMA) measurements, *J. Aerosol Sci.*, 40, 134–151, 2009.
- [51] Putaud, J. P. (2012): Interactive comment on “Aerosol hygroscopicity at Ispra EMEP-GAW station” by M. Adam et. al., *Atmos. Chem. Phys. Discuss.*, 12, C1316–C1322.
- [52] Doherty, et al., 2005. A comparison and summary of aerosol optical properties as observed in situ from aircraft, ship, and land during ACE-Asia. *Journal of Geophysical Research* 110, D04201.
- [53] Quinn, P. K., et al. (2005) , Impact of particulate organic matter on the relative humidity dependence of light scattering: A simplified parameterization, *Geophys. Res. Lett.*, 32, L22809, doi:10.1029/2005GL024322.
- [54] Gasso S., et al. (2000), Influence of humidity on the aerosol scattering coefficient and its effect on the upwelling radiance during ACE-2, *Tellus*, Ser. B, 52, 546 – 567.
- [55] Clarke, A., et al. (2007), Biomass burning and pollution aerosol over North America: Organic components and their influence on spectral optical properties and humidification response, *J. Geophys. Res.*, 112, D12S18, doi:10.1029/2006JD007777.
- [56] Hanel, G. (1976). The Properties of Atmospheric Aerosol Particles as Functions of Relative Humidity at Thermodynamic Equilibrium with Surrounding Moist Air. In *Advances in Geophysics*, Vol. 19, H. E. Landsberg and J. Van Mieghem, eds., Academic Press, New York, pp. 73–188.
- [57] Angstrom, A. (1961): Techniques of Determining the Turbidity of the Atmosphere, *Tellus*, 13, 214–223.
- [58] King, M. D. and Byrne, D. M.: A method for inferring total ozone content from spectral variation of total optical depth obtained with a solar radiometer, *J. Atmos. Sci.*, 33, 2242–2251, 1976.

- [59] Eck, T. F., Holben, B. N., Reid, J. S., Dubovic, O., Smirnov, A., O'Neil, N. T., Slutsker, I., and Kinne, S.: Wavelength dependence of the optical depth of biomass burning, urban, and desert dust aerosols, *J. Geophys. Res.*, 104(D24), 31 333–31 349, 1999.
- [60] Eck, T. F., Holben, B. N., Dubovic, O., Smirnov, A., Slutsker, I., Lobert, J. M., and Ramanathan, V.: Column-integrated aerosol optical properties over the Maldives during the northeast monsoon for 1998–2000, *J. Geophys. Res.*, 106, 28 555–28 566, 2001a.
- [61] Eck, T. F., Holben, B. N., Ward, D. E., Dubovic, O., Reid, J. S., Smirnov, A., Mukelabai, M. M., Hsu, N. C., O'Neil, N. T., and Slutsker, I.: Characterization of the optical properties of biomass burning aerosols in Zambia during the 1997 ZIBBEE field campaign, *J. Geophys. Res.*, 106(D4), 3425–3448, 2001b.
- [62] Kaufman, Y. J., Aerosol optical thickness and atmospheric path radiance, *J. Geophys. Res.*, 98, 2677–2992, 1993.
- [63] O'Neill, N. T., Dubovic, O., and Eck, T. F. (2001): Modified Angstrom exponent for the characterization of submicrometer aerosols, *Appl. Opt.*, 40(15), 2368–2375.
- [64] O'Neill, N. T., Eck, T. F., Smirnov, A., Holben, B. N., and Thulasiraman, S.: Spectral discrimination of coarse and fine mode optical depth, *J. Geophys. Res.*, 108(D17), 4559, doi:10.1029/2002JD002975, 2003.
- [65] Pedros, R., Martinez-Lozano, J. A., Utrillas, M. P., Gomez-Amo, J. L., and Tena, F. (2003): Column-integrated aerosol, optical properties from ground-based spectroradiometer measurements at Barrax (Spain) during the Digital Airborne Imaging Spectrometer Experiment (DAISEX) campaigns, *J. Geophys. Res.*, 108(D18), 4571, doi:10.1029/2002JD003331.
- [66] Kaskaoutis, D. G. and Kambezidis, H. D. (2006): Investigation on the wavelength dependence of the aerosol optical depth in the Athens area, *Q. J. R. Meteorol. Soc.*, 132, 2217–2234.
- [67] Schmid, B., Hegg, D.A., Wang, J., Bates, D., Redemann, J., Russell, P.B., Livingston, J.M., Jonsson, H.H., Welton, E.J., Seinfeld, J.H., Flagan, R.C., Covert, D.S., Dubovik, O., Jefferson, A., (2003). Column closure studies of lower tropospheric aerosol and water vapor during ACE-Asia using airborne Sun photometer and airborne in situ and ship-based lidar measurements. *Journal of Geophysical Research* 108 (D23), 8656.
- [68] Martinez-Lozano, J.A., Utrillas, M.P., Tena, F., Pedros, R., Canada, J., Bosca, J.V., Lorente, J., (2001). Aerosol optical characteristics from summer campaign in an urban coastal Mediterranean area. *IEEE Transactions on Geoscience and Remote Sensing* 39, 1573–1585.
- [69] Aspens D. E. (1982), Local-field effect and effective medium theory: A microscopic perspective *Am. J. Phys.* 50, 704–709.
- [70] Lorentz, H. A. (1880). Ueber die Beziehung zwischen der Fortpflanzungsgeschwindigkeit des Lichtes und der Körperdichte. *Ann. P hys. Chem.* 9, 641–665.
- [71] Lorenz, L. (1880). Ueber die Refractionconstante. *Ann. P hys. Chem.* 11, 70–103.
- [72] Schuster, G.L., Dubovik, O. and Holben, B.N. (2006). Angstrom Exponent and Bimodal Aerosol Size Distributions. *J. Geophys. Res.* 111: 7207.
- [73] Fitzgerald, J. W. (1975) Approximation formulas for the equilibrium size of an aerosol particle as a function of its dry size and composition and ambient relative humidity. *J. Appl. Meteorol.*, 14, 1044–1049.
- [74] Sheridan, P. J., Delene D. J., and Ogren J. A. (2001), Four years of continuous surface aerosol measurements from the Department of Energy's Atmospheric Radiation Measurement Program Southern Great Plains Cloud and Radiation Testbed site, *J. Geophys. Res.*, 106, 20,735–20,747.
- [75] Whitby, K. (1978), The physical characteristics of sulfur aerosols, *Atmos. Environ.*, 12, 135–159.
- [76] Seinfeld, J., and S. Pandis (1998), *Atmospheric Chemistry and Physics: From Air Pollution to Climate Change*, Wiley.
- [77] Kuśmierczyk-Michulec, J. (2009). Ångström coefficient as an indicator of the atmospheric aerosol type for a well-mixed atmospheric boundary layer: Part 1: Model development. *Oceanologia*, Vol. 51, p. 5–39.
- [78] Liou, K. N. (2002), *An Introduction to Atmospheric Radiation*, 583pp., Elsevier, New York.
- [79] Wang, J., and S. T. Martin (2007), Satellite characterization of urban aerosols: Importance of including hygroscopicity and mixing state in the retrieval algorithms, *J. Geophys. Res.*, 112, D 17203, doi:10.1029/2006JD008078.

# Efficient Solution of Constraint Satisfaction Problems by Equivalent Transformation

Hiroshi Mabuchi<sup>1</sup>

<sup>1</sup> Faculty of Software and Information Science, Iwate Prefectural University, Takizawa, Iwate, Japan

## ABSTRACT

*In many conventional programming languages, programs are constructed from built-in data structures and built-in constraints. Due to the limitation of the expressive power, the computation may become very inefficient when they are used to solve large and complicated problems. In order to overcome the difficulty, we adopt a computing framework of "problem solving based on equivalent transformation (ET)." In this framework, a problem can be solved by simplifying declarative descriptions of the problem on the equivalent transformation basis, and the correctness of computation can be guaranteed. Furthermore, users can easily introduce new various data structures and constraint-solving rules necessary for the improving of the constraint-solving algorithms. In this paper, we show that "problem solving based on equivalent transformation" is useful to avoid the combinatorial explosion when solving large constraint satisfaction problems.*

**KEYWORDS:** *Combinatorial explosion, Constraint satisfaction problem, Equivalent transformation, Transformation rule*

## I. INTRODUCTION

In constraint logic programming languages [3,5,9,10,23], a system has constraint atoms and algorithms for solving them. The "built-in" approach of combining constraint atoms enables users to program. This approach offers an advantage of guaranteeing the correctness of a solving method, because a system provides a constraint-solving algorithm. If a system has constraint atoms which are efficient for problem solving, users can create efficient programs easily. Constraint logic programming languages, however, have also disadvantages. Due to dependency on a pre-supported constraint-solving algorithm, expressive power for programming is limited. If its limit is violated, the computation efficiency may drastically decrease. In such a case, the "built-in" approach can not improve the constraint-solving algorithm. It is desirable for users to be able easily to add to or improve data structures or rules which represent constraints. The "built-in" approach prevents free programming which efficiently enables users to solve problems.

As a result, it may cause crucial problems when large-scale and complicated problems are solved. This paper proposes to solve problems by the "expansive" approach, where without depending only on a constraint-solving algorithm possessed in a system, users can improve the algorithm and define new rules for constraint-solving. First, this paper provides an example of unsolvable problems: an attempt to solve a problem under a constraint-processing algorithm possessed in systems of constraint logic programming languages may cause combinatorial explosion. Next, this paper demonstrates that a better result can be obtained by improving constraint atoms and algorithms for solving them so as to carry out constraint processing suitable for the problem. The "expansive" approach enables users to define efficient constraint atoms and constraint-solving algorithms for a given problem, and consequently the approach may derive an efficient solving method. Constraint Handling Rules (CHR) [8] is a kind of expansion of Constraint Logic Programming (CLP). In CLP, rules to solve constraints are built in a system, but in CHR, users can define some rules to solve constraints, the correctness of which is assured based on logical inference. Making use of user-defined rules to solve constraints presents difficulties in assuring to the correctness of solving method. In the "expansive" approach, users must guarantee the correctness of a solving method; therefore, such theoretical foundation (computation model) that users can easily guarantee the correctness of the solving method is required. In this study, the equivalent transformation (ET) computation model [1,14] is used to solve constraint satisfaction problems (CSPs) of Number-Place Problems. In CHR, users can define some rules to solve constraints, but rules in CHR constitute only a part of rules in the ET computation model [2]. In the ET computation model, rules

which can not be described by formulas can be defined as well as rules dealt with in CHR. For example, basic transformation rules for equality constraint described in [13] can not be dealt with in CHR. Solutions to CSPs can be classified into systematic search algorithms, represented by search based on backtracking, and stochastic search algorithms, represented by hill-climbing method. Systematic search algorithms guarantees the completeness of the algorithm but is not suitable for solving large-scale CSPs [4,7,15,21,24]. On the other hand, in lieu of guaranteeing the completeness of the algorithm, stochastic search algorithms can deliver practical approximate solutions at high-speed. However, its problem is that it falls into local optima while searching for solutions [6,16,19,20].

In this paper, the computing framework of “Problem Solving based on ET,” which effectively performs computations while preserving the algorithm's correctness In terms of problems in obtaining a solution set, the completeness of algorithms defined by conventional studies on CSP solving is that all solutions can be obtained. If an algorithm is complete and sound (obtained solutions are always correct), then that algorithm is correct, is utilized to solve CSPs and the effectiveness of the proposed method is demonstrated [17,18]. In this computing framework, a problem can be solved by simplifying declarative descriptions of the problem using ET, and the correctness of computation can be guaranteed over a broader range than the framework of logic paradigm. In the computing framework for problem solving based on ET, a problem is successively simplified into different problems by selecting and applying an appropriate rule from many ET rules; by showing that each transformation rule causes the equivalent transformation, computation can be guaranteed without changing the meaning of the given problem. Furthermore, this computing framework allows an easy introduction of the new data structures and rules necessary for improving the constraint-solving algorithms.

## II. COMPUTATION BY EQUIVALENT TRANSFORMATION

This study adopts, for problem solving, the computation model called “equivalent transformation”, where computation is regarded as equivalent transformation of declarative descriptions. This section describes its outline.

### 2.1. Equivalent Transformation of Declarative Descriptions

In our approach, a problem is formalized by a declarative description, which is a set of extended definite clauses, where we can treat various data structures including multisets, strings, and constraints, as well as usual terms [12]. A declarative description consists of the union of the definition part  $D$  and the query part  $Q$ . Given declarative description  $D \vee Q$  of a problem, query part  $Q$  is said to be transformed correctly in one step into new query part  $Q'$  by an application of a rewriting rule, iff declarative descriptions  $D \vee Q$  and  $D \vee Q'$  are equivalent, i.e., they have the same meaning. A rewriting rule is considered to be correct, iff its application always results in correct transformation. A correct rewriting rule is referred to as an equivalent Transformation rule (ET rule).

### 2.2. Problem Solving Based on Equivalent Transformation

In problem solving based on equivalent transformation, a declarative description is successively simplified into different declarative descriptions by ET rules, and from the simplified declarative description the solution may be obtained. If ET rules are employed in all transformation steps, the answer is guaranteed to be correct.

Rules used for transformations should be only those which transform a declarative description correctly. The rules in which the conditions to apply are true can be repeatedly used in any order. The system selects a rule to apply depending on computational situations. Each rule should include

- conditions that decide the applicability of the rule.
- definitions that determine a new set of clauses.

### 2.3. Variety, Correctness and Confluence of Computation

ET approach has the following properties.

#### [Variety of computation]

This approach can use not only unfolding rules [22] but also other various ET rules as transformation rules. By nondeterministic selection of ET rules at each step of computation, a variety of computation becomes possible.

#### [Correctness of computation]

Strict correctness is guaranteed in problem solving based on equivalent transformation. The correctness of rules can be determined without considering interrelations with other rules. As long as (correct) ET rules are applied, no matter what the rules are and in what order they are applied, correctness of the result of computation can be assured.

**[Confluence of computation]**

Meaning (which is defined in [12] by the name of declarative semantics) of a declarative description at each step of computation is preserved by an ET rule applied. Therefore, the confluence of solutions of a problem is achieved. It is obvious that the confluence of declarative descriptions is unnecessary for correct computation.

**2.4. Advantages of ET Approach**

ET approach has the advantages of

- describing various expressive rules since it offers abundant data structures.
- controlling processing flexibly since the order of computation is not fixed.
- improving algorithms at a lower cost by the introduction and the deletion of rules.

Furthermore, this paper shows that efficient constraint processing is possible since users are allowed to define constraint atoms without depending only on the “built-in” constraint atoms.

**III. PROBLEM AND ITS FORMALIZATION**

This section defines constraint satisfaction problem, explains number-place problem as an example, and formalizes the problem in terms of declarative descriptions.

**3.1. Constraint Satisfaction Problem and Its Example**

Constraint satisfaction problem (CSP) [24,25] is generally defined by the following three sets:  $I$ , a set of  $n$ -variables ( $X_1, X_2, \dots, X_n$ ); domain ( $D_1, D_2, \dots, D_n$ ), a set of the values which variables could take; and  $C : \{C_i(\dots X_j \dots)\}$ , a constraint which should be satisfied by the values of the variables. The objective of CSP is assignment of values to all variables in such a way that it satisfies all constraints in a given problem. In this study, number-place problems are used as examples of constraint satisfaction problems. Number-place is a puzzle in which numbers from 1 to 9 are placed in each small blank square (Fig. 1). There are two constraints:

(Constraint 1)

The numbers 1 through 9 will be placed into each small blank square.

(Constraint 2)

The same number can not be placed in any one column or row, nor within any one medium-sized box surrounded by a thicker border.

	6		2		4		5	
4	7			6			8	3
		5		7		1		
9			1		3			2
	1	2						9
6			7		9			8
		6		8		7		
1	4			9			2	5
	8		3		5		9	

Fig. 1 Number-place problem

**3.2. Declarative Descriptions Representing Problems**

This section formalizes problems in terms of declarative descriptions. Constraints to be satisfied when solving a numberplace problem are to satisfy a given assignment of the problem (given assignment predicate) and to adhere to the constraints of the problem (NP constraints predicate). These are represented with the following clause. The syntax of declarative descriptions is expressed by S-expressions. Symbols starting with “\*” represent variables.

```
(answer *numberplace) ←
(given_assignment *numberplace),
(NP_constraints *numberplace).
```

“given assignment” predicate is defined as follows. The “?” marks represent anonymous variables, each of which is different from all others.

```
(given_assignment *numberplace)←
```

```
(= *numberplace ((? 6 ? 2 ? 4 ? 5 ?)
(4 7 ? ? 6 ? ? 8 ?)
(? ? 5 ? 7 ? 1 ? ?)
(9 ? ? 1 ? 3 ? ? 2)
(? 1 2 ? ? ? ? ? 9)
(6 ? ? 7 ? 9 ? ? 8)
(? ? 6 ? 8 ? 7 ? ?)
(1 4 ? ? 9 ? ? 2 5)
(? 8 ? 3 ? 5 ? 9 ?))).
```

A variable, \*numberplace, is equal to the list which represents the given assignment of a problem. “NP constraints” predicate is expressed in accordance with (Constraint 1) and (Constraint 2) in Section 3.1. Fig. 2 shows the predicates which define the “NP constraints” predicate.

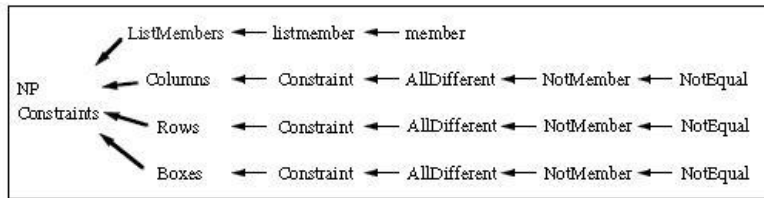


Fig. 2 Predicates which define “NP constraints” predicate

Member atom representing Constraint 1, providing that a variable is any of the numbers 1 through 9, is represented as follows:

```
(member *a (1 2 3 4 5 6 7 8 9))
```

AllDifferent atom representing Constraint 2, providing that elements of the list are different from each other, is represented as follows:

```
(AllDifferent (*a 6 *b 2 *c 4 *d 5 *e))
```

AllDifferent predicate is defined with Notmember predicate providing that an element does not belong to a given list. Notmember predicate is defined with NotEqual predicate providing that two arguments are not equal.

#### IV. RULES FOR SIMPLE CONSTRAINT ATOMS

In the problem solving based on equivalent transformation, various rules that are defined based on the declarative descriptions are applied. The problem can be successfully solved when all atoms in a clause are eliminated. In the problem shown in Section 3.2, first the answer clause is transformed and through various transformations, the NP constraints atom is transformed only into member atoms and NotEqual atoms. This section defines rules for these atoms.

##### 4.1. Rules for Member Atoms

In the previous section, it was shown that the NP constraints atom is transformed into only member atoms and NotEqual atoms. It is hard to transform the clause further without increasing the number of clauses if we pay attention only to one atom. We think the following example using two atoms.

```
(member *a (1 2 3 4 5 6 7 8 9))
(NotEqual *a 6)
```

In this case, since NotEqual atom shows that the variable \*a is not 6, 6 can be eliminated from the list (the second argument) of the member atom. However, the cost of such transformation is rather high because a computational cost of the order in the square of the number of atoms in order to find the two atoms, which are to be transformed, is required; therefore, it would be very efficient if the information of one atom could be spread to other atoms.

This study introduces a new data structure called an i-var [11]. An i-var is defined as a variable which has been given information. An i-var has the form in which a variable is followed by a symbol, “~”, and ends with S-expressions such as “apple” or “(1 2 3)”, as with ? ~apple or \*x~(1 2 3). Then S-expressions are called informations and the whole variable is called an i-var. A variable followed by nothing is called a pure variable. Users can freely get, replace, or eliminate information from i-var. Also, users can freely define the meaning of the information which the variable has. In the two atoms shown above, the member atom is transformed and the

variable \*a is changed to an i-var in which the variable \*a must be one of the numbers from 1 to 9. The change from a pure variable to an i-var instantly spreads over the entire clause. As a result, the NotEqual atom mentioned above is also changed into

$$(\text{NotEqual } *a \sim (1\ 2\ 3\ 4\ 5\ 6\ 7\ 8\ 9)\ 6).$$

All member atoms are transformed and all variables are changed to i-vars. Therefore, only NotEqual atoms remain in the body of the clause.

#### 4.2. Rules for NotEqual Atoms

NotEqual atom is a constraint such that two arguments are not equal. The candidate elimination means to eliminate elements (candidates) that do not obviously satisfy a constraint from elements (candidates) in the information of an i-var. The method for eliminating unnecessary numbers from candidates consists of the following procedure: when one argument in an atom is already decided as a number, the other variable in the atom can not be the same number, so the number can be eliminated from the candidates. When numbers in the information of a variable are reduced to only one number, the variable is unified with the number. Some examples of the rules are shown below.

- “candidate elimination” rule

When one argument is a number and the other argument is an i-var, the number is eliminated from the candidates in the i-var.

$$(\text{NotEqual } *a \sim (1\ 2\ 3\ 4)\ 4)$$

In such an atom, since the variable \*a can not be equal to the number 4, 4 is eliminated from the candidates, and this atom can be eliminated. The change in the information instantly spreads over the entire clause, and the atoms that have the variable \*a change.

$$*a \sim (1\ 2\ 3\ 4) \rightarrow *a \sim (1\ 2\ 3)$$

- “unification” rule

When either i-var reduces numbers in the information to one number, the variable is unified with the number, and the number is eliminated from the candidates in the other i-vars.

$$(\text{NotEqual } *a \sim (1\ 2\ 3\ 4)\ *b \sim (4))$$

In this case, since the numbers of the variable \*b are reduced to only one number, \*b is unified with the number, 4. As a result, since it is clear that the variable \*a is not 4, 4 is eliminated from the candidates in the variable \*a, and this atom can be eliminated.

$$*b \rightarrow 4, *a \sim (1\ 2\ 3\ 4) \rightarrow *a \sim (1\ 2\ 3)$$

Another rule is the “number check” rule, such that when both arguments in a NotEqual atom are numbers, checks are made to determine whether the numbers are different and then, when possible, the atom is eliminated. This rule also eliminates the entire clause when the elements consist of the same number.

#### 4.3. “Splitting” Rule

There may remain atoms in which candidates can not be reduced only using the rules described in the preceding section. This is because since there are nine possible values for one variable, both variables in the atom may be variables whose candidates are two or more. An example of such a NotEqual atom is shown as follows.

$$(\text{NotEqual } *a \sim (3\ 5\ 7\ 9)\ *b \sim (5\ 9))$$

Since the candidates of the variable \*b is reduced to two numbers, the “splitting” rule is employed, according to which a clause is separated into two clauses. When the “splitting” rule is applied, the clause is branched into two clauses: one clause of the variable \*b is unified with 5 and the other clause of the variable \*b is unified with 9. Computation proceeds in each clause and the clause that causes any contradiction is eliminated. However, computation efficiency usually decreases when the branching of a clause occurs. Therefore, less priority should be given to the “splitting” rule, in order to avoid the branching of a clause when possible.

## V. EXPLOSION OF PROCESSING TIME

The results obtained by solving problems by using the rules described in the previous section are shown as follows. The problem is number-place problem of size  $25 \times 25$ , i.e., 25 rows and 25 columns. The number of blank squares is the number of variables. The more the number of variables is, the greater amount of the computation is required. The horizontal axis in the graph in Fig. 3 shows the number of blank squares, i.e.,

the number of variables. 0 indicates that values are assigned to all variables. This graph shows the amount of processing time. The vertical axis shows the processing time required to obtain answers. From Fig. 3, the processing time does not change up to about 200 variables but the processing time drastically increases when the number of variables surpasses that extent: about 5 seconds for 225 variables, about 3.5 minutes for 250 variables, about 17 minutes for 275 variables, and about 100 minutes for 286 variables, and the problem with 300 or more variables can not be solved. This is because a clause has been separated into many clauses and a combinatorial explosion has occurred.

The next section introduces a new constraint processing to solve such a difficulty.

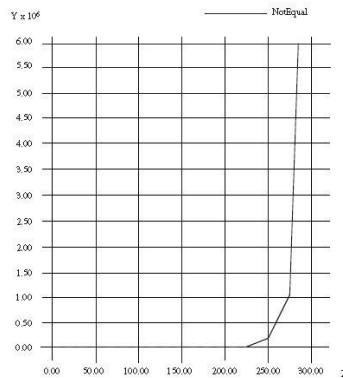


Fig. 3 Results of 25 × 25 puzzles

## VI. INTRODUCTION OF NEW RULES FOR ALLDIFFERENT ATOMS

This section improves the constraint-solving algorithms by introducing new constraints atoms to solve problems more efficiently.

### 6.1. Changing of Constraint Atoms

As described in Section 3.2, an AllDifferent atom is transformed into NotMember atoms. A NotMember atom is transformed into NotEqual atoms. That is, the candidate elimination is performed using constraints of NotEqual atom which is the simplest in the atoms. This is because constraints of NotEqual atom are the simplest and easiest to deal with. We do not transform AllDifferent atom into NotMember atoms, but instead we regard AllDifferent atom as the smallest unit and try to perform the candidate elimination, i.e., we deal with more complicated atoms. The reason is that since information in AllDifferent atom is more than that in NotMember atom, the candidate elimination can be performed by good use of those information (Fig. 4).

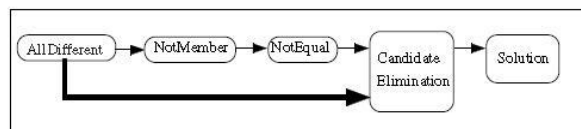


Fig. 4 Removing NotMember and NotEqual atoms

The next section defines the rules to perform constraint processing using constraints of AllDifferent atom where all elements in the list are different.

### 6.2. Rules for AllDifferent Atoms

This section defines the candidate elimination rules for AllDifferent atoms.

- “candidate elimination” rule

Elements that are identical to the numbers are all eliminated from the candidates of other i-vars.

$$\begin{aligned}
 &(\text{AllDifferent } (3 \text{ *a}^{\sim}(2 \ 3 \ 4) \ 5 \ \text{*b}^{\sim}(2 \ 3 \ 4 \ 5))) \\
 &\quad \downarrow \\
 &(\text{AllDifferent } (\text{*a}^{\sim}(2 \ 4) \ \text{*b}^{\sim}(2 \ 4)))
 \end{aligned}$$

- “unification” rule

When an i-var reduces candidates to one number, the variable is unified with the number.

(AllDifferent (\*a~(2 3 4) \*b~(2 3 4) \*c~(3)))



(AllDifferent (\*a~(2 3 4) \*b~(2 3 4) 3))

- “number decision” rule

(AllDifferent (\*a~(5 7 9) \*b~(5 9) \*c~(4 5 9) \*d~(4 5))

In this example, variable \*a can be determined as 7. The reason is as follows. The candidates of \*b, \*c or \*d are contained either in any two or in all three of 4,5,9. The number of candidates is three of 4,5,9 and the number of variables is also three of \*b, \*c, \*d. Then, the relation between the variables and the candidates (numbers) should be one-to-one. Therefore, three numbers of 4,5,9 are used as the values of \*b, \*c, \*d. \*a can be determined as 7 by removing 4,5,9 from the candidates of \*a.

## VII. COMPARISON AND CONSIDERATION

This section offers a comparison between results obtained through constraint processing using constraints of NotEqual atoms and those using constraints of AllDifferent atoms.

### 7.1. A Comparison in The Case of The 9 × 9 Puzzle

Table 1 shows a comparison between the results obtained by applying the candidate elimination rule to NotEqual atoms and those obtained by applying the candidate elimination rule to AllDifferent atoms for the same problem. In the processing time and the number of rule applications, the respective values of AllDifferent atoms when each value of NotEqual atoms equals 1 are shown.

Table 1 Results of the 9 × 9 Puzzle (Fig.1)

Atom	NotEqual	AllDifferent
Processing Time	1	0.37
Number of Rule Applications	1	0.01

The comparison above demonstrates that applying the candidate elimination rule to AllDifferent atoms enables the user to obtain better results on the processing time and the number of rule applications.

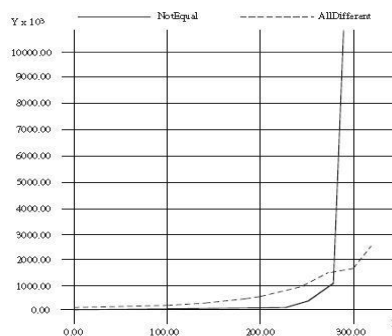


Fig. 5 Comparison of results of 25 × 25 puzzles

### 7.2. A Comparison in The Case of 25 × 25 Puzzles

Fig. 5 shows the results obtained by solving 25 × 25 puzzles (problems), which are discussed in Section V, through applying the candidate elimination rule to AllDifferent atoms. When the number of variables is 275 or less, the processing time is shortened by transforming the NP constraints atom to NotEqual atoms for constraint processing. When the number of variables is higher than that, the processing time required explodes, and consequently it is impossible to obtain a solution for this problem with 325 variables. However, in the case of constraint processing by using constraints of AllDifferent atom, even if the number of variables increases, we are able to continue performing computation. As shown in Fig. 5, we can obtain the solutions of a problem without an explosion of processing time. Thus the improvement in constraint processing enables us to solve problems which have previously been unsolvable.

### 7.3. Characteristics of Constraint Processing

The use of constraints of NotEqual atom is explained below. An AllDifferent atom is transformed into NotMember atoms. A NotMember atom is transformed into NotEqual atoms. The number of AllDifferent atoms is three times the number of squares in a set of squares. The number of NotEqual atoms is a value obtained by multiplying the number of AllDifferent atoms and the number of possible combinations for any two elements selected from the set of squares; therefore, the number of NotEqual atoms is enormously larger than that of AllDifferent atoms. For example, in the case of a  $9 \times 9$  puzzle, the number of AllDifferent atoms is 27, while that of NotEqual atoms is 972. In the case of a  $25 \times 25$  puzzle, the former is 75, while the latter 22,500. All atoms obtained in the cases above should be eliminated by applying transformation rules. Therefore, the larger the number of atoms is, the higher the number of rule applications becomes. Reducing the number of rule applications, however, may not lead to the shortening of processing time. The application of the “candidate elimination” rule to AllDifferent atoms has the following advantage. As described in Section 6.2, if there are two or more numbers in a body atom, the elimination of two or more numbers can be performed at a time regarding a variable (or two or more variables). Compared to the candidate elimination using constraints of NotEqual atom, the number of transformations is one, but a burden of one transformation becomes heavier. Because NotEqual atom is the most simplified, its constraint processing is also simple. The simpler the processing is, the shorter the processing time becomes, though the number of rule applications is larger.

Since the information in an AllDifferent atom is more than that in a NotEqual atom, we can define various rules for constraint processing by good use of those information. The unique rule, which uses constraints of AllDifferent atom, is called the “number decision” rule (See Section 6.2). When the number of variables to which a value can be assigned is only one, this rule enables assignment of the value to the variable. When this rule is applied to a NotEqual atom, a variable can not be unified with a number unless the number of candidates of a variable is one. However, only when this rule is applied to an AllDifferent atom, a variable can be unified with a number by using other information even when the number of candidates of a variable is not one. This is because elements of the list in the AllDifferent atom do not break the relations among the 9 elements which are different each other in specified squares.

### 7.4. Effect of Global Processing

As shown in Fig. 5, when the number of variables is 275 or less, constraint processing by using constraints of NotEqual atom shortens the processing time, and when it is over 275, the processing time explodes. This is because when a problem is a small-scale one, the smaller the cost required for single processing, the better the results obtained are; on the other hand, as the size of a problem becomes larger, the clause is branches explosively. Branching of the clause reduces the efficiency of computation, as in the case of backtracking. An explosive branch makes computation impossible. Since constraint processing by using constraints of NotEqual atom can perform only local processing – comparison of two elements in the atom, it is difficult to determine the values of variables; therefore, branches of clauses cause. Constraint processing by using constraints of AllDifferent atom enables the user to get solutions without causing an explosion in processing time. This is because the effective rules suppress the clause’s branching, though the cost required for single processing is large. It is clear that the larger the size of a problem is, the more effective such a global processing becomes. Such a global processing can be obtained by the user’s improving constraint-solving algorithms. From the observations above, it is clear that a large-scale and complicated problem should be solved not only through local processing but also through global processing. Therefore, we need a computing framework which defines a processing scheme suitable for a problem and improves the system.

## VIII. EFFECT OF USER-DEFINED CONSTRAINT PROCESSING

### 8.1. Definition of Flexible Constraint Processing

In various constraint logic programming languages, including CHIP [5] and Prolog III [3], the domains of constraints have been fixed, the constraint solvers of which have been provided by system designers. In other programming languages, the user also solves problems making use of subroutines and libraries. Therefore, the user is not allowed to change or improve rules and data structures which constitute algorithms, resulting in the incapability of the user when a problem goes beyond the range of the provided system. A computing framework, where a problem is solved by equivalent transformations, enables the user to share the rules as a library. Furthermore, as shown in Section VI, the user is allowed to define rules and data structures which carry out constraint processing suitable for a problem. If the builtin constraint-solving algorithms are suitable for a problem solving, the user easily obtains effective solutions. If not, the computing framework in the present study allows the user to compensate new data structures and constraint-solving rules to obtain effective solutions. Therefore, whenever the user solves complicated knowledge processing problems, the user becomes capable of extending the system.

## 8.2. Data Structures and ET Rules

In the computing framework proposed by this study, data structures, rules, and control descriptions of computation can be extended freely irrespective of the restrictions of the fixed framework. Section 4.1 introduces a new data structure called an i-var. Such data structures are transformed by equivalent transformation rules. Various constraints are also transformed by equivalent transformation rules. These rules can be easily defined by the definition of a predicate. Therefore efficient data structures, efficient rules, and efficient control can be easily and simply obtained from the specification of a problem.

## 8.3. Ensuring The Correctness of Solving Method

When the system provides constraint-solving algorithms, it ensures the correctness of constraints to be treated. When a user improves and defines newly constraint atoms, the user should ensure the correctness of solving method; therefore, such theoretical foundation that the user can easily guarantee the correctness of the algorithm is required. The framework of "problem solving based on equivalent transformation," on the other hand, strictly ensures the correctness of a solution. In this computing framework, since each rule transforms equivalently and correctly a declarative description at each computation step, the application of those rules in any order as long as they are correct ensures the correctness of a solution. Thus, rules transform mutually independently and correctly, a requirement which is called the "independence of rules." Therefore, the extension of data structures, changes in rules and the addition of rules due to a change in constraint atoms (as long as the new rules are correct) present no barrier to improving algorithms with the correctness of solving methods preserved.

## IX. CONCLUSIONS

This paper has solved number-place problems using a computing framework of "problem solving based on equivalent transformation," and showed the effectiveness of the method. Since this computing framework allows for easy introduction of new data structures or rules while preserving the algorithm's correctness, adding better data structures and rules to the system makes it possible for computations to be performed in a more efficient manner.

## REFERENCES

- [1] Akama,K. and Nantajeewarawat,E., "Formalization of the Equivalent Transformation Computation Model," *Journal of Advanced Computational Intelligence and Intelligent Informatics*, vol.10, no.3, pp.245–259, 2006.
- [2] Chippimolchai,P., Akama,K., Ishikawa,T., and Wuwongse,V., "Correct Computation with Multi-Head Rules in the Equivalent Transformation Framework," *Proc. of the 4th International Conference on Intelligent Technologies*, pp.531–538, 2003.
- [3] Colmerauer,A., "An introduction to Prolog III," *Communications of the ACM*, vol.33, no.7, pp.69–90, 1990.
- [4] Dechter,R., "Constraint Processing," Morgan Kaufmann Publishers, 2003.
- [5] Dincbas,M., et al., "The Constraint Logic Programming Language CHIP," *Fifth Generation Computer Systems*, Tokyo, Japan, 1988.
- [6] Frank,J., Cheeseman,P., and Stutz,J., "When Gravity Fails: Local Search Topology," *Journal of Artificial Intelligence Research*, vol.7, pp.249–281, 1997.
- [7] Freuder,C.E., et al., "Systematic Versus Stochastic Constraint Satisfaction," *IJCAI-95*, pp.2027–2032, 1995.
- [8] Frühwirth,T., "Theory and Practice of Constraint Handling Rules," *Journal of Logic Programming*, Special Issue on Constraint Logic Programming, vol.37, nos1-3, pp.95–138, 1998.
- [9] Jaffar,J. and Lassez,J.-L., "Constraint Logic Programming," *Proc. 14th Ann. ACM Symp. Principles of Programming Languages*, pp.111–119, 1987.
- [10] Jaffar,J. and Maher,M., "Constraint Logic Programming, A Survey," *J. of Logic Programming*, vol.19/20, pp.503–581, 1994.
- [11] Koike,H., Akama,K., and Mabuchi,H., "Dynamic Interaction of Syntactic and Semantic Analyses Based on the Equivalent Transformation Computation Model," *Journal of Advanced Computational Intelligence and Intelligent Informatics*, vol.10, no.3, pp.302–311, 2006.
- [12] Lloyd,J.W., "Foundations of Logic Programming," Second Edition, Springer-Verlag, 1987.
- [13] Mabuchi,H., Akama,K., Miura,K., and Ishikawa,T., "Constraint Solving Specializations for Equality on an Interval-Variable Domain," *Journal of Advanced Computational Intelligence and Intelligent Informatics*, vol.11, no.2, pp.210–219, 2007.
- [14] Mabuchi,H., Akama,K., and Wakatsuki,T., "Equivalent Transformation Rules as Components of Programs," *International Journal of Innovative Computing, Information and Control*, vol.3, no.3, pp.685–696, 2007.
- [15] Mackworth,A., "Constraint Satisfaction," In *Encyclopedia of Artificial Intelligence* (ed.) Shapiro, S.C.), vol.1, pp.205–221, JohnWiley & Sons, Inc., 1987.
- [16] Minton,S., Johnston,M.D., Philips,A.B., and Laird,P., "Minimizing Conflicts: A Heuristic Method for Constraint Satisfaction and Scheduling Problems," *Artificial Intelligence*, vol.58, pp.161–205, 1992.
- [17] Miyajima,S., Akama,K., Mabuchi,H., and Wakamatsu,Y., "Automatic Detection of Incorrect Rules in Equivalent Transformation Programs," *International Journal of Innovative Computing, Information and Control*, vol.5, no.8, pp.2203–2218, 2009.
- [18] Miyajima,S., Akama,K., and Mabuchi,H., "Algorithmic Debugging of Equivalent Transformation Programs using Oracle Rules," *International Journal of Innovative Computing, Information and Control*, vol.7, no.8, pp.4703–4716, 2011.
- [19] Mizuno,K., Kanoh H., and Nishihara,S., "Solving Constraint Satisfaction Problems by an Adaptive Stochastic Search Method," *Journal of Information Processing Society of Japan*, vol.39, no.8, pp.2413–2420, 1998.
- [20] Morris,P., "The Breakout Method for Escaping from Local Minima," *AAAI-93*, pp.40–45, 1993.
- [21] Nishihara,S., "Fundamentals and Perspectives of Constraint Satisfaction Problems," *Journal of Japanese Society for Artificial Intelligence*, vol.12, no.3, pp.351–358, 1997.
- [22] Pettorossi, K. and Proietti, M., "Transformation of Logic Programs: Foundations and Techniques," *Journal of Logic Programming*, vol.19/20, pp.261–320, 1994.

- [23] Stuart Russell, Peter Norvig, "Artificial Intelligence, A Modern Approach," Second Edition, Prentice Hall Series in Artificial Intelligence, Pearson Education, 2003.
- [24] Tsang,E., "Foundations of Constraint Satisfaction," Computation in Cognitive Science, Academic Press, 1993.
- [25] van Hentenryck,P., Simonis,H., and Dincbas,M., "Constraint satisfaction using constraint logic programming," Artificial Intelligence, vol.58, pp.113–159, 1992.

# Experimental Analysis & Designing of abrication Method Of Shear Fatigue Strength Of Glass Fiber Epoxy And Chapstan E-Glass Epoxy Laminates

Pns Srinivas<sup>1</sup>, Movva Mounika<sup>2</sup>, M.Rajya Lakshmi<sup>3</sup>.

<sup>1</sup> M.Tech PVP Institute Of Engineering & Technology, Kanuru, Vijayawada.

<sup>2</sup> Asst Professor Of Mechanical Department In PVP Institute Of Engineering & Technology, Kanuru, Vijayawada.

<sup>3</sup> Asst Professor Of Mechanical Department In PVP Institute Of Engineering & Technology, Kanuru, Vijayawada.

## ABSTRACT

The present project work mainly is focusing on development of manufacturing process and establishing critical test procedures for the polymer reinforced composite materials to be used in automobile & power plant equipments. This experiment played an important role in estimation of stiffness of the laminate which in turn helps for the testing to evaluate the stiffness of the laminate for further mathematical analysis. The evaluating elastic properties and the flexural stiffness of the composite beam by theoretical calculation is compared with experimental value analysis and from which the relations of mechanical properties are derived. This reduction in stiffness can further be improved by advanced manufacturing process such as compressor moulding, macro sphere moulding & auto clave moulding and the results obtained from the analytical testing are used to calibrate the load transducers. The load transducer shows a linear response to the load from this is clearly evident that the testing could be able to generate the useful data for evaluating the fatigue failure behavior of the composites. The data acquisition system from standard manufacturer of model TSI-608 which exactly meets requirements. A continuous plot of time verses load could be obtained We can say that the required data can be generated as per expectations, which could be utilized to establish the fatigue failure behavior any kind of composite laminate.

**KEYWORDS:** glass epoxy composites, fatigue test rig, transducer, pressure plate, CATIA

## I. INTRODUCTION

The laminated composite materials usage is increasing in all sorts of engineering applications due to high specific strength and stiffness. Fiber reinforced composite materials are selected for weight critical applications and these materials have good rating as per the fatigue failure is concerned. Present work is aimed to analyze the behavior of each laminate under the flexural fatigue test rig. Therefore here different types of composite materials are selected for test specimens. For this load transducer, the accuracy level required in transducer body is an important task. As selection of a transducer and work for its consistency is important consideration. Therefore a sensitive, consistently strong transducer to meet the axial tension-compression fatigue loading is required. (2)To provide dynamic sensibility to the transducer, foil type resistance strain gauges are used. The geometric shape of the load transducer is an important factor to be considered, to impart sufficient strain to the strain gauge, which in turn generates a noticeable signal with noticeable amplitude in the form of a voltage signal. The dynamic nature of loading could be read in the form of a signal is possible only with the iso-elastic type of strain gauges. In order to get the information after which it fails software is created which produces the waves depicting the response of the transducer to the loads applied on it. The present project work mainly is focusing on development of manufacturing process and establishing critical test procedures for the polymer reinforced composite materials to be used in certain engineering applications.

## II. FATIGUE

The flexural fatigue failure in laminated composite materials is a very common failure mode in most of the FRP components. As reinforced polymers used in weight critical applications, often over designed to compensate fatigue failure lead to the increase in weight which in turn hampers the objective of designer. In this

connection the investigation on flexural fatigue failure behavior of laminate to be used in the component is very important. As standard equipment and test procedures are not available.

## **2.1 Fatigue**

When a material is subjected to repeated stresses or loads, it fails below the yield stress. Such type of failure of a material is known as fatigue.

### **2.1.1 Characteristics of Fatigue**

- In metals and alloys, the process starts with dislocation movement, eventually forming persistent slip bands that nucleate short cracks.
- Fatigue is a stochastic process, often showing considerable scatter even in controlled environments.
- The greater the applied stress range, the shorter the life.
- Fatigue life scatter tends to increase for longer fatigue lives.
- Damage is cumulative. Materials do not recover when rested.
  
- Fatigue life is influenced by a variety of factors, such as temperature, surface finish microstructure, presence of oxidizing or inert chemicals, residual stresses, contact, etc.

## **2.2 Flexural Fatigue**

When a material is subjected to variable bending stresses or loads, it fails below the yield stress.

## **2.3 Fatigue Test Applications**

Fatigue testing helps determine how a material or product design will perform under anticipated service conditions. Many fatigue tests repeat the application of loads by controlling stress that is repeated for millions of cycles. In many engineering applications, products or materials experience vibration or oscillatory forces so it's important to predict and prove fatigue life, or cycles to failure under loading conditions. There are as many specialized fatigue testing protocols or test methods as there are products designed for fatigue applications. A few are supported as industry standard test methods but most designs are unique so machines are configured to match their needs. Metals and metal substitutes such as advanced composites are commonly used for fatigue resistant designs, so standards are more available. Low Cycle Fatigue (LCF) or strain controlled tests, High Cycle Fatigue (HCF) or load controlled tests, and even Random Spectrum tests are now common. Medical implants for orthopedic and intravascular use are also widely tested to FDA requirements.(4)

## **2.4 Mechanism of Fatigue Failure in Laminated Composites**

“Composites are a combination of a reinforcement fiber in a polymer resin matrix, where the reinforcement has an aspect ratio that enables the transfer of load between fiber, and the fibers are chemically bonded to the resin matrix. This precise definition accounts for the attributes of composites as an engineering material and differentiates them from a lot of combined materials having a lesser degree of synergy between the individual components. Cyclic deformation process in fiber-reinforced materials differs widely from those in homogenous isotropic materials. For example, crack nucleation plays a significant role in the latter; in the former, cracks and failure zones are often formed in the very first few cycles. In fact, there are often voids and defects in the material even before cycling begins. Secondly, fiber reinforced materials are characterized by a high degree of anisotropy; the ratio of longitudinal to transverse moduli varies from about 5 for glass fiber-polymers to about 25 for graphite or boron fiber-polymers. The stress field around a flaw in such a highly anisotropic medium is significantly different from one in isotropic material consequently, while homogeneous isotropic materials usually fail in fatigue by the nucleation of a crack which propagates in single mode, composite materials generally exhibit a variety of failure modes including matrix crazing or micro cracking, individual fiber failures resulting from statistically distributed flaw strengths, debonding, delamination, void growth etc. In addition, several of these failure modes are generally present at any given time prior to failure.

Further, failure mechanisms in the fiber are different from those in the matrix. It is well established, for example, the glass by itself does not exhibit dynamic fatigue failure but fails in „static „ fatigue as a result of thermally activated stress corrosion reactions of water vapor at surface flaws. When glass fiber are enclosed in a polymer matrix, and subjected to cyclic loading, it is not clear whether there would be reactions at the entire glass polymer interface due to moisture absorption through the polymer layer, or whether matrix micro cracks, alone (resulting from cyclic failure), would provide a conduit for preferential attack by water vapor over a localized area on the fibers at the crack front leading to further crack growth and eventual fatigue failure of the composite.(5) From this description it is clearly evident that the fatigue life of composite laminate is influenced

by many factors. The degree of significance of the above mentioned factors cannot be established with confidence. This present work is aimed at establishing a suitable test procedure for the fatigue life characteristics with a low cost test rig to meet the real time design requirements. The features of the test rig are explained in following script. As the test proceeds for so many number of load cycles (is of order  $10^6$  cycles) the generated from dynamic transducer cannot record manually. Then the signal conditioning system coupled with analog to digital conversion electronic circuit and the data logging software incorporated in the test rig. This logged data can be analyzed to establish the failure behavior and fatigue life characteristics of the composite laminates. This method of testing can be utilized for fatigue applications.



Fig 1. Positioning of composite material in vertical direction in Pictorial view of Fatigue Test Rig



Fig 2. Positioning of composite material in horizontal direction in Pictorial view of Fatigue Test Rig

The Bending fatigue test rig is capable of simulating bending fatigue load of 0 to 1000N on the test coupon at a frequency of 94 cycles per minute. The king pin is assembled to the dovetail mechanism which could be fixed at desired eccentricity. That provides desired bending force on the specimen.

### **2.5.1 Important Components of Test Rig**

- [1] Load cell
- [2] Specimen holding beam
- [3] Dovetail assembly
- [4] Induction motor
- [5] Adjustable columns(Sliding )
- [6] Electronic circuit(Signal Conditioning System)
- [7] Data acquisition software
- [8] Connector from the electronic circuit to the computer. Printer(7)

### 2.5.2 Working Principle of Test Rig

The schematic diagram of test rig as shown in Fig. 3.2. is self explanatory. The hinge eccentricity from the center of the crank is directly proportional to the deflection of the composite specimen. And this deflection resisting force is experienced by the linkage which is equipped with strain measurement. The strain gauge bonded to the linkage (load cell) elongates and contracts along with the load cell which in turn imbalances the balanced bridge circuit connected to the strain gauge. The output voltage of the bridge circuit is directly proportional to the deflection load of the composite specimen. As crank rotates with the constant rpm of 94 the strain measuring system develops voltage proportional to the degree of deflection. The voltage waveform is a pure sine wave. The cyclic load applied to the composite specimen generates a fatigue crack at the fixed end A from the Fig. 2.2.

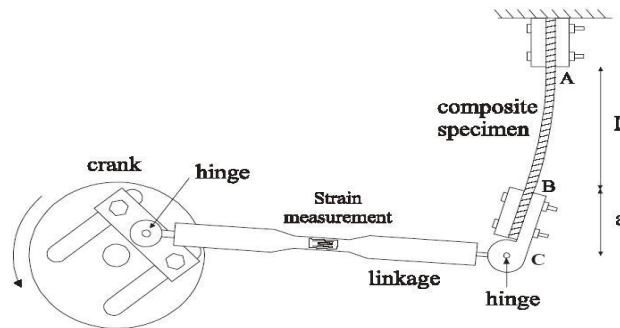


Fig.3. Schematic line diagram of Hinge Eccentricity, Load Cell and Specimen Holding Arrangement

Which in turn reduces the stiffness of the composite specimen and that is been clearly reflected on the voltage output from the strain measuring bridge circuit. The amplitude of wave form decreases as the damage progresses in the due course as the cyclic loading proceeds from 0 cycles to n number of cycles. This diminishing wave form reveals the health of the laminate as the time progresses. The recording of data in digital form could lead to analyze the fatigue damage pattern accurately. (9)

### 3.5.3 Specifications of the Test Rig

Bending load capacity	-----	0 to 1200N
Frequency	-----	1.57 to 10 RPS
Specimen specifications	-----	200x40x6 mm
Eccentricity	-----	0 to 250 mm

## III. LOAD CELL

**Introduction:** Load cell is a very important component which senses load and delivers a voltage analog signal, which is proportional to the intensity of load. This consists of a metallic body designed to meet the requirements of the working load range, generally it is made of aluminum alloy. The foil type strain gages are fixed to the body of the load cell. When the body of the load cell is subjected to load, the strain induced is transmitted to the strain gage. Dynamic load sensor (LOAD CELL) is important component of the test rig.(10)

### Selection of a Transducer:

The selection of the correct load transducer is followed by the following steps:

1. Material selection.
2. Proposing geometric models.
  - ❖ High sensitive type
  - ❖ Medium sensitive type

The material selection is based on the elastic property that is young's modulus. This should be capable of providing sufficient elastic strain for a given load application range. As per the present load application range of 0 -1000 N the material selected for this application is an aluminum alloy of Young's modulus 70 GPA.

**a. High Sensitive Type Load Cells**

**Ring type load cell:** The ring type load cell body is made of Aluminum. This is proposed in view of simulating more strain in the segments of hollow cylindrical segments, when the body is subjected to tensile and compressive stress. The ring type load cell is furnished in Fig. 4.1. The ring portion of the load cell body is first part of the body to undergo strain by virtue of changing its shape, which is a perfect circular to oval shape. When the load cell is subjected to tensile load, the inner portion of the body is subjected to tensile strain and the outer portion is subjected to compressive strain. This is proposed in the view of gaining strong signal from the bridge circuit.

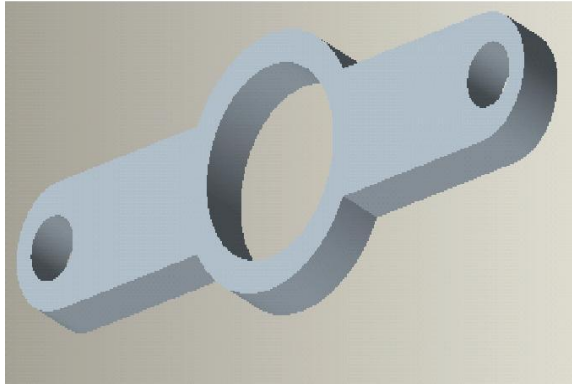


Fig. 4. Ring Type Load Cell

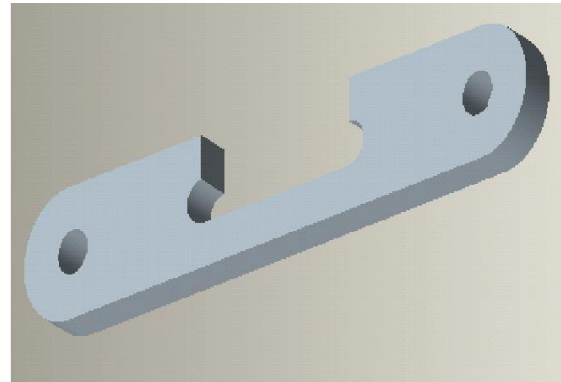


Fig. 5. C-Type Load Cell

**“C” type load cell:** The C type load cell is supposed to be strained in the thinner portion of the body. **b. Medium Sensitive Type Load Cells**

**H-Type Load Cell:** “H” type of load cell body is proposed to meet the dynamic loading situation of the flexural fatigue test rig.

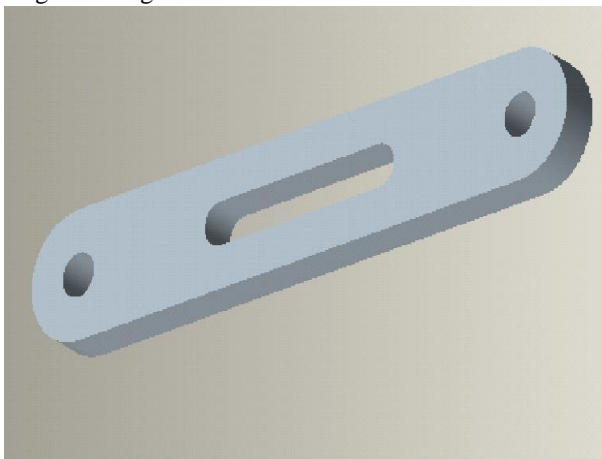


Fig. 6. H-Type Load Cell

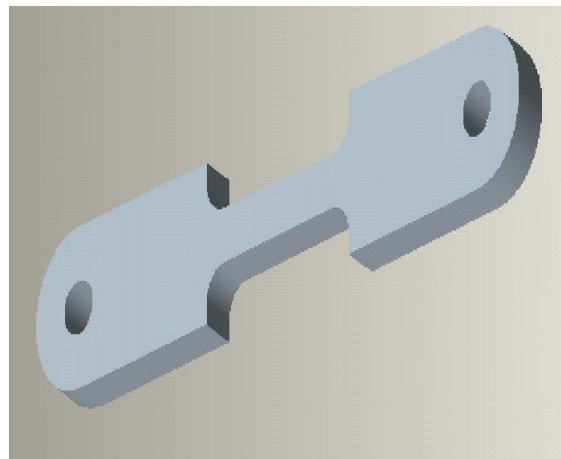


Fig.7.-Type Load Cell

**“I” Type Load Cell:** “I” type load cell having the thinnest gauge portion among the proposed load cell body models.

**Pillar Type Load Cell:** Among the load cell bodies proposed are observed carefully, and then the cylindrical gauge portion is proposed in view of achieving same strain on the gauge bonding area of the load cell body.

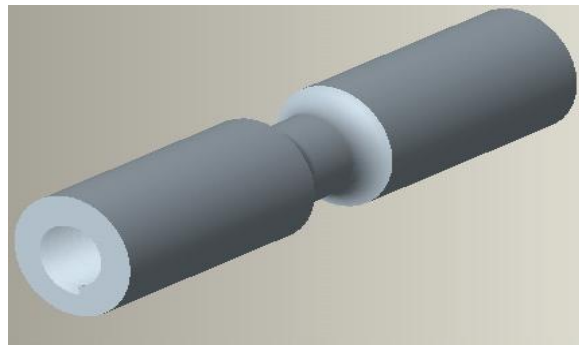


Fig.8. Pillar Type Load Cell

#### IV. ELECTRONIC CIRCUIT

**Introduction:** The electronic circuits are also very important a component of system and this are capable of amplifying the analog signal coming from the load cell and digitizes it to have provision of storing the data accurately to analyzing the data regarding stiffness degradation behavior of the specimen.

##### 4.1 Electronic Circuit for Signal Conditioning and Data Logging Systems

Dynamic load sensing is a mechanism, which senses the fluctuating loads with respect to time. A load cell (strain gage type) is a transducer, which senses the varying loads and changes its dimensions proportional to stress. The strain gage is incorporated in the bridge circuit and change in its resistance due to strain will unbalance the bridge. This unbalance voltage is amplified by the instrumentation amplifier. (12)A real time application of dynamic load sensing which convert the analog voltage from instrumentation amplifier to digital voltage by an ADC. This digital voltage is fed to computer via USB port. The sensing element which is an electrical type load cell senses the strain. The strain gage is glued to the load cell. The resistance of the load cell is 350 ohms resistors. This bridge is excited by the 10volts DC supply. Under no load condition i.e., when strain gage is not strained the bridge is under balanced condition. When load is applied on the load cell, the dimensions of strain gage gets changed thereby its resistance is varied. The amount of strain applied on the load cell proportionally changes the resistance of the strain gage. This change in resistance causes the bridge to unbalance. (13)This unbalanced voltage is proportional to the load applied on the specimen. In the first stage of amplification the gain has been limited to only 100 even though the capability of AD620AN is having a gain of 1000. This decision has been taken by carefully observing characteristics of the instrumentation amplifier to avoid unnecessary interference. The typical circuit to the signal conditioning system is shown in following Fig. 5.1.

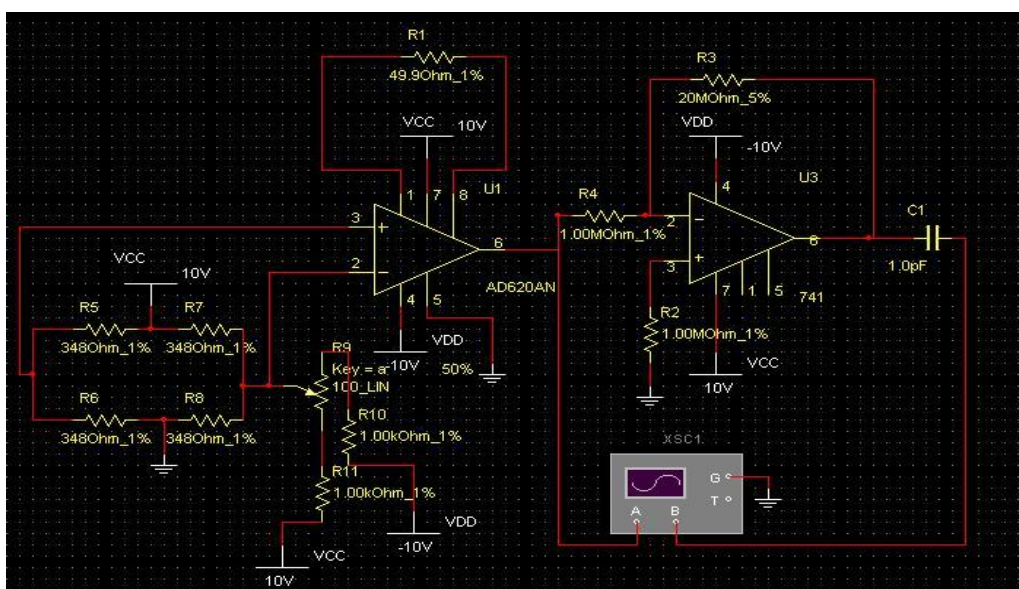


Fig 9.Signal conditioning circuit layout

## V. EXPERIMENTATION

### Introduction to Flexural Fatigue Experimentation

The present experimentation is aimed to understand the flexural fatigue behavior under high cycle fatigue conditions of Glass Fiber Epoxy, Chapsten E-Glass Epoxy and Glass Fiber Polyester Epoxy laminates. Before getting into the experimentation work, the evaluation of mechanical properties of glass fiber epoxy laminates is very important. A laminates of 200mm length, 40mm width and 6mm thickness were prepared. And from this laminates tensile tests were conducted for calculating the starting load on specimens for conducting fatigue test.

### 5.1 Loading Criteria for Flexural Fatigue Analysis of Glass Fiber Epoxy Laminates

For simulating high cycle flexural fatigue on test coupons, the calculations were made to estimate the bending loads considered to simulate stresses of the order of 50% of maximum tensile strength. To estimate the bending load, tensile tests were carried out on laminates. The tensile test results of specimens of Glass fiber epoxy, Chapsten E-glass epoxy and Glass fiber polyester epoxy are furnished in table No. 6.1.

And the corresponding bending loads to be applied are calculated with reference to the beam bending equation.  $M/I = F/Y$

The specimen is fixed to fatigue testing rig in cantilever mode, then the Maximum bending moment  $M = WL$  where  $W$  is the bending load applied on the specimen. The distance from the neutral axis to the surface of specimen is  $Y$ , which is equal to half the thickness of the specimen.

$$Y = t/2$$

Moment of Inertia of the specimen  $I = bh^3/12$  and Bending stresses induced in the specimen

$F = 1/2(\text{Ultimate Tensile strength of the specimen})$  From the above theory, bending load for each specimen is obtained.

#### a) Metallic Mould

The mould is made of MS material. To prevent the leakage of resin, four dams were fixed through nuts and bolts on a 10 mm thick MS plate which is machined by facing operation on lathe machine. The mould cavity area is 300X300 mm<sup>2</sup>

The mould with above specifications as shown in the figure 6.1. The required pressure is applied through pressure plate by tightening the nuts and bolts, the arrangement of which is shown in figure 6.2.



Fig. 10. Representation of Mould



Fig. 11. Representation of Pressure Plate

#### b) Pressure Plate

20 mm thick MS pressure plate with flat turned surface finish ensuring perfect flatness is used in order to prevent crippling and flexing due to compressive forces produced due to the top cover plate.

With the above mentioned precautions a laminate, of good quality can be made as shown in figure 6.3. From this laminate the test coupons are cut with required specifications which have already been discussed.

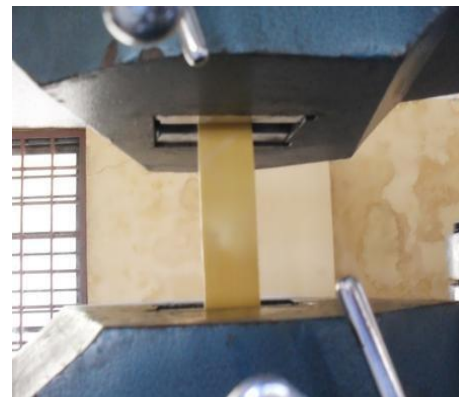


Fig 12. Laminate Moulded from the Metallic Mould by Compression Moulding Technique

**5.2 Tensile Tests**

Tensile tests are performed on the specimens and the tabulated values are furnished in table 6.1. The specifications of the test specimen are 200mm length, 6mm thickness and 40mm width. Following figures related to tensile tests conducted on various specimens. The figure represents the tensile test in progress. The figures to furnish below are specimens subjected to tensile test.

Specimens	Max strength(MPa)	Tensile
Glass fiber epoxy	358	
Chapsten E-glass epoxy	207	
Glass fiber polyester Epoxy	74.5	



**Table 1. Tensile Test Results**

**Fig. 13. Tensile Test in Process**



Fig. 13.1 Tensile Test Specimens of Glass Fiber Epoxy, Chapsten E-Glass Epoxy and Glass Fiber Polyester Epoxy

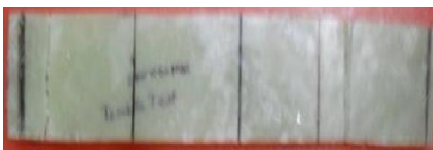


Fig. 13.2 Glass Fiber Epoxy Specimen after Tensile Test



Fig 13.3 Chapsten E-Glass Epoxy Specimen after Tensile Test



Fig. 13.4 Glass Fiber Polyester Epoxy Specimen after Tensile Test

## VI. RESULTS AND DISCUSSIONS

### Introduction

The present project work is aimed at establishing certain mechanical properties while designing fiber reinforced components for engineering applications. This experiment played an important role in estimation of stiffness of the laminate which in turn helps the user of the testing to evaluate the stiffness of the laminate for further mathematical purposes. The evaluating elastic properties and estimating the flexural stiffness of the composite beam and from the analytical evaluation of flexural stiffness has been matched with the theoretical calculations. This loss in stiffness of composite laminate is due to inherent defects generally occurs during welding and curing of the reinforced component. This reduction in stiffness can further be improved by advanced manufacturing process such as compressor moulding and auto clave moulding and the results obtained from the analytical testing are used to calibrate the load transducers. The load transducer shows a linear response to the load from this is clearly evident that the testing could be able to generate the useful data for evaluating the fatigue failure behavior of the composites. This data acquisition load generates the digital of time verses voltage by converting this data into time verses voltage with suitable multiplying factors. The data acquisition system from standard manufacturer of model pci-207 which exactly meets requirements. A continuous plot of time verses load could be obtained. We can say that the required data can be generated as per expectations, which could be utilized to establish the fatigue failure behavior any kind of composite laminate.

### 6.1 Flexural Fatigue Failure Behaviour of Glass Fiber Epoxy Laminate

Flexural fatigue failure behavior of laminates exhibits stiffness decay with respect to number cycles of load application. In this work ORIGIN LAB curve fitting tool is used to plot the data, number of cycles verses instantaneous maximum bending load within the cycle. The total scheme of experimentation is conducted at constant amplitude of bending. This phenomenon of bending load for yielding constant deflection is also known as stiffness. The test specimen used is shown in Fig. 7.1.



Fig. 14. Glass Fiber Epoxy Test Specimen

From the data logging system, the converted data is load applied on the specimen and number of cycles is given in the table 7.1. This data is used in plotting stiffness degradation curves.

Table 2. Stiffness Degradation Data of Glass Fiber Epoxy laminate

Number of Cycles	LOAD in NEWTONS				
0	320.006	5096.22	168.473	14894.6	116.910
100.48	311.663	5532.68	168.306	15305.93	114.223
219.8	291.354	4981.61	164.48	15769.08	113.781
		6055.49	163.633	16552.51	113.09
		6305.12	163.08	17397.17	113.046

345.4	281.055	6355.36	162.17	18012.61	111.728
405.06	278.333	6466.83	160.97	18552.7	108.632
538.51	278.356	6531.2	160.5	19196.4	104.075
591.89	270.37	6590.86	157.48	19915.45	100.07
676.67	267.555	6626.97	157.167	21078.82	95.11
797.56	267.553	6653.66	154.957	22000.41	88.041
904.32	264.895	6686.63	152.7	22564.04	87.966
943.57	262.481	6714.89	152.586	23242.28	84.687
1029.92	242.97	6749.43	152.16	23831.03	83.902
1146.1	234.243	6772.98	150.94	24287.9	77.38
1890.28	226.802	6821.65	150.982	24689.82	73.771
2138.34	225.75	7380.57	149333	25170.24	70.9
2474.32	223.974	7567.4	148.687	25481.1	68.147
2701.97	221.938	7892.4	145.935	25865.75	67.971
2739.65	219.28	8262.91	145.701	25906.57	65.935
2797.74	206.40	8700.94	142.19	26602.08	65.77
2824.43	202.321	9132.7	140.777	27245.78	65.16
2964.16	198.327	9679.05	137.973	28164.23	63.473
3058.36	195.506	9964.8	137.25	29088.96	62.413
3110.17	193.661	10489.17	133.216	29665.15	62.03
3303.28	185.08	11366.8	132.632	30506.67	60.127
3496.39	182.853	11999.51	130.713		
4114.97	179.851	12767.24	126.624		
4491.77	177.786	13547.53	125.163		

The data obtained from the experiments is plotted in Fig. 7.2. Results obtained reveal that the nature of behavior of the material is revealing exponential decay in its mechanical properties due to fatigue. This type of plotting is normally known as “Stiffness Degradation Curve plotting”. From the figure it is clear that the bending load is dropped from

320N to 60.127N and attained pivoting state where further reduction in stiffness is not noticed. Pivoting state is noticed at 25,000cycles.

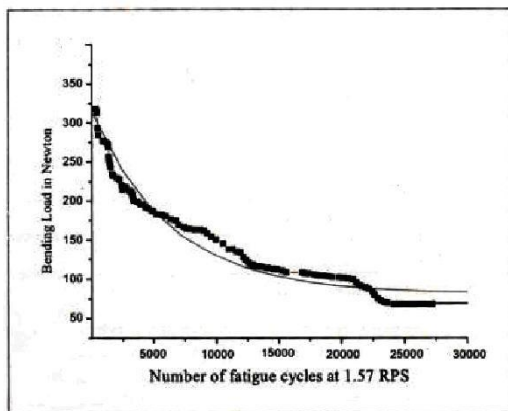


Fig. 14.1 Stiffness Degradation behaviour of Glass Fiber Epoxy laminate Number of Fatigue Cycles at 1.57 RPS for Glass Fiber Epoxy Laminate

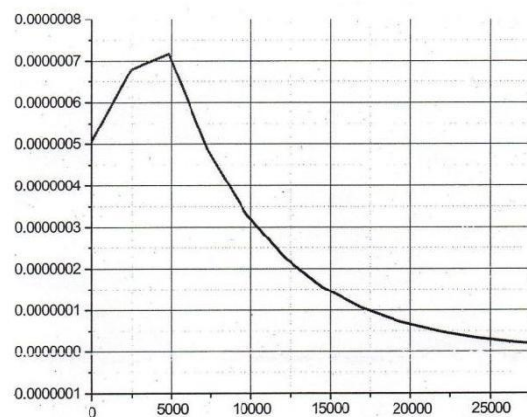


Fig. 14.2 Second order differential curve of Glass Fiber Epoxy laminate derived from Fig.

7.2 Flexural Fatigue Failure Behaviour of Chapsten E-Glass Epoxy Laminate

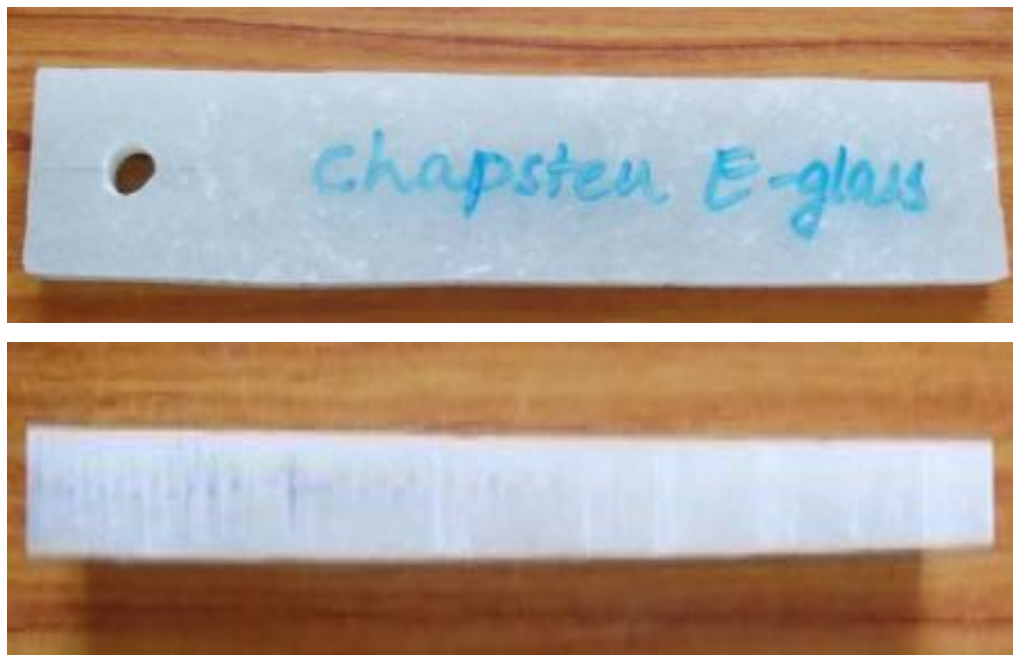


Fig. 15. Chapsten E-Glass Epoxy Test Specimen

The Flexural fatigue analysis data obtained from the experiment for Chapsten E-glass epoxy laminate is given in table 7.2. And the stiffness degradation is plotted in Fig.7.5. From this figure it is observed that the bending load dropped from 318.764N to 27.416N. Compared to Glass fiber epoxy specimen stiffness degradation curve, it is observed that there is smooth reduction in stiffness. The stiffness at the pivoting state is 27.416N as per the experiment. The stiffness of the specimen at the pivoting state is 8.6% of the virgin specimen.

Table 3. Stiffness Degradation Data of Chapsten E-Glass Epoxy laminate

Number of Cycles	LOAD in NEWTONS				
0	318.764	7353.88	79.787	18454.02	34.801
65.94	203.285	7523.44	74.421	18977.65	34.46
202.53	122.103	7656.89	71.113	19501.28	34.12
244.92	120.388	8247.21	68.1	20024.91	33.775
281.03	119.051	8597.32	65.6	20548.54	33.433
310.86	115.772	8685.24	54.7	21072.17	33.091
438.03	110.53	8859.51	47.73	21595.8	32.75
477.28	108.383	8913.43	46.77	22119.43	32.406
507.11	107.142	8962.47	45.356	22643.06	32.064
582.47	105.698	9014.62	44.756	23166.69	31.722
610.73	104.392	9452.74	43.9	23690.32	31.38
723.77	102.612	9924.73	42.235	24213.95	31.04
761.45	101.331	10732.22	41.766	24755.32	30.7
1339.21	98.353	11219.35	40.565	25296.69	30.354
1734.85	97.95	11763.48	39.96	25838.06	30.112
2391.11	97.62	12132.83	38.91	26379.43	29.67
2634.46	97.21	12764.03	38.565	26290.8	29.33
3367.65	96.73	13217.72	38.223	27462.17	28.985
4461.94	94.842	13741.35	37.881	28003.54	28.643
		14264.98	37.54	28544.91	28.3
		14788.61	37.2	29086.28	27.96

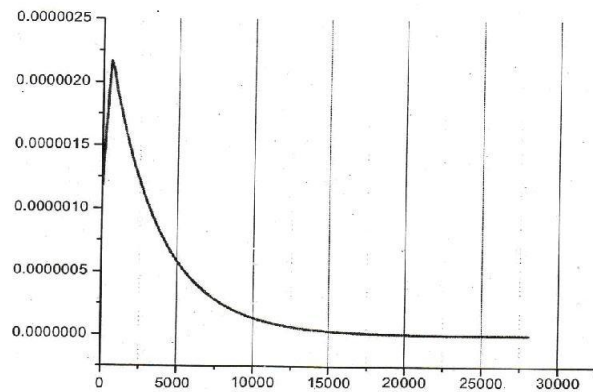
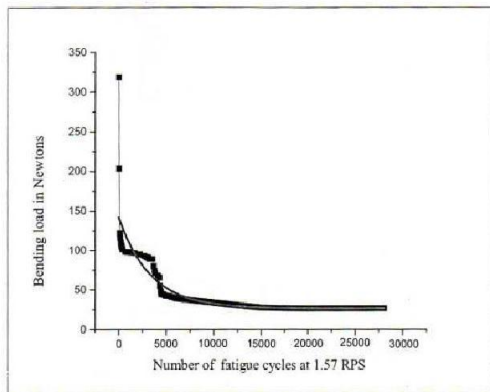


Fig. 16.1. Stiffness Degradation behaviour of Chapsten E-Glass Epoxy laminate Number of Fatigue Cycles at 1.57 RPS for Chapsten E-Glass Epoxy Laminate.

Fig. 16.2. Second order differential curve of Chapsten E-Glass Epoxy laminate derived from Fig. 6.5.

The experiments carried out in the laminates of Glass Fiber Epoxy, Chapsten E-Glass Epoxy and Glass Fiber Polyester Epoxy clearly exhibited a variation in the residual load bearing capacity after pivoting state. The graphical representation in Fig. 16.1. The stiffness degradation process of each specimen under goes basically in three stages, in the first stage the stiffness reduction rate is very fast this is due to the top and bottom layers of the laminates are subjected to maximum strain which leads to the failure being the glass reinforcement is pure elastic in nature. In the second stage as the stress levels on the subsequent layers reduces as the distance from the neutral layer is continuously decreasing. In the third stage of the failure already broken fibers provides a cushioning effect and resist the free bending of the specimen hence the stiffness degradation tends to towards zero. The results clearly establishes that the Glass Fiber Polyester Epoxy, exhibited very slow stiffness reduction rate when compared to the other specimens and the residual bending load bearing (residual stiffness) is also maximum i.e. 58.617N and the Stiffness retention after pivoting state is 73.26%. Hence it can be recommends that the Glass Fiber Polyester Epoxy material is best for fatigue critical applications.

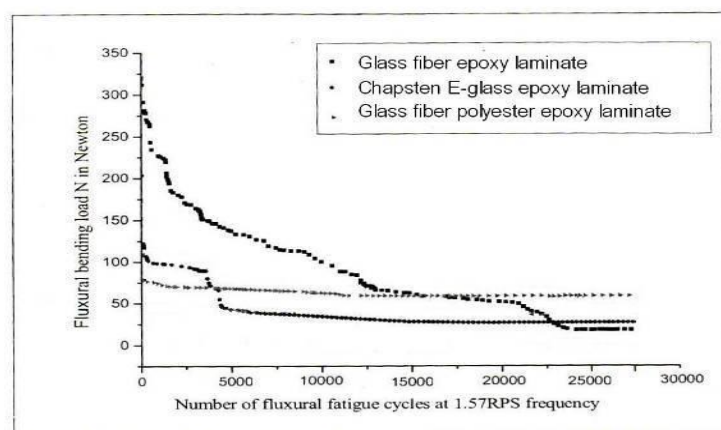


Fig. 16.3. Consolidated Flexural Fatigue Test Results of Glass Fiber Epoxy, Chapsten E-Glass Epoxy and Glass Fiber Polyester Epoxy laminates.

## VII. CONCLUSION

From the experimental investigation:

1. Flexural fatigue failure behavior of Glass Fiber Polyester Epoxy laminate composite exhibited better results.
2. The results clearly establish that the Glass Fiber Polyester Epoxy laminate exhibited very slow stiffness reduction rate when compared to the other specimens.

3. The residual bending load (residual stiffness) is also maximum i.e. 58N and the Stiffness retention after pivoting state is 72.5% of the virgin specimen.
4. Hence it can be recommended that the Glass Fiber Polyester Epoxy laminate is good for flexural fatigue critical applications such as wind turbine blades, Air craft wing and auto motive leaf spring constructions.

### REFERENCES

- [1] Saud Aldajah Ammar Al-omari and Ashraf Biddah Accelerated weathering effects on the mechanical and surface properties of CFRP composites Vernon T. Bechel, John D. Camping, Ran Y. Kim
- [2] 2. Cryogenic/elevated temperature cycling induced leakage paths in PMCs Composites Part B: Engineering, Volume 36, Issue 2, March 2005
- [3] Sandhya Rao, RMVGK Rao Cure studies on bifunctional epoxy matrices using a domestic microwave oven Polymer Testing, Volume 27, Issue 5, August 2008
- [4] S. Birger, A. Moshonov, S. Kenig The effects of thermal and hygrothermal ageing on the failure mechanisms of graphite-fabric epoxy composites subjected to flexural loading Composites, Volume 20, Issue 4, July 1989
- [5] [5]Mechanical Properties Of Composite Material Using Natural Rubber With Epoxy Resin Dr. Hani Aziz Ameen 9/3/2008
- [6] Fatigue Strength Assessment Of A Short Fibre-Reinforced Plastic Based On The Energy Dissipation G. Meneghetti\*, M. Quaresimin\*\*, M. De Monte\*\*
- [7] Experimentally Investigation Effect Of Geometrical Cross- Section On Fatigue Strength Of Aluminum Alloy (6063) Ghazi S. Al-Marahleh and Khaleel Abushgair Received: July 19, 2010
- [8] Fatigue and Ultrasonic Testing of Epoxy-Glass Composites M. Rojek, J. Stabik\*, S. Sokół
- [9] Mechanical Measurements by Thomas G.Beckwith, Roy D. Marangoni, John H. Lienhard Fifth edition an imprint of Addison Wesley Longman, Inc First ISE reprint 1999
- [10] The Pressure and Strain Handbook, Vol.29, Omega Engineering.
- [11]
- [12]

# An Evaluation of Software Development Methodology Adoption by Software Developer in Sri Lanka

C.D. Manawadu<sup>1</sup>, Md Gapar Md Johar<sup>2</sup>, S.S.N. Perera<sup>3</sup>

<sup>1</sup>Advanced Technology Center, Zone24x7 Private Limited, Colombo, Sri Lanka

<sup>2</sup>Faculty of Information Science & Engineering, Management and Science University, Selangor, Malaysia

<sup>3</sup>Department of Mathematics, University of Colombo, Colombo, Sri Lanka

## ABSTRACT:

Software development methodology usage and the adoption by software developers is an area which is crucial to understand. Currently available research in this area is limited and finding the evolution of software development methodology in the Sri Lankan context is vital for this booming industry. In this research the main objective is to find out how the evolution of software development methodology took place in history in Sri Lanka and what are the current methodologies adopted by the software developer in Sri Lanka. The research will be carried out by both qualitative and quantitative methods with the facilitation of the software development companies and software developers in Sri Lanka. The outcome of this research will be a stepping stone for future research on this area and the impact for future software development practitioners while adopting software development methodologies.

**KEYWORDS:** Adoption, Methodologies, Software Developer, Software Development, , Sri Lanka, ,

## I. INTRODUCTION

Software development is a booming industry and it employs a massive number of knowledge workers in the current society. Evolution of this great industry has only taken few decades however it has influenced and revolutionized businesses more promisingly than the other industries in general. Looking back at the evolution of the software development industry, it can be said that the 1960s were boom years for entrepreneurial firms established to sell programming and system design skills under contract in a market where the rapidly expanding use of computers created a high demand for those skills. The first of these companies Computer Usage Corporation—was founded earlier, in 1955,(Kubie, 1994) but by the end of the 1960s, there were thousands of such firms. Most such companies were small, but a handful was large enough to go public, employing hundreds of programmers.(Campbell-Kelly, Winter 1995). In January 1967, International Computer Programs (ICP) in Indianapolis, Indiana, began publishing a quarterly catalog of computer programs available for sale, and the software product industry began to take shape. (Johnson, 2002).A major event that helped set the stage for the dramatic growth of software products in the 1970s and 1980s was IBM's decision to partially unbundle its software products in 1969. Emerson Pugh, a well-known computer historian, describes the "Origins of Software Bundling" at IBM. Then Watts Humphrey, a key software executive at IBM in the 1960s and later, covers his experiences in "Software Unbundling: A Personal Perspective," and Burton Grad provides "A Personal Recollection: IBM's Unbundling of Software and Services." (Grad & Johnson, 2002)

In today's context, according to Software Magazine, the top 500 companies in the computer software and services industry generated \$640 billion dollars in revenue in 2012 and employed more than 4.1 million people who design, program, maintain, sell, or support computer software and services.(Desmond, 2012) One key factor lies for the success of the software industry which is the software development methodology that binds the people, processes, technology and tools. Hence a software development methodology is an integral part of software development. It ensures quality is given prominence and provides a consistent and standard delivery approach for software within any software development team environment. Hence it facilitates multiple stakeholders of a software development project to be interconnected and move forward with accomplishing objectives as the software development activities evolves. Exploring into the Sri Lankan context of software development, the IT industry in Sri Lanka was established about one and a half to two decades ago, with a large number of small and medium enterprises. Current estimates place the total number of entities offering services

in the software development industries in Sri Lanka at over 200.(SLASSCOM, 2012)Current there is no literature that studies about the adaption of software development methodology in the Sri Lankan context. Further similar studies in the Asian region have been less. Hence this papers purpose is to prepare a detailed case study in the context of Sri Lankan Software Development Methodology adoption which is needed to be studied extensively.

Therefore the aim of this study and the driving Research Questions for this study are:

- How did the Software development methodology adoption occur in Sri Lanka
- What is the current methodologies adopted by Sri Lankan Software developers

Since a vast majority of the current studies on the use of software development methods highlight the experiences of US and the European organizations. In contrast, little is reported on how those methods are actually being practiced within a small Asian country, and how successful they have been. (Rahim, Seyal, & Rahman, 1998) Therefore this research is motivated by the knowledge gap in the literature on comprehensive studies that describe the adaption of software development methodologies in a country. The research relevance can be considered high because the main objective of software engineering is the development of high-quality, on-time, and within budget software projects, which can only be delivered with the utilization of a systematic development process, as has been proven in other engineering disciplines. Therefore, this study contributes to organize the diverse and partial views of software development methodology adoption. The remainder of the paper is structured as follows. In Section 2, we discuss the existing literature that is available with similar studies from other parts of the world. Section 3 describes the research methodology approach used in the paper and demonstrates how the research was conducted. Section 4 discusses in detail the results and in discussion mode the outcome of the study which would be beneficial to practioners and researchers. In Section 5 we concluded the paper with limitations and future work.

## **II. LITERATURE REVIEW**

In the literature review, the research will look at some of the key software development methodologies including waterfall, spiral, prototyping, rapid application development, rational unified processes and agile. In here the research will look at their evolution and present some of the benefits and drawbacks each of these methodologies possesses. Hence through this background study, it will be helpful for the researcher to identify some of the most used software development methodologies and understands its evolution which will be helpful to directly map towards the Sri Lankan evolution and the adoption by the software developer.

### **Waterfall Methodology**

The evolution of software development life cycles (SDLC) starts in the mid twentieth century. According to Boehm (1988) prior to the year 1956, the software was developed by Code & Fix technique which included two steps: step 1, write some code, and step 2, fix the problems of this code. However in 1956, the experience recognizes the problems with more large software development, and then, a model stagewise was originated. This model stipulates that the software should be developed in successive stages: operational plan, operational specifications, code specification, code parameters test, integration test, shakedown (test and implementation), and system evolution. (Boehm, 1988) Royce (1970) proposed the Waterfall methodology in order to avoid the difficult nature of “code and fix” approach. He proposed the construction of a prototype, and involvement of the users in several phases. The methodology was also proposed initially to deal with the increasing complexity of aerospace software, which included development of software packages for spacecraft mission planning, commanding and post-flight analysis. In various researches the Waterfall Model is classified as a traditional methodology (Dyck & Majchrzak, 2012).The central concept of the waterfall methodology is the integrated verification and validation of the results by the customer in order to complete a certain phase (Royce, 1970).Taking on a process-centered perspective, the supportive disciplines of the waterfall methodology are mainly quality management and documentation. (Dyck & Majchrzak, 2012) An underlying implication of the waterfall methodology is that both problem and solution can be fully described upfront (Agresti, 1986), further introduces the requirements, analysis and design phases before coding(Rodríguez-Martínez, Mora, & Alvarez, 2009). This tends the software development team to focus on clear and concise requirements before moving through to development and hence deal with unwanted rework. Discussing on the negative side of the waterfall methodology, researchers negatively emphasize on the waterfall methodology on extensive documentation (Royce, 1970). In this context, some sources criticize that testing activities also start too late and without any customer involvement (Hindel, H'ormann, M'uller, & Schmied, 2006).

Considering other process oriented characteristics, the waterfall methodology describes a sequential proceeding strategy also covering all phases from requirements to operations, while not explicitly covering maintenance and disassembly (Royce, 1970). Even though there are many criticisms for the Waterfall model, it has been the base for several subsequent models and the first to suggest the iteration and feedback issues; (Rodríguez-Martínez et al., 2009)

### **Spiral Methodology**

Spiral methodology adds the risk analysis phase as a critical part of its definition, as well as the notion of an incremental development. (Rodríguez-Martínez et al., 2009). Much has been written about the value of risk reduction, especially as it is applied to software project management. A progressive approach to reduce risks for software development was defined by Barry Boehm. The approach involves working in incremental steps or phases to reduce software development risks. (Weckman, Colvin, Gaskins, & Mackulak, 1999). In each phase of this spiral approach, the objectives and risks associated with those objectives are defined. Then the necessary sub-tasks or prototypes needed to resolve those risks are developed. Finally simulations and models are executed to verify that the objectives can be achieved. (Weckman et al., 1999) One difficulty was determining where the elaborated objectives, constraints, and alternatives come from. Another difficulty in applying the spiral model across an organization's various projects was that the organization has no common reference points for organizing its management procedures, cost and schedule estimates, and so on. This is because the cycles are risk driven, and each project has different risks. (Boehm, 1988) Quality is built into spiral model by means of activities involved at each phase, like risk analysis, prototype development, development plan, validation and verification, integration and acceptance testing. Each phase ensures that development is not moved to the next phase unless the previous phase is satisfied in terms of its activities. There is thorough analysis of requirements and risks even before the development starts, which guarantees that system contains only those requirements that are feasible and possible to implement. Furthermore, development phase of spiral performs step by step analysis of the product which ensures that no faults are escaped. (Boehm, 1988)

### **Prototyping Methodology**

Prototyping suggest the development of an initial first operational version of the system in a quickly way (prototype), before to the full development. (Rodríguez-Martínez et al., 2009). The software industry has adopted this industrial technique to construct prototypes as models, simulations, or as partial implementations of systems and to use them for a variety of different purposes, e.g., to test the feasibility of certain technical aspects of a system, or as specification tools to determine user requirements. (Carr & Verner, 1997) Prototyping, on the other hand, can be viewed a 'process' (Floyd, 1984) which is either a well-defined phase within the software development life cycle, or is an 'approach' that influences the whole of it (Budde et al., 1992). The prototyping process can encourage the efficient development of applications by breaking a complex and often ill-defined problem into several comprehensive yet smaller and simpler parts (Kaushaar and Shirland, 1985). A prototyping development approach can help build, and subsequently refine, a product to meet end-user or market expectations. (Gomaa H., 1983). Researchers have also noted that prototyping enables us to partition the development process into smaller, easier to handle steps (Kaushaar and Shirland, 1985), is cost-effective (Boehm et al., 1984, Gordon and Bieman, 1994, Palvia and Nosek, 1990), improves communication between development personnel (Alavi, 1985) helps determine technical feasibility (Floyd, 1984), is a good risk management technique (Tate and Verner, 1990) and results in greater user involvement and participation in the development process (Naumann and Jenkins, 1982). It would appear that the prototype process would not be appropriate when user needs are static or well-defined, or when development experience with similar applications has been extensive (Kraushaar & Shirland, 1985). Evolutionary prototyping, however, can lead to problems when performance is not adequately measured and either inefficient code is retained in the final product or the prototype demonstrates functionality that is unrealizable under normal usage loads. (Gordon & Bieman, 1995)

### **Rapid Application Development (RAD)**

RAD proposes scenario-based analysis, the use of CASE tools and the component specification for maximum reuse (in the modern RAD concept). (Rodríguez-Martínez et al., 2009). James Martin coined the term RAD in the early 1990s to distinguish the methodology from the traditional waterfall model for systems development. "RAD refers to a development life cycle designed to give much faster development and higher quality results than the traditional life cycle. It is designed to take maximum advantage of powerful development software that has evolved recently." (Martin, 1991) While no universal definition of RAD exists, it can be characterized in two ways: as a methodology prescribing certain phases in software development (similar in principle to the spiral, iterative models of software construction), and as a class of tools that allow for speedy

object development, graphical user interfaces, and reusable code for client/server applications. (Agarwal, Prasad, Tanniru, & Lynch, 2000) The essential characteristics of RAD tools include the capability for planning, data and process modeling, code generation, and testing and debugging. RAD methodologies encompass three-stage and four-stage cycles. The four-stage cycle consists of requirements planning, user design, construction, and cutover, while in the three-stage cycle, requirements planning and user design are consolidated into one iterative activity. (Agarwal et al., 2000). In a typical RAD life cycle, the requirements specification and design phases consume approximately 30% of the total effort (Martin, 1991)RAD lacks suitable representations for managing the co-operative systems development process currently. (Beynon-Davies & Holmes, 2002). RAD is accused of being anti-quality. It is commonly believed speed and quality are incompatible in software development. You can have one or the other but not both at the same time. On the other hand, supporters of RAD argue that modern quality principles are inherent in RAD. Fitness for purpose, avoiding waste, getting things right the first time, individual responsibility for quality, and meeting customer requirements is as engraved in RAD as in quality. What RAD tries to avoid is the bureaucratic nature of current quality control and assurance practice. (Howard, 2002). Other major concerns with RAD include the costs of maintaining clean rooms and of funding the extensive user involvement required for prototyping. Many organizations have found the culture changes required for RAD impossible to achieve either within the business as a whole or within project teams. (Howard, 2002)

### **Rational Unified Process (RUP)**

RUP combines a two-dimensional (phases, workflows/activities) model with an iterative/incremental approach. (Rodríguez-Martínez et al., 2009). The Rational Unified Process is a Software Engineering Process. It provides a disciplined approach to assigning tasks and responsibilities within a development organization. Its goal is to ensure the production of high-quality software that meets the needs of its end-users, (Kruchten, 1999) within a predictable schedule and budget.(Jacobson, Booch, & Rumbaugh, 1999)

The software lifecycle is broken into cycles, each cycle working on a new generation of the product. The Rational Unified Process divides one development cycle in four consecutive phases (Kruchten, 1996)

- Inception phase
- Elaboration phase
- Construction phase
- Transition phase

Each phase is concluded with a well-defined milestone, a point in time at which certain critical decisions must be made, and therefore key goals must have been achieved (Boehm, 1996). The advantages of RUP have been the aesthetic clarity which makes the management point of RUP very easy, whereas the lacking details required supporting Software Engineers lacking is the key issue for its negative feedback over the years. (Hull, Taylor, Hanna, & Millar, 2002)

### **Agile Methodology**

Agile methodologies are a new host of methodologies that claim to overcome the limitations of traditional plan-driven SDMs. The “Agile Manifesto” published by a group of software practitioners outlines the principles of agile systems development(Chan & Thong, 2009). In short, these principles emphasize the importance of individuals and their interactions, customer collaboration, early and continuous delivery of software, and the capability to respond to volatile requirements. Examples of agile methodologies that align with the Agile Manifesto include Extreme Programming (XP), Crystal methods, Lean Development, Scrum, and Adaptive Software Development(Highsmith, 2002) Highsmith (2002)suggested that the differences between traditional SDMs and agile methodologies rest on two assumptions about customers. First, traditional SDMs assume that customers do not know their requirements but developers do, whereas agile methodologies assume that both customers and developers do not have full knowledge of system requirements at the beginning (Highsmith, 2002). Second, traditional SDMs assume customers are short-sighted, and thus developers have to build in extra functionalities to meet the future needs of customers, often leading to over designed systems (Highsmith, 2002). On the other hand, agile methodologies emphasize simplicity—the art of maximizing the work not done(Lindstrom & Jeffries, 2004). Also, the differences in philosophy between traditional SDMs and agile methodologies lead to differences in a number of practices and requirements, such as planning and control, role assignment among developers, customer's role, and technology used (Nerur, Mahapatra, & Mangalaraj, 2005).In 2001, the “agile manifesto” was written by the practitioners who proposed many of the agile

development methods. The manifesto states that agile development should focus on four core values<sup>1</sup>:(Dyba & Dingsøyr, 2008)

- Individuals and interactions over processes and tools.
- Working software over comprehensive documentation.
- Customer collaboration over contract negotiation.
- Responding to change over following a plan.

Most studies reported that agile development practices are easy to adopt and work well. Benefits were reported in the following areas: customer collaboration, work processes for handling defects, learning in pair programming, thinking ahead for management, focusing on current work for engineers, and estimation. (Dyba & Dingsøyr, 2008) With respect to limitations, the lean development technique did not work well for one of the teams trying it out, pair programming was seen as inefficient, and some claimed that XP works best with experienced development teams. A further limitation that was reported by one of the studies, which has also been repeatedly mentioned in the literature (McBreen, 2002), was the lack of attention to design and architectural issues.(Stephens & Rosenberg, 2003)

### **III. RESEARCH METHODOLOGY**

This research is an exploratory study. The research adopted a hybrid approach mainly based on quantitative research methodologies which slightly combined with qualitative research methodologies. As this is a relatively new research domain with insufficient academic research contribution, we had to consult the online articles, success stories, case studies and personal experiences shared by practitioners in the industry in Sri Lanka. To serve the need of quantitative research, a web based survey comprising of questionnaire was designed to approach practitioners who have experience working in software development methodologies in Sri Lanka. The questionnaire was sent through emails, community groups, and discussion boards to a large pool of practitioners. The data was collected over a period of four months from June, 2013 to October, 2013. The overall relevant response rate was 41% due to specific and technical nature of the survey. The questionnaire was open for all to access. We scanned data of 51 respondents, which were found more relevant and complete for evaluation of the results. Microsoft excel and SPSS were mostly used to evaluate the respondents' results. The questionnaire was divided into four parts. It contains total 28 close and open ended questions to capture the views of IT professionals. In the first section, we asked the demographic information of respondents, while the second section captured the particulars of the respondent's company. The third section was related to the organizations and individuals current & past experience of software development methodologies usage and some of the rankings related to effectiveness of using specific methodologies listed. Section 4 was designed to capture the perception of the future usage of software development methodology in the organization and at individual level. The responses were quite diverse according to the professional experience of the respondents. In order to become more focused, we identified the respondents which were specific and practically working in the particular roles (Software Engineers, Software Architects, QA Engineers and Project Managers). Informal interviews were also conducted to refine the respondent findings. The results presented here are formulated by compiling the literature reviews, the survey and informal interviews conducted. Descriptive statistics (mean and standard deviation) were used to analyze scores and to derive gaps of the current effective of software development methodology usage. Further similar analysis was used to derive results of future preferred methodology adoption. Percentage and graph based analysis was used to summarize and present the other findings of the research.

### **IV. RESULTS AND DISCUSSION**

This section summarizes research findings and results.

#### **A. Particulars of Respondents**

First section of research questionnaire was designed to obtain the respondents' demography. It included very general questions such as respondents' professional experience and current position etc. The respondent sample was quite diverse, that's why we got variation in their opinions and observations. Over here we have presented the averaged results of our findings. Altogether we got 51 responses. These were covering around 30 unique software development R & D companies spread across Sri Lanka. All most every company was attached to a global software development. From the respondents, 8% respondents had professional experience over 9 years, 32% respondents had professional experience between 4 - 9 years, 52% respondents had professional experience between 1 - 4 years and 8% respondents had less than 1 year of experience altogether. The diversity in professional expertise enabled us to get a better understanding of the situation. Participation of respondents on the basis their current position is shown in the table 1.

Table 1 Respondent’s Professional Division

Designation	Percentage %
Software Engineers	60
Software Quality Assurance Engineers	8
Software Architects	16
Project Managers	12
Other	4

**B. Particulars of Respondents’ Companies**

Second section collects the information related to respondents’ companies in which they were working at the time of survey conducted. Questions related to respondents’ companies e.g. no of employees and types of solutions developed were gathered. This section analyzes the information related to respondents’ IT companies’ software development practices. Respondents worked with companies of different size which varies from Less than 5 employees to more than 150 employees working companies. 44% of the respondents worked in companies comprising more than 150 employees. 40% respondents worked in companies having employees between 75 to 150. 8% of the respondents worked in companies having employees between 25 - 75. The remaining 8% respondents fell into the category of having employees below 25 in their companies. These companies fall into the falling types of solutions that were developed in-house. E-commerce/cloud-based/web applications (e.g. Web portals), Mobile Application Development(e.g. Android Apps), Real time applications (e.g. process control, manufacturing), Management information systems (e.g. decision support), Transaction processing systems (e.g. payroll, POS, accounting, inventory), Embedded systems (e.g. software running in consumer devices or vehicles), Systems software (e.g. telecommunications software), Interactive Multimedia Applications (e.g. Games), Legacy Transformation Systems (e.g. .Net porting). Figure 1 depicts the distribution of solutions developed by these companies.

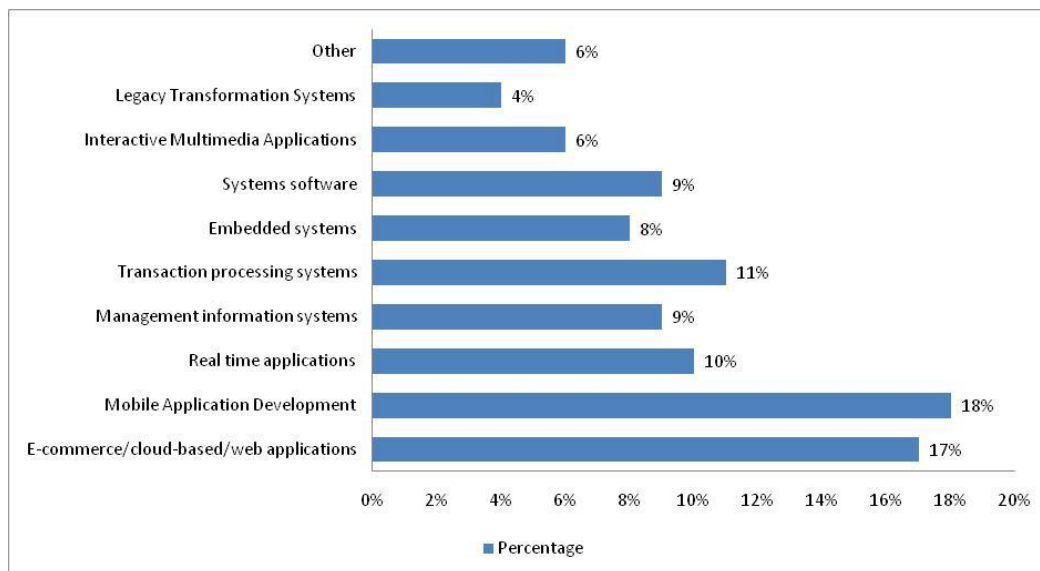
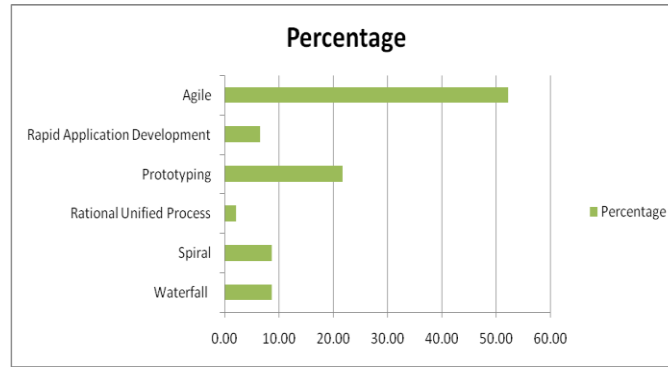


Figure 1 : Solutions Developed

**C. Current and past analysis of Software Development Methodology usage**

Third section of the questionnaire collected the current and past usage analysis of software development methodologies and rating of effectiveness of each methodology used currently were gathered. Out of the 51 respondents, 100% of the respondents confirmed that their organizations use a software development methodology. When questioned on the current methodologies used in the companies projects as an overall indicator, 52.17% of the participants stated using agile, while the rest of the distribution was spread among RAD, prototyping, RUP, spiral and waterfall methodologies. Statistics are illustrated in figure 2.



**Figure 2 : Current usage of software development methodologies**

The survey also gathered the mostly used software development methodology in the company. According to the results 68% of the participants indicated it was Agile and the next mostly used methodology was named as waterfall which was 21% of the total percentage. When inquired on the opinion on why it is used mostly in your organizations projects? 43% of the respondents stated that is most practical and effective, 29% stated its client specific, 18% According to company policy, 7% percent stated its less defects and re-work and 4% stated its suitable for outsourcing projects.

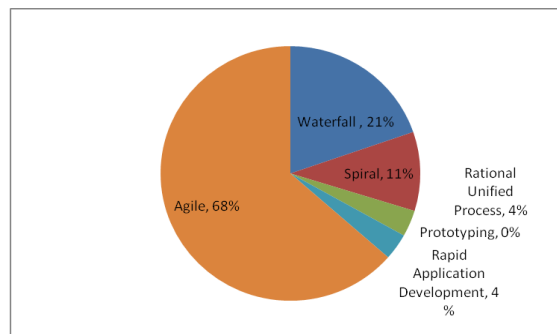


**Figure 3 : Mostly used software development methodology**

When we asked the question of what is the software development methodology used in your first project, as depicted in figure 4 above, 52% of the respondents stated it was waterfall, 24% stated it was prototyping, and the rest stated they used Spiral, RAD and Agile in a distribution of 8 percentage each respectively, which working on their first project. While we inquired on the reason, most of the respondents mentioned that it was due to organizations policy and client demand at that time. A considerable percentage mentioned it is due to only available option and the most effective at that time. Another percentage mentioned knew nothing about the other methods.

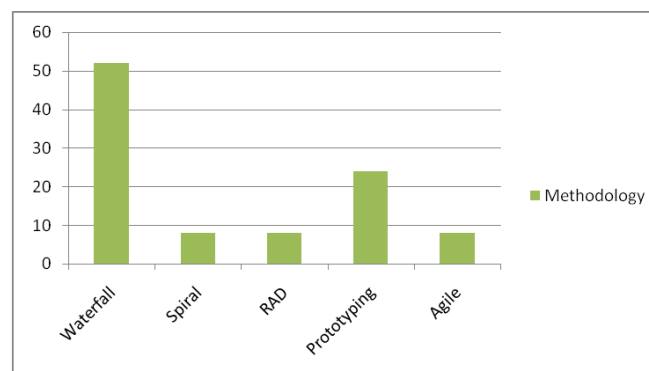


**Figure 4 : Methodology used in first project?**

To analyze the effectiveness of these methodologies being used, a five-point Likert scale was used to establish the level of effectiveness of current methodologies. Out of the six general methodologies used which were Waterfall, Spiral, RUP, Prototyping, RAD and Agile, the results are summarized in Table 2 below. Out of the analysis below, it clearly draws out the Agile methodology as the most effective methodology as per current status among the participants. While we interviewed few individuals for their opinion on this results, they agreed on the view of the results expressed, however considering the compared methodologies in place. However they also mentioned there are limitations that were existing even though the majority of practitioners have listed this one out. Further we clearly see that there is a high standard deviation of data analysis for Prototyping and RAD methodologies. In all categories, this reflects, hence we feel that the current usage of these methodologies may differ from each respondents experiences. Also we feel due to this high variance, these two methodologies have not been consistently used within the development scope of projects in Sri Lanka. Considering the lowest effective results that have been listed out, we feel that waterfall methodology has been the least effective with the rates identified below. However with a slight difference where the Project Managers has slightly preferred it. This may be due to the nature of project management compared with Waterfall. Looking into the Software Engineers result outcomes, it clearly indicates that the current developers prefer the agile context. While interviewing few of the Software Engineers, we gathered that the adoption has occurred from traditional based methods such as waterfall to prototype and then from it to agile practice. Most of these developers has indicated that they have used waterfall method at the initial stages of their careers. Looking at their experience profiles, during the past decade of working in the industry, most of them have used waterfall as the main methodology. Therefore we can clearly identify that Sri Lankan software R & D companies have approached this method at a early stage of development.

One clear reason for moving from these standard methodologies to more iterative based once has been the fact that the traditional once have always caused re-work and client dissatisfaction over quality on the longer run. Further we gathered that most of the projects had not been completed on time using the traditional methods. Always there had been project estimation slippages due to client not been part of the requirements engineering initially. As per the literature review on the methodologies presented, the drawbacks listed out in section 2 has a very direct relation to most of the comments shared by the interviewed software engineers. Mainly with comparison of the results depicted in table 2, the preference for Prototype has also been remarkably higher from the Software Engineers aspects. This is also a indication that iterative work is much preferred by developers in the current context rather than finishing large phases of work which would be ineffective for better productive results.

Table 2. Effectiveness of methodologies used

Methodology	All categories		Software Engineering		Software Architects		Quality Assurance		Project Management	
	Mean	SD	Mean	SD	Mean	SD	Mean	SD	Mean	SD
Waterfall	2.72	0.67	2.53	0.63	2.6	0.54	3.0	0.00	3.67	0.57
Spiral	3.2	0.64	3.20	0.67	3.2	0.83	3.0	0.00	3.33	0.57
Rational Unified Process	2.92	0.40	2.87	0.35	2.8	0.44	3.5	0.70	3.00	0.00
Prototyping	3.56	0.91	3.73	0.79	3.2	0.83	3.0	1.41	3.67	1.52
Rapid Application Development	3.32	0.98	3.47	1.06	3.2	0.83	3.0	1.41	3.00	1.00
Agile	4.64	0.56	4.60	0.63	5.0	0.00	4.5	0.70	4.33	0.57

## D. Future effectiveness of Software Development Methodology usage

Table 3. Future Effectiveness of SDM

Methodology	All categories		Software Engineering		Software Architects		Quality Assurance		Project Management	
	Mean	SD	Mean	SD	Mean	SD	Mean	SD	Mean	SD
Waterfall	2.72	0.84	2.67	0.82	2.0	0.82	3.0	0.00	3.67	0.58
Spiral	3.12	0.83	3.27	0.70	2.50	1.29	3.00	0.00	3.00	1.00
Rational Unified Process	2.92	0.64	3.00	0.53	2.25	0.96	3.50	0.71	3.00	0.00
Rapid Application Development	3.36	0.99	3.6	0.91	2.50	1.29	3.50	0.71	3.00	1.00
Scrum	4.64	0.49	4.67	0.49	4.75	0.50	4.50	0.71	4.33	0.58
Extreme Programming (XP)	4.16	0.75	4.07	0.80	4.25	0.50	4.00	1.41	4.33	0.58
Crystal Methods	3.20	0.58	3.13	0.52	3.00	0.00	4.00	1.41	3.33	0.58
Feature Driven Development (FDD)	3.00	1.47	2.87	1.46	2.50	1.73	4.00	0.00	4.33	0.58
Dynamic Systems Development Methodology (DSDM)	3.36	0.64	3.33	0.62	3.00	0.00	3.50	0.71	4.00	1.00
Adaptive Software Development (ASD)	3.36	0.64	3.40	0.74	3.00	0.58	3.50	0.71	3.67	0.58

Another analysis that was carried out to determine the future effectiveness of using specific software development methodologies. The participants were asked to rate the effectiveness using a five-point Likert scale. We added few of the agile methodologies and we dropped out the prototyping methodology as we thought it wouldn't be effectively used in the future with the diverse use of agile methods. We added Scrum, Extreme Programming (XP), Crystal Methods, Feature Driven Development (FDD), Dynamic Systems Development Methodology (DSDM), Adaptive Software Development (ASD) since the literature on SDM usage indicated to us that the future would be more relevant for these methodologies. Apart from that we also validated Waterfall, Spiral, RUP, and RAD, which the detailed results are summarized in Table 3 above.

The analysis gave use clear insights that the Agile methods are the most effective in terms of usage for future software development projects. Out of our sample participants, 4.64 and 4.16 mean values were retrieved for Scrum and XP agile methodologies respectively for the five-point Likert scale questions we raised on effectiveness. However Scrum methodology had the least standard deviation of 0.49 as a overall level, and further the same level of mean and standard deviations were shown comparing results from Software Engineers, Architects, QA's and Project Managers. Thus it is evident that Scrum is a popular agile methodology which is emerging within the Sri Lankan software development context and the likelihood of companies and developers using and preferring it as a methodology is viable.

However the effectiveness of XP was also similar, but it changed slightly while analysing the results with non-software engineering practioners. Through the literature and knowledge gained, XP is far more superior for Software Engineers and its core principles lie on coding. hence that could have been the reason for Software Engineers to prefer it for future usage and other not having the same opinion.

Out of the ten methodologies analyzed the least favorite for the future is the Waterfall methodology. Almost all the categories of roles has evaluated it as a least effective, other than a slight preference shown by the Project Managers. We feel that some of the Project Managers would have seen it effective as their discipline would have been skillfully mastered while using the methodology.

We also like to emphasize over here that Feature Driven Development (FDD) showed promise, but it has a very high standard deviation among all categories. Thus indicating to us that it is a methodology that some of the developers are aware and maybe some developers have not used its benefits in real practice.

Thus again with the analyze it denotes that the Sri Lankan software developer and related discipline community feels that the adoption of the software development methodology in the Sri Lankan perspective goes mainly to the agile methodologies which are in use. Hence in comparison to the changes of usage in the world Sri Lanka is also changing similarly as per our analysis.

## V. CONCLUSION

The research was a preliminary study of a larger research that is been carried out currently. Hence the main goal of the research was to understand the current usage of software development mythologies used by the software developers in Sri Lanka. Also to understand how the methodology usage has evolved during the past decade. We used both quantitative and qualitative methods to carry out our research and we had selected participants from Sri Lankan software industry for this research. The findings of the research was that many organizations and developers in the current context use Agile methodologies for the software development. Currently they are satisfied with its attributes and further many of them recommend its effectiveness for future use as well. Therefore we can clearly say that the Sri Lankan developer community in parallel with what is currently happening the words are more aligned. Further the findings of how the development methodology evolved during past years was gathered. Most of the past decade development activities has triggered with the waterfall and traditional methodologies and now it has slowly evolved into agile methodologies. However the surprising and promising factor is that most of the developers and organizations use at least one of the identified methodologies to perform software development. Discussing on the limitations of this study, it could be said that if the sample of this study was increased it would have given a more better outcome. Hence to provide further research into this area, we could propose that methodology specific study comparing effectiveness to the Sri Lankan context be studies in order to support future practitioners in determining which methodology they could use in which circumstances.

## REFERENCES

- [1] Agarwal, R., Prasad, J., Tanniru, M., & Lynch, J. (2000). Risks of rapid application development. *Commun. ACM*, 43(11es), 1. doi: 10.1145/352515.352516
- [2] Agresti, W. W. (1986). The conventional software life-cycle model: Its evolution and assumptions. *New Paradigms for Software Development. IEEE CS*, 2-5.
- [3] Alavi, M. (1985) An Assessment of the Prototyping Approach to Systems, *Communications of the ACM*, 27, 6, 556-564.
- [4] Beynon-Davies, P., & Holmes, S. (2002). Design breakdowns, scenarios and rapid application development. *Information and Software Technology*, 44(10), 579-592. doi: [http://dx.doi.org/10.1016/S0950-5849\(02\)00078-2](http://dx.doi.org/10.1016/S0950-5849(02)00078-2)
- [5] Boehm, B.W., Gray, T.E. and Seewaldt, T. (1984) Prototyping Versus Specifying: A Multiproject Experiment, *IEEE Transactions on Software Engineering*, SE-10, 4, 290 -402.
- [6] Boehm, B. (1988). A Spiral Model of Software Development and Enhancement. *IEEE Computer*.
- [7] Boehm, B. (1996). Anchoring the Software Process. *IEEE Softw.*, 13(4), 73-82. doi: 10.1109/52.526834
- [8] Boehm, B., Egyed, A., Kwan, J., Port, D., Shah, A., & Madachy, R. (1998). Using the WinWin Spiral Model: A Case Study. *Computer*, 31(7), 33-44. doi: 10.1109/2.689675
- [9] Budde, R., Kautz, K., Kuhlenkamp K., Zullighoven, H. (1992) What is Prototyping? Information Technology & People, 6, 2-4, 89-95.
- [10] Campbell-Kelly, M. (Winter 1995). Development and Structure of the International Software Industry, 1950–1990. *Business and Economic History*, 24(2), 84-85.
- [11] Carr, M., & Verner, D. J. (1997). Prototyping and Software Development Approaches.
- [12] Chan, F. K. Y., & Thong, J. Y. L. (2009). Acceptance of agile methodologies: A critical review and conceptual framework. *Decis. Support Syst.*, 46(4), 803-814. doi: 10.1016/j.dss.2008.11.009
- [13] Desmond, J. P. (2012). Software 500: Revenue Up 17 Percent. *Software Magazine*. Retrieved from <http://softwaremag.com/content/ContentCT.asp?P=3374> website:
- [14] Dyba, T., & Dingsøyr, T. (2008). Empirical studies of agile software development: A systematic review. *Inf. Softw. Technol.*, 50(9-10), 833-859. doi: 10.1016/j.infsof.2008.01.006
- [15] Dyck, S., & Majchrzak, T. A. (2012). Identifying Common Characteristics in Fundamental, Integrated, and Agile Software Development Methodologies. Paper presented at the Proceedings of the 2012 45th Hawaii International Conference on System Sciences.
- [16] Floyd, C. (1984) A Systematic Look at Prototyping, in: Budde, R.,Kuhlenkamp, K., Mathiassen, L. and Zullighoven, H. (Eds.) *Approaches to Prototyping*, Springer-Verlag: Heidelberg, 1-17.
- [17] Gomaa, H. (1983) The Impact of Rapid Prototyping on Specifying User Requirements, *ACM SIGSOFT Software Engineering Notes* 8, 2, 17-28.
- [18] Gordon, V.S. and Bieman, J.M. (1994) Rapid Prototyping: Lessons Learned, *IEEE Software*, 12, 1, 85-95
- [19] Grad, B., & Johnson, L. (2002). The Start of the Software Products Industry. *IEEE Ann. Hist. Comput.*, 24(1), 3-4. doi: 10.1109/mahc.2002.988573

- [20] Highsmith, J. (2002). Agile software development ecosystems: Addison-Wesley Longman Publishing Co., Inc.
- [21] Hindel, B., H'ormann, K., M'uller, M., & Schmied, J. (2006). Basiswissen Software-Projektmanagement - Aus- und Weiterbildung zum Certified Professional for Project Management nach iSQI. Paper presented at the Aus- und Weiterbildung zum Certified Professional for Project Management nach iSQI-Standard.
- [22] Howard, A. (2002). Rapid Application Development: Rough and Dirty or Value-for-Money Engineering? COMMUNICATIONS OF THE ACM, 45.
- [23] Hull, M. E. C., Taylor, P. S., Hanna, J. R. P., & Millar, R. J. (2002). Software development processes — an assessment. Information and Software Technology, 44(1), 1-12. doi: [http://dx.doi.org/10.1016/S0950-5849\(01\)00158-6](http://dx.doi.org/10.1016/S0950-5849(01)00158-6)
- [24] Jacobson, I., Booch, G., & Rumbaugh, J. (1999). The unified software development process: Addison-Wesley Longman Publishing Co., Inc.
- [25] Johnson, L. (2002). Creating the Software Industry: Recollections of Software Company Founders of the 1960s. IEEE Ann. Hist. Comput., 24(1), 14-42. doi: 10.1109/85.988576
- [26] Kraushaar, J. K., & Shirland, L. E. (1985). A prototyping method for applications development by end users and information systems specialists. MIS Q., 9(3), 189-197. doi: 10.2307/248948
- [27] Kruchten, P. (1996). A Rational Development Process, CrossTalk. Hill AFB, UT: STSC.
- [28] Kruchten, P. (1999). The Rational Unified Process: an introduction: Addison-Wesley Longman Publishing Co., Inc.
- [29] Kubie, E. C. (1994). Recollections of the first software company. IEEE Ann. Hist. Comput., 16(2), 65-71. doi: 10.1109/85.279238
- [30] Lindstrom, L., & Jeffries, R. (2004). Extreme programming and agile software development methodologies. Information Systems Management 21(3), 41-60.
- [31] Martin, J. (1991). Rapid Application Development. New York: Macmillan.
- [32] McBreen, P. (2002). Questioning Extreme Programming: Addison-Wesley Longman Publishing Co., Inc.
- [33] Nerur, S., Mahapatra, R., & Mangalaraj, G. (2005). Challenges of migrating to agile methodologies. Commun. ACM, 48(5), 72-78. doi: 10.1145/1060710.1060712
- [34] Nauman, J.D. and Jenkins, M. (1982) Prototyping: The New Paradigm for Systems Development, MIS Quarterly, 6, 3, 29-44.
- [35] Palvia, P. and Nosek, J.T. (1990) An Empirical Evaluation of System Development Methodologies, Information Resources Management Journal, 3,23-32.
- [36] Rahim, M. M., Seyal, A. H., & Rahman, M. N. A. (1998). Use of software systems development methods An empirical study in Brunei Darussalam. Information and Software Technology, 39(14-15), 949-963. doi: [http://dx.doi.org/10.1016/S0950-5849\(97\)00052-9](http://dx.doi.org/10.1016/S0950-5849(97)00052-9)
- [37] Rodríguez-Martínez, L. C., Mora, M., & Alvarez, F. J. (2009). A Descriptive/Comparative Study of the Evolution of Process Models of Software Development Life Cycles (PM-SDLCs). 298-303. doi: 10.1109/enc.2009.45
- [38] Royce, W. W. (1970). Managing the Development of Large Software Systems. Proceedings of the IEEE WESCON, 1-9.
- [39] SLASSCOM. (2012). Sri Lanka Advantage - The Sri Lankan IT-BPO Industry Retrieved 02/21/2013, 2013
- [40] Stephens, M., & Rosenberg, D. (2003). Extreme Programming Refactored: The Case Against XP: APress L. P.
- [41] Verner, J., Tate, G. and Cerpa, N. (1995) Prototyping: Some New Results, Information and Software Technology, 38, 12, 743-755.
- [42] Weckman, J., Colvin, T., Gaskins, R. J., & Mackulak, G. T. (1999). Application of simulation and the Boehm spiral model to 300-mm logistics system risk reduction. Paper presented at the Proceedings of the 31st conference on Winter simulation: Simulation---a bridge to the future - Volume 1, Phoenix, Arizona, USA.

## Harmonic Filter Design for HvdC Lines Using Matlab

<sup>1</sup>P.Kumar , <sup>2</sup>P.Prakash

<sup>1</sup> Power Systems Division Assistant Professor DEEE, P.A. College of Engineering and Technology, Pollachi  
<sup>2</sup> VLSI Design,, Assistant Professor DEEE, P.A. College of Engineering and Technology, Pollachi

**ABSTRACT:** This paper presents harmonic filter design for HVDC lines using MATLAB version R2009a. Non-linear devices such as power electronics converters can inject harmonics alternating currents (AC) in the electrical power system. The number of sensitive loads that require ideal sinusoidal supply voltage for their proper operation has been increasing. To maintain the quality limits proposed by standards to protect the sensitive loads, it is necessary to include some form of the filtering device to the power system. Harmonics also increases overall reactive power demanded equivalent load. This paper deals with the design of three phase filter banks connected in parallel to achieve optimal control for harmonic elevation problems.

**KEYWORDS:** harmonic filter, sensitive loads, reactive power, three phase filter banks, optimal control, harmonic elevation problems.

### I INTRODUCTION

Advancement in technology of semiconductor devices has led to a revolution in electronic technology over the past decade. However rise in the power quality (PQ) problem is due to power equipments which include adjustable-speed motor drives (ASDs), electronic power supplies, direct current (DC) motor drives, battery chargers, electronic ballasts. The distortion in current is due to the nonlinearity of the resistor. The nonlinear loads are constructed by nonlinear devices, in which the current is not proportional to the applied voltage. The concept of current distortion is illustrated in the figure 1. In figure 1 a sinusoidal voltage is applied to a simple nonlinear resistor in which the voltage and current vary according to the curve shown. From figure 1 we observe, the voltage is perfectly sinusoidal, the resulting current is distorted.

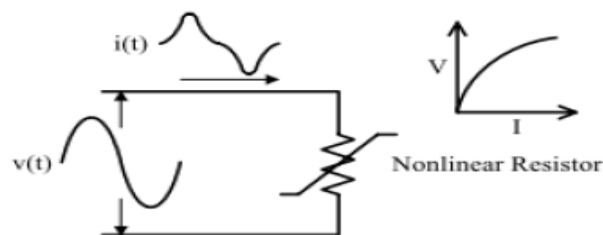


**Figure.1 Current distortion caused by nonlinear resistance**

The Non-linear loads seem to be the main source of harmonic distortion in a power distribution system. The Non-linear loads produce harmonic currents and inject it into the power distribution network at the point of common coupling (PCC). These harmonic current can interact negatively with a broad range of power systems equipment such as transformers, motors and produce more losses, overheating and overloading.

### II SOLUTIONS FOR HARMONIC DISTORTION PROBLEMS

There are set of conventional solutions to the harmonic distortions which have existed for a long time. Some of them are as follows

1) The passive filtering is the simplest conventional solution to mitigate the harmonic distortion. The passive filtering mechanisms do not depend upon an external power supply. Although simple, the use of passive elements does not respond correctly to the dynamics of the power distribution systems. Also the use of passive elements at high power level makes the filter heavy and bulky. The passive filters are known to cause resonance, thus affecting the stability of the power distribution systems. 2) The active power filter (APF) provides solution for harmonic distortion mitigation. The active filters are made of passive and active components and require an external power source. The APF utilize power electronics technologies to produce current components that

cancel the harmonic currents from the non-linear loads. With the APF the switching frequency noise requires additional filtering to prevent with other sensitive equipments.

3) The passive high-pass filter (HPF) used in addition to the conventional APF for mitigating harmonics. This combination is known to be hybrid APF. The main objective of hybrid APF is to improve the filtering performance of high-order harmonics while providing a cost-effective low order harmonic mitigation.

### III MATHEMATICAL ANALYSIS OF HARMONICS

#### 3.1 TOTAL HARMONIC DISTORTION

The basic parameter that is used for the harmonic analysis is the total harmonic distortion (THD). The total harmonic distortion (THD) gives the common measurement indices of harmonic distortion. THD applies to both current and voltage and is defined as the root-mean-square (rms) value of the harmonics divided by the rms value of the fundamental and then multiplied by 100%. The THD is given by the following equation.

$$THD = \frac{\sqrt{\sum_{h>1}^{h_{max}} M_h^2}}{M_1} \times 100 \quad (1)$$

Where  $M_h$  is the rms value of harmonic component  $h$  of the quantity  $M$ .

THD of the current varies from a few percent to more than 100%. THD of the voltage is usually less than 5%. Voltage THDs below 5% are widely considered to be acceptable, while values above 10% are definitely unacceptable and will cause problems for sensitive equipment and loads. The biggest problem with harmonics is voltage waveform distortion. We can calculate a relation between the fundamental and distorted waveforms by finding the sum of the squares of all harmonics generated by a single load, and then dividing this number by the nominal 50/60 Hz waveform value. We do this by a mathematical calculation known as Fast Fourier Transform (FFT) Theorem. This calculation method determines the total harmonics distortion (THD) contained within a nonlinear current or voltage waveform.

#### 3.2 FOURIER SERIES

Fourier series are used in the analysis of periodic functions or periodic signals into the sum of oscillating function called sines and cosines. Many of the phenomena studied in engineering and science are periodic in nature eg. the current and voltage in an alternating current circuit. These periodic functions can be analyzed into their constituent components (fundamentals and harmonics) by a process called Fourier analysis. By definition, a periodic function,  $f(t)$  is that where  $f(t) = f(t+T)$ . This function can be represented by a trigonometric series of elements consisting of a DC component and other elements with frequencies comprising the fundamental component and its integer multiple frequencies. This applies if the following so-called Dirichlet conditions are met:

If a discontinuous function,  $f(t)$  has a finite number of discontinuities over the period  $T$

If  $f(t)$  has a finite mean value over the period  $T$

If  $f(t)$  has a finite number of positive and negative maximum values

The expression for Fourier series expansion is given as follows,

$$f(t) = \frac{a_0}{2} + \sum_{n=1}^{\infty} [a_n \cos(n\omega_0 t) + b_n \sin(n\omega_0 t)] \quad (2)$$

Where  $\omega_0 = 2\pi / T$

We can further simplify equation (1), we get

$$f(t) = c_0 + \sum_{n=1}^{\infty} c_n \sin(n\omega_0 t + \phi_n) \quad (3)$$

Where

$$c_0 = \frac{a_0}{2}, c_n = \sqrt{a_n^2 + b_n^2}, \phi_n = \tan^{-1}\left(\frac{b_n}{a_n}\right)$$

$(n \omega_0)n^{th}$  order harmonic of the periodic function

$c_0$  magnitude of the DC component

$c_n$  and  $\phi_n$  magnitude and phase angle of the  $n^{th}$  harmonic component

The component with  $n = 1$  is the fundamental component. Magnitude and phase angle of each harmonic determine the resultant waveform  $f(t)$ .

The equation (3) can be written in complex form as,

$$f(t) = \sum_{n=1}^{\infty} c_n e^{jn\omega_0 t} \quad (4)$$

Where  $n=0, \pm 1, \pm 2$

$$c_n = \frac{1}{T} \int_{-T/2}^{T/2} f(t) e^{-jn\omega_0 t} dt \quad (5)$$

The main source of harmonics in power system is the static power converter. Under ideal operation condition, harmonics generated by a  $p$  pulse power converter are characterized by,

$$I_n = \frac{I_1}{n}, \text{ and } n = pl \pm 1 \quad (6)$$

where  $n$  stand for the characteristic harmonics of the load;  $l=1, 2, \dots$  and  $p$  is an integer multiple of six.

The figure below gives the example of harmonic spectrum

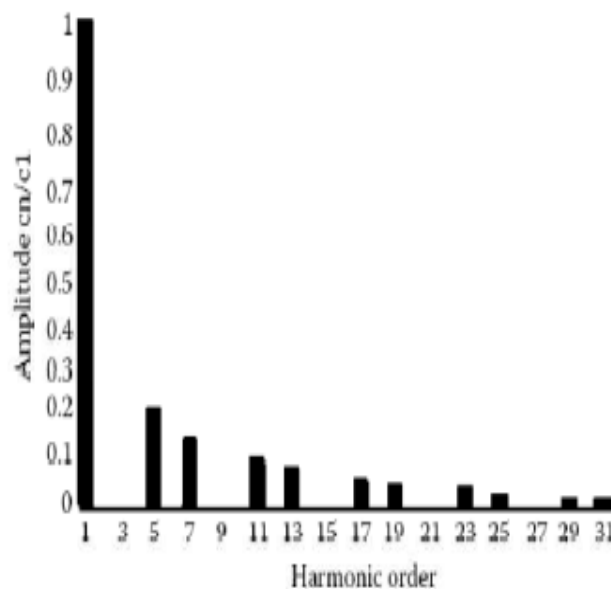
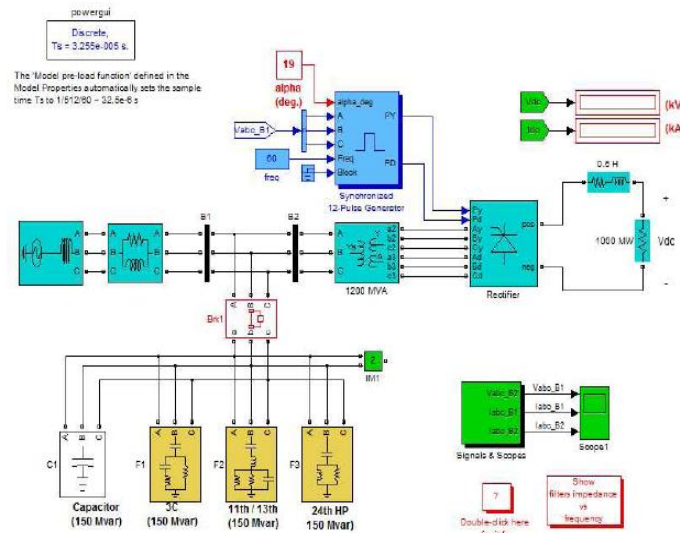


Figure 2. Example of harmonics spectrum

#### IV SIMULATION AND RESULTS

The figure 3 represents the simulink model of proposed system created in MATLAB. The three phase harmonic filters are connected between the buses B1 and B2 through breaker. For analysis of the harmonics two cases were taken. Case 1 with the three phase harmonics filters connected to the lines and the case 2 with the harmonic filters not connected to the lines.



**Figure 3. Simulink model of the proposed system**

Three-phase harmonic filters are shunt elements that are used in power systems for decreasing voltage distortion and for power factor correction. Nonlinear elements such as power electronic converters generate harmonic currents or harmonic voltages, which are injected into power system. The resulting distorted currents flowing through system impedance produce harmonic voltage distortion. Harmonic filters reduce distortion by diverting harmonic currents in low impedance paths. Harmonic filters are designed to be capacitive at fundamental frequency, so that they are used for producing reactive power required by converters and for power factor correction. The HVDC (High Voltage Direct Current) rectifier is built up from two 6-pulse thyristor bridges connected in series. The converter is connected to the system with a 1200-MVA three phase transformer (three windings). A 1000-MW resistive load is connected to the DC side through a 0.5 H smoothing reactor. The filters are made of the following four components of the powerlib/Elements library:

1. One capacitor banks (C1) of 150 Mvar modeled by a “Three-Phase Harmonic Filters “are used in HVDC line.
- (i). One C-type high-pass filter to the 3<sup>rd</sup> (F1) of 150 Mvar
- (ii). One double-tuned filter 11<sup>th</sup> /13<sup>th</sup> (F2) of 150 Mvar
- (iii). One high-pass filter tuned to the 24<sup>th</sup> (F3) of 150 Mvar.

In order to achieve an acceptable distortion, several banks of filters of different types are usually connected in parallel. The combinations of different banks are derived from basic filters Butterworth Chebyshev and Causer filters. The most commonly used filter types are

1. Band-pass filters, which are used to filter lowest order harmonics such as 5<sup>th</sup> ,7<sup>th</sup> ,11<sup>th</sup> ,13<sup>th</sup> etc. Band-pass filters can be tuned at a single frequency(single tuned filter) or at two frequencies(double-tuned filter)
2. High-pass filters, which are used to filter high-order harmonics and cover a wide range of frequencies. A special type of high-pass filter, the C-type high-pass filter, is used to provide reactive power and avoid parallel resonances. It also allows filtering low order harmonics (such as 3<sup>rd</sup>), while keeping zero losses at fundamental frequency.

The figure below shows the different types of three-phase RLC harmonic filter.

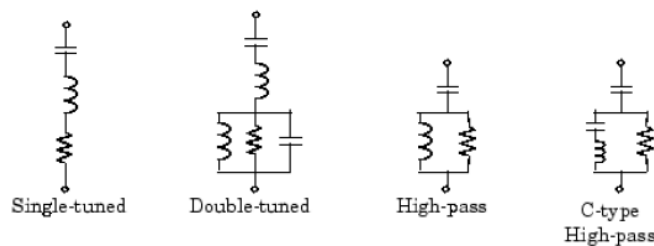


**Figure 4. Different types of three-phase RLC harmonic filter**

The simulink model of the proposed system is given in figure 2. The power converter usually act as nonlinear source injecting harmonics into the system. The three phase harmonic filter is installed between the buses B1 and B2.

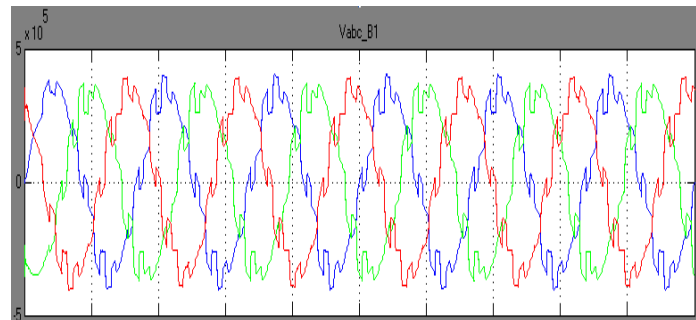


Figure 5. Three phase voltage at the bus B1 without harmonic filter

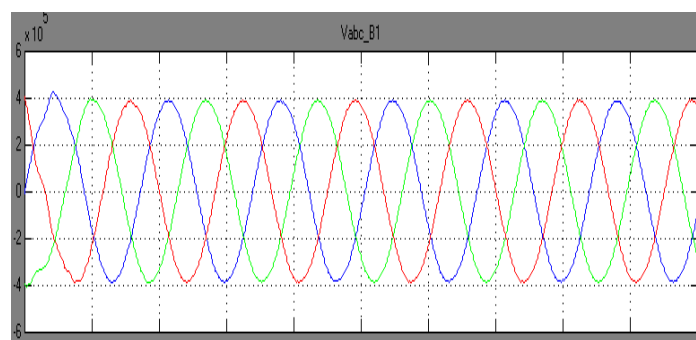


Figure 6. Three phase voltage at the bus B1 with harmonic filter

Figures 4 and 5 gives the simulation results of the three phase voltage at the bus B1 with and without harmonic filters. From figure 4 we observe that in the absence of three phase harmonic filters the three phase voltage at the bus B1 getting distorted due to the harmonics injected by the rectifier, which is the non-linear load in this case.

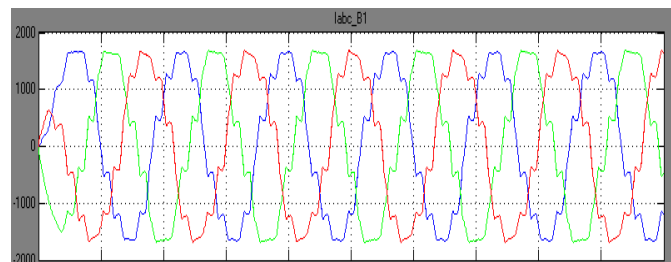


Figure 7. Three phase current at the bus B1 without harmonic filter

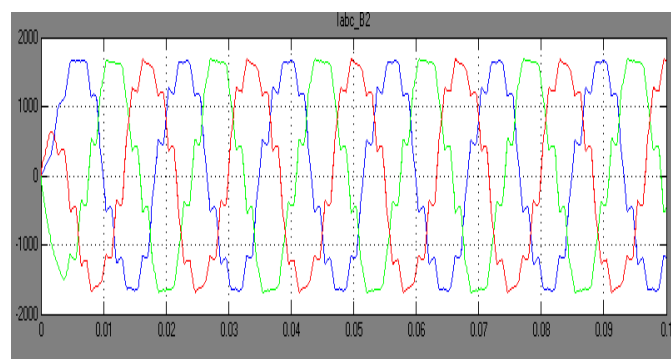


Figure 8. Three phase current at the bus B2 without harmonic filter

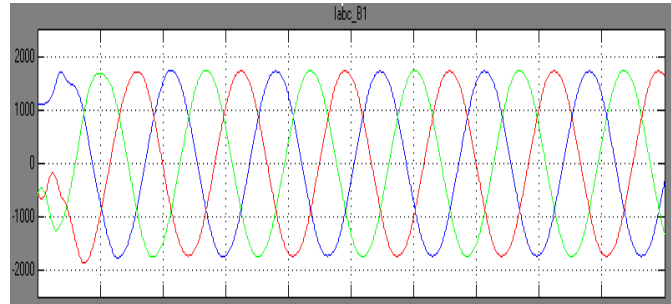


Figure 9. Three phase current at the bus B1 with harmonic filter

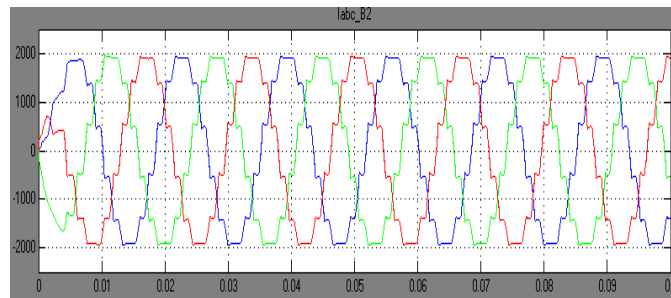


Figure 10. Three phase current at the bus B2 with harmonic filter

Figures 6 and 7 gives the simulation results of three phase currents at the buses B1 and B2 without harmonic filters. Figures 8 and 9 gives the simulation results of three phase currents at the buses B1 and B2 with harmonic filters. On comparison of figures 6,7 and 8,9 we observe that in the absence of three phase harmonic filters the three phase currents at the bus B1 and B2 getting distorted due to the harmonics injected by the non-linear load.

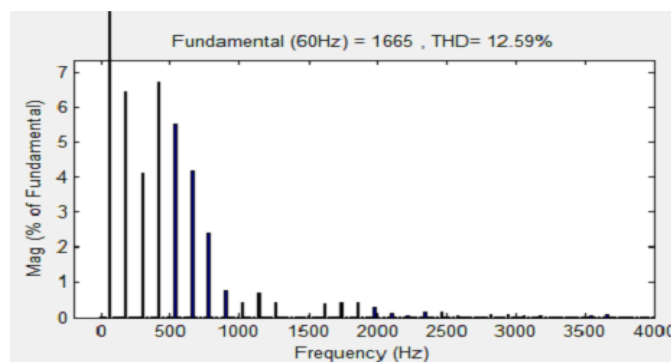


Figure 11. Harmonic spectrum of three-phase currents at bus B2 without harmonic filter

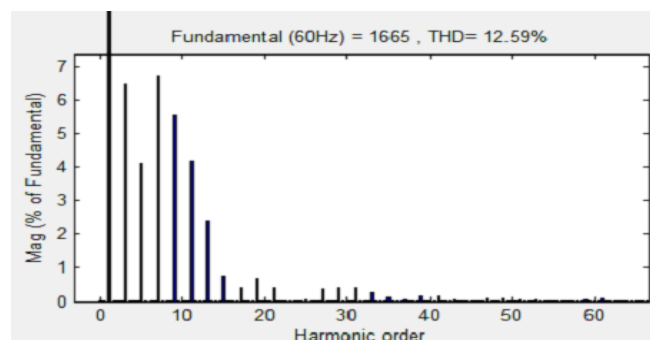


Figure 12. Harmonic order of three-phase currents at bus B2 without harmonic filter

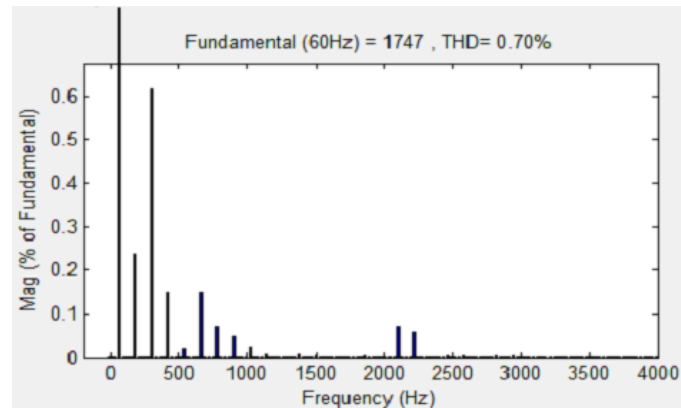


Figure 13. Harmonic spectrum of three-phase currents at bus B2 with harmonic filter

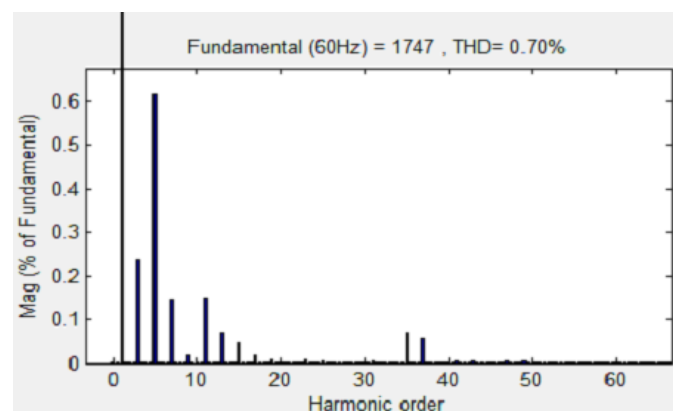


Figure 14. Harmonic order of three-phase currents at bus B2 with harmonic filter

On comparison on figures 10, 11 with figures 11, 12 we observe that the total harmonic reduction (THD) was considerably reduced from 12.59% for the case without harmonic filters to 0.70% for the case with harmonic filters. The simulation is performed for the test case with alpha 19 degree. Simulations can be performed for various values of alpha and the impact on the DC level and on generated harmonics can be noted.

## V CONCLUSION

There will be an increasing economical impact on the operation of electrical power system due to losses in the system. In this study the HVDC model in MATLAB/SIMULINK is used with different three phase filter banks to reduce the distortion and to increase the power quality of the system. Three phase harmonic filter used in this work for decreasing the voltage distortion and for power factor correction. The focus of this work is to have economical impact of the electrical power system through harmonics, distortion reduction and to increase the power quality of the system.

## VI SCOPE OF FUTURE WORK

This work can be extended in future with different filter combinations for decreasing the harmonics. Advanced modifications can be imparted to this filter design to address various power quality issues and to provide the end users with reliable source of power.

## REFERENCES

- [1] Himabindu. T, Jayaprakash, "Performance of single phase shunt active filter based on P-Q technique using matlab/simulink", International Journal of Engineering Research and Technology, vol.1, Issue 9, November 2012.
- [2] P.Thirumoorthi, Jyothis Francis and N.Yadaiah, "Power conditioning in battery chargers using shunt active power filter through neural network", International Journal of Advances in Engineering & Technology, March 2012.
- [3] R.Sriranjani and S.Jayalalitha, "Investigation the performance of the various types of harmonic filters", World Applied Sciences Journal 17(5):643-650 2012.
- [4] C. Nalini Kiran, Subhransu Sekhar Dash, and S. Prema Latha, "A Few Aspects of Power Quality Improvement Using Shunt Active Power Filter," International Journal of Scientific & Engineering Research, vol.2, Issue 5, May 2011.

- [5] Shu,Z.,S.Xie and Q.Li,2011, "Single phase back to back converter for active power balancing, reactive power compensation and harmonic filtering in traction power system",IEEE Trans.Power Electronics,26:2.
- [6] S. Mikkili and A. K. Panda, "APF for mitigation of current harmonics with p-q and id-iq control strategies using pi controller," Journal of Trends in Electrical Engineering, Vol. 1, No. 1, pp. 1-11, May 2011.
- [7] Seema P. Diwan, Pradeep Diwan, a.P Vaidya,"Simulation Studies of Single phase Shunt Active Filter with the DC Capacitor Voltage Control,"IEEE,2011.
- [8] Attia, A. H., El-Metwally, M. and Fahmy O.M., "Harmonic distortion effects and mitigation in distribution systems", Journal of American Science, 2010 vol.6, no.10, pp.173-183.
- [9] Rahmani, S., Mendalek, N., and Al-Haddad, K., "Experimental Design of a Nonlinear Control Technique for Three-Phase Shunt Active Power Filter", IEEE Transactions on Industrial Electronics, Volume 57, No. 10, pp.3364-3375, 2010.
- [10] Aaron Vander Meulen and John Maurin, Application Engineers, Current source inverter vs.Voltage source inverter topology. August 2010.
- [11] Chen, C.I., Chang, G.W., Hong, R.C., and Li, H.M.,"Extend Real Model of Kalman Filter for Time-Varying Harmonics Estimation", IEEE Transactions on Power Delivery, Volume 25, No. 1, pp. 17-26, 2010.
- [12] Jaume Miret, Miguel Castilla, Jose Matas, Josep M.Guerrero, Juan C.Vasquez, "Selective harmonic-compensation control for single phase active power filter with high harmonic rejection",IEEE transactions on industrial electronics,vol.56,no.8,August 2009.
- [13] P. Kumar and A.Mahajan, "Soft computing techniques for the control of an active power filter," IEEE Trans. Power Del.,vol.24,no.,pp.452-461,Jan 2009.
- [14] L.Asiminoaci, F.Blaabjerg, S.Hansen, and P.Thogersen, "Adaptive compensation of reactive power with shunt active power filters, IEEE Trans.Ind.Appl., vol.44, no.3, pp.867877,May/Jun 2008.
- [15] Abdusalam, M., P. Poure and S.Saadate, 2008. "Hardware implementation of a three phase active filter system with harmonic isolation based on self tuning filter", IEEE.
- [16] Harmonics and Power System, Francisco C. De LA ROSA, Distribution Control System, Inc, Hazelwood, Missouri, USA.
- [17] Basic Electronics Eighth Edition, by Bernard Grob.

## Adsorption Capacity of Nicotine From Tobacco Products By Different Adsorbents

<sup>1</sup>Zamzam Basher\* , <sup>2</sup>A.K.Gupta And <sup>3</sup>Amit Chattrre

1,2,3,PhD. Student , Professor , Associate Professor Department of Chemistry , Faculty of basic science, SHIATS ,Allahabad-211007(U.P.).

### ABSTRACT:

This study determined the adsorption capacity of nicotine content of tobacco in four cigarettes brands . The method was used to estimate the nicotine in tobacco products by an Ultraviolet-Visible Spectrophotometer. The results for nicotine content that was adsorbed highest in coconut fibre and saw dust , followed by tea waste.

**KEYWORDS:** UV-Vis Spectrophotometer, tobacco, nicotine, adsorption.

### I. INTRODUCTION

The highly toxic chemical in tobacco alkaloids is nicotine,3-(1-methyl-2-pyrrolidinyl) pyridine present in the leaves of *Nicotiana tabacum* [1]. Nicotine is one of the several thousands of compounds , identified in tobacco . The determination of nicotine is an important analysis for the tobacco industry, as the quality and usability of the product can be determined by its nicotine content [2]. Nicotine content in cigarettes has been reported in several studies [3-4] based on the dose reduction resulting from cigarette smoke as the main control in estimating the concentration of nicotine produced by smoking . Nicotine can be found in tobacco particulate matter and in tobacco smoke [5]. Nicotine in tobacco smoke is converted to its volatile and available free-base from through the action of gaseous ammonia [6]. Various methods have been employed to determine the nicotine content in tobacco, including solvent extraction followed by gas-chromatographic-mass spectrometric analysis [7] or liquid chromatography with ultra violet visible (UV-Vis) spectrophotometer [8]. Most technologies are expensive . Activated carbons are widely used as adsorbents for purification of aqueous solutions . In separation science the process of adsorption has an edge over other methods ,due to its simplicity and sludge free clean operation used for nicotine separation [9]. The objective of this study is to estimate the nicotine content of 4 popular cigarettes and to compare the ability of coconut fibre , saw dust and tea waste as adsorbents for nicotine content in tobacco .

### II. MATERIALS & METHODS

Brand of cigarettes used in this study were Gold, Capstan , Gudang garam and Tradition purchased from a local supermarket. Cigarettes were taken out of their rolling paper dried to weighing. 0.5g of individual tobacco were weighed, placed in a 100 ml beaker and treated with boiling water in a well-closed flask, after twenty-four hours the liquid was treated with 10 ml of adsorbing solution (0.01 NaOH in 10% ethanol) . Subsequently solution of nicotine extract was stirred for 3 hours . The liberated solution of nicotine is distilled off in a current of steam, in such a way that the volume of liquid in the flask is reduced 3/4<sup>th</sup> to 2/3<sup>rd</sup> . When the volume of distillate attains two to three times less then that of the original liquid the distillation was stopped.

### III. RESULTS AND DISCUSSION

The results obtained in the estimation of nicotine adsorption of four cigarettes brands by coconut fibre , saw dust and tea waste,used as adsorbents were determined by the UV-Vis spectrophotometer method. The data of the table(1) envisages that, the initial concentration of nicotine in four cigarettes Gold , Capstan , Gudang garam and Tradition were  $3.3106 \times 10^{-3}$  ,  $2.9867 \times 10^{-3}$  ,  $3.9196 \times 10^{-3}$  ,  $4.5351 \times 10^{-3}$  mg/L respectively, while the initial concentration of nicotinic acid that was used as standard was  $1.5031 \times 10^{-3}$  mg/L . The concentrations of nicotine in four cigarettes that adsorbed by coconut fibre , saw dust and tea waste is shown in the table :

**Table 1 :** Adsorption of Nicotine of cigarettes in mg/L by the adsorbents.

cigarette	Coconut fibre		Saw dust		Tea waste	
	$C_f$	$C_{ad}$	$C_f$	$C_{ad}$	$C_{final}$	$C_{ad}$
Gold	$1.1143 \times 10^{-3}$	$2.1963 \times 10^{-3}$	$1.3022 \times 10^{-3}$	$2.0084 \times 10^{-3}$	$2.2805 \times 10^{-3}$	$1.0301 \times 10^{-3}$
Capstan	$0.7774 \times 10^{-3}$	$2.2092 \times 10^{-3}$	$0.9912 \times 10^{-3}$	$1.9954 \times 10^{-3}$	$1.8788 \times 10^{-3}$	$1.1079 \times 10^{-3}$
Gudang garam	$1.0431 \times 10^{-3}$	$2.8765 \times 10^{-3}$	$1.3735 \times 10^{-3}$	$2.5461 \times 10^{-3}$	$2.0149 \times 10^{-3}$	$1.9047 \times 10^{-3}$
Tradition	$1.1662 \times 10^{-3}$	$2.5980 \times 10^{-3}$	$1.9242 \times 10^{-3}$	$2.6109 \times 10^{-3}$	$3.7642 \times 10^{-3}$	$0.7709 \times 10^{-3}$
Nicotinic acid	$1.9371 \times 10^{-3}$	$0.3379 \times 10^{-3}$	$1.1337 \times 10^{-3}$	$0.3694 \times 10^{-3}$	$1.9371 \times 10^{-3}$	$0.1296 \times 10^{-3}$

Where  $C_f$  = The final concentration of nicotine in equilibrium.

$C_{ad}$  = The concentration of adsorbed nicotine by adsorbents.

Adsorption of nicotine was measured at specified time using three adsorbents like coconut fibre, saw dust and waste tea leaves for four different cigarettes. From Fig 1 to 3 the plot reveals that the amount of nicotine removed by coconut fibre and saw dust were higher, then the amount of nicotine was removed by using waste tea leaves. The result showed that coconut fibre and saw dust had more efficiency than waste tea leaves as adsorbents to remove nicotine in cigarettes. Therefore active carbon fibres of coconut with unmatched pore structure and surface characteristics that have materials and high efficiency for a number of application, these organic materials can be used for adsorption of wide number of molecules of organic matter as observed by Manocha [10].

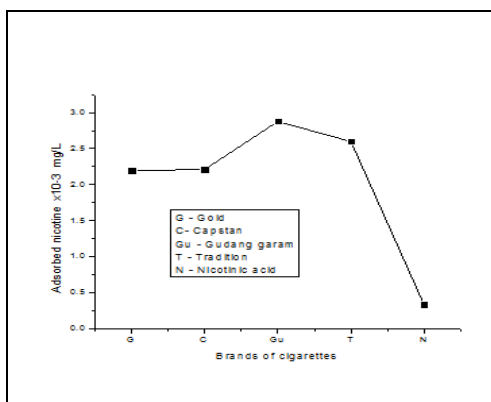


**Figure 1 :**The nicotine adsorption capacity of four cigarettes by coconut fibre

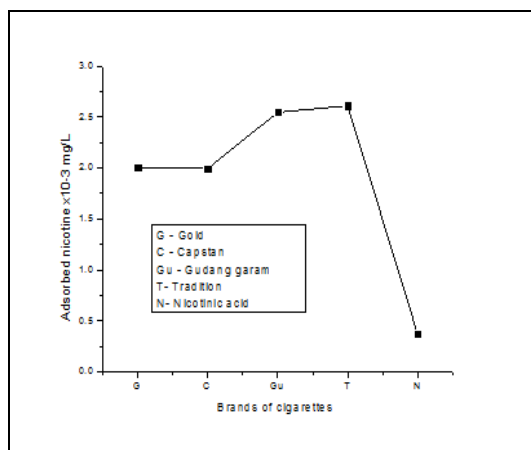


**Figure 2 :**The nicotine adsorption capacity of four cigarettes by saw dust.

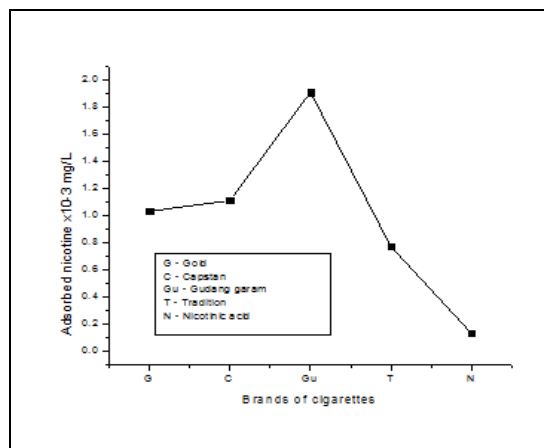


**Figure 3 :**The nicotine adsorption capacity of four cigarettes by tea waste.

The above figures showed that the amount of adsorbed nicotine by coconut fibre and saw dust was higher in Gudang garam than Tradition, Capstan and Gold respectively, while the amount of adsorbed nicotine by tea waste was higher in Gudang garam than Capstan, Gold and Tradition respectively. Therefore the percentage of nicotine was higher in Gudang garam than the other studied cigarettes.

#### IV. CONCLUSION

In the current study the nicotine content of tobacco in 4 popular brands of cigarettes was determined by using UV-Vis spectrophotometer after using different adsorbents. The results showed that the concentration of nicotine that adsorbed by coconut fibre and saw dust was higher than the concentration of nicotine that adsorbed by tea waste. The coconut fibre and saw dust had higher efficiency as adsorbents in respect to nicotine adsorption.

#### REFERENCES

- [1] Ching, Wu; William, F. Siems; Herbert H; Hill, J. and Rich, M. Hannan., Analytical determination of nicotine in tobacco by supercritical fluid Chromatography-ion mobility detection. *Journal of Chromatography A*, 1998. **811**(1-2): p. 157-161.
- [2] Henningfield, J.E; Radzius, A. and Cone, E.J. Estimation of available nicotine content of six
- [3] smokeless tobacco products. *Tobacco Control*, 1995. **4**(1): p. 57.
- [4] Henningfield, J.E; Hariharan, M. and Kozlowski, L.T. Nicotine content and health risks of
- [5] cigars. *JAMA: The Journal of the American Medical Association*, 1996. **276**(23): p. 1857.
- [6] Henningfield, J.E; Fant, R.V; Radzius, A. and Frost, S. Nicotine concentration, smoke pH and whole tobacco aqueous pH of some cigar brands and types popular in the United States. *Nicotine & Tobacco Research*, 1999. **1**(2): p. 163.
- [7] Ferris Wayne, G; Connolly, G. and Henningfield, J. Brand differences of free-base nicotine
- [8] delivery in cigarette smoke: the view of the tobacco industry documents. *Tobacco Control*,
- [9] 2006. **15**(3): p. 189.
- [10] James, F. Pankow; Brian, T. Mader; Lorne, M. Isabelle; Wentai Luo, Andrea
- [11] Pavlick and Cikui Liang. Conversion of nicotine in tobacco smoke to its volatile and available free base form through the action of gaseous ammonia. *Environmental Science & Technology*,
- [12] 1997. **31**(8): p. 2428-2433.
- [13] Hariharan, M. and VanNoord, T. Liquid chromatographic determination of nicotine and
- [14] cotinine in urine from passive smokers: comparison with gas chromatography with a nitrogen-
- [15] specific detector. *Clinical Chemistry*, 1991. **37**(7): p. 1276.
- [16] Uryupin, A. and Fomina, L. Analysis of tobacco smoke condensates. *Journal of Analytical*
- [17] *Chemistry*, 2005. **60**(8): p. 784-787.
- [18] 9. Jyotsna Lal. *Chromium and fluoride removal by low cost adsorbents* proceedings The Third international
- conference on Environmental Science and Technology Houston, Texas USA 6-9 August 2007
- [19] Manocha. Porous carbons, Sadhana, (28), Parts 1 & 2, February/April 2003, pp. 335-348.

## An Automated Image Segmentation Scheme for Iris Recognition

Dr. G. Saravana Kumar<sup>1</sup>, J. Munikrishnan<sup>2</sup>, Manimaraboopathy<sup>3</sup>

1 Professor, Dept of ECE, Vel Tech High Tech Dr Rangarajan Dr Sakunthala Engineering College, Chennai

2 Research Scholar, St Peter's University, Chennai

3 Dept of ECE, Vel Tech High Tech Dr Rangarajan Dr Sakunthala Engineering College,, Chennai

### ABSTRACT:

The paper proposes an automated segmentation system, which localizes the iris region from an eye image and also isolates the eyelid, eyelash as well as the reflection regions. This automatic segmentation was achieved through the utilization of the circular Hough transform in order to localize the iris as well as the pupil regions, and the linear Hough transform has been used for localizing the eyelid occlusion. Thresholding has been employed for isolating the eyelashes as well as the reflections. Now, the segmented iris region has been normalized in order to eliminate the dimensional inconsistencies between the iris regions. This was achieved by applying a version of Daugman's rubber sheet model, in which the iris is modeled as a flexible rubber sheet, which is unpacked into a rectangular block with constant polar dimensions. Ultimately, the iris features were encoded by convolving the normalized iris region with the 1D Log-Gabor filters and phase quantizing the output to produce a bit-wise biometric template. For metric matching, the Hamming distance has been chosen, which provides a measure of number of disagreed bits between two templates.

**KEYWORDS:** Image segmentation, Image localization, Circular Hough transform, Thresholding, Log-Gabor filter, Hamming distance

### I. INTRODUCTION

Various facets of modern life demand identity validation for human beings to provide unique access, ensure protection and confirmation to their transactions. The archetypal examples are authenticated entry to buildings, ATMs. The conventional authentication mechanisms accomplish this objective by providing Identification Cards, Numeric and alphanumeric characters based passwords to end-users. The ruggedness of this system can be improved by utilizing unique features of physiological characteristics of human beings. A biometric system is a pattern recognition system that operates by acquiring biometric data from an individual, extracting a feature set from the acquired data and comparing this feature set against the template set in the database [1]. The existing visual recognition techniques authentication is based on identity fed by individuals. The performance measure of automated recognition algorithms is reliability. A relatively high variability value among instances of different classes compared to variability value for a given class will yield good reliability. One of the main performance constraints for a face recognition system is the input image, "facial image". The resultant changes due to face's collateral features such as different expressions, age and image acquisition set up deviations cause quality deterioration of the image. This introduces drastic success rate reduction of matching algorithms amounts to 43%-50%. The existing face recognition algorithms exhibit a superior inter class variability management over intra class variability. The human iris, which is the annular part between the pupil and the white sclera, has a complex pattern determined by the chaotic morphogenetic processes during embryonic development. The iris pattern is unique to each person and to each eye and is essentially stable over a lifetime. Furthermore, an iris image is typically captured using a noncontact imaging device, which is of great importance in practical applications. Iris recognition is a biometric recognition technology that utilizes the pattern recognition techniques based on the high quality images of iris. The advantage of iris recognition techniques among a gamut of visual recognition techniques is founded on the inimitable iris pattern of each individual. The prevailing matching algorithms exploit this characteristic to ascertain individuals. This uniqueness supports large size iris databases, low false rate matching algorithm development. The basic block diagram of an iris recognition system is shown in Fig.1.

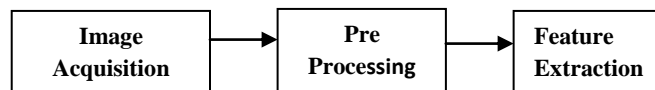


Figure 1: Block diagram of Iris recognition System

Typical Iris recognition system consists of mainly three modules. They are image acquisition, pre processing stage as well as feature extraction and encoding. Image acquisition is a module which involves the capturing of iris images with the help of sensors. Pre-processing module provides the determination of the boundary of iris within the eye image and then extracts the iris portion from the image in order to facilitate its processing. It involves stages like iris segmentation, iris normalization and image enhancement. The performance of the system has been analyzed in the feature extraction and encoding stage.

## II. LITERATURE SURVEY

In the recent years, drastic improvements have been accomplished in the areas like iris recognition, automated iris segmentation, edge detection, boundary detection etc.

### 2. 1. Integro Differential Operator

This approach [1] is regarded as one of the most cited approach in the survey of iris recognition. Daugman uses an integrodifferential operator for segmenting the iris. It finds both inner and the outer boundaries of the iris region. The outer as well as the inner boundaries are referred to as limbic and pupil boundaries. The parameters such as the center and radius of the circular boundaries are being searched in the three dimensional parametric space in order to maximize the evaluation functions involved in the model. This algorithm achieves high performance in iris recognition. The boundary decision techniques navigate from rough texture to smoother details resulting in a single pixel precision estimate of center coordinates, radius of iris and image. Owing to boundary concentricity non assumption pupil search constrained by normal approach.

### 2. 2. Edge Detection

The edge detection has been performed through the gradient-based Canny edge detector, which is followed by the circular Hough transform [2], which is used for iris localization. The final issue is the pattern matching. After the localization of the region of the acquired image which corresponds to the iris, the final operation is to decide whether pattern matches with the previously saved iris pattern. This stage involves alignment, representation, goodness of match and also the decision. All these pattern matching approaches relies mainly on the method which are closely coupled to the recorded image intensities. If there occurs a greater variation in any one of the iris, one way to deal with this is the extraction as well as matching the sets of features that are estimated to be more vigorous to both photometric as well as geometric distortions in the obtained images. The advantage of this method is that it provides segmentation accuracy up to an extent. The drawback of this approach is that, it does not provide any attention to eyelid localization (EL), reflections, eyelashes, and shadows which is more important in the iris segmentation.

### 2. 3. Heterogeneous Segmentation

This automation algorithm performs localization, separation operation on eye image yielding iris region, eyelid, and eyelash. This algorithm uses two variants of Hough transform namely linear Hough transform localizing eyelid occlusion and circular Hough transform for iris localization, pupil localization. A new iris segmentation approach, which has a robust performance in the attendance of heterogeneous as well as noisy images, has been developed in this. The segmentation approach provides three parameters two spatial coordinates and intensity value for each image pixel. The possession of homogeneous characteristics by image, constrains edge detector algorithm. An Intermediate image is generated by applying fuzzy-K-means algorithm. The intermediate image is derived from pixel-by-pixel classification. The Intermediate Generation image offers parameter to propel edge detection algorithm performance.

### 2. 4. Characteristics of Segmentation Algorithms

Iris recognition algorithm performance improvement is based on two parameters precision, swiftness. The desirable characteristics are,

- Specularities exclusion
- Iris detection / Localization
- Non iris images rejection
- Iris Center Localization estimate
- Circular iris boundary localization

- Non Circular iris boundary localization
- Eyelid localization
- Sharp irregularity management

Extracting iris images from moderate non cooperative eye images and severe non cooperative eye images is the performance metric for iris segmentation algorithm. The desired characteristics of the algorithm are,

- Spatial location based clustering
- False location minimization
- Enhancement of global convergence ability

The various categories of techniques are summarized in Table 1.

Figure 1: Block diagram of Iris recognition System

S. No.	Method name	Operation
1	Adaboost-Cascade iris detector	Iris detection
2	Puling and Pushing (PP) method	i. Circular iris boundary localization ii. Shortest path to the valid parameters
3	Cubic Smoothing Spline	Non circular iris boundaries detection
4	Statistically Learned Prediction Model	Eyelash, Eyelid detection
5	8-neighbour connection based clustering	Region based clustering
6	Semantic Priors	Iris extraction
7	Integro differential constellation	Segmentation
8	1-D Horizontal rank filter	Eyelid localization
	Eyelid curvature model	

The existing segmentation methods yield less segmentation accuracy in many areas such as boundary detection, iris detection, pupil and limbic boundary detection. The main limitation identified as lack of segmentation accuracy. The literature survey suggests need for novel, reliable and robust automatic segmentation method.

### III. ALGORITHM PROPOSITION

This paper presents an iris identification approach which involves feature extraction of iris images followed by masking and matching algorithm. Hamming distance is used in order to classify iris codes. The proposed algorithm flow is shown in Figure 2.

#### 3. 1. Image Acquisition and Pre Processing

The step is one of the most important and deciding factors for obtaining a good result. A good and clear image eliminates the process of noise removal and also helps in avoiding errors in calculation. In this case, computational errors are avoided due to absence of reflections, and because the images have been taken from close proximity. This paper uses the image provided by CASIA (Institute of Automation, Chinese Academy of Sciences, these images were taken solely for the purpose of iris recognition software research and implementation. The proposed algorithm flow is shown in Figure 2.

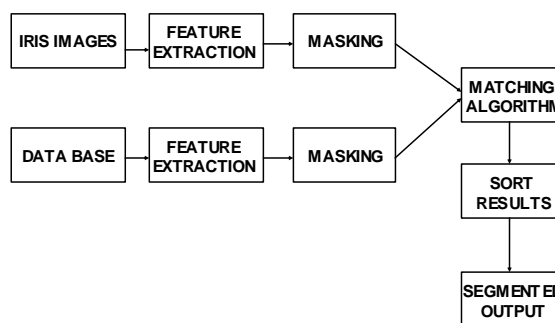


Figure 2: Proposed Algorithm Flow

Infra-red light was used for illuminating the eye, and hence they do not involve any specular reflections. Some part of the computation which involves removal of errors due to reflections in the image was hence not implemented. Since it has a circular shape when the iris is orthogonal to the sensor, iris recognition algorithms typically convert the pixels of the iris to polar coordinates for further processing. An important part of this type of algorithm is to determine which pixels are actually on the iris, effectively removing those pixels that represent the pupil, eyelids and eyelashes, as well as those pixels that are the result of reflections. In this algorithm, the locations of the pupil and upper and lower eyelids are determined first using edge detection. This is performed after the original iris image has been down sampled by a factor of two in each direction (to 1/4 size, in order to speed processing). The best edge results came using the canny method. The pupil clearly stands out as a circle and the upper and lower eyelid areas above and below the pupil is also prominent. A Hough transform is then used to find the center of the pupil and its radius. Once the center of the pupil is found, the original image is transformed into resolution invariant polar coordinates using the center of the pupil as the origin. This is done since the pupil is close to circular. Although not always correct, it is assumed that the outer edge of the iris is circular as well, also centered at the center of the pupil. From this geometry, when the original image is transformed into polar coordinates, the outer boundary of the iris will appear as a straight (or near straight) horizontal line segment. This edge is determined using a horizontal Sobel filter. After determination of the inner and outer boundaries of the iris, the non-iris pixels within these concentric circles must be determined. Thresholding identifies the glare from reflections (bright spots), while edge detection is used to identify eyelashes.

### 3. 2. Chinese Academy of Sciences - Institute of Automation (CASIA) eye image database

The Chinese Academy of Sciences - Institute of Automation (CASIA) eye image database contains 756 grayscale eye images with 108 unique eyes or classes and 7 different images of each unique eye. Images from each class are taken from two sessions with one month interval between sessions. The images were captured especially for iris recognition research using specialized digital optics developed by the National Laboratory of Pattern Recognition, China. The eye images are mainly from persons of Asian decent, whose eyes are characterized by irises that are densely pigmented, and with dark eyelashes. Due to specialized imaging conditions using near infra-red light, features in the iris region are highly visible and there is good contrast between pupil, iris and sclera regions. A part of CASIA eye image database is shown in Figure 3.

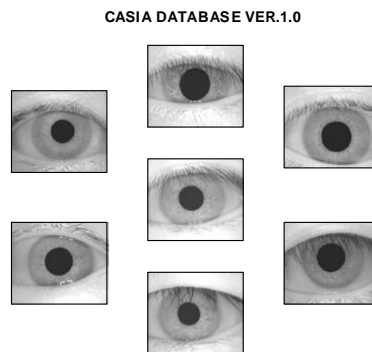


Figure 3: CASIA eye image database

### 3. 3. Iris Localization / Segmentation

Without placing undue constraints on the human operator, image acquisition of the iris cannot be expected to yield an image containing only the iris. Rather, image acquisition will capture the iris as part of a larger image that also contains data derived from the immediate surrounding eye region. The part of the eye carrying information is only the iris part. It lies between the sclera and the pupil. Therefore, prior to performing iris pattern matching, it is important to localize that portion of the acquired image that corresponds to an iris. In particular, it is necessary to localize that portion of the image derived from inside the limbus (the border between the sclera and the iris) and outside the pupil. Further, if the eyelids are occluding part of the iris, then only that portion of the image below the upper eyelid and above the lower eyelid should be included. Typically, the limbic boundary is imaged with high contrast, owing to the sharp change in eye pigmentation that it marks. The upper and lower portions of this boundary, however, can be occluded by the eyelids. The papillary boundary can be far less well defined. The image contrast between a heavily pigmented iris and its pupil can be quite small.

Further, while the pupil typically is darker than the iris, the reverse relationship can hold in cases of cataract: the clouded lens leads to a significant amount of backscattered light. Like the pupillary boundary, eyelid contrast can be quite variable depending on the relative pigmentation in the skin and the iris. The eyelid boundary also can be irregular due to the presence of eyelashes. Taken in tandem, these observations suggest that iris localization must be sensitive to a wide range of edge contrasts, robust to irregular borders, and capable of dealing with variable occlusion. The first stage of iris recognition is to isolate the actual iris region in a digital eye image. The iris region can be approximated by two circles, one for the iris/sclera boundary and another, interior to the first, for the iris/pupil boundary. The eyelids and eyelashes normally occlude the upper and lower parts of the iris region. Also, specular reflections can occur within the iris region corrupting the iris pattern. This technique is required to isolate and exclude these artifacts as well as locating the circular iris region. The success of segmentation depends on the imaging quality of eye images. Images in the CASIA iris database do not contain specular reflections due to the use of near infra-red light for illumination. Also, persons with darkly pigmented irises will present very low contrast between the pupil and iris region if imaged under natural light, making segmentation more difficult. The segmentation stage is critical to the success of an iris recognition system, since data that is falsely represented as iris pattern data will corrupt the biometric system performance.

### 3.4. Hough Transform

The Hough transform is a standard computer vision algorithm that can be used to determine the parameters of simple geometric objects, such as lines and circles, present in an image. The circular Hough transform can be employed to deduce the radius and centre coordinates of the pupil and iris regions. Firstly, an edge map is generated by calculating the first derivatives of intensity values in an eye image and then thresholding the result. From the edge map, votes are cast in Hough space for the parameters of circles passing through each edge point. These parameters are the centre coordinates  $x_c$  and  $y_c$ , and the radius  $r$ , which are able to define any circle. A maximum point in the Hough space will correspond to the radius and centre coordinates of the circle best defined by the edge points. The motivation for this is that the eyelids are usually horizontally aligned, and also the eyelid edge map will corrupt the circular iris boundary edge map if using all gradient data. Taking only the vertical gradients for locating the iris boundary will reduce influence of the eyelids when performing circular Hough transform, and not all of the edge pixels defining the circle are required for successful localisation. Not only does this make circle localization more accurate, it also makes it more efficient, since there are less edge points to cast votes in the Hough space. The resultant images yielded by Hough transform application are shown in Figure 4.

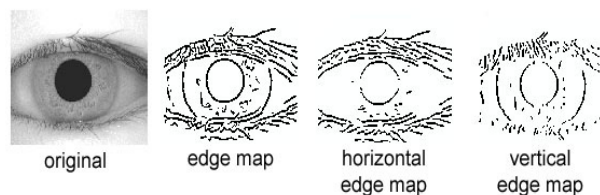


Figure 4: Edge maps of an eye image

Circular Hough transform is used for detecting the iris and pupil boundaries. This involves first employing canny edge detection to generate an edge map. Gradients were biased in the vertical direction for the outer iris/sclera boundary. Vertical and horizontal gradients were weighted equally for the inner iris/pupil boundary. In order to make the circle detection process more efficient and accurate, the Hough transform for the iris/sclera boundary was performed first, then the Hough transform for the iris/pupil boundary was performed within the iris region, instead of the whole eye region, since the pupil is always within the iris region. After this process was complete, six parameters are stored, the radius, and x and y centre coordinates for both circles. Eyelids were isolated by first fitting a line to the upper and lower eyelid using the linear Hough transform. A second horizontal line is then drawn, which intersects with the first line at the iris edge that is closest to the pupil. The second horizontal line allows maximum isolation of eyelid regions. Canny edge detection is used to create an edge map, and only horizontal gradient information is taken. For isolating eyelashes in the CASIA database a simple thresholding technique was used, since analysis reveals that eyelashes are quite dark when compared with the rest of the eye image.

### 3. 5. Iris Localization / Segmentation

Once the iris region is segmented, the next stage is to normalize this part, to enable generation of the iris code and their comparisons. Since variations in the eye, like optical size of the iris, position of pupil in the iris, and the iris orientation change person to person, it is required to normalize the iris image, so that the representation is common to all, with similar dimensions. Normalization process involves unwrapping the iris and converting it into its polar equivalent. It is done using Daugman's Rubber sheet model shown in Figure 5. The centre of the pupil is considered as the reference point and a remapping formula is used to convert the points on the Cartesian scale to the polar scale. The radial resolution was set to 100 and the angular resolution to 2400 pixels. For every pixel in the iris, an equivalent position is found out on polar axes. The normalized image was then interpolated into the size of the original image, by using the `interp2` function. The dimensional inconsistencies between eye images are mainly due to the stretching of the iris caused by pupil dilation from varying levels of illumination. Other sources of inconsistency include, varying imaging distance, rotation of the camera, head tilt, and rotation of the eye within the eye socket. The normalisation process will produce iris regions, which have the same constant dimensions, so that two photographs of the same iris under different conditions will have characteristic features at the same spatial location.

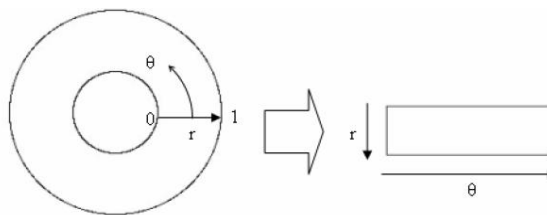


Figure 5: Daugman's rubber sheet model

### 3. 6. Feature Encoding

The final process is the generation of the iris code. For this, the most discriminating feature in the iris pattern is extracted. The phase information in the pattern only is used because the phase angles are assigned regardless of the image contrast. Amplitude information is not used since it depends on extraneous factors. In order to provide accurate recognition of individuals, the most discriminating information present in an iris pattern must be extracted. The template that is generated in the feature encoding process will also need a corresponding matching metric, which gives a measure of similarity between two iris templates. This metric should give one range of values when comparing templates generated from the same eye, known as intra-class comparisons, and another range of values when comparing templates created from different irises, known as inter-class comparisons. These two cases should give distinct and separate values, so that a decision can be made with high confidence as to whether two templates are from the same iris, or from two different irises.

## IV. IMPLEMENTATION

### 4.1. Hamming Distance

For matching, the Hamming distance was chosen as a metric for recognition, since bit-wise comparisons were necessary. The Hamming distance gives a measure of how many bits are the same between two bit patterns. The weighted Euclidean distance (WED) can be used to compare two templates, especially if the template is composed of integer values. The weighting Euclidean distance gives a measure of how similar a collection of values are between two templates. If two bits patterns are completely independent, such as iris templates generated from different irises, the Hamming distance between the two patterns should equal 0.5. This occurs because independence implies the two bit patterns will be totally random, so there is 0.5 chance of setting any bit to 1, and vice versa. Therefore, half of the bits will agree and half will disagree between the two patterns. If two patterns are derived from the same iris, the Hamming distance between them will be close to 0.0, since they are highly correlated and the bits should agree between the two iris codes. The calculation of the Hamming distance is taken only with bits that are generated from the actual iris region. The Hamming distance algorithm employed also incorporates noise masking, so that only significant bits are used in calculating the Hamming distance between two iris templates. Now when taking the Hamming distance, only those bits in the iris pattern that corresponds to '0' bits in noise masks of both iris patterns will be used in the calculation.

## V. RESULTS

The implementation provides a Graphical User Interface (GUI) as shown in Figure 6.

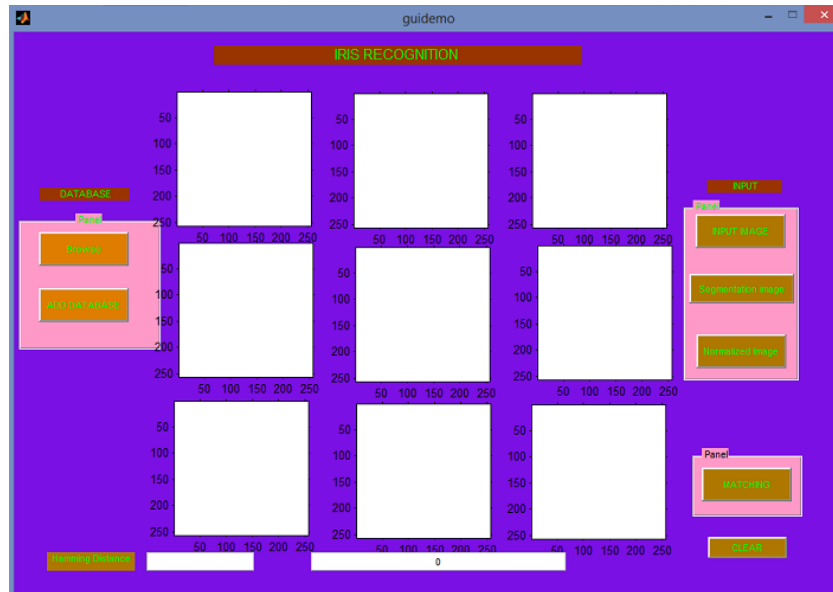


Figure 6: GUI for Iris recognition

Figure 7 shows comprehensive result stages obtained by the proposed algorithm .



Figure 7: Iris recognition implementation

## VI. CONCLUSION

The major contributions of this paper is to demonstrate an effective approach for phase-based iris recognition as proposed in Section 3. Experimental performance evaluation using the CASIA iris image. Database clearly demonstrates that the use of the segmentation scheme for iris images makes it possible to achieve highly accurate iris recognition with a hamming distance as authentication criterion. This paper optimizes the trade-off between the iris data size and recognition performance in a highly flexible manner.

## REFERENCES

- [1] J. Wayman, A. Jain, D. Maltoni, and D. Maio, *Biometric Systems*. Springer, 2005.
- [2] A. Jain, R. Bolle, and S. Pankanti, *Biometrics: Personal Identification in a Networked Society*. Kluwer, 1999.
- [3] J. Daugman, "High-Confidence Visual Recognition of Persons by a Test of Statistical Independence," *IEEE Trans. Pattern Analysis and Machine Intelligence*, vol. 15, no. 11, pp. 1148-1161, Nov. 1993.
- [4] L. Ma, T. Tan, Y. Wang, and D. Zhang, "Efficient Iris Recognition by Characterizing Key Local Variations," *IEEE Trans. Image Processing*, vol. 13, no. 6, pp. 739-750, June 2004.
- [5] W. Boles and B. Boashash, "A Human Identification Technique Using Images of the Iris and Wavelet Transform," *IEEE Trans. Signal Processing*, vol. 46, no. 4, pp. 1185-1188, Apr. 1998.
- [6] C. Tisse, L. Martin, L. Torres, and M. Robert, "Person Identification Technique Using Human Iris Recognition," *Proc. 15th Int'l Conf. Vision Interface*, pp. 294-299, 2002.
- [7] R. Wildes, "Iris Recognition: An Emerging Biometric Technology," *Proc. IEEE*, vol. 85, no. 9, pp. 1348-1363, Sept. 1997.
- [8] B.V.K. Vijaya Kumar, C. Xie, and J. Thornton, "Iris Verification Using Correlation Filters," *Proc. Fourth Int'l Conf. Audio- and Video-Based Biometric Person Authentication*, pp. 697-705, 2003.
- [9] Z. Sun, T. Tan, and X. Qiu, "Graph Matching Iris Image Blocks with Local Binary Pattern," *Advances in Biometrics*, vol. 3832, pp. 366-372, Jan. 2006.
- [10] C.D. Kuglin and D.C. Hines, "The Phase Correlation Image Alignment Method," *Proc. Int'l Conf. Cybernetics and Soc.* '75, pp. 163-165, 1975.
- [11] K. Takita, T. Aoki, Y. Sasaki, T. Higuchi, and K. Kobayashi, "High-Accuracy Sub pixel Image Registration Based on Phase-Only Correlation," *IEICE Trans. Fundamentals*, vol. E86-A, no. 8, pp. 1925-1934, Aug. 2003.
- [12] K. Takita, M.A. Muquit, T. Aoki, and T. Higuchi, "A Sub-Pixel Correspondence Search Technique for Computer Vision Applications," *IEICE Trans. Fundamentals*, vol. 87-A, no. 8, pp. 1913-1923, Aug. 2004.
- [13] K. Ito, H. Nakajima, K. Kobayashi, T. Aoki, and T. Higuchi, "A Fingerprint Matching Algorithm Using Phase-Only Correlation," *IEICE Trans. Fundamentals*, vol. 87-A, no. 3, pp. 682-691, Mar. 2004.
- [14] K. Ito, A. Morita, T. Aoki, T. Higuchi, H. Nakajima, and K. Kobayashi, "A Fingerprint Recognition Algorithm Using Phase-Based Image Matching for Low-Quality Fingerprints," *Proc. 12th IEEE Int'l Conf. Image Processing*, vol. 2, pp. 33-36, Sept. 2005.
- [15] K. Ito, A. Morita, T. Aoki, T. Higuchi, H. Nakajima, and K. Kobayashi, "A Fingerprint Recognition Algorithm Combining Phase-Based Image Matching and Feature-Based Matching," *Advances in Biometrics*, vol. 3832, pp. 316-325, Jan. 2006.
- [16] H. Nakajima, K. Kobayashi, M. Morikawa, A. Katsumata, K. Ito, T. Aoki, and T. Higuchi, "Fast and Robust Fingerprint Identification Algorithm and Its Application to Residential Access Controller," *Advances in Biometrics*, vol. 3832, pp. 326-333, Jan. 2006.
- [17] Products Using Phase-Based Image Matching, Graduate School of Information Sciences, Tohoku Univ., <http://www.aoki.ecei.tohoku.ac.jp/research/poc.html>, 2008.
- [18] K. Miyazawa, K. Ito, T. Aoki, K. Kobayashi, and H. Nakajima, "An Efficient Iris Recognition Algorithm Using Phase-Based Image Matching," *Proc. 12th IEEE Int'l Conf. Image Processing*, vol. 2, pp. 49-52, Sept. 2005.
- [19] K. Miyazawa, K. Ito, T. Aoki, K. Kobayashi, and H. Nakajima, "A Phase-Based Iris Recognition Algorithm," *Advances in Biometrics*, vol. 3832, pp. 356-365, Jan. 2006.
- [20] CASIA Iris Image Database, Inst. Automation, Chinese Academy of Sciences, <http://www.sinobiometrics.com/>, 2008.
- [21] Iris Challenge Evaluation (ICE), Nat'l Inst. Standards and Technology, <http://iris.nist.gov/ice/>, 2008.
- [22] R.C. Gonzalez and R.E. Woods, *Digital Image Processing*, second ed. Prentice Hall, 2002.
- [23] L. Masek and P. Kovesi, "Matlab Source Code for a Biometric Identification System Based on Iris Patterns," School of Computer Science and Software Eng., Univ. of Western Australia, <http://people.csse.uwa.edu.au/pk/studentprojects/libor/>, 2003.
- [24] ICE 2005 Results, Nat'l Inst. Standards and Technology, [http://iris.nist.gov/ICE/ICE\\_2005\\_Results\\_30March2006.pdf](http://iris.nist.gov/ICE/ICE_2005_Results_30March2006.pdf), 2008.
- [25] B. Efron, "Bootstrap Methods: Another Look at the Jackknife," *Annals of Statistics*, vol. 7, no. 1, pp. 1-26, 1979.
- [26] R.M. Bolle, N.K. Ratha, and S. Pankanti, "Error Analysis of Pattern Recognition Systems: The Subsets Bootstrap," *Computer Vision and Image Understanding*, vol. 93, no. 1, pp. 1-33, Jan. 2004.
- [27] K. Ito, T. Aoki, H. Nakajima, K. Kobayashi, and T. Higuchi, "A Palmprint Recognition Algorithm Using Phase-Based Image Matching," *Proc. 13th IEEE Int'l Conf. Image Processing*, pp. 2669-2672, Oct. 2006.
- [28] B.V.K. Vijaya Kumar, M. Savvides, K. Venkataramani, and C. Xie, "Spatial Frequency Domain Image Processing for Biometric Recognition," *Proc. Ninth IEEE Int'l Conf. Image Processing*, vol. 1, pp. 53-56, 2002.
- [29] K. Venkataramani and B.V.K. Vijaya Kumar, "Performance of Composite Correlation Filters for Fingerprint Verification," *Optical Eng.*, vol. 43, pp. 1820-1827, Aug. 2004.
- [30] B.V.K. Vijaya Kumar, A. Mahalanobis, and R. Juday, *Correlation Pattern Recognition*. Cambridge Univ. Press, 2005.

# DWDM Link with Multiple Backward Pumped Raman Amplification

Awab Fakh<sup>1</sup>, Santosh Jagtap<sup>2</sup>, Shraddha Panbude<sup>3</sup>

1,2,3 Vidyalkankar Institute of Technology, Wadala, India

## ABSTRACT:

Faced with the challenge of dramatically increasing capacity while constraining costs, carriers have two options either to install new fiber or increase the effective bandwidth of existing fiber. The technology of dense wavelength-division multiplexing (DWDM) has recently resulted in a considerable increase in the transmission capacity of fiber-optic communication systems up to several terabits per second. The further improvement of the transmission capacity of such systems can be achieved through the expansion of the spectral range of WDM transmission toward the short-wavelength region. Therefore in this report we have proposed and investigated the new trends and progress of fiber Raman amplification for dense wavelength division multiplexing photonic communication networks. Forty individual channels carrying PRBS data are transmitted over a 50 km length of ITU-T G.652 single mode dispersive fiber. The design objective is to utilize distributed Raman amplification to compensate for the link attenuation thereby effectively increasing the inter-EDFA span in a longer-haul link.

**KEYWORDS:** PRBS, Digital Crossconnect System (DCS), phonons, Dense wavelength division multiplexing (DWDM), stimulated raman scattering (SRS), raman amplification, pump evolution, EDFA

## I. INTRODUCTION

It is needless to mention that the 21st century activities will be drastically hindered without the advent of modern communication system [1]. Off all, the most advanced communication system has been culminated in the form of Internet, allowing all computers on the planet and in the orbit to be connected to each other simultaneously. While telecommunication remains as a major medium and has its own demand for higher bandwidth, the demand for even higher bandwidth is sky rocketed by exponential growth of the Internet traffic. The cumulative demand for bandwidth poses a serious limitation for the existing carrier technologies. High demand coupled with high usage rates, a deregulated telecommunications environment, and high availability requirements is rapidly depleting the capacities of fibers. Faced with the challenge of dramatically increasing capacity while constraining costs, carriers have two options: Install new fiber or increase the effective bandwidth of existing fiber. Laying new fiber is the traditional means used by carriers to expand their networks. Deploying new fiber, however, is a costly proposition. It is estimated at about dollar 70,000 per mile, most of which is the cost of permits and construction rather than the fiber itself. Laying new fiber may make sense only when it is desirable to expand the embedded base. Increasing the effective capacity of existing fiber can be accomplished in two ways [1], increase the bit rate of existing systems or increase the number of wavelengths on a fiber.

In section II, a detailed explanation of Dense Wavelength Division Multiplexing (DWDM) technology is mentioned. Section III describes the basic concept of Raman amplification, comparison of Raman amplifiers with Erbium Doped Fiber Amplifiers (EDFA) and the use of Raman Amplification in DWDM system. In section IV, the design and simulation results of a 40 channel DWDM link with backward pumped Raman amplification is mentioned. The paper ends with section V, which includes the summary and the future scope of Raman amplification in DWDM systems.

## II. DENSE WAVELENGTH DIVISION MULTIPLEXING (DWDM)

In fiber-optic communications, wavelength-division multiplexing (WDM) is a technology which multiplexes multiple optical carrier signals on a single optical fiber by using different wavelengths ( $\lambda$ s) of laser light to carry different signals as shown in figure 1. DWDM is the clear winner in the backbone. It was first deployed on long-haul routes in a time of fiber scarcity. Then the equipment savings made it the solution of choice for new long-haul routes, even when ample fiber was available [3]. While DWDM can relieve fiber exhaust in the metropolitan area, its value in this market extends beyond this single advantage. Alternatives for capacity enhancement exist, such as pulling new cable and SONET overlays, but DWDM can do more. What delivers additional value in the metropolitan market is DWDMs fast and flexible provisioning of protocol and bit rate-transparent, data-centric, protected services, along with the ability to offer new and higher-speed services at less cost. The need to provision services of varying types in a rapid and efficient manner in response to the changing demands of customers is a distinguishing characteristic of the metropolitan networks. With SONET, which is the foundation of the vast majority of existing MANs, service provisioning is a lengthy and complex process. Network planning and analysis, ADM provisioning, Digital Crossconnect System (DCS) reconfiguration, path and circuit verification, and service creation can take several weeks. By contrast, with DWDM equipment in place provisioning new service can be as simple as turning on another light wave in an existing fiber pair.

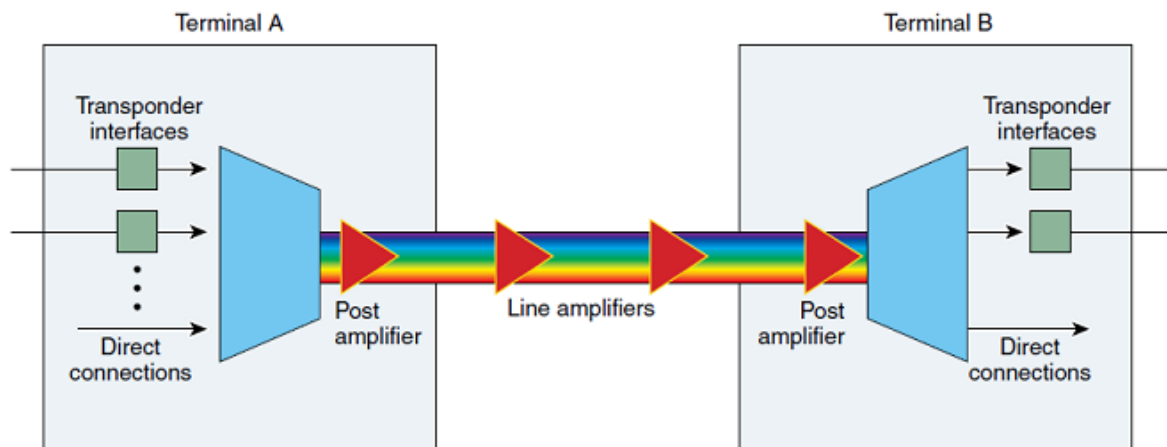


Fig. 1: WDM Technology [2]

Potential providers of DWDM-based services in metropolitan areas, where abundant fiber plant already exists or is being built, include incumbent local exchange carriers (ILECs), competitive local exchange carriers (CLECs), inter-exchange carriers (IXCs), Internet service providers (ISPs), cable companies, private network operators, and utility companies. Such carriers can often offer new services for less cost than older ones. Much of the cost savings is due to reducing unnecessary layers of equipment, which also lowers operational costs and simplifies the network architecture. Carriers can create revenue today by providing protocol transparent, high-speed LAN and SAN services to large organizations, as well as a mixture of lower-speed services (Token Ring, FDDI, Ethernet) to smaller organizations. In implementing an optical network, they are ensuring that they can play in the competitive field of the future.

## III. RAMAN AMPLIFICATION IN DWDM SYSTEM

Raman amplification is based on stimulated Raman scattering (SRS) a non-linear effect in fiber optical transmission that results in signal amplification if optical pump waves with the correct wavelength and power are launched into the fiber [4]. One of the most recent and interesting developments includes the constructive usage of the so-called Raman effect in optical amplifiers [8]. A Raman amplifier uses intrinsic properties of silica fibers to obtain signal amplification. This means that transmission fibers can be used as a medium for amplification, and hence that the intrinsic attenuation of data signals transmitted over the fiber can be combated within the fiber. An amplifier working on the basis of this principle is commonly known as a distributed Raman amplifier (DRA). The physical property behind DRAs is called SRS. This occurs when a sufficiently large pump is co-launched at a lower wavelength than the signal to be amplified. The Raman gain depends strongly on the pump power and the frequency offset between pump and signal. Amplification occurs when the pump photon gives up its energy to create a new photon at the signal wavelength plus some residual energy, which is absorbed as phonons (vibrational energy) as shown in figure 2.

As there is a wide range of vibrational states above the ground state, a broad range of possible transitions, are providing gain. This is shown by figure 2. Generally, Raman gain increases almost linearly with wavelength offset between signal and pump peaking at about 100 nm and then dropping rapidly with increased offset. Figure 3 shows a typically measured Raman gain curve [9]. The position of the gain bandwidth within the wavelength domain can be adjusted simply by tuning the pump wavelength. Thus, Raman amplification potentially can be achieved in every region of the transmission window of the optical transmission fiber. It only depends on the availability of powerful pump sources at the required wavelengths. The disadvantage of Raman amplification is the need for high pump powers to provide a reasonable gain. This opens a new range of possible applications. It is possible, for instance, to partially compensate fiber attenuation using the Raman effect and, thus, to increase the EDFA locations. This saves costs as less EDFAs are needed on the link, and the number of sites to be maintained is reduced [8], [11].

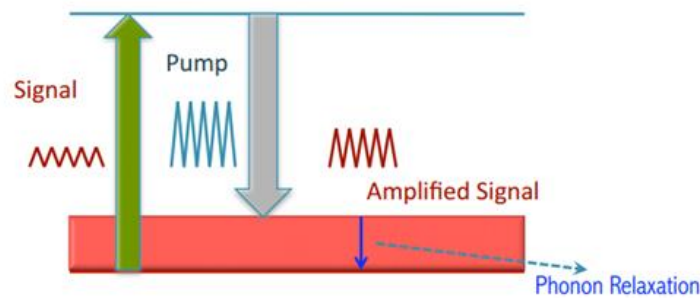


Fig. 2: System Configuration [8]

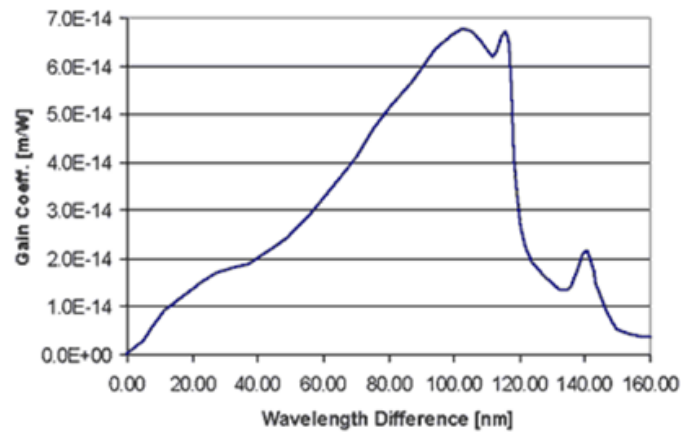


Fig. 3: Typical Raman gain curve versus wavelength offset [9]

Raman amplifiers offer several advantages compared to EDFAs, including the following:

- Low noise build-up.
- Simple design, as direct signal amplification is achieved in the optical fiber, and no special transmission medium is needed.
- Flexible assignment of signal frequencies.
- Broad gain bandwidth.

However, despite the many advantages of Raman amplification, there can be some degradation effects. For example, not only the specially launched pump waves but also some of the WDM channels may provide power to amplify the other channels. This would result in power exchange between WDM channels and thus cross-talk leading to signal degradation. These negative effects occur in unidirectional and bidirectional WDM transmission. So for accurate analysis of advanced WDM systems, it is crucial to model all Raman interactions. Additionally, degrading effects like spontaneous Raman scattering and backward Rayleigh scattering have to be considered. Raman amplifiers are topologically simpler to design than doped-fiber amplifiers, as the existing transmission fiber can be used as a medium if properly pumped. However, the selection of pump powers and wavelengths, as well as the number and separation of pumps, strongly determines the wavelength behaviour of Raman gain and noise.

When building distributed Raman amplifiers, designers face the question of using forward or backward pumping (or even both) with respect to signal propagation. The backward pumping scheme is most commonly used as it offers several advantages. Pump noise strongly affects the WDM signals to be amplified if forward pumping is applied, as the Raman process is nearly instantaneous [5], [6]. When the Raman pump wave has slight random power fluctuations in time, which is almost always the case, individual bits might be amplified differentially, which leads to amplitude fluctuations or jitters. If backward pumping is applied the amplitude fluctuations will be averaged out [7].

#### 4. 40 Gbps DWDM Link with Backward Pumped Raman Amplification

This example simulates a realistic scenario of a 40Gbps DWDM link with inter-channel spacing of 50 GHz. Forty individual channels carrying PRBS data are transmitted over a 50 km length of ITU-T G.652 single mode dispersive fiber. The design objective is to utilize distributed Raman amplification to compensate for the link attenuation thereby effectively increasing the inter-EDFA span in a longer-haul link. Figure 4 below shows a snap-shot of the layout. The multi-line capability of OptSims CW laser model makes it very convenient to generate the source-grid for simulating WDM channels.

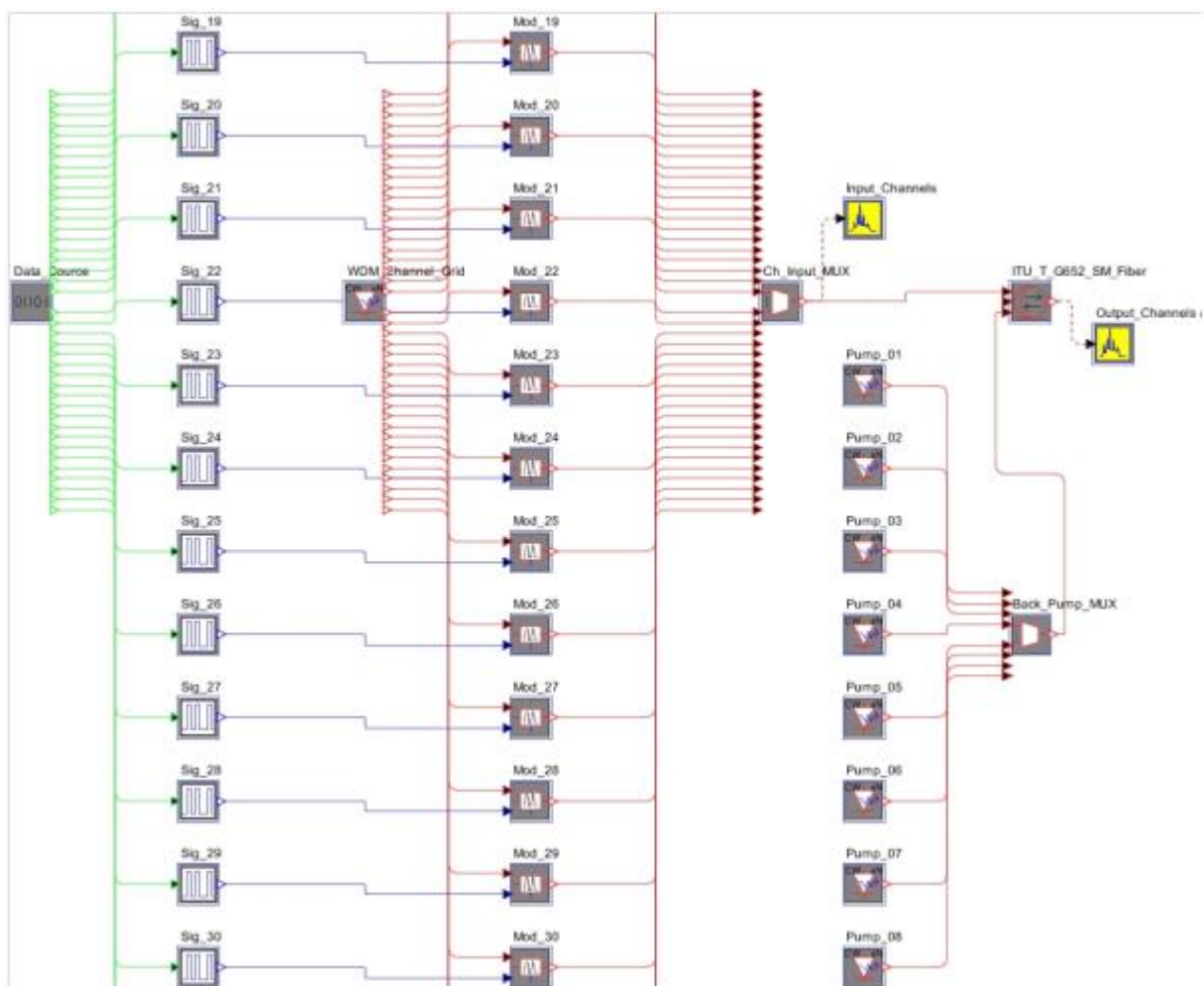


Fig. 4: Sectional snap-shot of a 40-channel DWDM link layout

#### 4.1 Spectrum of Channels

Since backward pumping helps in averaging out power ripples at the receiver end, we choose a backward pumping scheme that employs eight CW pump signals with carefully chosen nominal wavelengths and power values. Figure 5 and figure 6 depicts spectra of input and output channels in presence of backward pumping respectively.

## 4.2 Backward Pump Characteristics

Raman amplification is a wide-band phenomenon having a highly irregular gain profile over wavelength. The highest Raman gain is observed for a frequency differential range (range of difference between pump signal and data signal nominal frequencies) of 8 to 12 THz. Outside this range, the gain profile exhibits a sharp decline. Therefore, if the number of pumps, their wavelengths, and the power values are chosen carefully, we can achieve the desired gain shape for the input DWDM channels. Figure 7 shows a graph of the backward output spectral density. It is observed that the pump is given at a wavelength of 1330 nm. Power of 0.44 W is launched in the backward channel at 1330 nm as shown in figure 8. It can also be observed that the noise power in the channel is very low. The backward gain ranges from -20 dB to -50 dB in the range of 1300 to 1400 nm as shown in figure 9. Outside this range the backward gain is as low as -66 dB. Figure 10 depicts the backward effective noise figure. Effective noise figure of approximately 40 dB is obtained at 1330 nm. The signal to noise ratio obtained is 180 dB as shown in figure 11.

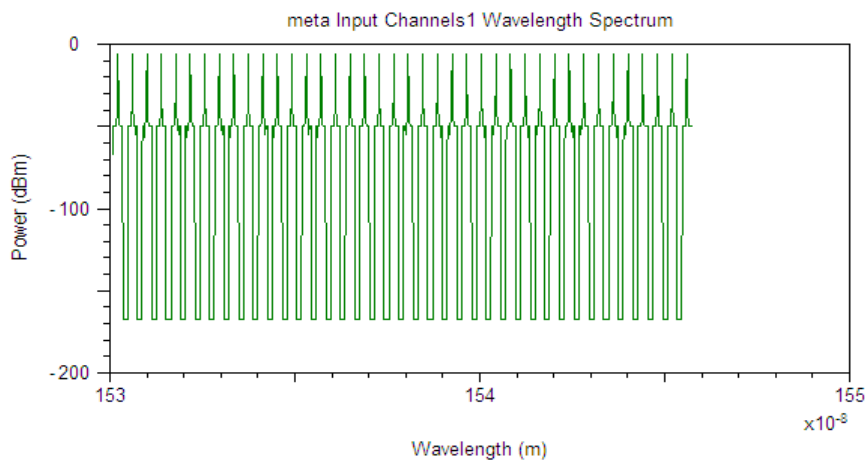


Fig. 5: 40 channel input wavelength spectrum

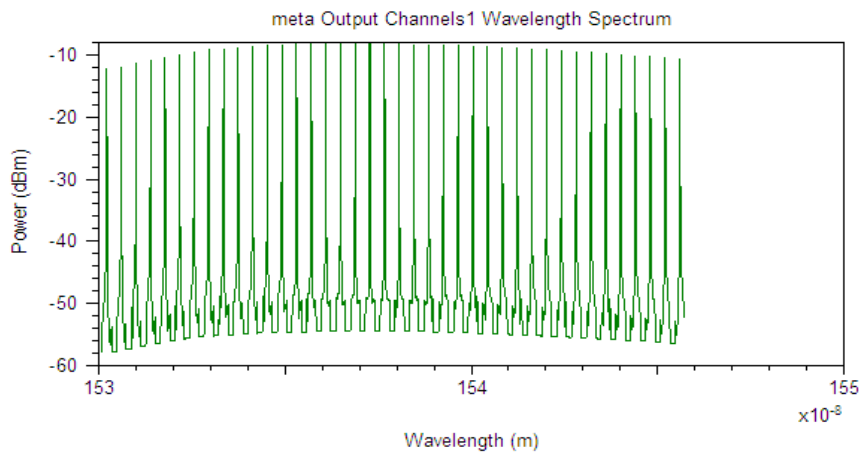


Fig. 6: Output with backward pumping

## 4.3 Characteristic of Output Signal

The output signal is observed at 1550 nm. As shown in figure 12, forward gain of 6.2 dB is obtained at 1550 nm. It can be seen in figure 13 that power of 1 mW is launched into the fiber at 1550 nm and a final power of 5 mW is obtained at 1550 nm. The forward effective noise figure is shown in figure 14. Effective noise figure of -3.35 dB is obtained at 1550 nm. Figure 15 shows that signal to noise ratio at 1550 nm is 40 dB.

## 4.4 Pump Evolution

The output spectrum above takes in to account the pump signal and the signal-signal interactions. Besides, the pumps interact with each other, too. Shorter wavelength pumps provide power to longer wavelength pumps. As a result, we can expect rise in longer wavelength pump powers and corresponding depletion of shorter wavelength pumps at the launch end of the fiber. The pump evolution and signal power evolution are shown in figure 16 and figure 17 respectively.

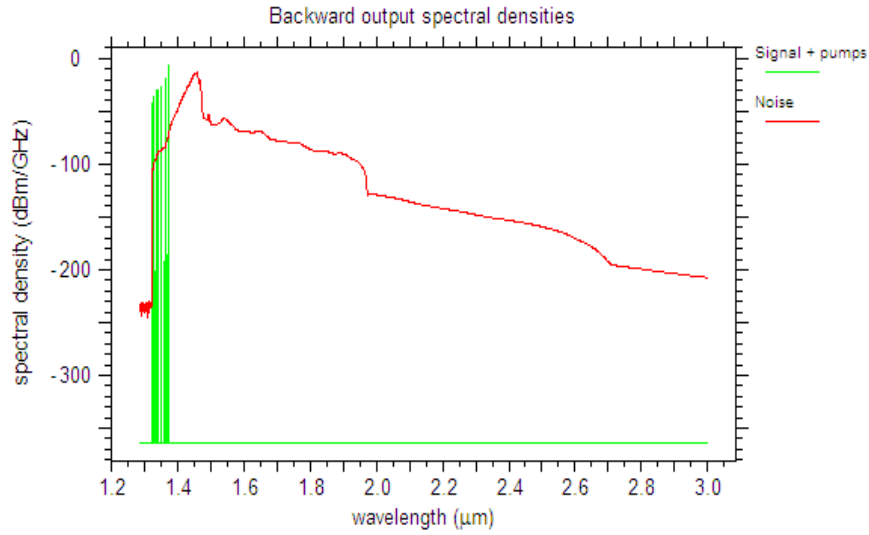


Fig. 7: Backward output spectral density

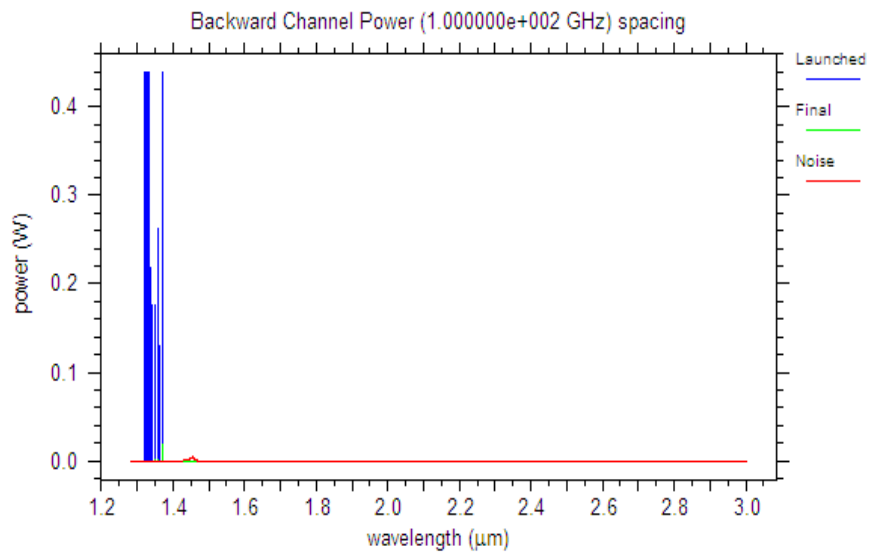


Fig. 8: Backward channel power

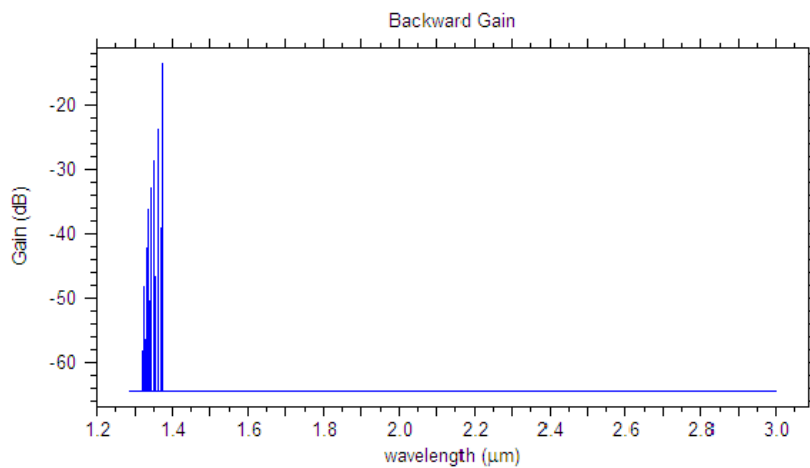


Fig. 9: Backward gain

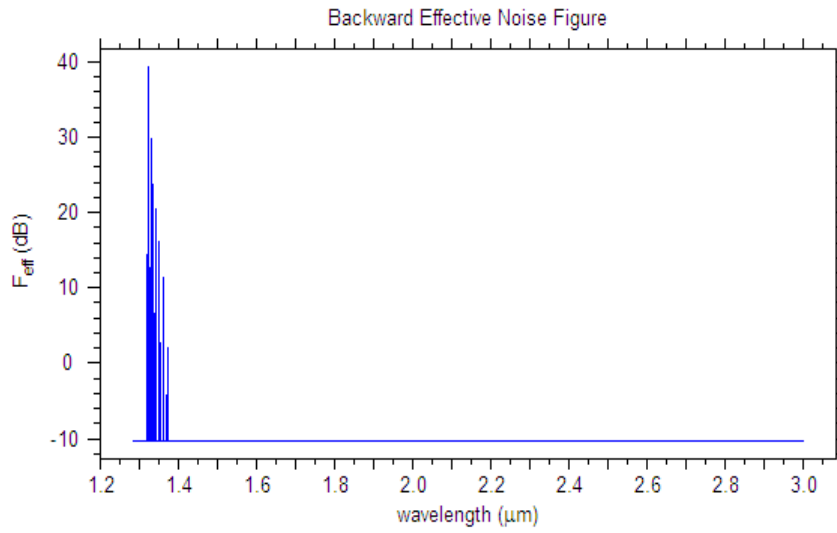


Fig. 10: Backward Effective Noise Figure

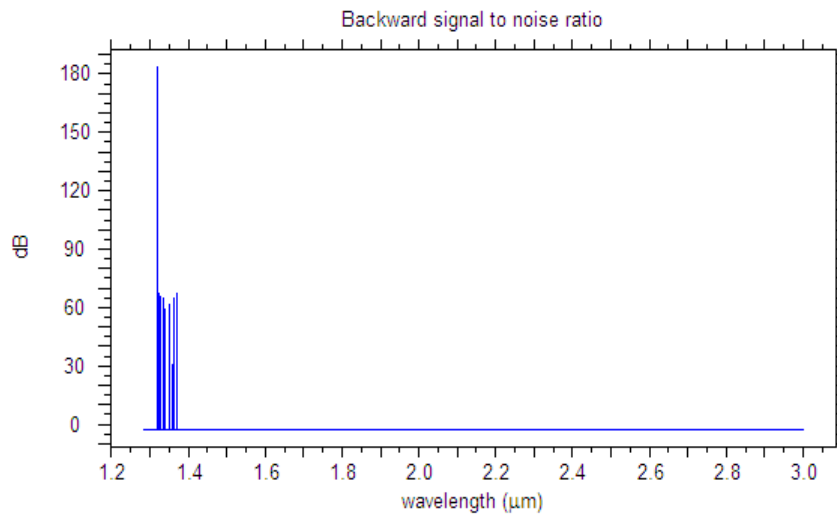


Fig. 11: Backward Signal to Noise Ratio

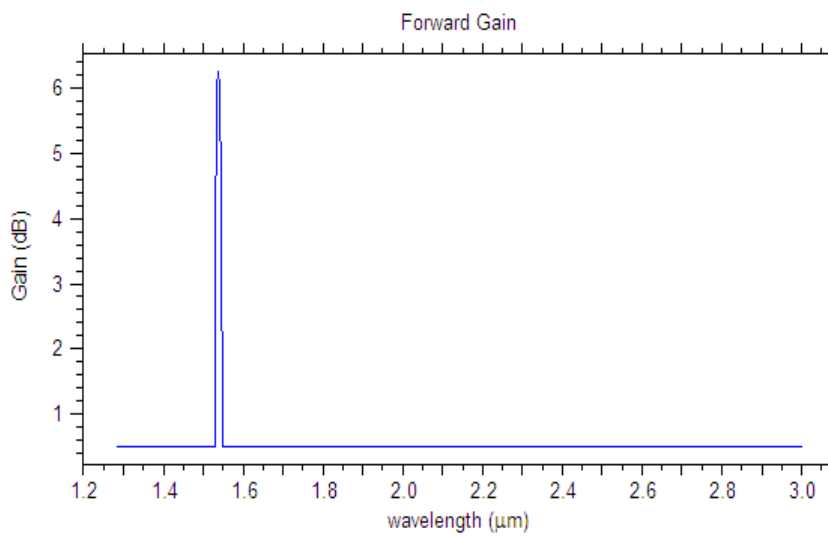


Fig. 12: Forward Gain

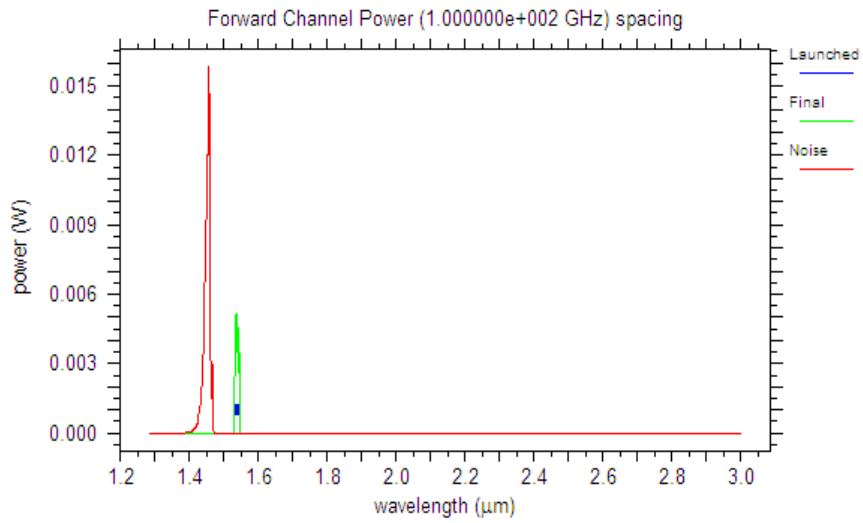


Fig. 13: Forward Channel Power

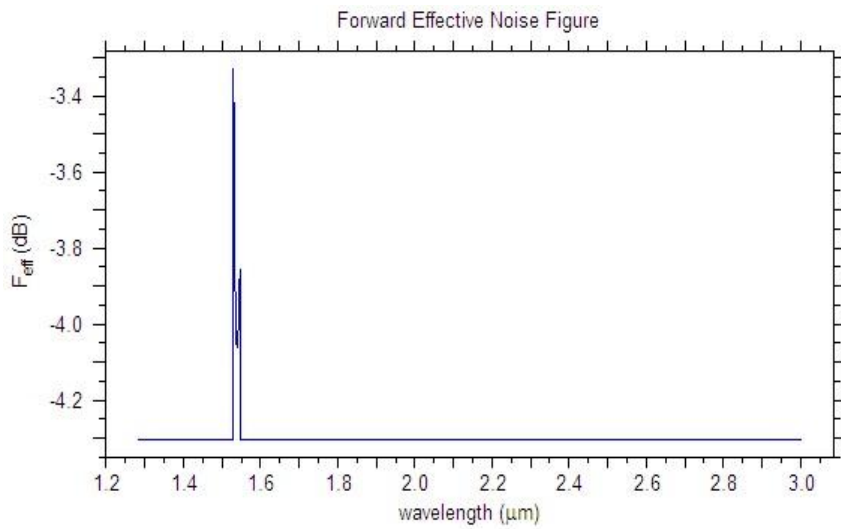


Fig. 14: Forward Effective Noise Figure

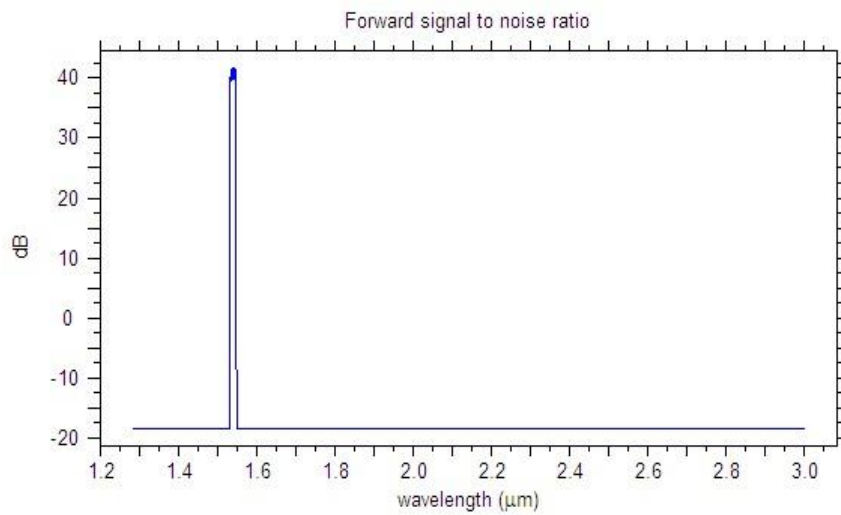


Fig. 15: Forward Signal to Noise Ratio

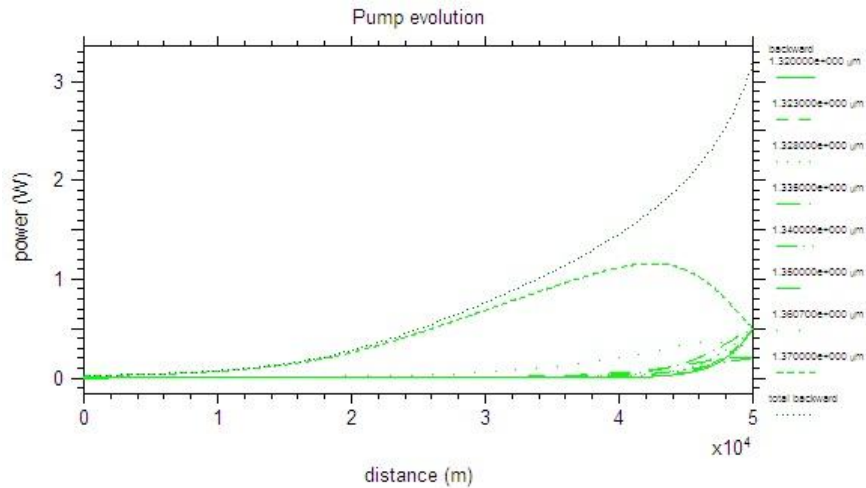


Fig. 16: Pump Evolution

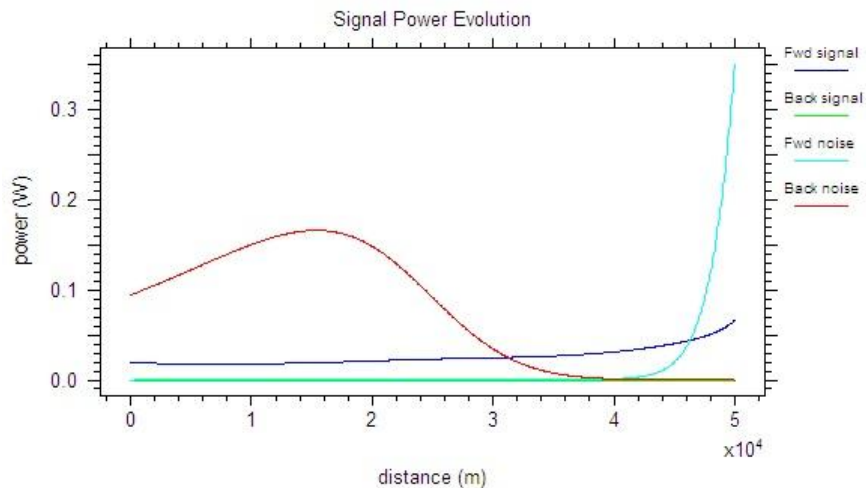


Fig. 17: Signal Power Evolution

#### IV. CONCLUSIONS

The advantages of fiber Raman amplifiers over the optical amplifiers include the possibility to operate in any wavelength region and superior noise performance of distributed amplification, as well as permits, with the appropriate choice of pump wavelengths and powers, flattening of the gain profile over the whole bandwidth. This report describes the simulation of a realistic scenario of a 40Gbps DWDM link with interchannel spacing of 50 GHz. Forty individual channels carrying PRBS data are transmitted over a 50 km length of ITU-T G.652 single mode dispersive fiber. The multi-line capability of OptSims CW laser model makes it very convenient to generate the source-grid for simulating WDM channels. Since backward pumping helps in averaging out power ripples at the receiver end, we chose a backward pumping scheme that employs eight CW pump signals with carefully chosen nominal wavelengths and power values. Power of 0.44 W is launched into the backward channel at 1330 nm. Noise figure of 40 dB is obtained at this wavelength. The output signal observed at 1550 nm has a gain of 6.2 dB and noise figure of -3.35 dB. Thus distributed Raman amplification is used to compensate for the link attenuation thereby effectively increasing the inter- EDFA span in a longer haul link.

#### V. ACKNOWLEDGEMENT

The authors are thankful to Vidyalankar Institute of Technology, India for providing the necessary facilities for carrying out this work and Ms.Jovita Serrao for her valuable guidance .

## REFERENCES

- [1] Raman Amplification Design in WDM systems, The International Engineering Consortium
- [2] Anis Rahman, A Review of DWDM: The Heart of Optical Networks
- [3] Introduction to DWDM Technology, Cisco Systems, Inc.
- [4] Clifford Headley, Govind Agrawal, Raman Amplification in Fiber Optical Communication Systems
- [5] A.N.A. Mohammed, M.M.E. El-Halawany, A.N. Zaki Rashed, M.M. Eid "Recent Applications of Optical Parametric Amplifiers in Hybrid WDM/TDM Local Area Optical Networks," IJCSIS International Journal of Computer Science and Information Security, Vol. 3, No. 1, pp. 14-24, July 2009.
- [6] J.W. Nicholson, "Dispersion Compensating Raman Amplifiers With Pump Reflectors for Increased Efficiency," Journal of Lightwave Technology, Vol. 21, No. 8, pp. 1758-1762, Aug. 2003.
- [7] M.C. Fugihara, A.N. Pinto, "Low-Cost Raman Amplifier for CWDM Systems," Microwave and Optical Technology Letters, Vol. 50, No. 2, pp. 297-301, Feb. 2008.
- [8] M. Wasfi, "Optical Fiber Amplifiers Review," International Journal of Communication Networks and Information Security (IJCNIS), Vol. 1, No. 1, pp. 42-47, Apr. 2009.
- [9] S. Raghuaawansh, V. Guta, V. Denesh, S. Talabattula, "Bi-directional Optical Fiber Transmission Scheme Through Raman Amplification: Effect of Pump Depletion," Journal of Indian Institute of Science, Vol. 5, No. 2, pp. 655-665, Dec. 2006.
- [10] A.N.A. Mohammed, A.F.A. Saad, A.N. Zaki Rashed, M.M. Eid, "Characteristics of Multi-Pumped Raman Amplifiers in Dense Wavelength Division Multiplexing (DWDM) Optical Access Networks," IJCSNS International Journal of Computer Science and Network Security, Vol. 9, No. 2, pp. 277-284, Feb. 2009.
- [11] J. Bromage, "Raman Amplification for Fiber Communications Systems," Journal of Lightwave Technology, Vol. 22, No. 1, pp. 79-93, 2004.
- [12] W. H. KNox, "The Future of Wavelength Division Multiplexing," OPN Trends, Vol. 18, No. 1, pp. 5-6, March 2001.

# Fingerprint Recognition Using Genetic Algorithm and Neural Network

Purneet Kaur <sup>1</sup>, Jaspreet Kaur <sup>2</sup>,

<sup>1</sup> Student of Baba Banda Singh Bahadur Engineering College, Fatehgarh Sahib

<sup>2</sup> Assist.prof.of Baba Banda Singh Bahadur Engineering College, Fatehgarh Sahib.jaspreet

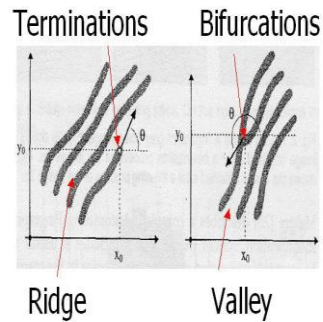
## ABSTRACT:

Fingerprints are the most used biometric feature for the person identification. During research it has been observed that there are number of approaches has been implemented for recognition of fingerprints. Different algorithms and techniques have been used for enhancement purpose, minutiae extraction and for matching. In this thesis work a novel technique to enhance our results by using the combination of genetic algorithm and neural network. As we know that both techniques are the world's best techniques. Genetic algorithm is used for the extraction of minutiae and neural network is used for the recognition of a fingerprint. Firstly, fingerprint image has been enhanced using histogram equalization process so that our algorithm also capable of predicting good results even for dull or low intensity images too. Then Morphological Image Processing operations using MATLAB 2011b has applied for thinning the lines up to the predefined extent so that it will not further destroy or harm our structure of the image. After that we proceed towards predicting of discontinuities using Genetic Algorithm approach based upon nth last segment. Here genetic algorithm is used to find the best possibility for each discontinues segment in an image. Lastly Enhanced image has fed to NN (neural networks) based trained system to diagnose and match finger print with data set. Several features will be used to train the network so that precision will be made in recognition of finger print.

**KEYWORDS:** Biometrics, fingerprints, minutiae enhancement, ridge endings, feature extraction, genetic algorithm, neural network

## I. INTRODUCTION

One of the topics of continuing interest in forensics is the automatic identification or verification of human users, where the applications are broad, including simple logins into computers, authorized access to systems, banking transactions and highly-secure infrastructure [1]. The most common biometric traits used by recognition applications are: fingerprints, retina, iris, hand geometry, face, veins, handwriting, voice, etc. Among all these fingerprints are today the most widely used biometric features for personal identification [2]. It has some features such as uniqueness, lifelong unchanged and inseparable with the body. As one of most reliable biometric identification technology, the fingerprint has been used for hundreds of years [3]. Most automatic systems for fingerprint comparison are based on minutiae matching [4]. Minutiae characteristics are local discontinuities in the fingerprint pattern which represent terminations and bifurcations. A ridge termination is defined as the point where a ridge ends abruptly. A ridge bifurcation is defined as the point where a ridge forks or diverges into branch ridges (Fig. 1). Reliable automatic extracting of minutiae is a critical step in fingerprint classification. The ridge structures in fingerprint images are not always well defined, and therefore, an enhancement algorithm, which can improve the clarity of the ridge structures, is necessary. Skin on human fingertips contains ridges and valleys which together forms distinctive patterns. These patterns are fully developed under pregnancy and are permanent throughout whole lifetime. Prints of those patterns are called fingerprints. Injuries like cuts, burns and bruises can temporarily damage quality of fingerprints but when fully healed, patterns will be restored. Through various studies it has been observed that no two persons have the same fingerprints, hence they are unique for every individual.



“Figure(1.1)Ridge and valley structure”

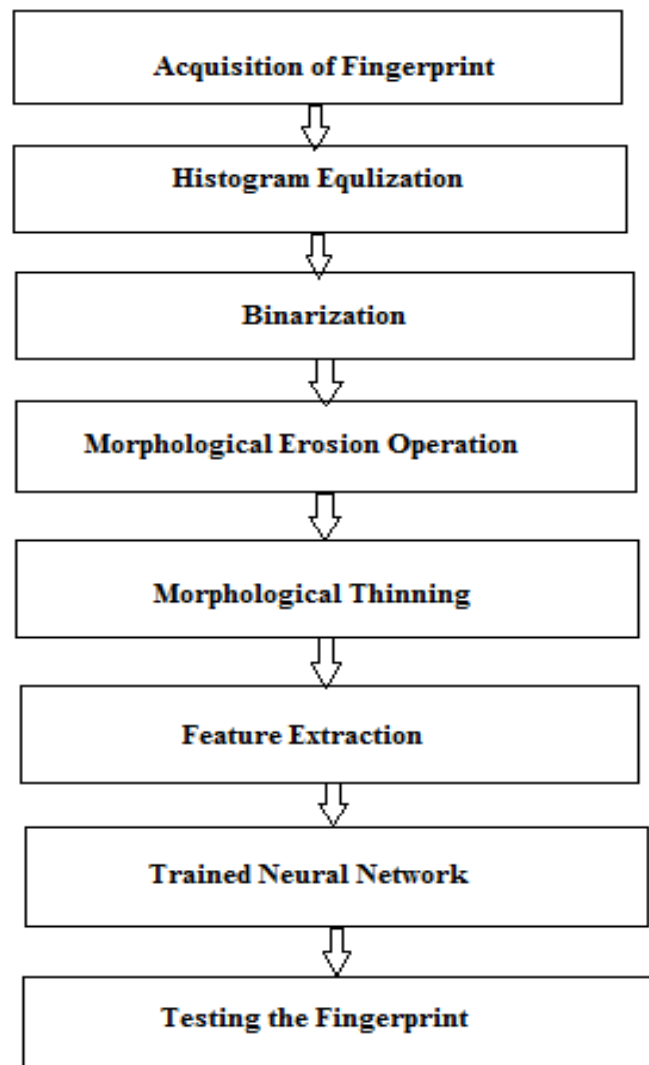


“ Figure(1.2)Fingerprint”

The performance of minutiae extraction algorithm is heavily depends upon the quality of input image. In fingerprint image minutiae can be precisely located from the thinned ridges. Fingerprint recognition methods can be grouped into three major classes: (i) correlation-based matching, (ii) minutiae based matching, and (iii) ridge feature-based matching [5]. While minutiae-based methods are the most popular because of their temporal performances, the correlation-based matching is considered to be more reliable, but very time consuming at the same time [6]. Minutiae-based recognition performs poorly on very well on low quality and partial input fingerprints [7]. The loss of singularity points makes ridge feature-based recognition and indexing techniques impossible to apply [8]. It can be observed from the previous work that there are number of algorithms has been used for the enhancement of the fingerprint image which consists of normalization, ridge orientation estimation, ridge frequency estimation , region of interest extraction, filtering, binarization, morphological thinning then the final step minutiae extraction and matching. For the filtering purposes, Gabor filter is the most common filter. Most of the existing enhancement techniques are based on Gabor filter. Gabor filter is both frequency and orientation selective tuned by ridge direction and ridge frequency. It works on both spatial and frequency domains [9].The main drawback of these methods lies in the fact that false estimate of local ridge direction will lead to poor enhancement. But the estimate of local ridge directions is unreliable in the areas corrupted by noise where enhancement is most needed [10]. Gabor filter is time consuming and parameter selection such as ridge centre frequency, radial bandwidth and central orientation, requires an empirical setup. Moreover, this is very old method.

Fingerprint recognition is always a field of research for researchers and security industries. Here we are developed a noble technique to enhance fingerprint results. To achieve a better result of matching we proposed a method of fingerprint recognition system using Genetic Algorithm and Neural Network. In this study, we apply a histogram equalization method for the enhancement of fingerprint image which is then followed by binarization and morphological operations. Optimization technique is used for the minutiae extraction and these extracted features are given to train the neural network. Enhanced image will fed to NN (neural networks) based trained system to diagnose and match finger print with data set. Several features will be used to train the network so that precision will be made in recognition of finger print. Here we are first discussing about optimization technique using genetic algorithm and neural network, these both are the world's best techniques.

### Proposed Algorithm



“Figure2. Algorithm”

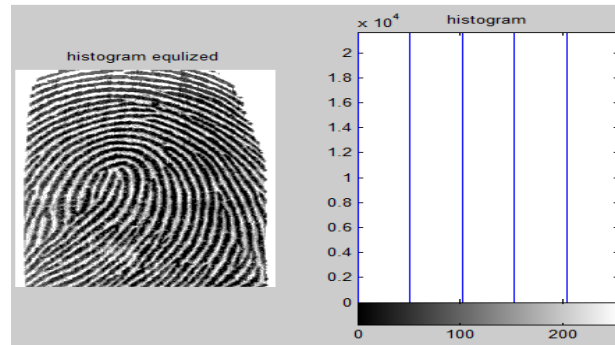
In this proposed work we introduce a new algorithm of fingerprint recognition system. It is very well known that to develop a reliable fingerprint recognition system image enhancement and features extraction are needed. This proposed algorithm is divided into main three stages: Preprocessing, post processing and final minutiae matching stage. Preprocessing stage involved enhancement of image by using histogram equalization, binarization and morphological operations after applying this enhancement algorithm a binarized thinned image has been obtained. In second stage minutiae are extracted from the enhanced fingerprint by using the optimization technique. Final stage is the recognition of the fingerprint which has been done with the help of neural network.

#### “A. Acquisition of Fingerprint”

A number of methods are used to acquire fingerprints. The quality of the fingerprint image is very crucial for the recognition process. It is always prefer to use a good quality of fingerprint sensor hat can tolerate the miscellaneous skin types, dryness or humidity of the fingerprint.

#### “B. Image Enhancement”

**Histogram Equalization:** This is the first step which is used for the image enhancement process. It is a technique for adjusting the pixel intensities of image to enhance the contrast [4]. Through this adjustment the intensities can be better distributed on the histogram. This allows the lower contrast region of the image gain the higher one. The original histogram of image is of bimodal type. After the histogram equalization the histogram of the image occupies all the range from 0 to 255 and the contrast of the image is enhanced.



“Figure3. Histogram equalized”

**Binarization:** The operation that converts the gray scale image into binary image is known as binarization. It is used to transform 8-bit gray fingerprint image into 1-bit image with 0 value for ridges and 1 value for furrows.

**Morphological Erosion:** Morphological techniques are used as pre-processing and post-processing such as filtering and thinning. There are two fundamental morphological operations, dilation and erosion, in terms of union (or intersection) of an image with a translated shape (structuring element).

**Morphological Thinning:** The final enhancement method prior the minutiae extraction is thinning. Thinning is a morphological operation that erodes the pixels. Thinned image helps minutiae extraction. The thinning of the image is to reduce the ridges till the ridges one pixel wide.



“Figure4. The results of main enhancement steps: (a) Binarized image (b) image obtained after erosion operation (c) Thinned image”

### “C. Feature Extraction”

After a fingerprint image has been enhanced the next step is to extract the minutiae from the enhanced image. In this present work genetic algorithm based optimization technique has been used for this purpose. Genetic algorithm is the heuristic search and optimization technique that mimic the process of natural evolution. It was first developed by John Holland from the University of Michigan in 1975 [11]. It was proven to be the most powerful optimization technique. Genetic algorithms are considered to be the part of the evolutionary algorithms which produce the solution to the optimization problems. In a genetic algorithm, a population of a candidate solution (called individuals) to an optimization problem is evolved toward better solutions. Each candidate solution has a set of properties (its chromosomes and genotype) which can be mutated and altered; traditionally, solutions are represented in binary as strings of 0s and 1s, but other encodings are also possible. The evolution usually starts from a population of randomly generated individuals and is an iterative process, with the population in each iteration called a generation. In each generation, the fitness of every individual in the population is evaluated; the fitness is usually the value of the objective function in the optimization problem being solved. The more fit individuals are stochastically selected from the current population, and each individual's genome is modified (recombined and possibly randomly mutated) to form a new generation. The new generation of candidate solutions is then used in the next iteration of the algorithm. Commonly, the algorithm terminates when either a maximum number of generations has been produced, or a satisfactory fitness level has been reached for the population. Before applying GA firstly the enhanced binary thinned image is to convert into RGB image so that the extracted minutiae can show with a color. In this work we have extracted the ridge endings in the fingerprint image which will be the input of the neural network for training. Similarly, extract the ridge endings of the image in the database which are going to be tested. Figure (4) shows the extracted ridge endings showing with green color.



“Figure5. Extracted ridge endings”

#### “D. Training of Neural Network”

The ability of the ANN to learn given patterns makes them suitable for such applications. Fingerprint recognition is one such area that can be used as a means of biometric verification where the ANN can play a critical role. An ANN can be configured and trained to handle such variations observed in the texture of the fingerprint. Artificial Neural networks have been proved very effective in performing complex function in various fields. In this research work neural network has been used for the recognition of fingerprints. Firstly the neural network has been trained before test the matching operation. Extracted features of all the images in the data set are the input of the neural network. With the help of these inputs the network has been trained and the network should be trained till then we get the minimum MSE value so that the desired number of true results can be obtained. Retrain the network at least twenty times. For training the network, MATLAB neural network toolbox has been used.

“E. Testing the Fingerprint:” This is the final step of the proposed work. To test or recognize the fingerprint first take any image from the data set and fed that image to the trained network then it gives the result by showing whether it matches to the right person or wrong. For instance, second sample of 6<sup>th</sup> person has taken for testing then it showed that fingerprint is matched with 6<sup>th</sup> person. If it matched to another person instead of 6<sup>th</sup> person then the results is considered to be false. In this way all the fingerprints in the database has been tested.

## II. EXPERIMENTAL RESULTS

We worked on 128 images of 16 persons, each has 8 samples. The data base has been taken from <http://www.advancedsourcecode.com/fingerprintdatabase.asp>. All the images in database are in TIF format (Tagged Image File). TIF is lossless, which is considered the highest quality format for commercial work. It is the most versatile and TIF does not have compression. The work has been done in MATLAB 7.12.0(R2011a).

“Table1. Results”

Total No. of Samples	No. of tested Samples	No. of Correctly predicted samples	Correct Rate	Incorrect Rate
128	112	77	68.75%	31.25%

### III. CONCLUSION”

A method of fingerprint recognition based on Neural Network is presented. Our feature selection method is based on Genetic algorithm. The fingerprint image is enhanced before extracting features. Enhancement method included histogram equalization, binarization, morphological operations, it has made a great improvement of recognition accuracy for recognition method. The combination of both genetic algorithm and neural network techniques provided the better and efficient method for fingerprint biometric. Experimental results show that the presented method has the better recognition accuracy compared with the previous fuzzy logic based recognition methods.

### REFERENCE

- [1] Mona Omidyeganeh, Abbas Javadtala, Shahrokh Ghaemmaghami, Shervin Shirmohammadi “A Robust Wavelet-based Approach to Fingerprint Identification” 2012 IEEE International Conference on Multimedia and Expo Workshops.
- [2] Radu Miron, Tiberiu Letia “Fuzzy Logic Method for Partial Fingerprint Recognition” AQTR IEEE, pp 602-607, 2012
- [3] Wang Wenchao, Sun Limin “A Fingerprint Identification Algorithm Based on Wavelet Transformation Characteristic Coefficient”
- [4] S Greenberg, M Aladjem, D Kogan, and I Dimitrov, “Fingerprint image enhancement using filtering techniques”, ICPR, Vol. 3, pp. 326–329, 2000.
- [5] D. Maltoni, “A Tutorial on Fingerprint Recognition”, Biometric Systems Laboratory - DEIS - University of Bologna, 2005.
- [6] K. Abbad, N. Assem, H. Tairi and A. Aarab, "Fingerprint Matching Relying on Minutiae Hough Clusters", ICGST - GVIP Journal, ISSN: 1687-398X, Volume 10, Issue 1, February 2010, pp. 39-44.
- [7] A. N. Marana, A. K. Jain, “Ridge-Based Fingerprint Matching Using Hough Transform”, Computer Graphics and Image Processing, SIBGRAPI, 2005, p. 112-119.
- [8] H. Le, D. Bui, "Online fingerprint identification with a fast and distortion tolerant hashing", Journal of Information Assurance and Security 4, 2009, p. 117-123.
- [9] L. Hong, Y. Wan, A. Jain, “Fingerprint Image Enhancement: Algorithm and Performance Evaluation”, IEEE Trans. Pattern Analysis & Machine Intelligence, Vol. 20, no.8, pp.777-789, 1998
- [10] G. Milici, G Raia, S. Vitabile, F. Sorbello, “ Fingerprint Image Enhancement Using Directional Morphological Filter” IEEE Trans. Digital Object Identifier, Vol. 2, pp.967-970, 2005
- [11] Holland j., Adaption in Natural and Artificial System, The University of Michigan Press, 1975

## Content Based Medical Image Retrieval – Performance Comparison of Various Methods

Harishchandra Hebbar<sup>1</sup>, Niranjan U C<sup>2</sup>, Sumanth Mushigeri<sup>3</sup>

<sup>1,3</sup>School of Information Sciences, Manipal University

<sup>2</sup>MDN Labs, Manipal

### ABSTRACT

Present healthcare system calls for standardization and interoperability of images acquired by various equipment manufacturers. The healthcare system is also not limited to a single super-specialty hospital where state of the art machines and excellent physicians are available but should also these services need to be available in remote places too. Nowadays, number of images acquired by the hospitals is increasing due to the various modalities available to identify accurately the cause of the deceases. This results in more number of medical images being stored in the database in hospitals. The interpretation of these medical images becomes even more critical, as it may contain the information which cannot be perceived by human eye. Therefore the images need to be annotated appropriately while it is stored so that, retrieval of the images of interest can be done quickly. The manual annotation is very cumbersome process when large number of images is involved in the retrieval process. Hence it is necessary to have an efficient Content Based Image Retrieval System which is user friendly and user definable in terms of speed and Precision.

**Keywords:** CBIR, Histogram, Retrieval time, Precision, Recall, CDF, GLCM, DICOM, RSNA,

### I. INTRODUCTION

All human beings have the inherent nature of organizing the objects based on their perception. When we have very few items to arrange or organize, we can do so manually with ease. When the number increases, we need the help of an intelligent machine to do the same. In case of non-medical images variation in perception can be acceptable, since it may not have major impact even if there is some error. However in case of medical images a small error may have serious implications, which should not be overlooked. Hence it is important to compare medical images “based on the content” rather than only on perception. Looking for the contents which are not visible to the human eye calls for extracting features of the image, storing it in the database and retrieving based on the query.

Figure 1 describes the general block diagram of Image Retrieval System where, features extracted from query image are compared with the features in the image database. Pre calculating the features of the images in

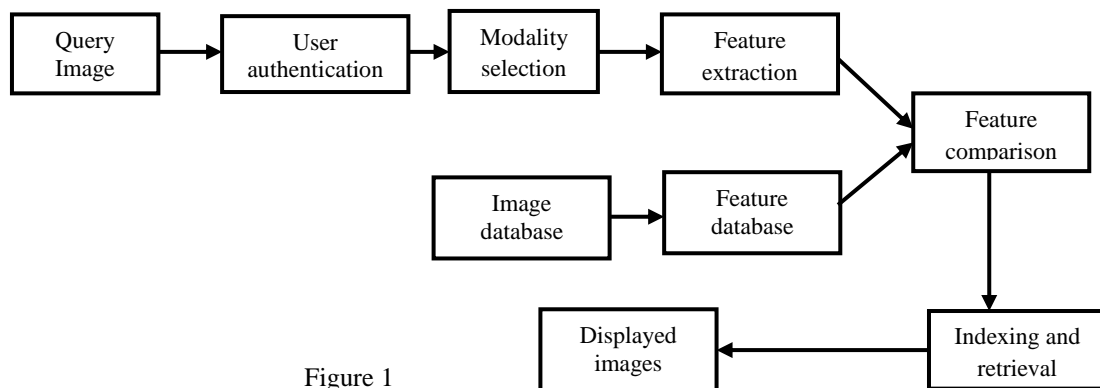


Figure 1

the image database reduces the time required for comparison and retrieval. However the challenge lies in finding

the right features of the image so that, retrieved image is accurate and the retrieval time is also less. User authentication is needed to restrict only the authorized user to use the system. The modality selection helps to categorize correct modality images to be compared for retrieval. Most of the times, it may not be sufficient to have one feature comparison to retrieve the image accurately. It may be necessary to refine the query process by extracting more than one feature (for example intensity, shape, edge, texture) so that, retrieved image is more precise.

As the medical images in the PACS system at present need to conform to the DICOM (Digital Imaging and Communication in Medicine) standard, the size of any medical image is well defined by National Electrical Manufacturer's Association (NEMA) specification. The medical equipment used in the imaging process in hospitals or diagnostic centers need to conform to standards defined by NEMA.

In order to provide efficient patient care many hospitals are implementing Picture Archival and Communication Systems (PACS). In a practical scenario mid-sized hospitals cannot afford to have the PACS due to the initial investment which is quite huge. These hospitals can have the services of PACS through a Wide Area Network (WAN). Size of the medical image being very large, transmission of these images to a distant healthcare setup will be limited by the bandwidth of the Wide Area Network or Internet. The image viewing at a remote station will be a very slow process and likely to cause severe delay which is a great concern for a physicians if he/she wants to view these images before treatment. Hence it is necessary to have an efficient Content Based Image Retrieval System which is user friendly and user definable in terms of speed and Precision.

## **II. SIGNIFICANCE OF CBIR IN HEALTHCARE**

Images in medical domain are being captured only when the exact diagnosis need to be carried out. The images are very rich in their content and the information may not be clearly visible to physicians for visual inspection. These images are being large in size and require accurate interpretation a good Content Based Image Retrieval system will definitely help physicians in their decision by comparing it with similar cases in the image database.

Many Image Retrieval systems that have been developed are independently accessed and are usually text based. These systems have been developed mainly to categorize pictures which are generally non – medical. Here image perception is of higher priority than the content and thus text based retrieval is appropriate.

Apart from the rich information contained in the medical images, medical images also contain meta data information such as image modality, image slice number, patient age, gender, family status. Use of meta data along with the content of the image will prove to be more accurate in medical image retrieval, than using content alone.

Much of the radiological practice is currently not based on the quantitative image analysis, but on heuristics. Such heuristics may fail some time in variety of circumstances such as poor quality of imaging equipment, associated noise during the imaging procedure, lack of experienced technician, poor quality imaging station. Computer assisted image interpretation and retrieval will assist radiologists in correct interpretation. Image retrieval system combined with decision support system will be a real advantage in proper diagnosis.

There is a need to address the challenge of a specialized internet based Content Based Medical Image Retrieval (CBMIR) system that can help the doctors or medical practitioners across the globe in referring the existing medical records before taking a final decision over the diagnosis. If the system is distributed and accessible to the physicians, there will be definitely improvement in the quality of healthcare.

## **III. CBIR SYSTEM EVALUATION**

In the general image retrieval domain, it is difficult to compare any two retrieval systems. Still, there are several articles on the evaluation of imaging systems in medicine or on general evaluation of clinical systems.

Henning Muller [1] provides an overall view of the various CBIR systems being developed. It would be hard to name or compare them all but some well-known examples include Candid, Photobook and Netra that all use simple color and texture characteristics to describe the image content. Using higher level information, such as segmented parts of the image for queries, was introduced by the Blobworld system. PicHunter on the other hand is an image browser that helps the user to find an exact image in the database by showing to the user images on screen that maximizes the information gain in each feedback step. A system that is available free of charge is the GNU Image Finding Tool (GIFT). Some systems are available as demonstration versions on the web such as

Viper, WIPE or Compass.

A single example result does not reveal a great deal about the real performance of the system and is not objective as the best possible query result can be chosen arbitrarily by the authors.

The commonly used measurement parameters in CBIR are:

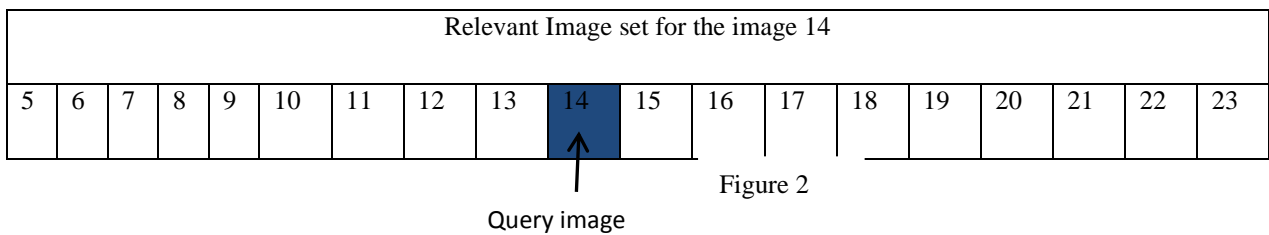
1. Retrieval Time (tr): The time taken by the system to display relevant images to the given query image

$$2. \text{Precision (P)} = \frac{\text{number of relevant items retrieved}}{\text{number of items retrieved}}$$

$$3. \text{Recall (R)} = \frac{\text{number of relevant items retrieved}}{\text{number of relevant items}}$$

Defining the relevant image set can be done in various ways. This paper defines a set of “n” images which are varying by some factor as defined by the user. A total of 1720 images procured from Radio diagnosis department of K.M.C Manipal hospital is maintained in the database. The images are of different modality like CT, MR, US & CR and of dimension (256 x 256, 2500x2048, etc..)

Figure 2 shows the relevant set for the query image 14.



#### IV. RETRIEVAL METHODS IMPLEMENTED

Retrieval time (tr) comparison of eight different methods is provided in section 4.6 in the form of a graph.

##### 4.1 Histogram Based Retrieval

One of the most commonly used parameters for image comparison is the color or intensity of the image. In our research we have emphasized on the gray level medical images. An experienced physician can interpret the images better than a lay man due to his experience in identifying similar images in the past. However subtle changes in the image cannot be easily observed. A histogram is the count of the number of pixels at each intensity level over the entire image. It is given by,

$$hist(r_k) = n_k$$

Where,  $k=0 \dots L-1$ ,

L is the number of intensity levels.

$n_k$  = number of pixels at gray level  $r_k$

It plots the number of pixels for each intensity value. By looking at the histogram for a specific image, a viewer will be able to judge the entire intensity distribution at a glance.

In histogram matching technique, the histogram of all the images in the database are computed and stored in a file. When a query image is given, the histogram of the query is computed and compared with the stored histograms. For each and every image in the database, the distance metric is calculated as,

$$histdist[dataset] = \sum_{j=0}^{255} | hist\_dataset[j] - hist\_query[j] |$$

Where,

- o j denotes the various gray levels ranging from 0 to 255.
- o hist\_query is the histogram of query image, hist\_dataset is histogram of the image in the database.

The images in the database nearly matching with the query image, have the least distance metric. The exact match is the one with the zero distance metric.

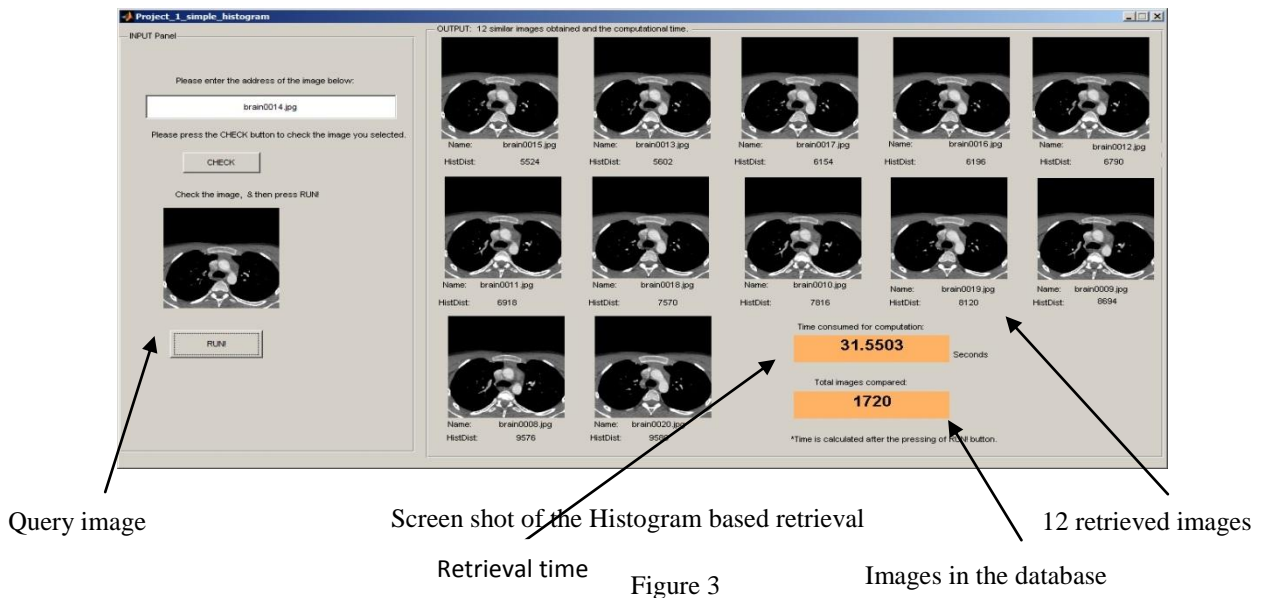


Figure 3

The result of the Histogram based retrieval is shown in Fig.3. Twelve closest images are displayed from a total 1720 images in the database. The total time for retrieval is 31.5503 seconds.

#### 4.2 Bit Plane Based Retrieval

In this method, the image is composed of eight one bit planes, ranging from bit plane 0 for the Least Significant Bit (LSB), to the bit plane 7 for Most Significant Bit (MSB) as shown in Fig.4. Usually most of the visually significant information is contributed by higher order bits and less by the least significant bits. An 8 bit image can have 256 different shades of gray, where 0 represents black and 255 represent white, and Integers between 0 and 255 represent various shades of gray. So out of the 8 bits, when 7th bit is set, it represents the intensities ranging from gray level 128 to 255, and, when 6th bit is set, it represents totally 128 gray levels in the range 64 to 127 and 192 to 255, and when 5th bit is set, represents totally 128 gray levels in the range 32 to 63; 96 to 127; 160 to 191 and 224 to 255 and so on.

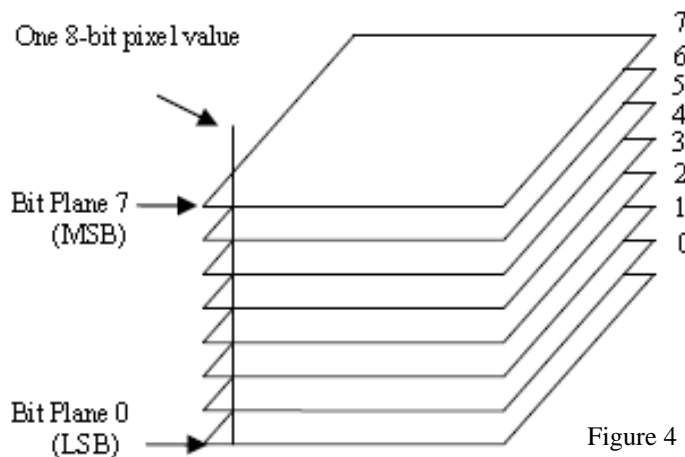


Figure 4

In this method, the number of occurrences of set bits in each bit plane is computed. The bit plane histogram is represented mathematically as,

$$hist\_databaset[i] = \sum_{x,y} \sum_{m,n} f(x,y)_i \quad (2.5)$$

Where,  $f(x,y)$  is the pixel value at  $(x,y)$  having  $i^{th}$  bit set to 1,  $i = 7,6..0$ .

**4.3 Hierarchical Bit Plane based retrieval**

To make the bit plane histogram matching more efficient, a method is proposed to discard the dissimilar images in the database by a method called Hierarchical bit plane histogram matching.

**4.3.1 Histogram percentage as threshold**

This method begins with the most significant bit (MSB), and is based on the distance metric equation. The distance metric at the MSB for each image in the database is compared with the threshold specified by the user in terms percentage of histogram. Those images in the database with the distance metric less than the specified threshold are retained for subsequent search at lower bit planes. This is continued till the least significant bit i.e. till the 0th bit is reached. This bit plane technique allows one to compare the query and database images with only one arithmetic operation per bit plane and hence needs less computational time and power compared to the traditional grayscale histogram matching.

**4.3.2 Image size as the threshold**

It is common that, the major object in an image is located at the center part of the image. In this method query image as well as the images in the database are re-sized according the percentage of the threshold specified by the user in terms of dimension. If image dimension is [m x n] and the percentage of the threshold is 90%, then image dimension is re-sized to 90% \* [m x n]. it has been observed that smaller dimension of the image takes less time for retrieval.

**Result of Histogram and Bit plane**

Table 1, shows comparison of four retrieval methods in terms of retrieval time, Precision and Recall parameters.

**Table 1**

Total number of images in the database= 1720

Sl.No	Retrieval Method	Retrieval time (Tr) in secs	Precision (P)	Recall (R)
1.	Histogram comparison	31.6323	1	0.667
2.	Bit plane histogram	4.27613	0.583	0.389
3.	Hierarchical bit plane 2% histogram as the threshold)	4.64211	1	0.667
4.	Hierarchical bit plane 98% size of the image as the threshold)	5.31345	1	0.667

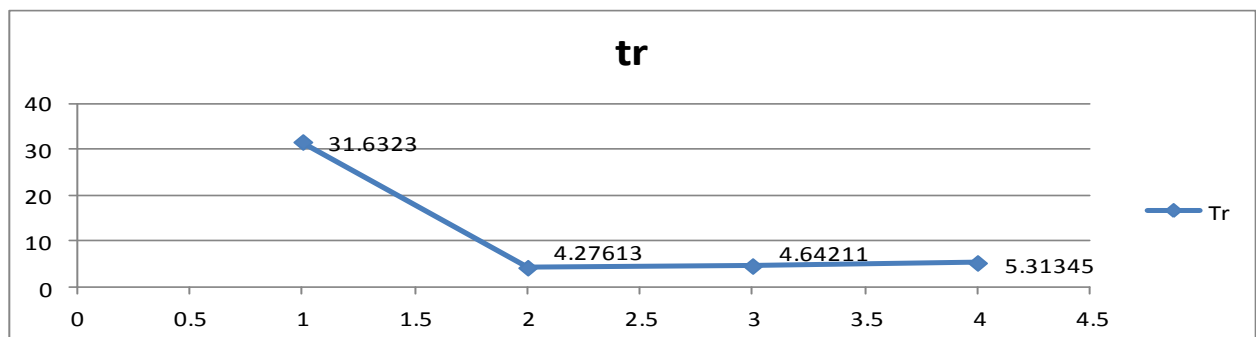


Fig. 5, Retrieval of four different methods

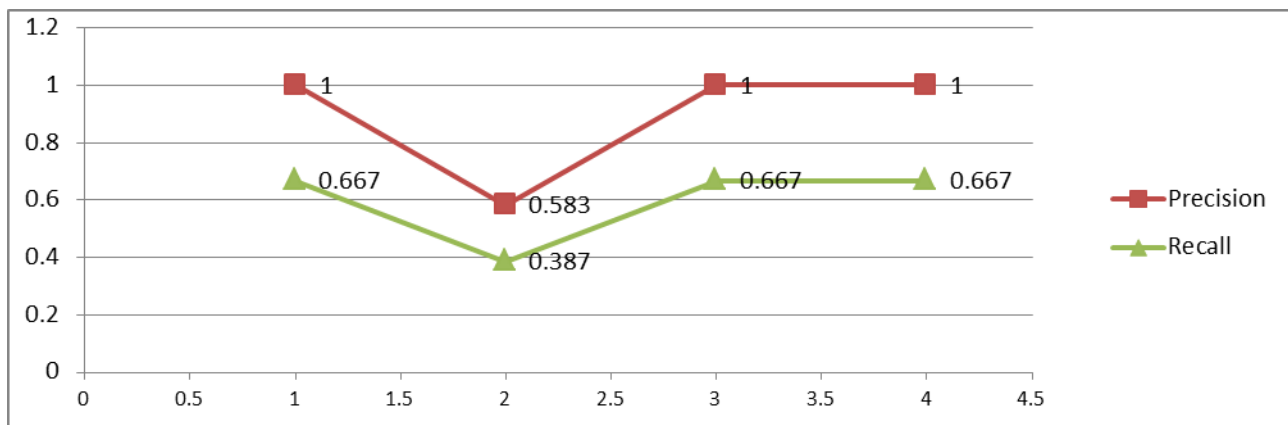


Fig. 6, Precision, Recall graph of four methods

From the graph in the Fig.5, it can be observed that, there is a considerable improvement in retrieval time in case of Bit plane histogram compared to that Simple histogram method. Fig.6 shows the Precision and Recall parameters of the four different methods implemented. From the above two graphs it can be observed that the least retrieval time ( $T_r$ ) amongst the four method is the Bit plane histogram (4.27613 sec). While retrieval time being the lowest in Bit plane method, the Precision and Recall values are 0.583 and 0.387 respectively, which is lower than the other 3 methods namely Histogram comparison, Hierarchical bit plane with Histogram as threshold and Hierarchical bit plane with size as the threshold. From the user's perspective the Precision and Recall being the most important parameters, Hierarchical bit plane with 2% histogram as the threshold is the best method amongst the four being described here. It is also observed that the Precision and Recall parameters remain same irrespective of the image dimension in the database.

The retrieval time will also depend on the speed and type of the processor on which the algorithm has been implemented. Results are obtained on a computer with Processor type: Intel i3-2370M CPU @ 2.4 GHz processor with 4 GB RAM.

#### 4.4 Cumulative Distribution Function (CDF) based retrieval

Medical images are of different dimension depending on the modality of the image as defined by Radiological Society of North America (RSNA). The pixel depth and image dimension vary depending on the size of the image. The comparison of images of different dimension will be difficult and needs sophisticated algorithms to match the two images in terms of intensity or histogram value. This puts extra computation time as well as complexity to the CBIR system. Another problem being the registration of the two images. In the pixel matching method where pixel intensity of the query and database images is compared, the rotation of the image leads to comparison of two dissimilar pixels. This requires image registration to be carried out before the comparison. This problem is overcome by CDF where The CDF of the query image and the images in the database are approximated by piecewise linear models with two parameters, slope and intercept at various grayscale intervals. The contiguous set of lines approximating the CDFs enables us to compare the query image and the images in the database with corresponding estimated slopes and intercepts. As the dynamic range of CDF is from 0 to 1, images of different sizes can be compared. Approximation of CDFs with lines further reduces the dimension of the image features and thus improves the speed of matching. Also, the monotonically increasing CDF is well suited for approximations with lines. Resolving the CDF with lines of different lengths recasts the matching to a hierarchical methodology.

Cumulative Distribution Function (CDF) for retrieving the medical images from the database provides a considerable reduction in the retrieval time and also flexibility to the user in terms of selecting suitable number of line segments ( $p$ ) and the percentage of CDF threshold depending on the situation providing control over precision and time of retrieval.

The Cumulative Distribution Function  $cdf(i)$  upto the gray level 'i' is given by:

$$cdf(i) = \sum_{j=0}^i h(j) = \sum_{j=0}^i \frac{n_j}{M.N} \quad 0 \leq i \leq 255 \quad (3.2)$$

Where,  $h(j)$  is the normalized histogram at gray level  $j$

$n_j$  is the number of pixels with gray level  $j$

$M.N$  is the size / dimension of the image

The CDF contains the same information as that of the histogram, but in another form. However, it has two interesting properties (a) It is a monotonically increasing quantity which allows fairly well approximation of the CDF with just a first order curve (b) It has a dynamic range between 0 and 1 which allows one to fit piecewise linear models on CDFs of images of any size.

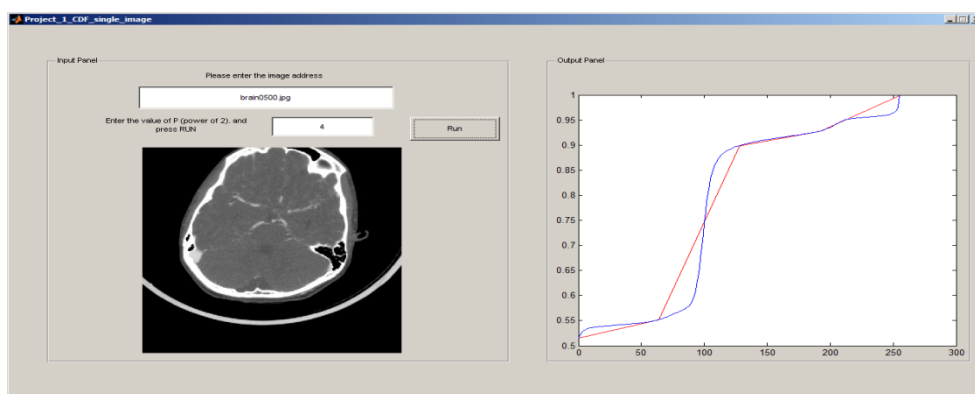


Fig 7. CDF of image brain0500.jpg with  $p=4$  and continuous cdf overlapped

#### 4.5 Edge and Texture based retrieval

It is also equally important to consider the edge / shape of the medical images for comparison especially in case of bone / skull images. As the edges give idea about the shape of the objects present in the image, they are useful for segmentation, registration and identification of objects. We have implemented edge detection using Sobel Operator. The Sobel operator consists of a pair of  $3 \times 3$  convolution kernels as shown in Fig.8. One kernel is simply the other rotated by  $90^\circ$ . Sobel operator is very simple and effective way for finding the edges in image.

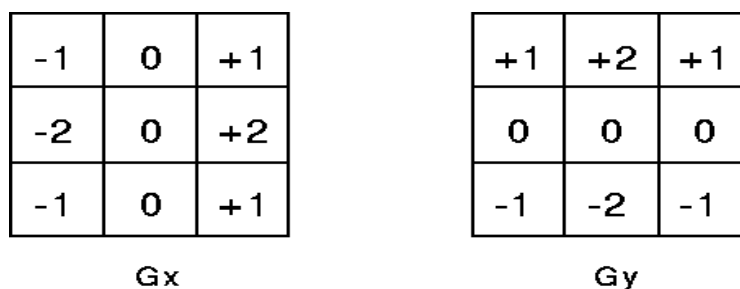


Fig 8

These kernels are designed to respond maximally to edges running vertically and horizontally relative to the pixel grid, one kernel for each of the two perpendicular orientations. The kernels can be applied separately to the input image, to produce separate measurements of the gradient component in each orientation (call these  $G_x$  and  $G_y$ ). These can then be combined together to find the absolute magnitude of the gradient at each point and the orientation of that gradient. An approximate gradient magnitude is computed using

$$|G| = |G_x| + |G_y|$$

The Edge =  $|G_d - G_q|$

Where  $G_d$  is the gradient of the database image

$G_q$  is the gradient of the query image

Texture is a very general notion that can be attributed to almost everything in nature. For a human, the texture relates mostly to a specific, spatially repetitive (micro) structure of surfaces formed by repeating a particular element or several elements in different relative spatial positions. Generally, the repetition involves local variations of scale, orientation, or other geometric and optical features of the elements. Texture features can be extracted in several methods, using statistical, structural, model based and transformation based, in which the most common way is, using the Gray Level Co- occurrence Matrix (GLCM). GLCM contains the second-order statistical information of spatial relationship of pixels of an image. From GLCM, many useful textural properties can be calculated to expose details about the image content. However, the calculation of GLCM is very computationally intensive and time consuming. After calculating GLCM, normalization is being carried out by dividing each element by the sum of all elements as shown in the equation below:

$$P_{i,j} = \frac{V_{i,j}}{\sum_{i,j=0}^{N-1} V_{i,j}}$$

Where,

- $V_{i,j}$  is the (i , j) element of the GLCM
- $P_{i,j}$  is the (i , j) element of the Normalized GLCM

From the normalized GLCM the following features have been extracted

- Contrast [T1]
- Dissimilarity [T2]
- Homogeneity [T3]
- Angular Second Moment [T4]
- Entropy [T5]
- 

The calculation of GLCM features is done by the following equation:

$$\text{Contrast [T1]} = \sum_{i,j=0}^{N-1} P_{i,j} (i - j)^2$$

$$\text{Dissimilarity [T2]} = \sum_{i,j=0}^{N-1} P_{i,j} |i - j|$$

$$\text{Homogeneity [T3]} = \sum_{i,j=0}^{N-1} \frac{P_{i,j}}{1 + (i-j)^2}$$

$$\text{Angular Second Moment [T4]} = \sum_{i,j=0}^{N-1} P_{i,j}^2$$

$$\text{Entropy [T5]} = \sum_{i,j=0}^{N-1} P_{i,j} (-\ln P_{i,j})$$

From the above equations the feature vector F is calculated as shown below.

$$F = [T1, T2, T3, T4, T5]$$

The magnitude of the feature vector  $F = T1+T2+T3+T4+T5$

The Similarity metric of the texture can be calculated as  $E_{\text{texture}} = |F_d - F_q|$

Where,

- $F_d$  = Magnitude of Feature Vector of Database Image
- $F_q$  = Magnitude of Feature Vector of Query Image

The results of our research work where we have implemented eight different methods are shown in are shown in Table 2.

#### 4.6 Retrieval time comparisons of various methods implemented

Sl.No	Method			Retrieval Time (Tr) in seconds
1.	Histogram			31.6323
2.	Bit plane	Simple		4.09868
3.	Hierarchical bit plane -1	20% histogram as threshold		4.51706
4.	Hierarchical bit plane -2	98% size as threshold		5.69741
5.	CDF	P = 3 [8 lines]		0.61504
6.	Hierarchical CDF	P = 3	1% of cdf diff as threshold	0.351143
7.	Edge based - 1	Sobel method		12.6268
8.	Texture based	GLCM method		0.401352

Table 2

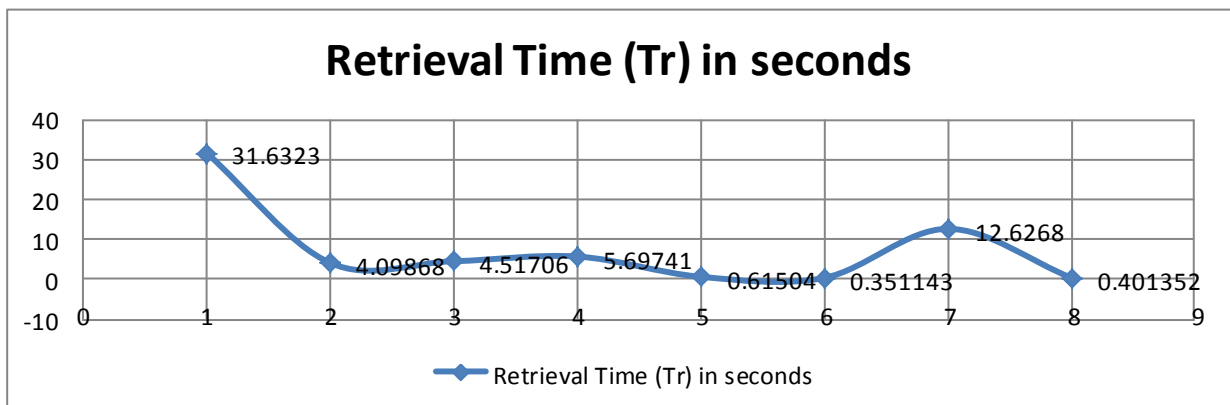


Fig. 9



Fig. 10. Retrieved images for query image brain0014.jpg with  $p=8$ , with 1% as CDF threshold

Figure 9 shows the retrieval time ( $t_r$ ) comparison of various methods implemented in our research work. Y- axis indicates the retrieval time ( $t_r$ ) in seconds. Figure 10 shows the screen shot for CDF based retrieval with  $p=8$  with 1% as CDF as the threshold.

X – axis indicates 8 different methods implemented. The details of the 8 different methods are given below:

1. Histogram based retrieval (without pre-stored features)
2. Simple Bit plane (pre-stored features)
3. Hierarchical Bit plane – 20% histogram as the threshold (pre-stored features)
4. Hierarchical Bit plane – 98% size as the threshold (pre-stored features)
5. CDF based retrieval ( $p=3$ ) (pre-stored features)
6. Hierarchical CDF based retrieval ( $p=3$ ) (pre-stored features)
7. Edge based retrieval (Sobel method) (pre-stored features)
8. Texture based retrieval (GLCM method) (pre-stored features)

## V. CONCLUSION AND FUTURE SCOPE FOR THE RESEARCH

Content-Based Image Retrieval (CBIR) is a very important research area with its innumerable applications especially in the medical and healthcare domain. Presently there is a substantial gap between CBIR, and its focus on raw image information and decision support systems, which typically enter the workflow beyond the point of image analysis itself. This gap represents what we believe is a major opportunity to develop decision support systems that integrate image features exploited in CBIR systems. With such integration, CBIR may be a starting point for finding similar images based on pixel analysis, but the process would be augmented by inclusion of image and non-image metadata as well as knowledge models, broadening the system from “image based search” to “case-based” search.

The present research work focuses on retrieval of images quickly based on three parameters namely Intensity, Texture and Shape. However including physician in the image retrieval loop (relevance feedback) will be better for accurate diagnosis. It would be better, if the physician is given a choice to select a specific area in the image and image is re-sized according to the selected area for better precision. However this will need extra time in terms of re-building the feature database.

The proposed system addresses global feature extraction of the images. However implementing local feature extraction based on automatic segmentation of the images may improve the accuracy of the system.

In our systems we have maintained single CDF feature database irrespective of line segments (2p) being selected by the user. Maintaining different feature databases as per the number of line segment should improve the retrieval time. This method could be explored in the future implementations.

In the texture comparison using GLCM we have taken into account the added values of the features (i.e. T1 + T2 + T3 + T4 + T5). Retrieval performance based on the individual GLCM features may give us more insight into the content of the medical images.

Extending the above features into the video images such as endoscopy may also help physicians in the diagnosis.

From the research perspective it is better to develop a standard CBIR frame work where various algorithms can be implemented on standard image database hosted at a central location. Giving options to students / researches to develop new algorithms and adding it to the existing methods will make the CBIR system usable by everyone.

### REFERENCES

- [1] Henning Muller, Nicolas Michoux, David Bandon, Antoine Geissbuhler. A review of content based image retrieval systems in medical applications – Clinical benefits and future directions. *International Journal on Medical Informatics* (2004) 73, 1-23.
- [1] Manjunath K N, Niranjana U C. Proceedings of the 2005 IEEE. *Engineering in Medicine and Biology*, 27<sup>th</sup> Annual Conference, Shanghai, China, September 1-4, 2005
- [2] Suyog Dutt Jain, Harishchandra Hebbar, K N Manjunath, U.C.Niranjana. Large Scale Distributed Frame work for Remote Clinical Diagnosis with Visual Query Support. *Distributed Diagnosis and Home Healthcare*, Pages: 1-16. ISBN: 1-58883 – 158 - 2.
- [3] K.N.Manjunath, A Renuka, U.C.Niranjana. Linear Models of Cumulative Distribution Function for Content –based Medical Image Retrieval. *Journal of Medical Systems* (2007) 31:433-443.
- [4] Ritendra Datta, Jia Li, James Z Wang. Content –Based Image Retrieval – Approached and Trends of the New Age. ACM1-58113-940-3/04/0010.
- [5] Ceyhun Burak Akgul, Daniel L Rubin, Sandy Napel, Christopher F Beaulieu, Hayit Greenspan, Burak Acar. *Journal of Digital Imaging*, 08 April 2010, Published online
- [6] Datta R, et al: Image retrieval: ideas, influences, and trends of the new age. *ACM Computer Survey* 40(2), 2008.
- [7] Smeulders AWM, et al: Content-based image retrieval at the end of the early years. *IEEE Trans Patt Anal Mach Intell* 22 (12):1349–1380, 2000.
- [8] Swain, M. J., and Ballard, D. H., “Color indexing for Content Based Image Retrieval” *International Journal of Computer Vision* 7(1):11–32, 1991.
- [9] Comaniciu D, Meer P, Foran DJ: Image-guided decision support system for pathology. *Mach Vis Appl* 11(4):213–224, 1999.
- [10] Kwak DM, et al: Content-based ultrasound image retrieval using a coarse to fine approach. *Ann N Y Acad Sci* 980:212–224, 2002.
- [11] Lim J, Chevallet J-P: Vismed: A visual vocabulary approach for medical image indexing and retrieval. in *Second Asia Information Retrieval Symposium*. 2005. Jeju Island, Korea.
- [12] Shyu CR, et al: ASSERT: a physician-in-the-loop content-based image retrieval system for HRCT image databases. *Comput Vis Image Underst* 75(1/2):111–132, 1999.
- [13] Cauvin JM, et al: Computer-assisted diagnosis system in digestive endoscopy. *IEEE Trans Inf Technol Biomed* 7 (4):256–262, 2003.
- [14] Güld MO, et al: Content-Based Retrieval of Medical Images by Combining Global Features. *Accessing Multilingual Information Repositories*. in *Accessing Multilingual Information Repositories*. 2005: Springer LNCS 4022.
- [15] Lubbers K, et al: A Probabilistic Approach to Medical Image Retrieval, in *Multilingual Information Access for Text, Speech and Images*. Springer Berlin, 2005, pp 761–772.

# Direct Method for Finding an Optimal Solution for Fuzzy Transportation Problem

A.Srinivasan<sup>1</sup>, G. Geetharamani<sup>2</sup>

<sup>1</sup> Department of Mathematics  
P.R Engineering College Thanjavur – 613 403, Tamilnadu, India

<sup>2</sup> Department of Mathematics  
Anna University Chennai, BIT Campus, Tiruchirappalli – 620 024, Tamilnadu, India

## ABSTRACT

In this paper we shall study fuzzy transportation problem, and we introduce an approach for solving a wide range of such problem by using a method which apply it for ranking of the fuzzy numbers. Some of the quantities in a fuzzy transportation problem may be fuzzy or crisp quantities. In many fuzzy decision problems, the quantities are represented in terms of fuzzy numbers may be triangular or trapezoidal. Thus, some fuzzy numbers are not directly comparable. First, we transform the fuzzy quantities as the cost, coefficients, supply and demands, in to crisp quantities by using Robust's ranking method [1] and then by using the classical algorithms we solve and obtain the solution of the problem. The new method is a systematic procedure, easy to apply and can be utilized for all types of transportation problem whether maximize or minimize objective function. At the end, this method is illustrated with a numerical example.

**Mathematics Subject Classification:** 90C70, 90C08

**Keywords:** Fuzzy ranking, fuzzy sets (normal and convex), Membership

**Functions, Trapezoidal fuzzy number, Triangular fuzzy number, Optimal Solution, Transportation problem.**

## I. INTRODUCTION

The transportation problem is a special linear programming problem which arises in many practical applications. In this problem we determine optimal shipping patterns between origins or sources and destinations. Suppose that  $m$  origins are to supply  $n$  destinations with a certain product. Let  $a_i$  be the amount of the product available at origin  $i$ , and  $b_j$  be the amount of the product required at destination  $j$ . Further, we assume that the cost of shipping a unit amount of the product from origin  $i$  to destination  $j$  is  $c_{ij}$ , we then let  $x_{ij}$  represent the amount shipped from origin  $i$  to destination  $j$ . If shipping costs, are assumed to be proportional to the amount shipped from each origin to each origin to each destination so as to minimize total shipping cost turns out to be a linear programming problem. Transportation models have wide applications in logistics and supply chain for reducing the cost. When the cost coefficients and the supply and demand quantities are known exactly. A fuzzy transportation problem is a transportation problem in which the transportation cost, supply and demand quantities are fuzzy quantities.

In many fuzzy decision problems, the data are represented in terms of fuzzy numbers. In a fuzzy transportation problem, all parameters are fuzzy numbers. Fuzzy numbers may be triangular or trapezoidal. Thus, some fuzzy numbers are not directly comparable. Comparing between two or multi fuzzy numbers and ranking such a numbers is one of the important subjects, and how to set the rank of fuzzy numbers has been one of the main problems. Several methods are introduced for ranking of fuzzy numbers. Here we use Robust's ranking method [1] which satisfies the properties of compensation, linearity and additivity. This method is very easy to understand and apply.

## II. PRELIMINARIES

### 1.1 Fuzzy Set:

A fuzzy set is characterized by a membership function mapping element of a domain, space, or the universe of discourse  $X$  to the unit interval  $[0, 1]$ . (i.e.)  $A = \{(x, \mu_A(x)); x \in X\}$ . Here  $\mu_A: X \rightarrow [0, 1]$  is a mapping called the degree of membership function of the fuzzy set  $A$  and  $\mu_A(x)$  is called the membership value of  $x \in X$  in the fuzzy set  $A$ . These membership grades are often represented by real numbers ranging from  $[0, 1]$ .

### 1.2 Normal fuzzy set :

A fuzzy set  $A$  of the universe of discourse  $X$  is called a normal fuzzy set implying that there exist at least one  $x \in X$  such that  $\mu_A(x) = 1$ .

### 1.3 Convex:

A fuzzy set  $A$  is convex if and only if, for any  $x_1, x_2 \in X$ , the membership function of  $A$  satisfies the inequality  $\mu_A(\lambda x_1 + (1 - \lambda)x_2) \geq \min(\mu_A(x_1), \mu_A(x_2))$ ,  $0 \leq \lambda \leq 1$ .

### 1.4 Triangular Fuzzy Number:

For a triangular fuzzy number  $A(x)$ , it can be represented by  $A(a, b, c; 1)$  with membership function  $\mu(x)$  given by

$$\mu(x) = \begin{cases} \frac{x-a}{b-a}, & a \leq x \leq b \\ 1, & x = b \\ \frac{c-x}{c-b}, & b \leq x \leq c \\ 0, & \text{otherwise} \end{cases}$$

### 1.5 Trapezoidal fuzzy number:

For a trapezoidal fuzzy number  $A(x)$ , it can be represented by  $A(a, b, c, d; 1)$  with membership function  $\mu(x)$  given by

$$\mu(x) = \begin{cases} \frac{x-a}{b-a}, & a \leq x \leq b \\ 1, & b \leq x \leq c \\ \frac{d-x}{d-c}, & c \leq x \leq d \\ 0, & \text{otherwise} \end{cases}$$

### 1.6 $\alpha$ -Cut:

The  $\alpha$ -cut of a fuzzy number  $A(x)$  is defined as  $A(\alpha) = \{x / \mu(x) \geq \alpha, \alpha \in [0, 1]\}$ .

### 1.7 Arithmetic operations between two triangular and trapezoidal fuzzy numbers fuzzy numbers:

Addition and Subtraction of two triangular fuzzy numbers can be performed as

$$\tilde{A} + \tilde{B} = (a_1 + b_1, a_2 + b_2, a_3 + b_3)$$

$$\tilde{A} - \tilde{B} = (a_1 - b_1, a_2 - b_2, a_3 - b_3)$$

Addition and Subtraction of two trapezoidal fuzzy numbers can be performed

$$\begin{aligned} \tilde{A} + \tilde{B} &= (a_1 + b_1, a_2 + b_2, a_3 + b_3, a_4 + b_4), \\ \text{as} \\ \tilde{A} - \tilde{B} &= (a_1 - b_1, a_2 - b_2, a_3 - b_3, a_4 - b_4) \end{aligned}$$

### III. ROBUST'S RANKING TECHNIQUE [1]

Robust's ranking technique [1] which satisfy compensation, linearity, and additively properties and provides results which are consistent with human intuition. If  $\tilde{a}$  is a fuzzy number then the Robust's ranking is defined by

$$R(\tilde{a}) = \int_0^1 0.5(a'_\alpha, a''_\alpha) d\alpha, \text{ Where } (a'_\alpha, a''_\alpha) \text{ is the } \alpha\text{-level cut of the fuzzy number } \tilde{a}.$$

In this paper we use this method for ranking the objective values. The Robust's ranking index  $R(\tilde{a})$  gives the representative value of fuzzy number  $\tilde{a}$ . It satisfies the linearity and additive property.

### IV. FUZZY TRANSPORTATION MODEL FORMULATION

We deal with the production and transportation planning of a certain manufacturer that has production facilities and central stores for resellers in several sites in Chennai. Each store can receive products from all production plants and it is not necessary that all products are produced in all production units.

Assume that a logistics center seeks to determine the transportation plan of a homogeneous commodity from  $m$  sources to  $n$  destinations. Each source has an available supply of the commodity to distribute to various destinations, and each destination has a forecast demand of the commodity to be received from various sources. This work focuses on developing a Fuzzy linear programming method for optimizing the transportation plan in fuzzy environments.

#### 1.8 Index sets

- $i$  index for source, for all  $i = 1, 2, \dots, m$
- $j$  index for destination, for all  $j = 1, 2, \dots, n$
- $g$  index for objectives, for all  $g = 1, 2, \dots, k$

#### 1.9 Decision variables

$x_{ij}$  units transported from source  $i$  to destination  $j$  (units)

#### 1.10 Objective functions

$\tilde{Z}$  Transportation costs (Rs.)

#### 1.11 Parameters

$\tilde{C}_{ij}$  Transportation cost per unit delivered from source  $i$  to destination  $j$  (Rs/unit)

$\tilde{S}_i$  Total available supply at each source  $i$  (units)

$\tilde{D}_j$  Total forecast demand at each destination  $j$  (units)

#### 1.12 Objective functions

Minimize total transportation costs

$$\text{Min } \tilde{Z} = \sum_{i=1}^m \sum_{j=1}^n \tilde{c}_{ij} x_{ij}$$

Constraints on total available supply for each source  $i$

$$\sum_{i=1}^n x_{ij} = \tilde{S}_j$$

Constraints on total forecast demand for each destination  $j$

$$\sum_{j=1}^m x_{ij} = \tilde{D}_i$$

If any of the parameters  $x_{ij}$ ,  $S_i$ , and  $D_j$  is fuzzy, the total transportation cost  $Z$  becomes fuzzy as well. The conventional transportation problem defined then turns into the fuzzy transportation problem.

**V. FUZZY TRANSPORTATION MODEL ILLUSTRATION**

Consider transportation with  $m$  fuzzy origins (rows) and  $n$  fuzzy destinations (columns). Let  $\tilde{C}_{ij} = [c_{ij}^{(1)}, c_{ij}^{(2)}, c_{ij}^{(3)}, c_{ij}^{(4)}]$  be the cost of transporting one unit of the product from  $i^{\text{th}}$  fuzzy origin to  $j^{\text{th}}$  fuzzy destination.  $\tilde{S}_i = [s_i^{(1)}, s_i^{(2)}, s_i^{(3)}, s_i^{(4)}]$  be the quantity of commodity available at fuzzy origin  $i$ ,  $\tilde{D}_j = [d_j^{(1)}, d_j^{(2)}, d_j^{(3)}, d_j^{(4)}]$  the quantity of commodity needed at fuzzy destination  $j$ .  $X_{ij}$  is quantity transported from  $i^{\text{th}}$  fuzzy origin to  $j^{\text{th}}$  fuzzy destination. The above fuzzy transportation problem can be stated in the below tabular form.

	1	2	...	n	Fuzzy Supply
1	$\tilde{C}_{11}x_{11}$	$\tilde{C}_{12}x_{12}$	...	$\tilde{C}_{1n}x_{1n}$	$\tilde{S}_1$
2	$\tilde{C}_{21}x_{21}$	$\tilde{C}_{22}x_{22}$	...	$\tilde{C}_{2n}x_{2n}$	$\tilde{S}_2$
m	$\tilde{C}_{m1}x_{m1}$	$\tilde{C}_{m2}x_{m2}$	...	$\tilde{C}_{mn}x_{mn}$	$\tilde{S}_m$
Fuzzy Demand	$\tilde{D}_1$	$\tilde{D}_2$		$\tilde{D}_n$	$\sum_{j=1}^n \tilde{D}_j = \sum_{i=1}^m \tilde{S}_i$

Where  $\tilde{C}_{ij} = [c_{ij}^{(1)}, c_{ij}^{(2)}, c_{ij}^{(3)}, c_{ij}^{(4)}]$

$\tilde{X}_{ij} = [x_{ij}^{(1)}, x_{ij}^{(2)}, x_{ij}^{(3)}, x_{ij}^{(4)}]$

$\tilde{S}_i = [s_i^{(1)}, s_i^{(2)}, s_i^{(3)}, s_i^{(4)}]$

$\tilde{D}_j = [d_j^{(1)}, d_j^{(2)}, d_j^{(3)}, d_j^{(4)}]$

**VI. METHODOLOGY [4]**

**Step 1:** Construct the transportation table from given fuzzy transportation problem.

**Step 2:** Subtract each row entries of the transportation table from the respective row minimum and then subtract each column entries of the resulting transportation table from respective column minimum.

**Step 3:** Now there will be at least one zero in each row and in each column in the reduced cost matrix. Select the first zero (row-wise) occurring in the cost matrix. Suppose  $(i, j)^{\text{th}}$  zero is selected, count the total number of zeros (excluding the selected one) in the  $i^{\text{th}}$  row and  $j^{\text{th}}$  column. Now select the next zero and count the total number of zeros in the corresponding row and column in the same manner. Continue it for all zeros in the cost matrix.

**Step 4:** Now choose a zero for which the number of zeros counted in step 3 is minimum and supply maximum possible amount to that cell. If tie occurs for some zeros in step 3 then choose a  $(k, l)^{\text{th}}$  zero breaking tie such that the total sum of all the elements in the  $k^{\text{th}}$  row and  $l^{\text{th}}$  column is maximum. Allocate maximum possible amount to that cell.

**Step 5:** After performing step 4, delete the row or column for further calculation where the supply from a given source is depleted or the demand for a given destination is satisfied.

**Step 6:** Check whether the resultant matrix possesses at least one zero in each row and in each column. If not, repeat step 2, otherwise go to step 7.

**Step 7:** Repeat step 3 to step 6 until and unless all the demands are satisfied and all the supplies are exhausted.

### VII. NUMERICAL EXAMPLE

**Example 5.1** Consider the following fuzzy transportation problem.

A company has four sources  $S_1, S_2, S_3,$  and  $S_4$  and four destinations  $D_1, D_2, D_3,$  and  $D_4$  the fuzzy transportation cost for unit quantity of the product from  $i^{\text{th}}$  source to  $j^{\text{th}}$  destination is  $C_{ij}$  where

$$[\tilde{C}_{ij}]_{4 \times 4} = \begin{pmatrix} (5,10,15) & (5,10,20) & (5,15,20) & (5,10,15) \\ (5,10,20) & (5,15,20) & (5,10,15) & (10,15,20) \\ (5,10,20) & (10,15,20) & (10,15,20) & (5,10,15) \\ (10,15,25) & (5,10,15) & (10,20,30) & (10,15,25) \end{pmatrix}$$

and fuzzy availability of the product at source are  $(10,15,20), (5,10,15), (20,30,40), (15,20,25)$  and the fuzzy demand of the product at destinations are  $(25,30,35), (10,15,20), (5,15,20),$

$(10,15,25)$  respectively. The fuzzy transportation problems are

	$D_1$	$D_2$	$D_3$	$D_4$	FUZZY CAPACITY
$S_1$	(5,10,15)	(5,10,20)	(5,15,20)	(5,10,15)	(10,15,20)
$S_2$	(5,10,20)	(5,15,20)	(5,10,15)	(10,15,20)	(5,10,15)
$S_3$	(5,10,20)	(10,15,20)	(10,15,20)	(5,10,15)	(20,30,40)
$S_4$	(10,15,25)	(5,10,15)	(10,20,30)	(10,15,25)	(15,20,25)
FUZZY DEMAND	(25,30,35)	(10,15,20)	(5,15,20)	(10,15,25)	

**Solution:**

**Step 1:** Construct the transportation table from given fuzzy transportation problem.

$$\begin{aligned} \text{Min} Z = & R(5,10,15)x_{11} + R(5,10,20)x_{12} + R(5,15,20)x_{13} + R(5,10,15)x_{14} \\ & R(5,10,20)x_{21} + R(5,15,20)x_{22} + R(5,10,15)x_{23} + R(10,15,20)x_{24} \\ & R(5,10,20)x_{31} + R(10,15,20)x_{32} + R(10,15,20)x_{33} + R(5,10,15)x_{34} \\ & R(10,15,25)x_{41} + R(5,10,15)x_{42} + R(10,20,30)x_{43} + R(10,15,25)x_{44} \end{aligned}$$

Now we calculate  $R(5,10,15)$  by applying Robst's ranking method. The membership function of the triangular fuzzy number  $(5,10,15)$  is

$$\mu(x) = \begin{cases} \frac{x-5}{5}, & 5 \leq x \leq 10 \\ 1, & x = 10 \\ \frac{15-x}{5}, & 10 \leq x \leq 15 \\ 0, & \text{otherwise} \end{cases}$$

The  $\alpha$ -Cut of the fuzzy number  $(5,10,15)$  is  $(a'_\alpha, a''_\alpha) = (5\alpha + 5, 15 - 5\alpha)$  for

which  $R(a_{11}) = R(5,10,15) = \int_0^1 0.5(a'_\alpha, a''_\alpha) d\alpha = \int_0^1 0.5(20) d\alpha = 10$

Proceeding similarly, the Robust's ranking indices for the fuzzy costs  $a_{ij}$  are calculated

$$R(a_{1,2})=11.25, R(a_{1,3})=13.75, R(a_{1,4})=10, R(a_{2,1})=11.25, R(a_{2,2})=13.75,$$

as:  $R(a_{2,3})=10, R(a_{2,4})=15, R(a_{3,1})=11.25, R(a_{3,2})=15, R(a_{3,3})=15,$

$$R(a_{3,4})=10, R(a_{4,1})=16.25, R(a_{4,2})=10, R(a_{4,3})=20, R(a_{4,4})=16.25$$

Rank of All Supply  $R(10,15,20)=15, R(5,10,15)=10, R(20,30,40)=30, R(15,20,25)=20$

Rank of All Demand  $R(25,30,35)=30, R(10,15,20)=15, (5,15,20)=13.75, R(10,15,25)=16.25$

We replace these values for their corresponding  $\tilde{a}_{ij}$  in which result in a convenient transportation problem

	$D_1$	$D_2$	$D_3$	$D_4$	CAPACITY
$S_1$	10	11.25	13.75	10	15
$S_2$	11.25	13.75	10	15	10
$S_3$	11.25	15	15	10	30
$S_4$	16.25	10	20	16.25	20
DEMAND	30	15	13.75	16.25	

**Step 2:** Subtract each row entries of the transportation table from the respective row minimum and then subtract each column entries of the resulting transportation table from respective column minimum.

	$D_1$	$D_2$	$D_3$	$D_4$	CAPACITY
$S_1$	0	1.25	3.75	0	15
$S_2$	1.25	3.75	0	5	10
$S_3$	1.25	5	5	0	30
$S_4$	6.25	0	0	6.25	20
DEMAND	30	15	13.75	16.25	

**Step 3:** Now there will be at least one zero in each row and in each column in the reduced cost matrix. Select the first zero (row-wise) occurring in the cost matrix. Suppose  $(i, j)^{th}$  zero is selected, count the total number of zeros (excluding the selected one) in the  $i^{th}$  row and  $j^{th}$  column. Now select the next zero and count the total number of zeros in the corresponding row and column in the same manner. Continue it for all zeros in the cost matrix.

	$D_1$	$D_2$	$D_3$	$D_4$	CAPACITY
$S_1$	0	1.25	3.75	0	15 (2)
$S_2$	1.25	3.75	0	5	10 (1)
$S_3$	1.25	5	5	0	30 (1)
$S_4$	6.25	0	10	6.25	20 (1)
DEMAND	30	15	13.75	16.25	
	(1)	(1)	(1)	(1)	

**Step 4:** Now choose a zero for which the number of zeros counted in step 3 is minimum and supply maximum possible amount to that cell. If tie occurs for some zeros in step 3 then choose a  $(k,l)^{th}$  zero breaking tie such that the total sum of all the elements in the  $k^{th}$  row and  $l^{st}$  column is maximum. Allocate maximum possible amount to that cell.

	$D_1$	$D_2$	$D_3$	$D_4$	CAPACITY
$S_1$	0(15)	1.25	3.75	0	0
$S_2$	1.25	3.75	0	5	10
$S_3$	1.25	5	5	0	30
$S_4$	6.25	0	10	6.25	20
DEMAND	15	15	13.75	16.25	

**Step 5:** After performing step 4, delete the row or column for further calculation where the supply from a given source is depleted or the demand for a given destination is satisfied.

	$D_1$	$D_2$	$D_3$	$D_4$	CAPACITY
$S_1$	0(15)	1.25	3.75	0	0
$S_2$	1.25	3.75	0	5	10
$S_3$	1.25	5	5	0	30
$S_4$	6.25	0	10	6.25	20
DEMAND	15	15	13.75	16.25	

**Step 6:** Check whether the resultant matrix possesses at least one zero in each row and in each column. If not, repeat step 2, otherwise go to step 7.

**Step 7:** Repeat step 3 to step 6 until and unless all the demands are satisfied and all the supplies are exhausted.

	$D_1$	$D_2$	$D_3$	$D_4$	CAPACITY
$S_1$	10(15)	11.25	13.75	10	15
$S_2$	11.25	13.75	10(10)	15	10
$S_3$	11.25(10)	15	15(3.75)	10(16.25)	30
$S_4$	16.25(5)	10(15)	20	16.25	20
DEMAND	30	15	13.75	16.25	

The total cost associated with the allocation is 812.5

### VIII. CONCLUSIONS

The Direct method provides an optimal solution directly, in less iteration, for the transportation problems. As this method consumes less time and is very easy to understand and apply, so it will be very helpful for decision makers who are dealing with logistic and supply chain problems.

### REFERENCES

- [1]. A.Solairaju and R.Nagarajan "Computing Improved Fuzzy Optimal Hungarian Assignment Problems with Fuzzy Costs under Robust Ranking Techniques"(2010)
- [2]. A.Srinivasan and G.Geetharamani "Method for solving fuzzy assignment problem using ones assignment method and Robust's ranking technique" Applied Mathematical Sciences, Vol.7,2013,no.113,5607-5619.
- [3]. A.ZADEH "Fuzzy Set"(1965)
- [4]. AbdulQuddos, Shakeel Javaid, M.M Khalid " A New Method for Finding an Optimal Solution for Transportation Problems" International Journal on Computer Science and Engineering (IJCSSE), ISSN : 0975-3397 ,Vol. 4 No. 07 July 2012.
- [5]. George J.Klir/Bo Yuan "Fuzzy Sets and Fuzzy logic Theory and Applications"
- [6]. H.J Zimmermann, "Fuzzy set theory and its Applications", third Ed., kluwer Academic, Boston 1996.
- [7]. Hamdy A. Taha, "Operations Research", an introduction 8<sup>th</sup> Ed.(2007)
- [8]. JieLu.Guangquan Zhang and DaRuan.Fengjie Wu "Multi objective Group Decision Making Methods, Software and Applications with Fuzzy Set Techniques".
- [9]. Kadhivel.K,Balamurugan.K,"Method For Solving Hungarian Assignment Problems Using Triangular And Trapezoidal Fuzzy Number" (2012)
- [10]. M.Hellmann "Fuzzy logic Introduction"
- [11]. R.R Yager,"A procedure for ordering fuzzy subsets of the unit interval, information Sciences",24,(1982),143-161
- [12]. Y. L. P. Thorani, P. PhaniBushmanRao, and N. Ravi Shankar "Ordering Generalized Trapezoidal Fuzzy Numbers Using Orthocentre of Centroids"

## Polynomials having no Zero in a Given Region

<sup>1</sup>M. H. Gulzar

<sup>1</sup>Department of Mathematics University of Kashmir, Srinagar 190006

### ABSTRACT:

In this paper we consider some polynomials having no zeros in a given region. Our results when combined with some known results give ring-shaped regions containing a specific number of zeros of the polynomial.

**Mathematics Subject Classification:** 30C10, 30C15

**Keywords and phrases:** Coefficient, Polynomial, Zero.

### I. INTRODUCTION AND STATEMENT OF RESULTS

In the literature we find a large number of published research papers concerning the number of zeros of a polynomial in a given circle. For the class of polynomials with real coefficients, Q. G. Mohammad [5] proved the following result:

**Theorem A:** Let  $P(z) = \sum_{j=0}^{\infty} a_j z^j$  be a polynomial of degree  $n$  such that

$$a_n \geq a_{n-1} \geq \dots \geq a_1 \geq a_0 > 0.$$

Then the number of zeros of  $P(z)$  in  $|z| \leq \frac{1}{2}$  does not exceed

$$1 + \frac{1}{\log 2} \log \frac{a_n}{a_0}.$$

Bidkham and Dewan [1] generalized Theorem A in the following way:

**Theorem B:** Let  $P(z) = \sum_{j=0}^{\infty} a_j z^j$  be a polynomial of degree  $n$  such that

$$a_n \leq a_{n-1} \leq \dots \leq a_{k+1} \leq a_k \geq a_{k-1} \geq \dots \geq a_1 \geq a_0 > 0,$$

for some  $k, 0 \leq k \leq n$ . Then the number of zeros of  $P(z)$  in  $|z| \leq \frac{1}{2}$  does not exceed

$$\frac{1}{\log 2} \log \left\{ \frac{|a_n| + |a_0| - a_n - a_0 + 2a_k}{|a_0|} \right\}.$$

Ebadian et al [2] generalized the above results by proving the following results:

**Theorem C:** Let  $P(z) = \sum_{j=0}^{\infty} a_j z^j$  be a polynomial of degree  $n$  such that

$$a_n \leq a_{n-1} \leq \dots \leq a_{k+1} \leq a_k \geq a_{k-1} \geq \dots \geq a_0$$

for some  $k, 0 \leq k \leq n$ . Then the number of zeros of  $P(z)$  in  $|z| \leq \frac{R}{2}, R > 0$ , does not exceed

$$\frac{1}{\log 2} \log \left\{ \frac{|a_n| R^{n+1} + |a_0| + R^k (a_k - a_0) + R^n (a_k - a_n)}{|a_0|} \right\} \text{ for } R \geq 1$$

And

$$\frac{1}{\log 2} \log \left\{ \frac{|a_n|R^{n+1} + |a_0| + R(a_k - a_0) + R^n(a_k - a_n)}{|a_0|} \right\} \text{ for } R \leq 1 .$$

M.H.Gulzar [3] generalized the above result by proving the following result:

**Theorem D:** Let  $P(z) = \sum_{j=0}^{\infty} a_j z^j$  be a polynomial of degree  $n$  with  $\text{Re}(a_j) = \alpha_j$ ,  $\text{Im}(a_j) = \beta_j$  such that for some  $k, \tau, \lambda, 0 < k \leq 1, 0 < \tau \leq 1, 0 \leq \lambda \leq n$ ,

$$k\alpha_n \leq \alpha_{n-1} \leq \dots \leq \alpha_{\lambda+1} \leq \alpha_{\lambda} \geq \alpha_{\lambda-1} \geq \dots \geq \tau\alpha_0 .$$

Then the number of zeros of  $P(z)$  in  $|z| \leq \frac{R}{c}$  ( $R > 0, c > 1$ ) does not exceed

$$\frac{1}{\log c} \log \left\{ \frac{\left[ |a_n|R^{n+1} + |a_0| + R^{\lambda}[\alpha_{\lambda} - \tau(|\alpha_0| + \alpha_0) + |\alpha_0| + |\beta_0| + |\beta_{\lambda}| + 2 \sum_{j=1}^{\lambda-1} |\beta_j|] \right] + R^n [|\alpha_n| - k(|\alpha_n| + \alpha_n) + \alpha_{\lambda} + |\beta_{\lambda}| + |\beta_n| + 2 \sum_{j=\lambda+1}^{n-1} |\beta_j|]}{|a_0|} \right\}$$

for  $R \geq 1$

and

$$\frac{1}{\log c} \log \left\{ \frac{\left[ |a_n|R^{n+1} + |a_0| + R[\alpha_{\lambda} - \tau(|\alpha_0| + \alpha_0) + |\alpha_0| + |\beta_0| + |\beta_{\lambda}| + 2 \sum_{j=1}^{\lambda-1} |\beta_j|] \right] + R^n [|\alpha_n| - k(|\alpha_n| + \alpha_n) + \alpha_{\lambda} + |\beta_{\lambda}| + |\beta_n| + 2 \sum_{j=\lambda+1}^{n-1} |\beta_j|]}{|a_0|} \right\}$$

In this paper we prove the following result:

**Theorem 1:** Let  $P(z) = \sum_{j=0}^{\infty} a_j z^j$  be a polynomial of degree  $n$  with  $\text{Re}(a_j) = \alpha_j$ ,  $\text{Im}(a_j) = \beta_j$  such that for some  $k, \tau, \lambda, 0 < k \leq 1, 0 < \tau \leq 1, 0 \leq \lambda \leq n$ ,

$$k\alpha_n \leq \alpha_{n-1} \leq \dots \leq \alpha_{\lambda+1} \leq \alpha_{\lambda} \geq \alpha_{\lambda-1} \geq \dots \geq \tau\alpha_0 .$$

Then  $P(z)$  has no zero in  $|z| < \frac{|a_0|}{M_1}$  for  $R \geq 1$  and no zero in  $|z| < \frac{|a_0|}{M_2}$  for  $R \leq 1$

where

$$M_1 = |a_n|R^{n+1} + R^n [|\alpha_n| - k(|\alpha_n| + \alpha_n) + \alpha_{\lambda}] + |\beta_{\lambda}| + |\beta_n| + 2 \sum_{j=\lambda+1}^n |\beta_j| + R^{\lambda} [\alpha_{\lambda} - \tau(|\alpha_0| + \alpha_0) + |\alpha_0| + |\beta_0| + |\beta_{\lambda}| + 2 \sum_{j=1}^{\lambda-1} |\beta_j|]$$

and

$$M_2 = |a_n|R^{n+1} + R^n [|\alpha_n| - k(|\alpha_n| + \alpha_n) + \alpha_{\lambda}] + |\beta_{\lambda}| + |\beta_n| + 2 \sum_{j=\lambda+1}^n |\beta_j| + R[\alpha_{\lambda} - \tau(|\alpha_0| + \alpha_0) + |\alpha_0| + |\beta_0| + |\beta_{\lambda}| + 2 \sum_{j=1}^{\lambda-1} |\beta_j|] .$$

Combining Theorem 1 with Theorem D, we get the following result:

**Theorem 2:** Let  $P(z) = \sum_{j=0}^{\infty} a_j z^j$  be a polynomial of degree  $n$  with  $\text{Re}(a_j) = \alpha_j$ ,  $\text{Im}(a_j) = \beta_j$  such that

for some  $k, \tau, \lambda, 0 < k \leq 1, 0 < \tau \leq 1, 0 \leq \lambda \leq n$ ,

$$k\alpha_n \leq \alpha_{n-1} \leq \dots \leq \alpha_{\lambda+1} \leq \alpha_{\lambda} \geq \alpha_{\lambda-1} \geq \dots \geq \tau\alpha_0.$$

Then the number of zeros of  $P(z)$  in  $\frac{|a_0|}{M_1} \leq |z| \leq \frac{R}{c}$  ( $R > 0, c > 1$ ) does not exceed

$$\frac{1}{\log c} \log \left\{ \frac{\left[ |a_n| R^{n+1} + |a_0| + R^{\lambda} [\alpha_{\lambda} - \tau(|\alpha_0| + \alpha_0) + |\alpha_0| + |\beta_0| + |\beta_{\lambda}| + 2 \sum_{j=1}^{\lambda-1} |\beta_j|] \right] + R^n [|\alpha_n| - k(|\alpha_n| + \alpha_n) + \alpha_{\lambda} + |\beta_{\lambda}| + |\beta_n| + 2 \sum_{j=\lambda+1}^{n-1} |\beta_j|]}{|a_0|} \right\}$$

for  $R \geq 1$

and the number of zeros of  $P(z)$  in  $\frac{|a_0|}{M_2} \leq |z| \leq \frac{R}{c}$  ( $R > 0, c > 1$ ) does not exceed

$$\frac{1}{\log c} \log \left\{ \frac{\left[ |a_n| R^{n+1} + |a_0| + R[\alpha_{\lambda} - \tau(|\alpha_0| + \alpha_0) + |\alpha_0| + |\beta_0| + |\beta_{\lambda}| + 2 \sum_{j=1}^{\lambda-1} |\beta_j|] \right] + R^n [|\alpha_n| - k(|\alpha_n| + \alpha_n) + \alpha_{\lambda} + |\beta_{\lambda}| + |\beta_n| + 2 \sum_{j=\lambda+1}^{n-1} |\beta_j|]}{|a_0|} \right\}$$

for  $R \leq 1$ ,

where  $M_1$  and  $M_2$  are as given in Theorem 1.

For different values of the parameters, we get many interesting results including some already known results.

## 2. Proofs of Theorems

**Proof of Theorem 1:** Consider the polynomial

$$\begin{aligned} F(z) &= (1-z)P(z) \\ &= (1-z)(a_n z^n + a_{n-1} z^{n-1} + \dots + a_1 z + a_0) \\ &= -a_n z^{n+1} + (a_n - a_{n-1})z^n + \dots + (a_1 - a_0)z + a_0 \\ &= -a_n z^{n+1} + a_0 + [(k\alpha_n - \alpha_{n-1}) - (k-1)\alpha_n]z^n + \sum_{j=\lambda+1}^{n-1} (\alpha_j - \alpha_{j-1})z^j \\ &\quad + \sum_{j=2}^{\lambda} (\alpha_j - \alpha_{j-1})z^j + [(\alpha_1 - \tau\alpha_0) + (\tau-1)\alpha_0]z + i \left\{ \sum_{j=\lambda+1}^n (\beta_j - \beta_{j-1})z^j \right. \\ &\quad \left. + \sum_{j=1}^{\lambda} (\beta_j - \beta_{j-1})z^j \right\} \end{aligned}$$

$= a_0 + G(z)$ , where

$$G(z) = -a_n z^{n+1} + a_0 + [(k\alpha_n - \alpha_{n-1}) - (k-1)\alpha_n]z^n + \sum_{j=\lambda+1}^{n-1} (\alpha_j - \alpha_{j-1})z^j \\ + \sum_{j=2}^{\lambda} (\alpha_j - \alpha_{j-1})z^j + [(\alpha_1 - \tau\alpha_0) + (\tau-1)\alpha_0]z + i \sum_{j=1}^{\lambda} (\beta_j - \beta_{j-1})z^j$$

For  $|z| \leq R$ , we have, by using the hypothesis

$$|G(z)| \leq |a_n|R^{n+1} + [(\alpha_{n-1} - k\alpha_n) + (1-k)|\alpha_n|]R^n + \sum_{j=\lambda+1}^{n-1} (\alpha_{j-1} - \alpha_j)R^j \\ + \sum_{j=1}^{\lambda} (\alpha_j - \alpha_{j-1})R^j + [(\alpha_1 - \tau\alpha_0) + (1-\tau)|\alpha_0|]R + \sum_{j=1}^n (|\beta_j| + |\beta_{j-1}|)R^j$$

which gives

$$|G(z)| \leq |a_n|R^{n+1} + R^n [|\alpha_n| - k(|\alpha_n| + \alpha_n) + \alpha_\lambda] + |\beta_\lambda| + |\beta_n| + 2 \sum_{j=\lambda+1}^n |\beta_j| \\ + R^\lambda [\alpha_\lambda - \tau(|\alpha_0| + \alpha_0) + |\alpha_0| + |\beta_0| + |\beta_\lambda| + 2 \sum_{j=1}^{\lambda-1} |\beta_j|] \\ = M_1 \quad \text{for } R \geq 1$$

and

$$|G(z)| \leq |a_n|R^{n+1} + R^n [|\alpha_n| - k(|\alpha_n| + \alpha_n) + \alpha_\lambda] + |\beta_\lambda| + |\beta_n| + 2 \sum_{j=\lambda+1}^n |\beta_j| \\ + R[\alpha_\lambda - \tau(|\alpha_0| + \alpha_0) + |\alpha_0| + |\beta_0| + |\beta_\lambda| + 2 \sum_{j=1}^{\lambda-1} |\beta_j|] \\ = M_2 \quad \text{for } R \leq 1.$$

Since  $G(z)$  is analytic in  $|z| \leq R$  and  $G(0)=0$ , it follows by Schwarz Lemma that

$$|G(z)| \leq M_1 |z| \quad \text{for } R \geq 1 \text{ and } |G(z)| \leq M_2 |z| \quad \text{for } R \leq 1.$$

Hence, for  $R \geq 1$ ,

$$|F(z)| = |a_0 + G(z)| \\ \geq |a_0| - |G(z)| \\ \geq |a_0| - M_1 |z| \\ > 0$$

if

$$|z| < \frac{|a_0|}{M_1}.$$

And for  $R \leq 1$ ,

$$|F(z)| = |a_0 + G(z)| \\ \geq |a_0| - |G(z)| \\ \geq |a_0| - M_2 |z| \\ > 0$$

if

$$|z| < \frac{|a_0|}{M_2}.$$

This shows that  $F(z)$  has no zero in  $|z| < \frac{|a_0|}{M_1}$  for  $R \geq 1$  and no zero in  $|z| < \frac{|a_0|}{M_2}$  for  $R \leq 1$ . But the zeros of

$P(z)$  are also the zeros of  $F(z)$ . Therefore, the result follows.

**REFERENCES**

- [1] M.Bidkham and K.K. Dewan, On the zeros of a polynomial, Numerical Methods and Approximation Theory,III , Nis (1987), 121-128.
- [2] A.Ebadian, M.Bidkham and M.Eshaghi Gordji, Number of zeros of a polynomial in a given domain,Tamkang Journal of Mathematics, Vol.42, No.4,531-536, Winter 2011.
- [3] M.H.Gulzar, On the Number of Zeros of a Polynomial in a Given Domain, International Journal of Scientific and Research Publications, Vol.3, Issue 10, October 2013.
- [4] M.Marden , Geometry of Polynomials , Mathematical surveys, Amer. Math. Soc. , Rhode Island , 3 (1966).
- [5] Q.G.Mohammad, Location of the zeros of polynomials, Amer. Math. Monthly , 74 (1967), 290-292.

# Simple Domestic Air Conditioning by using the Ice Thermal Storage Capacity

<sup>1</sup>Mohammed Hadi Ali  
<sup>1</sup>Lecturer University of Mustansiriyah

## ABSTRACT:

*In this paper, a special design of an experimental rig was used to study and evaluate the performance of using the ice thermal storage capacity for cooling purpose. Nowadays ice thermal storage system is mostly used because it is practical due to the large heat of fusion of ice to change into water. Thermal storage techniques have provided opportunities to store cooling energy in ice when the power price is relatively low.*

*The experimental rig that was built is a simple domestic air conditioning prototype that can be used to cool small spaces with ice bank which are prepared for this purpose.*

*Encouraging results were obtained in this paper where two different air flowrate was used to compare between them; it was found that the performance of using the ice storage capacity is effective in which the coefficient of performance (COP) is relatively high compared to a conventional air conditioning. The results showed that the COP for higher air flowrate is lower than the COP for lower air flowrate due to lower power consumed by the system. And the outlet temperature for the higher air flowrate is higher than the outlet temperature for the lower air flowrate due to the more time of contact between the air and the ice banks.*

*As a conclusion we found that the ice storage capacity process is an effective process of using a chiller or refrigeration plant to build ice during off-peak hours to serve part or the entire on-peak cooling requirement.*

## I. INTRODUCTION:

### Refrigeration:

Refrigeration can be defined as the process of removing heat from any substance which may be a solid, a liquid, or a gas; it maintains the temperature of the substance below that of its surroundings. Refrigeration is therefore the science of moving heat from low temperature to high temperature <sup>[ref. 1]</sup>.

There are two common methods of refrigeration; these methods are natural and mechanical. In the mechanical refrigeration a refrigerant which is a substance capable of transferring heat that it absorbs at low temperatures and pressures to a condensing medium. By means of expansion, compression, and a cooling medium, such as air or water, the refrigerant removes heat from a substance and transfers it to the cooling medium.

In the natural refrigeration, ice has been used in refrigeration since ancient times and it is still widely used. In this natural technique, the forced circulation of air or water passes around blocks of ice <sup>[ref. 2]</sup>. Some of the heat of the circulating air is transferred to the ice, thus cooling the air, particularly for air conditioning applications.

### Refrigeration by Natural Ice:

Historically, an inscription from 1700 BC in northwest Iran records the construction of an icehouse, "which never before had any king built." In China, archaeologists have found remains of ice pits from the seventh century BC, and references suggest they were in use before 1100 BC. Alexander the Great around 300 BC stored snow in pits dug for that purpose. In Rome in the third century AD, snow was imported from the mountains, stored in straw-covered pits, and sold from snow shops <sup>[ref. 3]</sup>.

Before the 19th century, there was no mechanical refrigeration, and all the artificial cooling of air has used ice, snow, cold water or evaporative cooling. In the 1800s natural refrigeration was a vibrant part of the economy. Natural ice harvested from the pristine rivers and lakes of the northern US was in demand <sup>[ref. 4]</sup>.

Ice harvesting is still a good way to beat the cost of refrigeration. In China, "Citizens collect ice blocks cut from the ice on the Songhua River in Mudanjiang, northeast China's and store ice cubes at their cellars in winter for summer use. They buried it in sawdust, ice can last all summer at zero cost and energy consumed <sup>[ref. 5]</sup>.

In natural ice refrigeration, cooling is accomplished by melting ice. Owing to its melting point of (0 °C), Ice is used as an effective cooling agent because to melt it, ice must absorb 333.55 kJ/kg (about 144 Btu/lb) of heat.

This method is used for small-scale refrigeration such as in laboratories and workshops, or in portable cooler, and foodstuff maintained near this temperature have an increased storage life.

**Sustainable cooling with thermal energy storage:**

Thermal energy storage (TES) is sometimes defined as a way of producing an energy sink or source, and provides methods and systems that allow storage of either cooling or heating produced at one period in time for later use at another period in time. TES results in two significant environmental benefits: (i) the conservation of fossil fuels through efficiency increases and/or fuel substitution, and (ii) reductions in emissions of such pollutants as CO<sub>2</sub>, SO<sub>2</sub>, NOx and CFCs [ref. 6].

Thermal storage can either take the form of sensible heat storage (SHS) or latent heat storage (LHS). Latent heat storage is accomplished by changing a material's physical state whereas SHS is accomplished by increasing a material's temperature [ref. 7].

Ice as (LHS) is one of the more common thermal storage materials used today. Ice provides one of the highest theoretical thermal storage densities (and, therefore, the lowest storage volumes). Ice systems have been shown to be excellent for smaller and even for some larger packaged installations [ref. 8].

The annual electricity consumption for air conditioning systems can account for over than 30%. Thus, stored energy for ice (focus on phase change) can be used instead of electricity when the demand for energy is high to reduce energy consumption in hot climates.

**II. THE RESEARCH GOAL:**

The goal of this research is to carry out a study of cooling system performance through a simple domestic air conditioning prototype by using the ice thermal storage capacity as an alternative method in air conditioning system for the following reasons:

1. To reduce the pollution and global warming by reducing the usage of oil fossil for producing electricity. With global warming, extremely hot weather may become more common, so, the ice thermal storage can provide potential solution for hot weather cooling issue [ref. 9], and avoid forced shutdown during hot weather.
2. To benefit from the lower electricity charge during night time, the ice thermal storage technology is an essential solution, where part of the electricity consumption during peak hours at mid-day could be shifted to off-peak hours at night [ref. 10].
3. It can be used to cool building spaces when the main electrical power is blackout.

**III. EXPERIMENTAL RIG DESIGN:**

An experimental rig was designed and fabricated for this research as shown in the schematic drawing and the experimental construction [figure 1] to represent a small prototype of a simple domestic air conditioning system using ice thermal storage to cool the air for small conditioned space with overall dimension of (3m X 2m X 2.8m height).

The unit has two parts, the first part is the cooling unit and the second is the power supply unit which includes a charger and battery.

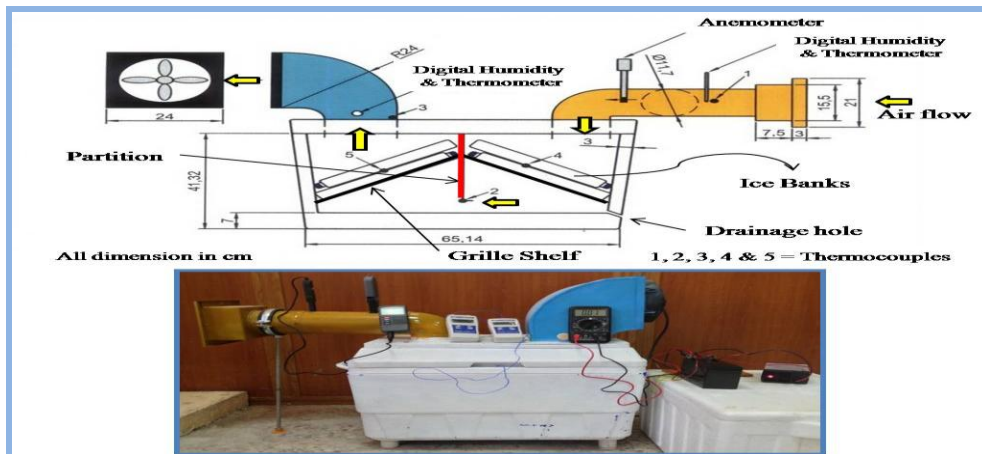


Figure (1): Schematic drawing & the Experimental rig of a simple domestic air conditioning.

### The cooling unit:

#### 1. The cooling box (container):

A plastic cold box of (60 X 40 X 50 cm) was designed and fabricated for the experimental study of this research as shown in the schematic drawing [Figure 1]. The box was partially divided into two chambers by using metallic plate (partition) without upper space in order to ensure that the cover is tightly closed to direct the air flow through a longitudinal lower space (passage) of about (50 mm) where the air flows through from the first to the second chamber.

Two grille shelves were placed in oblique position on both sides of the metallic central plate (partition), on each of them a bank of (11) ice contained in a thin sheet plastic bottles of (0.5 liter volume) to avoid direct contact of air with ice were placed and to be modeled as a component of a heat exchanger, these bottles are used to cool the air and reduce its humidity.

An opening draining hole of (12.5 mm) was made in one corner of the box to drain water that accumulates due to vapor condensation.

The box was lifted from ground by four legs, one of these legs is an adjustable leg to ensure that the condensate vapor to be accumulated at the draining hole to complete its draining out of the cooling box.

The box cover was fabricated with two opening on both sides to introduce two ducts, the first duct was made of galvanized plate with one end of rectangular cross section, its opening is square shaped of (240 x 240 mm), in which a fan is placed and fixed by screws at its end [figure 2].

The used fan is a DC motor has a maximum power of (80 Watt) and the working voltage is (12 Volt).



Figure (2): The air outlet duct and the used fan, the air inlet duct.

The second duct was made of plastic pipe (PVC) of (100 mm in diameter) and (600 mm length) ended by another diverging square shaped duct with grill made of galvanized sheet to produce uniform air flow [figure 2].

#### 2. Power supply unit:

This unit consists of two parts:

- a) The charger, which converts the electric voltage received from main circuit from (220V AC) to (14V DC) to charge the battery.
- b) The battery, it supplies electric power to the fan; the maximum obtained voltage is (14 Volt).

#### 3. The measuring instruments:

The measuring instruments used in this experiment are:

- 1- Two digital thermometers each of two thermocouple sockets in order to measure temperature in four positions [referring to figure 1]:
  - First thermocouple was connected to the first bank of ice bottles (4) which is insulated from the airflow.
  - The second thermocouple is connected to the second bank of bottles (5) which is insulated from the airflow.
  - The third thermocouple is connected to the central plate (2) to measure the temperature between the two ice banks.
  - The fourth thermocouple is connected to the duct at the cold air outlet (3).
- 2- Humidity meter: is placed in two positions, the first one inside the pipe to measure the RH, temperature (1) and dew point temperature of air entering the unit, the second one inside the duct fan to measure RH and the dew point temperature of the air leaving out the unit.
- 3- Air flow meter; to measure velocity of the air, it is placed inside the pipe at the air flow entrance.
- 4- Ammeter and voltmeter to measure the fan power consumed at different air flow passing through the experimental rig.

#### IV. THEORETICAL ANALYSIS:

To study the thermal energy system, it will consider in this paragraph the performance analysis of conventional domestic air conditioning using the ice thermal storage capacity.

To write down the energy balance for this system, the temperatures and the relative humidity and the dew point temperature of the contained vapor in the air flow were measured at different positions in the system, these positions are:

- The temperature and the relative humidity at inlet & outlet of air flow into the c box.
- The air mass flow rate ( $\dot{m}$ ) entering the system.
- The temperature of air flow between the two Ice banks.
- The consumed power of the fan by the ammeter and voltmeter.

The calculation can be done to find the required parameters and studying the performance of this system, by using the following formulas relating <sup>[ref. 11]</sup>.

##### 1) The Humidity Ratio:

To measure the humidity ratio of moist air ( $\omega$ ) which is the ratio of the mass of water vapor ( $m_w$ ) to the mass of dry air ( $m_a$ ).

$$\omega = \frac{m_w}{m_a} = \frac{R_a}{R_w} \cdot \frac{p_w}{p_{at} - p_w}$$

$R_a$  = the gas constant for dry = (0.2871) (J/kg.K)

$R_w$  = the gas constant for water vapor = (0.461) (J/kg.K)

$$\omega = 0.62198 \frac{p_w}{p_{at} - p_w}$$

##### 2) The Air pressure:

To measure the air pressure, the following equation is used:

$$p_a = p_{at} - p_w \quad \dots \dots Pa \left( \frac{N}{m^2} \right)$$

$p_w$  = vapor pressure at the dew point temp.

##### 3) The air mass flow rate:

The mass flow rate of the air passing through the system can be calculated by measuring the air volume of the air, which is equal to:

$$\dot{V} = A * v_{air}$$

Where:  $A$  = the cross-sectional area of the entrance pipe ( $m^2$ )

$$A = \frac{\pi}{4} * D_{pipe}^2$$

$D_{pipe}$  = the diameter of entrance pipe (m)

$v_{air}$  = the air velocity inside the entrance pipe (m/s).

The air mass ( $\dot{m}$ ) flow rate then can be calculated by using the following formula:

$$\dot{m} = \rho_m * \dot{V}$$

Where:  $\rho_m$  = the air density (mixture of dry air and vapor) .... (kg/m<sup>3</sup>)

$$\rho_m = \rho_a + \rho_w$$

$$\rho_a = \frac{p_a}{R_a * T}, \quad \rho_w = \frac{p_w}{R_w * T}$$

$\rho_a$  = the dry air density .... (kg/m<sup>3</sup>)

$\rho_w$  = the vapor density .... (kg/m<sup>3</sup>)

$T$  = temperature of dry air (°C)

##### 4) The Enthalpy of Moist air:

The moist air is a mixture of dry air and water vapor, so, the enthalpy of the moist air can be evaluated as:

$$h = h_a + \omega * h_w$$

where:  $h_a$  = the enthalpy of dry air (kJ/kg)

$h_w$  = the specific enthalpy of water vapor (kJ/kg)

$$h = h_a + \omega * h_w$$

$$h_a = C_{pa} * T$$

$$h_w = h_{g0} + C_{ps} * T$$

Where:  $h_{g0}$  = specific enthalpy of saturated water vapor at (0 °C), its value can be taken as (2500 kJ/kg).

In temperature range of (0 to 60 °C), the mean value of the specific heat of dry air ( $C_{pa}$ ) can be taken as (1.005 kJ/kg.K), and the specific heat of water vapor ( $C_{ps}$ ) can be taken as (1.88 kJ/kg.K), then the specific enthalpy of moist air ( $h$ ) is given by:

$$h = 1.005 * T + \omega * (2500 + 1.88 * T) \quad (kJ/kg)$$

**5) The Heat Loss by the air:**

When a moist air passing through a cooling or heating medium, it will loss or gain heat ( $Q$ ). That means there is a change in its state of temperature and content of water vapor (a change in the humidity ratio). It can be calculated as:

$$Q = \dot{m} * (h_2 - h_1)$$

Where:  $h_1$  = the enthalpy of inlet moist air (kJ/kg)

$h_2$  = the enthalpy of outlet moist air (kJ/kg)

Thus, the heat loss of air flow rate passing through a cooling system can be evaluated as:

$$Q = \dot{m} \{1.005 * (T_2 - T_1) + 2500 * (\omega_2 - \omega_1) + 1.88 * (\omega_2 * T_2 - \omega_1 * T_1)\}$$

And to calculate the average of heat removed ( $Q_{av}$ ) during any time of the cooling cycle, the trapezoidal rule can be used which states below:

$$Q_{av} = \frac{\Delta t}{t_c} * \left( \frac{Q_1 + Q_n}{2} + Q_2 + Q_3 + \dots + Q_{n-1} \right)$$

Where:  $\Delta t$  = the time interval (min)

$t_c$  = the period time of cooling (min)

**6) The System Performance:**

The system performance of a cooling system is expressed by the ratio of a useful heat gain to work done by the system, it is called as the coefficient of performance (COP), and it can be evaluated as follows:

$$COP = \frac{Q}{W}$$

Where:

$COP$  = coefficient of performance (dimensionless)

$W$  = the work done by the system ( kW )

The work done by the domestic air conditioning system in this project is equal to the power consumed by the working fan, and this power is equal to:

$$W = V.I$$

Where:

$V$  = the measured voltage of the power supply (Volt)

$I$  = the measured amperage to working fan (Ampere)

**V. RESULTS & DISCUSSION:**

The experiment's procedure was carried out to study the performance of the simple domestic air conditioning. The measuring values for the air flow velocity, temperatures, relative humidity, Dew point temperature and the power consumed by the working fan were measured by using ice packed in the bottles with a deep freeze temperature of ( - 6 °C) for two different air flowrate to make a comparison to study the effect on performance when the flowrate is altered.

Figure (3) shows the temperature variation through the cooling system for two different air flowrate [0.0321 and 0.0229 kg/s] with time for the air inlet temperature ( $T_1$ ), the air outlet temperature from the first ice bank ( $T_2$ ) and the air outlet temperature from the second ice bank to the outlet of the system ( $T_3$ ).

It was noticed from figure (3) that the temperature difference between inlet and outlet temperature is higher for low air flowrate (0.0229 kg/s) than for higher flowrate (0.0321 kg/s) due to more time of contact for the air with the ice blocks and this leads to better heat exchange between the air and ice block.

The figure shows too that the temperature leaving the first ice bank is highly decreased compared to the air temperature leaving the second ice bank. The difference is attributed to the fact that as the temperature difference decreases between the two heat mediums, this caused the transferred heat to be lowered as it is observed that for lower air flowrate ( $T_3 - T_2$ ) is lower than ( $T_3 - T_2$ ) for higher flowrate.

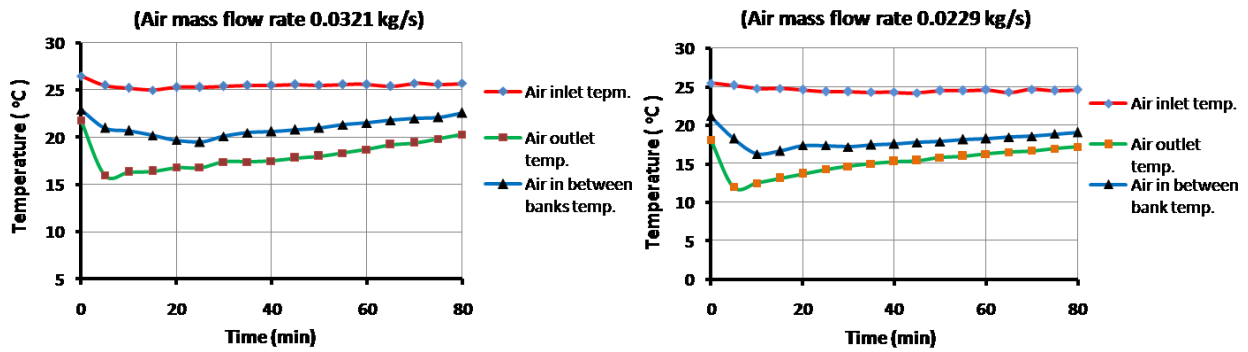


Figure (3): The graph showing the air temperature variation across the cooling system.

Figure (4) shows the vapor content variation of air at inlet and outlet for the cooling system for two different air flowrate, it shows the drop in vapor content with time at outlet as the air passes across the system. It is observed that more condensation occurs for the lower air flowrate (0.0229 kg/s) than for the higher air flowrate (0.0321 kg/s) due to more time of contact and better heat exchange between the air and ice block. As well, when a lower flowrate is used the heat loss of air is less and ice block will last and need more time to melt.

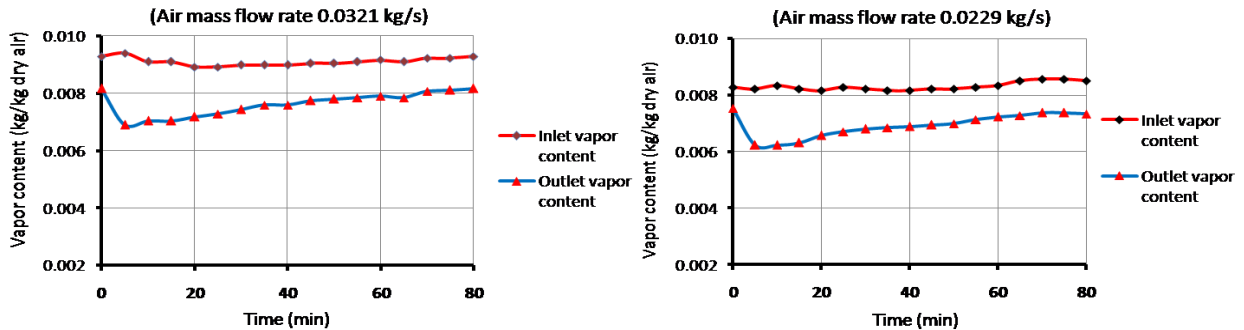


Figure (4): The graph showing the variation of air vapor content across the cooling system.

Figure (5) shows the heat loss of the air flowrate that is passing through the cooling system for the two different air flowrate with time, this heat represents the difference between the heat content of the entering air flow enthalpy ( $h_1$ ), and the leaving air flow enthalpy ( $h_2$ ) from the outlet of the cooling system. It is observed from figure (5) that the lost or removed heat from the air moving across the cooling system is decreased with lower air flowrate (0.0229 kg/s) than with higher air flowrate (0.0321 kg/s) because the air flowrate quantity plays as an active factor to dominate the increasing in heat exchange than increasing in temperature difference.

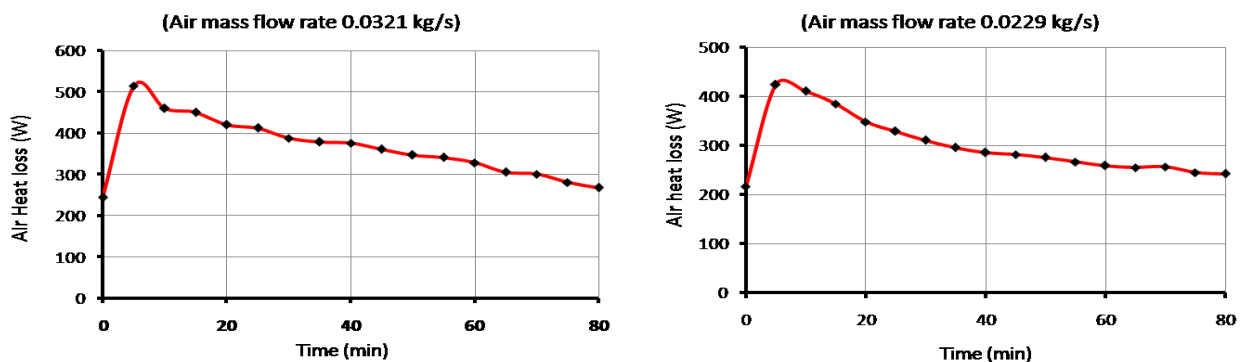


Figure (5): The graph showing the variation of the removed heat from the air with different flowrate.

Figure (5) shows too that the curve for the higher air flowrate (0.0321 kg/s) is steeper than the lower air flowrate which explains that with higher air flowrate the removed heat is faster than lower air flowrate (0.0229 kg/s), on contrary the curve for the lower air flowrate becomes flatter with time which means the heat is gradually removed from the ice pack of both banks.

Figure (6) shows the coefficient of performance (COP) for this cooling system. It is observed from this figure that the COP increases as the air flowrate is decreased; this is because as the air flowrate is decreased the fan consumes less power according to the fan third law.

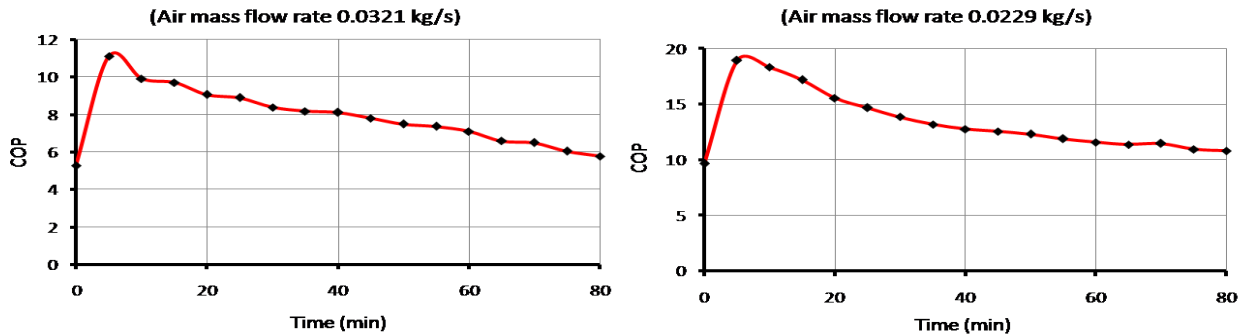


Figure (6): The graph showing the variation of COP of the cooling system with different air flowrate.

Figure (6) shows too that for higher air flowrate (0.0321 kg/s) the obtained COP has a maximum value of about (10) and it goes down with time, but for lower air flowrate (0.0229 kg/s) the obtained COP has a maximum value of about (19) and it goes down with time.

Figure (7) shows the average heat removed from the air with time for two different air flowrate. It is noticed from the figure that the average heat removed from the air is higher with higher air flowrate (0.0321 kg/s) which is approximately around (400 W) at the end of the test compared with lower air flowrate (0.0229 kg/s) which is approximately about (300 W) at the end of the test.

That means with lower air flowrate the ice pack will last and stand for more time to melt, whereas with high air flowrate the ice pack will melt faster but gives better heat removing to meet the heat demand for cooling.

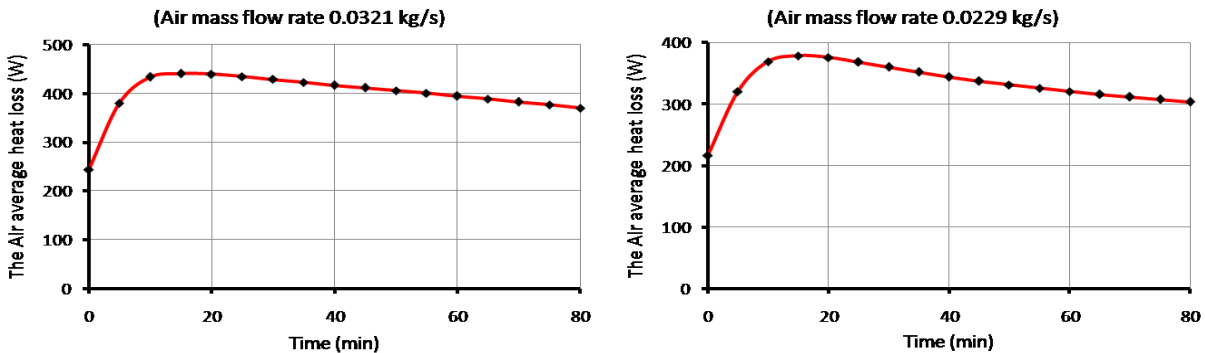


Figure (13): The graph showing the variation of average heat removed from the air with different air flowrate.

## VI. THE CONCLUSIONS:

As a conclusion, the results shows that the test carried out on this simple domestic air conditioning is a small prototype to simulate a bigger cooling system shows that using ice thermal storage capacity to decrease the cooling load on the cooling system at the on-peak time and in turn it will decrease the capacity of a cooling system for hot climate which means decreasing the system volume and for cooling a small spaces.

Beside what mentioned above, it will the pollution and global warming by reducing the usage of oil fossil for producing electricity, and to take the benefit of lower charge of electricity at the off-peak time.

It can be used too in developing countries where the electrical power is blackout at programmed time for shutting due to lake in electrical power supplying or at countryside and far away areas.

The COP of such systems will increase when the air flowrate decreases, but the removed heat (Q) will be less and with a lower air outlet temperature, in this case it needs more time to remove or absorb the same heat quantity from the cooling space, this point is open for discussion to balance between getting better COP or to meet the cooling load as fast as possible when using a cooling system using the ice thermal storage capacity.

## REFERENCES:

- [1] A. R. Trott, T. C. Welch, 2000 "Refrigeration and Air Conditioning", 3<sup>rd</sup> Edition, Butterworth-Heinemann, Reed Educational and Professional Publishing Ltd, Great Britain.
- [2] Ibrahim Dincer, 2003, "Refrigeration Systems and Application", John Wiley & Sons Ltd. England.
- [3] James, Peter; Nick Thorpe (1995), "Ancient Inventions", Random House USA Inc, United States.
- [4] George C. Briley, P.E., "100 Years of Refrigeration", A Supplement to ASHRAE Journal, November 2004. <http://www.ashrae.org/File%20Library/docLib/Public/ASHRAE-D-22923-20050105.pdf>
- [5] Lloyd Alter, "Natural Refrigeration; Collecting Ice in China", Clean Technology, January 15, 2007. <http://www.treehugger.com/clean-technology/natural-refrigeration-collecting-ice-in-china>.
- [6] Robert E. Wilson, Peter B. S. Lissaman, "Natural Refrigeration", National Science Foundation, 1974. [http://wind.nrel.gov/designcodes/papers/WilsonLissaman\\_AppAeroOfWindPwrMach\\_1974.pdf](http://wind.nrel.gov/designcodes/papers/WilsonLissaman_AppAeroOfWindPwrMach_1974.pdf)
- [7] Ibrahim Dincer, "The Role of Thermal Energy Storage System in Sustainable Development". [http://intraweb.stockton.edu/as/energy\\_studies/content/docs/FINAL\\_PAPERS/6A-3.pdf](http://intraweb.stockton.edu/as/energy_studies/content/docs/FINAL_PAPERS/6A-3.pdf)

- [8] Kenneth Ip PhD MSc MCIBSE CEng, Jonathan Gates BSc, "Thermal Storage for Sustainable Dwellings". <http://freespace.virgin.net/m.eckert/final%20maastricht.pdf>
- [9] Lucas B. Hyman, P. E., Leed AP, 2011, "Sustainable Thermal Storage System, Planning, Design and Application", McGraw-Hill Education: New York.
- [10] Haihua Zhao, Hongbin Zhang, Phil Sharpe, Blaise Hamanaka, Wei Yan, WoonSeong Jeong, "Ice Thermal Storage System for LWR Supplemental Cooling and Peak Power Shifting", Proceedings of ICAPP '10 San Diego, CA, USA, June 13-17, 2010. <http://www.inl.gov/technicalpublications/Documents/4502635.pdf>
- [11] Y. H. Yau, S. K. Lee, 2010, "Feasibility Study of Ice Slurry – Cooling Coil for HVAC and R Systems in a Tropical Building", Elsevier Ltd Applied Energy ISSN: 03062619 Year: 2010 Volume: 87 Issue. <http://libhub.sempertool.dk.tiger.sempertool.dk/libhub?func=search&fromSimpleSearch=1&query=Feasibility+Study+of+Ice+Slurry+%E2%80%93+Cooling+Coil+for+HVAC+and+R+Systems+in+a+Tropical+Building>
- [12] W. P. Jones, 2001, "Air Conditioning Engineering", 5<sup>th</sup> edition, Elsevier Science & Technology Books, USA.

## Design of A network Data Security Circuit

<sup>1</sup> Nuha Abdelmageed Tawfig Khalil, <sup>2</sup> Abdelrasoul Jabar Alzubaidi,

<sup>1</sup> Computer Department, Aljouf University, Sakaka – Saudi Arabia

<sup>2</sup> Electronics Engineering School, Sudan University of Science and technology, Khartoum – Sudan

### Abstract

To safeguard information during electronic communication and data transmission processes across unsecured networks and provide security requirements, including authentication, confidentiality, integrity and non-repudiation. To achieve this goal, this paper proposed to design of a network data security circuit using two Basic Stamp2 Microcontroller, two wireless X-Bee modules, two computer and BASCOM language (TC++ program language ) to generate non-standard algorithm ( logic algorithm ) for encrypted and decryption. The algorithm depends on ciphering the plaintext n times with n keys.

**Keywords:** Basic stamp2, ciphertext, Decrypted, Encryption, Network data security, plaintext, and X-Bee.

### I. INTRODUCTION

Security of network communications is arguably the most important issue in the world today given the vast amount of valuable information that is passed around in various networks. Information pertaining to banks, credit cards, social security numbers, personal details, and government policies are transferred from place to place with the help of networking infrastructure. The high connectivity of the World Wide Web (WWW) has left the world 'open'. Such openness has resulted in various networks being subjected to multifarious attacks from vastly disparate sources, many of which are anonymous and yet to be discovered. This growth of the WWW coupled with progress in the fields of e-commerce and the like has made the security issue even more important.

A typical method for security that is used To safeguard information during electronic communication and data transmission processes across unsecured networks and provide security requirements is encryption [1].

Encryption is the process of encoding messages (or information) in such a way that cannot be read by eavesdroppers or hackers, but that authorized parties can. In an encryption scheme, the message or information (referred to as plaintext) is encrypted using an encryption algorithm, turning it into an unreadable ciphertext. This is usually done with the use of an encryption key, which specifies how the message is to be encoded. An authorized party, however, is able to decode the ciphertext using a decryption algorithm, that usually requires a secret decryption key [2].

Implementing a demonstration project comprise of BASIC Stamp microcontroller, two wireless X-Bee modules, two computer and BASIC Stamp Editor v2.5 and Bascom language (TC++ program language) to protect information during electronic communication and data transmission across unsecured networks and most importantly to prevent data from falling into wrong hands.

### II. METHODOLOGY

Design of a network data security circuit consists of two elements:

#### A. Hardware components:

The hardware components for this research paper consists of Parallax, Inc.'s BASIC Stamp2 modules, X-Bee wireless modules and computer. Upon using all this materials, a transmitter and a receiver circuit will be build.

#### Microcontrollers

Microcontrollers are frequently used device in embedded computing in which the application varies from computing, calculating, smart decision-making capabilities, and processes the data. Most of the electrical/electronic device, sensors and high-tech gadget can be easily interface and interact with microcontrollers to automate a system structure. For this research BASIC Stamp2 is used [3].



**Computer**

To program the Basic Stamp2 with the windows interface, an IBM PC or compatible computer system the following components is needed [7] :

- IBM PC or compatible computer running windows 95, windows 98, or windows NT4.0 (S.P.3 recommended).
- 80468 (or greater) processor.
- 16 MB RAM (24 recommended).
- 1 MB free hard drive space.
- 256-color VGA video card (24 bit SVGA recommended).

**D25 connection**

The D25 connection used to connect Basic Stamp2 to computer parallel port for programming.

**B. Software:**

For this research there are two main softwares being used BASIC Stamp Editor v2.5 and Bascom language (TC++ program language ).

- BASIC Stamp Editor v2.5, used to program the Basic Stamp2 microcontroller.
- Bascom language (TC++ program language ) , used to write non-standard algorithm ( logic algorithm ) for encrypted and decryption.

The circuit design for this research is divided into two parts namely the transmitter and the receiver circuit. The interconnection for the transmitter and the receiver circuit are shown in Figure 3.

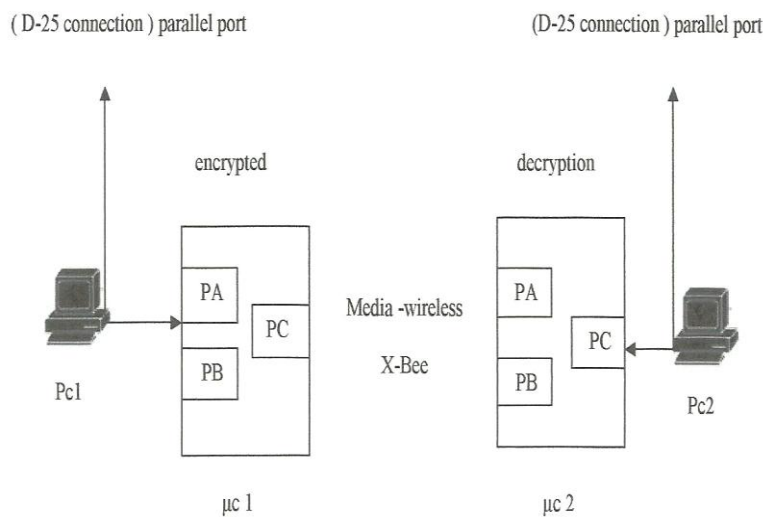


**Figure 3 : block diagram for the circuit**

In the transmitter circuit the message will be encrypted m times depending on the length of the key. The key will be converted to equivalent ASCII code. In this algorithm key will be inserted into the encrypted message after any encryption stage to form the new message for the next encryption stage. This process will be repeated m times. The number of the encryption stages will be given depending on the length of the key.

In the receive circuit the message will be decrypted by used the inverse method for encryption.

**III. RESULTS**

The flowchart of the program of the design of a network data security circuit is shown in Figure 4.

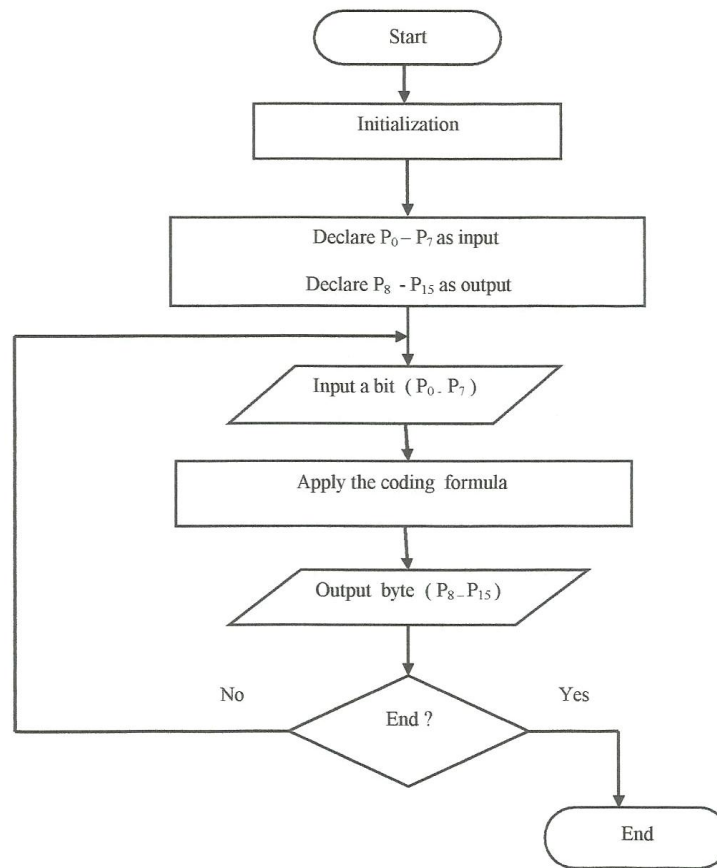


**Figure 4: flowchart of the program of the design of a network data security circuit**

#### IV. CONCLUSION

Design of a network data security circuit is the most important system to enhance security in transmission of data in network, to prevent data from falling into wrong hands and to provide the data security requirements, including integrity, authentication, non-repudiation and confidentiality. Design of a network data security circuit includes the following advantages:

- 1- Encrypted the message by using non-standard algorithm.
- 2- Very complicated because it encrypted and decrypted the message m times.

#### REFERENCES

- [1.] A Novel Scheme for Secured Data Transfer Over Computer Networks, Rangarajan Athi Vasudevan (University of Michigan, Ann Arbor, USA ranga@umich.edu). <http://arxiv.org/ftp/arxiv/papers/1002/1002.4530.pdf>.
- [2.] <http://en.wikipedia.org/wiki/Encryption>.
- [3.] International Symposium on Robotics and Intelligent Sensors 2012 (IRIS 2012), Wireless Traffic Light Controller for Emergency Vehicle through XBee and Basic Stamp Microcontroller, R.Hussin\*, R.C.Ismail, E.Murrari, A.Kamarudin, School of Microelectronic Engineering, University Malaysia Perlis (UniMAP), <http://www.sciencedirect.com/science/article/pii/S187705812026239?np=y>
- [4.] Basic Stamp 2 microcontrollers comparisons. Retrieved April 28, 2012 from [http://www.parallax.com/detail.asp?product\\_id=BS2-IC](http://www.parallax.com/detail.asp?product_id=BS2-IC) website of Parallax. Inc. developer and distributor of Basic Stamp 2 microcontroller.
- [5.] <http://www.parallax.com/BASICStampComparison/tabid/436/efault.aspx>.
- [6.] Basic Stamp 2 microcontrollers. Retrieved April 13, 2012 from <http://www.parallax.com/go/XBee> website of Parallax. Inc. developer and distributor of Basic Stamp 2 microcontroller.
- [7.] <http://books.google.com.sa/books?id=sQ9AigIIOkC&pg=PA41&dq=connect+basic+stamp+2+with+computer+by+parallel+port&hl=ar&sa=X&ei=2llpUqv0Aeno4gTZ34CICQ&ved=0CC4Q>.

# Key pad Based Online Examination System

S.G.Pardeshi<sup>1</sup>, K.S.Jadhav<sup>2</sup>

1. Government College of Engineering, Aurangabad, Maharashtra.

## **Abstract:**

Area of compact handheld devices using embedded system is attracting embedded designers nowadays. This paper present such one handheld embedded device which can be used for online examination system. This device is designed using microcontroller, keypad, LCD & RF transmitter and receiver. In present systems to conduct online examination system one desktop PC per candidate have to be used. This embedded device can be used to conduct online examination with only one desktop PC. Also the main objective of this On-line Examination System is to efficiently evaluate the candidate thoroughly through a fully automated system that not only saves lot of time but also gives fast & accurate results without using number of computers.

**Keywords:** Microcontroller, RF communication, Keypad

## **I. INTRODUCTION**

The purpose of On-line Examination System is to take online test in an efficient manner and with no time wasting for checking the paper.

These systems combine wireless handheld keypads with LCD Screen and master computer. When used by a skilled moderator, these systems create an interactive environment that can inspire honest feedback and generate quality data that can be instantly sorted in myriad ways. After the computer receives the group's input, the results are tallied for immediate display to the moderator, group members, and/or observers. This avoids data entry errors that can occur when converting paper information into electronic files. Using wireless keypads instead of computers for every student ("all those in increasing cost of examination...") allows a participant to respond anonymously, which may encourage more thoughtful and honest responses.

The purpose of the system is to develop Online Examination System., used to test the Domain knowledge of the students, and employees with respect to the particular technology. The manual procedure used for conducting exam is time consuming process and error prone due to human limitations. The System purpose is to completely automate the old manual procedure of conducting exam. It is very essential for an Institute to handle the Examinations and their results.

## **II. PREVIOUS WORK**

### **2.1 Current System**

The Current system of examinations is highly complicated and expensive. Whenever exams are to be conducted there are various tasks that have to be done again and again

- Setting question paper
- Checking for errors
- Printing question papers
- Scheduling Exams
- Conducting Exams
- Checking Answer Papers
- Preparing Result Charts
- Solving Question Papers

Online Examination System using Touchpad is known in the industry by many names including audience response system, interactive voting pads, audience voting keypads, and clickers. These handheld or wearable electronic devices quickly record member answers to questions during a exams, meeting, training, and survey activities. You'll find devices in conferences and seminars for opinion polling, benchmarking, and speaker feedback. In corporations for strategic planning and decision making and to share voting.

### III. PROPOSED SYSTEM HARDWARE

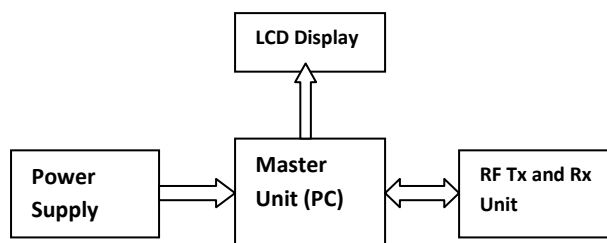


Figure 1 (a): Master Unit Block Diagram

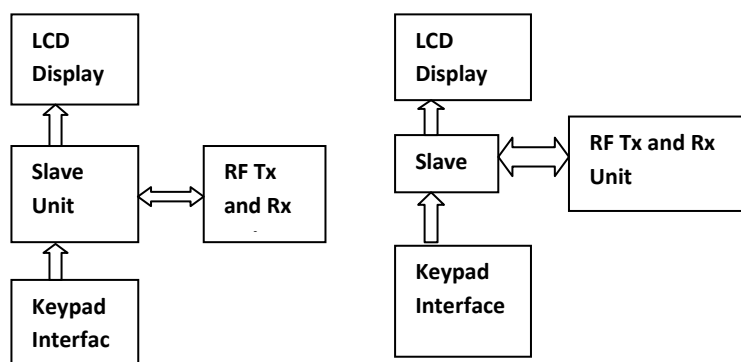


Figure 1 (b): Slave Unit Block Diagram

**Figure 1: Answering-pad Based Online Examination System**

#### 3.1 Master Unit

**3.1.1. RF Transmitter and Receiver:** It is a rate of oscillation in the range of about 3 kHz to 300 GHz, which corresponds to the frequency of radio waves, and the alternating currents which carry radio signals. RF usually refers to electrical rather than mechanical oscillations, although mechanical RF systems do exist (see mechanical filter and RF MEMS). Although radio *frequency* is a rate of oscillation, the term "radio frequency" or its acronym "RF" are also used as a synonym for radio – i.e. to describe the use of wireless communication, as opposed to communication via electric wires.

**3.1.2. Master Computer:** It consists of a Master computer which is connected to Internet for sending and receiving of the questions and answers. It is used for sending the data (Question Paper) to Slave Unit and also receiving the final data from the Slave Units.

**3.1.3 Power Supply Unit:** This block is used to produce a power supply of about +5V.

**3.1.4 LCD Display:** It is used to for Result display purpose.

#### 3.2 Slave Unit:

**3.2.1 Microcontroller:** ATmega32A microcontroller is used as controller of slave Unit.[3] It is CMOS,RISC, AVR ATmega32 8-BIT Microcontroller which is having In-system Programmable with Flash code storage, re-programmable up to 1000 times, 32 working registers, single clock cycle execution giving up to 1MIPs/MHz[2]

**3.2.2 GLCD:** This is a smaller version of our serial graphic LCD. The Serial Graphic LCD backpack is soldered to the 128x64 pixel GLCD and provides the user a simple serial interface to a full range of controls.[2] Besides writing text, this serial graphic LCD allows the user to draw lines, circles and boxes, set or reset individual pixels, erase specific blocks of the display, control the backlight and adjust the baud rate.[3]

**3.2.3 RF Transmitter & Receiver module:** It is a true single-chip transceiver, It is based on 3 wire digital serial interface and an entire Phase-Locked Loop (PLL) for precise local oscillator generation .so the frequency could be setting. It gives 30 meters range with onboard antenna. It is al Low power consumption IC.This module is used in this system to establish wireless communication between slave & master to exchange question-answers. [4]

### 3.3 Working

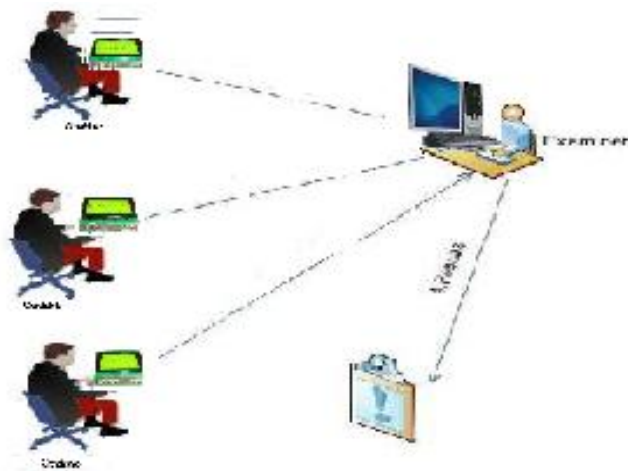


Figure 2: Working of System

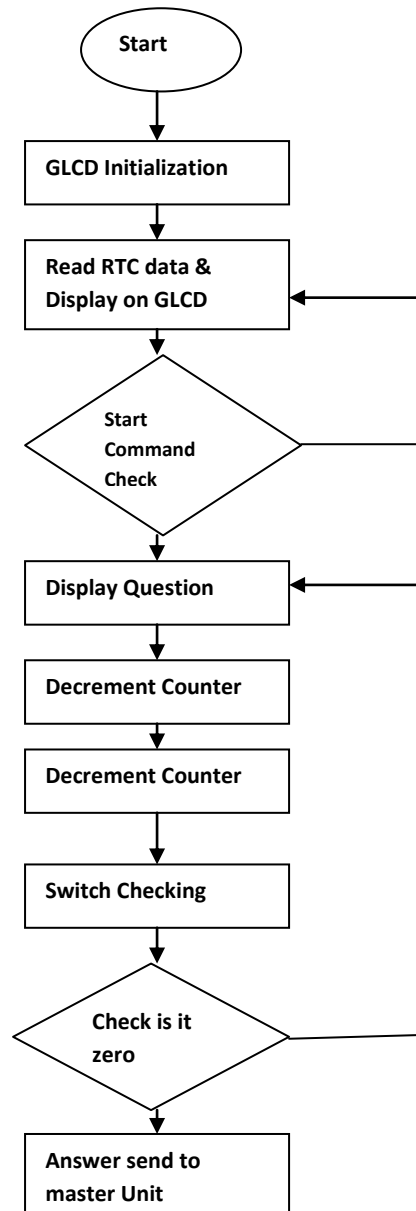
1. All the question paper sets will be stored in a Master Computer via Internet, from this Master computer it will be send to the Slave unit as per the prescribed time before the start of examination.
2. Initially there is no display of questions on the GLCD unit of Slave, after start command given from Master unit the Slave unit will turn on.
3. Then different set of objective questions with options will arrive as per the sequence on different Slave unit.
4. As the time starts the candidate will start solving the questions, at a time only one question will appear.
5. There are four buttons given on the device A, B,C,D by pressing the particular button the candidate can select the answer.
6. If the candidate wants to preview the previous question then by using the preview button he can go to the previous questions.
7. If the candidate wants to proceed with the question then by using the next button he can proceed with the questions
8. After time-up Master Unit will request Slave Unit to send the data.
9. Then all the data will appear at the Master Unit within few seconds, only one Slave will send the data at a time.
10. Simultaneously Master unit will start analyzing the answers with the standard format stored in it.
11. After completion the Master unit will display the result within some time.

### 3.4 Utilities

It includes:-

- Skip and come back to the question afterwards if needed.
- Displays the selected answer of attempted questions and can go to next or previous question and can either attempt or change the answer of the already attempted question.

## IV. SOFTWARE- FLOW CHART



## V. RESULT

Examination will start on every slave device only after receive command from master. Then each candidate has to enter his name and examination seat number on master pc. After completion of registration procedure candidate's examination time start & each question will be displayed sequentially as per the set for each slave.



Figure 3: Handheld Device (Slave Unit)

As shown in above Display each question is displayed with four objective answers Viz. A, B, C, D. Candidate has to submit one option and has to press *NEXT* switch for next question. Candidate can return to the previous question by pressing *PRV.* Switch.

## **VI. CONCLUSION**

An Answering-pad Based Online Examination System allows large groups of people to vote on a topic or answer a question. Each person has a device with which selections can be made. Each remote communicates with a computer via receivers located around the room or via a single receiver connected to the presenter's computer using a USB connector. After a set time – or after all participants have answered – the system ends the polling for that particular question and tabulates the results. Typically, the results are instantly made available to the participants via a bar graph displayed on the projector. An online Examination system forms the lifeline of the Educational Institutes to the functioning of the examination.

## **REFERENCE**

1. Li Jun, "Design of Online Examination System Based on Web Service & COM", The first International Conference on Information & Engineering", ICISC-2009.
2. Muhammad Ali Mazidi, Janice Gillispie Mazidi, Rolin McKinlay," The 8051 Microcontroller and Embedded Systems Using Assembly and C 2nd Edition (Paperback), Pearson Publication 2007.
3. Atmel Datasheets,"8-bit Microcontroller with 32Kbytes In-System Programmable Flash, Atmega32, Atmega32L", www.Atmel.com/Images/doc2503.pdf.
4. Devendra K. Mishra," Radio Frequency & Microwave Communication Circuit", Wiley Publication, 2004.

## Connectedness of e-Service Quality, e-Satisfaction and e-Loyalty. A Configuration Analysis with QDA Software.

Nanis Susanti<sup>1</sup>, Surachman<sup>2</sup>, Djumilah Hadiwidjojo<sup>3</sup>, Fatchur Rohman<sup>4</sup>

Department of Management, Faculty of Economics & Business, Brawijaya University, East Java, Indonesia

### ABSTRACT:

Marketing strategy of e-business should be adjusted to ensure that the customer is ready to make transaction online. This adjustment is primarily intended to foster customer trust related to privacy and economic risk. E-Trust in B2C e-commerce is more difficult to realize than an offline business. Gaps in e-Trust still exist, how the service without face to face interaction can logically satisfy. The perceptions of e-Service Quality can grow through Technology Readiness as well as Technology Acceptance, but e-Trust is more decisive in shaping of the service quality perception. This study aims to discover the customer's perspective on e-Service Quality and to analyze its relations with e-Satisfaction and e-Loyalty. Text corpus of satisfied customer review from the online store is used as the unit of hermeneutics analysis to reveal meaningful reviews. Purposive text sampling with detail in content and context is used to obtain a complete answer to the research question. MAXQDA11 software is used for the configuration analysis process on the connectivity among themes. The perspectives of e-Service Quality are discovered through Fun Shopping theme which is determined by: shopping experience, ease shopping, shopping problem handling and functional satisfaction. Customers' satisfaction perspective is the emotional e-Satisfaction through the emotional satisfaction in online shopping and the delight from family values. The fellow care and special attention are the value delivered by the company. Perspectives on e-Loyalty drawn from Loyal to Each Other: customer loyalty commitment, customer loyalty proof, and customer service staff dedication to serve. The perspective of e-Loyalty is determined by the e-Trust which is reflected from the themes of mutual trust (Trust Each Other). That is customer recognition to customer service team performance and recognition of the company's reputation offset with the company's trust to the customer.

**KEYWORDS:** Configuration Analysis, Customer Review, e-Satisfaction, e-Service Quality, e-Loyalty, e-Trust, Word of Mouse

### I. INTRODUCTION

Positive Word of Mouth is a shopping experience that is shared by satisfied customers to other people. In the era of Internet, WOM spread more widely and quickly through social media such as facebook, email, blog, twitter and others, so that it crosses the geographical boundary. Additionally, WOM activity in the internet can be stored for a long time because the messages are recorded on the medium used for sharing information. E-WOM is word of mouth via the Internet and *World of Mouse* is a term that is used for e-WOM [1]. Information spreading via Internet is very vast and it is able to penetrate the boundaries of place and time rapidly compared to offline. Customer review is the one of *Word of Mouse* platform. Nowadays consumer behavior has changed, especially in *Word of Mouse* activities. Rating system or product review to service quality or satisfaction in online shopping can take place instantaneously through a computer mouse device to the Web site. The availability of *Word of Mouse* is the valuable customers' voice data base. Several studies utilize this data base e.g. who investigated the behavior online customer in online feedback forums about dissatisfaction with *frequent-flier programs in the air industry* [2], investigated the importance of *listen in* conversations in social media discussion forum: *discussion forums, blogs, social networks, mainstream news, wiki, video and review sites*) to conclude the brand sentiment [3]. Internet Marketing minimizes transaction time, closeness the distance and place: "One of the best ways to initiate or to extend export activities used to be to exhibit at an overseas trade show. With the Web, it is not even necessary to attend trade shows to show one's ware. Electronic communication via the Internet is extending the reach of companies large and small to worldwide markets." [4]

## II. THEORY

### 2.1. e-Service Quality, e-Satisfaction and e-Loyalty

At the beginning of the online retail presence, Web performance and low prices will spur success. But regardless of the low price offers, they are not able to fix the issues of quality of service and frequently occur: the consumer canceled the transaction, the product is not delivered on time or even not sent, emails not replied, and the desired information cannot be accessed [5]. Customers are ready to pay higher prices for online shopping as long as they can see some values obtained for instance comfort, exclusivity, etc. [6] Quality of service is a prerequisite for determining customers' satisfaction and loyalty. Satisfied customers show their loyalty by repurchasing and doing WOM. In reality, there is doubt among many Internet users to conduct transactions in the Web, especially because of the privacy and trust towards Internet [7]. In general, the e-Service Quality is still low [8], customer dissatisfaction is encountered more in an online securities brokerage service [9]. In the context of online shopping, has conducted a review and synthesis of the literature on service quality delivery through Web sites and generate [10] four-dimensional conceptualization of core e-SERVQUAL (1) efficiency (2) reliability (3) fulfillment (4) privacy. Also, a three-dimensional quality of the particular online service recovery e-SERVQUAL is developed: (1) responsiveness (2) compensation (3) contact. A review and synthesis of 25 studies over the period 1996 to 2008 and establish eight scales of measurement of e-Service Quality [11]: (1) Web site design (2) personalization (3) empathy. There are five dimensions similar to those expressed by Zeithaml et al. (2002): (4) reliability (5) responsiveness (6) security (equal to the dimension of privacy), (7) fulfillment (8) information (equal to efficiency).

Important things considered by each researcher above is: the importance of the empathy dimension, that although there is no face to face interaction in the process of online services, some human contacts included in online services, such as e-mail communications [12]. The availability of individual customer attention shows empathy to customers. Some attributes of empathy dimensions expressed are: (1) good personal attention (2) adequate contact (3) address complaints friendly (4) consistently courteous. On the other hand, has built a proposition that connects Technology Readiness and e-Service Quality on E-Shopping Behavior. [13] The propose that the Technology Readiness of customer (customers' TR) will be a positive influence on the online Service Quality (e-SQ) perception, and these perceptions will positively influence the behavior of online shopping (e-SB). From these two concerns, researcher depict that Internet technology could replace the human absenteeism in Customer Service process, but technology should more concern in the two-way communication, with paying attention to the psychological aspects.

### 2.2. e-Trust

Some studies also relate the Satisfaction - Loyalty to e-Trust dimensions. There was a relationship between e-Trust with intention to shop online. The fulfillment of privacy enhance trust towards Internet, which is the feeling of free from specific threats such as citations or personal data theft, data misuse and computer viruses [14]. Six companies observed base on customer text comments (500-1000 characters) and customer rating. This observation conclude that e-Trust in B2C e-commerce is more difficult to realize than offline business, due to the presence of retailers in cyberspace that often face consumer views which are not too obvious or clear. Gaps in the consumer trust still exist, how e-tailer as "Strangers" can logically be expected [15]. From both of the studies, it is clear that e-Trust is a very important factor. Perceptions of e-Service Quality can grow through Technology Readiness, but the e-Trust seems to be more influential in shaping the perception of quality, and privacy is the dominant factor that shapes customer's trust.

### 2.3. e-WOM (Word of Mouse)

Internet is a medium that juxtaposes interpersonal relationships in terms of the absence face to face interaction and there is distance obstacle. Online interactions mostly appear in written forms, take place within the framework of direct communication (*real time*) or as an indirect interaction (*delayed*); but in this form, Internet has changed the act of writing into speech [16]. e-WOM are very open and easily accessible to Internet users. To obtain the data of e-WOM, this research utilizes an American Web sites by considering [17]: that secondary data required and easily available in the U.S. or Europe; tend to be not available or difficult to obtain outside the U.S., particularly in Asia and developing countries". Zappos.com, *an American online shoe store*, stores thousands of customer review data base that is easily accessed and downloaded. The text review is descriptive, and it describes the plot in detail. Researchers used the data of 15-month period (January 2011 to March 2012). A research that is using data provided by other parties described in Myers (2009:153) as same as using interviews or observations, to collect the data may also obtain data from the document.

Furthermore, it was stated that a document such as email, blog, webpage, corporate records, newspapers, and photographs depict things said or things that happen. It was also said that this document

provided facts or evidence in building a more complete picture than those provided only through interviews or observation. Internet is a vast medium, influential, and without obstructions. Internet is a very large database and can be scanned (observed), which provide a wide range of meaning or significance in individual communications or communications that present publicly [18]. Researchers use online customer review text as the primary data research is in line with the general definition of the document as "a written text" and should be studied as a social product [19]. By comparing some of the research findings in the context of offline and online shopping; the diverse of shopping motivations, the main dimensions of service quality, and gaps in the research results in explaining the phenomenon of online customer satisfaction and loyalty are reflected. This gap enables more efforts to discovering *Noema* (what is behind the phenomenon) in online customer satisfaction and loyalty deeper. Thus we need to understand what is presented or discussed by the online customer shopping experiences, about their satisfaction and loyalty more deeply. This understanding can be done by exploring the *Word of Mouse* in customer review text. Customer opinion in a product review on the Web site is the embodiment of *the Word of Mouse*, contains rating of good or bad with general comments; usually used the word choises for emphasis in assessing the quality of the product, often seen there is a strong expression of emotions verbally (through choice of words) or non-verbal cues (*orthographic*): capital letters, punctuation [20]. The importance of *customer review* for online customers is described by some researchers: (1) the feeling level of review readers, caused by the power (*valence*) of a review (2) when the readers feel the *resonance* of the reviewer, they assume that such reviews more trustworthy and useful, and give greater influence over their purchase intentions [21]. The depth and content of the information (*content* and *context*) of a review significantly affect consumer perceptions of source credibility and their intention to purchase decisions [22]. The depth of the reviews (*reviews depth*) has a positive and significant effect on the benefit of a good review both for *experience goods* and *search goods* [23]. The positive *Word of Mouse* may reduce the risk of purchase, increase the perception of the company, develop a psychological condition (e.g. relief), and fix interest in purchasing [24].

### III. METHODOLOGY

Exploration and explanation of this research reveal and explain the customer's perspective of e-Service Quality, e-Satisfaction and e-Loyalty. Exploration conducted on the customer's expression conveyed in a written form in the customer review text. The discussion associated with the phenomenon of online shopping, especially for product that has two categories at once. Shoes have both search product and experience product category in apparel product lines. This study uses data customer downloaded from the online web store Zappos.com (USA). Interpretive analysis conducted on the online customer's perspective which is written in the text of customer reviews. The purpose of the study is to explain the connectedness between e-Service Quality, E-Satisfaction and e-Loyalty. Interpretive analysis of the e-WOM data in the form of *customer* text produces main themes of research focus: e-Satisfaction and e-Loyalty.

Population is 1057 collection of text (*text corpus*) of customer review in January 2011 to March 2012 period (15 months) available in the Zappos.com Web site. Samples are text of customer reviews which meet the content and depth. According to the research conclusions of [25] that interest of borrowing books in the library is significantly affected by the length of the sentence read in the book reviews online. Also, it is concluded that book review depth (*rich lexical content*) will increase the intention to borrow books. Researchers have conducted initial observations that many customer reviews consist of many sentences and contain the depth of various customer expressions about their shopping experience. Initially all the text to be converted into Word format, *Times New Roman style, font 12*, with normal margins (*left and right 2.5 cm*). There is a text classification for 1057 customer review text based on the number of lines in each text as below:

TABLE 1. TEXT CLASIFICATION (BASE ON ROW NUMBER)

Category (row number)	January – June 2011	July – December 2011	January – June 2012	Number of Texts
1-5	476	156	48	680
6-10	142	87	47	276
11-15	36	16	12	64
>15	18	12	7	37
<b>Total</b>	672	271	114	1057

Source: Data Process

Raw data of social scientists consist of the meaningful words, not structured from human being fellowship. The characteristics of these social sciences are sometimes described as the double hermeneutic, 'subject' of social researcher and acts as an interpreter to the social situation of the society that is being studied [26]. Hermeneutic endeavor is to reveal the phenomenon through the *back and forth process* related to the whole text. Interpretations are continued to be improved as there are more text tackled by the researchers [27].

This research use data analysis steps of [28] stated that ideally, with an intellectual analysis and interpretation, raw data is processed and refined, summarized into meanings. Then it can then be presented in the form of a theoretical concept that brings new understanding through a process of refinement. The process of inductive logical reasoning, observation of individuals constructed in order to make a more general statement about the phenomenon. The sequences of qualitative data analysis are as follows: 1) *Coding* 2) *Noting* 3) *Abstracting and comparing* 4) *Check and Refinement* 5) *Generalizing* 6) *Theorizing*. There were a number of perceived obstacles that is the obstruction of the scope of qualitative approaches in the marketing research. These four scopes are characterized [29]: 1) The volume of data 2) Analysis complexity 3) Detail of classification records and 4) The speed and the flexibility of analysis. To overcome this problem, researchers use MAXQDA11 [30] software to process, organize, store, and display the output and to analyze the data. The data configuration simulation is conducted to see the connectedness between the themes. This configuration is very important to deal with the above constraints. Researchers utilize options in the software worksheet to describe the connectivity between themes and formulating propositions.

### 3.1. Step of Data Processing By Software MAXQDA11

Data processing by using *software* is able to provide an accurate theme-setting process, because code (label) on the themes recorded in the *software* system, so it can efficiently be displayed at any time. As well as to fix the code determination on a meaningful statement. The process which is recorded in a *software* system is able to produce summaries and data processing display efficiently. The outputs generated from data processing are as follows:

1. Table of the theme frequency
2. The connectedness Matrix and Chart of themes (*code relation matrix*) - (14x14 theme in this study)
3. Configuration table among themes (up to 5 themes) that describes connectedness (frequency) between the specified themes. Configuration table is used as the basis for preparing the premises.
4. Table of data (customer review text) which is included in the configuration. This table is used to construct the connectedness of meaningful statements of related review text, subsequently forming the premises.
5. Recap of all meaningful statement which are very helpful to establish propositions

The data processing are as follows:

1. Importing the entire text (35 customer reviews)
2. Inputting the 14 codes (Table 2) to the themes that have been estimated in early reading and understanding of customer review text.
3. Reread the texts and confirm the meaningful reviews in every segment of the text.
4. Displaying and printing the output of data processing required
5. Simulation of the themes on Configuration.

## IV. RESULT

The research question answered is present in Table 2. Perspectives of e-Service Quality are answered through the themes pleasant online shopping (shopping experiences, practical shopping, shopping problem handling and functional satisfaction). Customer perspective about satisfaction is the *emotional* e-Satisfaction that is the emotional satisfaction of online shopping and family values (caring about each other/ special attention) that provides excitement, happiness. Perspectives on e-Loyalty is the emergence of the theme of loyalty commitment, loyalty and dedication of proof serve by a team of customer service. Perspectives of e-Loyalty is determined by the e-Trust which is reflected from the theme of the recognition of the customer service team performance, recognition of the company's reputation and the trust company to the customer. There is a two-way connectivity both within trust and loyalty, namely the emergence of the theme of company trust (online store) to the customer and dedication to serve as company loyalty to customer. These findings are clasified as mutual trust and loyalty.

**Table 2. Theme (Code)**

No.	Theme	Perspective
1	Shopping Experience (Fu1)	e-Service Quality
2	Ease Shopping (Fu2)	
3	Shopping Problem Handling (Fu5)	
4	Functional Satisfaction (Fu3)	
5	Emotional Satisfaction (Fu4)	Emotional e-Satisfaction
6	Happiness (Fa1)	
7	Joyness (Fa2)	
8	Fellow Care (Fa3)	
9	Recognition of Customer Service Performance (T1)	e-Trust (Trust Each Other)
10	Recognition of Company Reputation (T2)	
11	Mutual Trust (T3)	
12	Commitment to Loyal (L1)	e-Loyalty (Loyal to Each Other)
13	Proof of Loyalty (L2)	
14	Dedication to Serve (L3)	

Source: Meaningful Statement in the Text Segment

**Table 3. Frequency of Theme**

Theme	Code	Frequency	Proportion (%)
1	Fu1	12	6.90
2	Fu2	17	9.77
3	Fu3	22	12.64
4	Fu4	25	14.37
5	Fu5	7	4.02
6	Fa1	6	3.45
7	Fa2	11	6.32
8	Fa3	7	4.02
9	T1	3	1.72
10	T2	22	12.64
11	T3	5	2.87
12	L1	15	8.62
13	L2	18	10.34
14	L3	4	2.30
<b>Total</b>		<b>174</b>	<b>99.98</b>

Source: Data Process

The proportion of the above themes can be grouped into four classifications themes as follows: The fun online shopping theme 47.70% (Fu1 s/d Fu5), The family theme 13.79% (FA1, FA2 and Fa3), The mutual trust theme 17.23% (T1, T2 and T3) and 21.26% The faithful to each other theme (L1, L2 and L3). Furthermore, configuration table is used to determine the inter-connectedness of the table among themes. The focus of the research is how the customer's perspective connects the e-Service Quality by e-Satisfaction and e-Loyalty. From the themes discovered, it reveals that the explanation of e-Service Quality creates a pleasant atmosphere of online shopping (*Fun Shopping*) which gives total satisfaction (functional and emotional

satisfaction). Kinship through customer service team attitude that cares about others and gives special attention, fosters emotional satisfactions: the joy and happiness. The joy and happiness complement the emotional satisfactions (*emotional e-Satisfaction*). Emotional e-Satisfaction connected with e-Trust customers are drawn from the recognition of the performance of the customer service team and recognition of the company's reputation. Trust of the company to the customer, strengthens customer recognition of the company's reputation. Furthermore, e-Trust is connected to e-Loyalty as follows: customer's trust which is reflected from the recognition of team performance and the recognition of the company's reputation are the basis for the customer to set their loyalty. The determination of customer loyalty includes commitment (promise) and proof. Customer loyalty is proved from the statements about: the time span has been a customer (and always satisfied), has been re-doing the shopping, have influenced others to become customers, has made the company the first place to shop online. From the process of meaningful reviews and coding processing, there are 174 meaningful statements in 14 themes (see Table 3.)

### 3.2. Connectedness of the Themes

Connectivity between themes is analyzed by using the data processing output (by MAXQDA11) in the form of a configuration table among themes. The process of establishing connectivity among themes by using the software of configuration table output MAXQDA11. Researchers determined nine (9) configurations based on the concept of logical frame of mind in the following order:

#### 1. Connectedness of Fun e-Shopping Themes

*Configuration 1:* Connecting the theme of shopping experience, ease online shopping, shopping problems handling, functional and emotional satisfaction (Fu1, fu2, Fu5, Fu3, Fu4)

#### 2. Connectedness of Family Value Themes

*Configuration 2:* Connecting Family Value theme with Trust Themes: joy, happiness, caring about others with the recognition of the customer service performance and recognition of the company reputation (Fa1, Fa2, Fa3, T1, T2)

*Configuration 3:* Connecting the Family Value themes with Loyalty themes: joyness, happiness, fellow care with the commitment to loyal and proof of the loyalty (Fa1, Fa2, Fa3, L1, L2)

#### 3. Connectedness Mutual Trust theme

*Configuration 4:* Connecting the Satisfaction themes with the Mutual Trust theme: functional satisfaction, emotional satisfaction with the recognition of customer service performance, recognition of the company's reputation and company trust (Fu3, Fu4, T1, T2, T3)

#### 4. Connectedness of Loyal to Each Other

*Configuration 5:* Connecting the Satisfaction theme with the Loyalty themes: functional satisfaction, emotional satisfaction with the commitment to loyal, loyalty proving and company dedication to serve (Fu3, Fu4, L1, L2, L3)

*Configuration 6:* Connecting the theme of Mutual Trust and Loyal to Each Other that are: recognition of customer service performance, recognition of the company's reputation with a commitment to loyal, loyalty proving and company dedication to serve (T1, T2, L1, L2, L3)

#### 5. Connectedness of particular themes

*Configuration 7:* Connecting a special theme with the Trust themes: fellow care, mutual trust and dedication to serve with the recognition of customer service performance and the recognition of company's reputation (Fa3, T3, L3, T1, T2)

*Configuration 8:* Connecting the special theme to the loyalty themes: fellow care, mutual trust and dedication to serve with commitment and loyalty proving (Fa3, T3, L3, L1, L2)

#### 6. Connectedness of themes associated with the Emotions with Trust and Loyalty

*Configuration 9:* Connecting the emotions themes with trust and loyalty: emotional satisfaction, joyness and happiness with the recognition of the company's reputation and proving loyalty (Fu4, FA1, FA2, T2, L2)

**3.3. Nine Theme Configurations**

The configuration table shows the emergence of a particular theme (shown by 1), contrary to the number 0. The Frequency indicates the number of reviews that have multiple themes observed. In this research found there are 5 reviews that contain theme Fu2, Fu3 and Fu4 (indicated by number 1) - in the first row. That can create Tabel 4. shown the connectedness (frequency) between themes. Detailed explanation as below:

*Configuration 1:* Connecting the Fun Online Shopping Theme with Satisfaction theme (Fu1, fu2, Fu5 with Fu3 and Fu4). From the 19 combinations of connectedness (*data process in this research*), the matrix frequency among themes is composed. The Matrix shows the number of review that has the theme connectedness. For example, the following matrix it is known that there are 7 customer reviews containing Fu1 and Fu3 theme. Then from the output of *Configuration\_Table\_detail* it can be seen that there is a number of texts which have connectivity among themes observed. Some numbers of the customer review text which have inter-connectedness themes is arranged into Table 5. The intersection shows some text of customer reviews which have the same connectedness. Then the meaningful statements in the text will be reassembled to form the premises. From the intersection, it is indicated that there is relationship between fun online shopping with satisfaction. All of these processes implemented to configuration 2 to 9 will be displayed:

**Table 4. Connectedness of Themes**

	Fu3	Fu4
Fu1	7	9
Fu2	14	12
Fu5	5	6

Source: Data Process

**3.4. The Way to Form the Proposition**

Table 5. (at the end of this section) is used to indicate the review that has connectedness of theme spesified. Taken as an example the review number 2, 6 and 16 rearranged as follow:

*Text Review 2* describe the conectivity between shopping experience with satisfaction (functional and emotional) “I felt the need to take a minute and share my thoughts with you. I had recently been trying to find a few pair of sneakers and was having no luck, partially due to no selection at local stores, and also a wide foot. ... I had purchased some sneakers from another website but got a few imitations and had trouble returning shoes that didn't fit. ... I honestly don't see myself ever shoe shopping in the store again”. R2Fu1 (*disatisfaction experience*) “But when my friend said to try it, I figured why not. Well, I placed my first order for two pair on a Saturday night. I choose regular shipping and to my delight they arrived on Monday morning!” R2Fu3 (*functional satisfaction*) “... Without your quick free shipping you wouldn't have won me over! ... PLEASE continue to offer the same shipping policy as you have no idea how many like me there are out there and don't share with you”. R2Fu4 (*emotional satisfaction*)

*Text Review 6* describe the conectivity between ease shopping with satisfaction (functional and emotional) “... Shopping at Zappos.com feels so comforting and secure. I feel like I never have to worry about my orders as service is easily attainable, shipping is incredibly fast (and free!)” R6Fu2 (*ease shopping*) “and your customer service representatives are simply amazing” R6Fu3 (*functional satisfaction*) “... I have never taken the time to thank a company for their services but with Zappos.com, I just had to!! ...” R6Fu4 (*emotional satisfaction*)

*Text Review 16* describe the conectivity between ease shopping with satisfaction (functional and emotional) “... My standard shoes didn't feel just right. ... My poor feet were not happy. I finally gave into the conclusion that I was refusing to accept. They didn't fit. What to do? I wore them outside, so I can't return them right?” R16Fu5 (*customer confidence to get shopping problem handling*) “... Did I mention the free shipping? Yup, free. Imagine my surprise to find my shoes on my doorstep, just over 12 hours from placing the order online!! Free overnight shipping, incredible R16Fu3 (*functional satisfaction*) “I contacted Zappos via live chat and talked to a wonderful rep. She told me that not only would they extend the courtesy of returning the shoes, but they would send me a different pair in exchange. Still free shipping!! Awesome. So

there I am sitting there completely pleased, having just been given everything that I wanted” R16Fu4 (emotional satisfaction)

**Conclusion:** Shopping experience determine customer to searching the store that they meet their need of satisfaction. Ease shopping give rise to both fungsional and emotional satisfaction, as the same as shopping problem handling. These connectedness used to establish proposition 1 (P1): Fun online shopping determine e-Satisfaction. The entire propositions below are formed by the same process of understanding.

- P1 Fun Online Shopping Determines e-Satisfaction
- P2 e-Satisfaction Encourages e-Trust
- P3 e-satisfaction cause e-loyalty
- P4 Family value promote positive Emotions
- P5 Emotional e-Satisfaction develop e-Trust
- P6 Family value promote e-Loyalty
- P7 E-trust determine e-loyalty
- P8 Mutual trust strengthen e-Satisfaction
- P9 Mutual trust strengthen e-Trust
- P10 Mutual Faithfulness promote e-Satisfaction
- P11 Mutual Faithfulness Strengthen e-Loyalty

**Table 5. The Text Review Related Connected of the Theme**

	Review Number	Intersection (Review)
<b>Fu1-Fu3</b>	01, 02, 06, 10, 13, 14, 16	
<b>Fu1-Fu4</b>	02, 06, 08, 11, 14, 16, 29, 34, 36	02, 06, 14, 16
<b>Fu2-Fu3</b>	01, 04, 05, 06, 12, 13, 16, 18, 21, 33, 35	04, 05, 06, 16, 18,
<b>Fu2-Fu4</b>	04, 05, 06, 16, 18, 19, 20, 29, 33, 34, 35, 36	33, 35
<b>Fu5-Fu3</b>	02, 15, 16, 25, 37	
<b>Fu5-Fu4</b>	02, 08, 15, 16, 25, 37	02, 15, 16, 25, 37

Source: Data Process

**3.5. Upcoming Research**

1. This study focuses on the online store customer settings in America. However, this study would be the basis for similar studies in the setting of online store in Indonesia. A qualitative research is needed to continue an understanding and the concept of e-Service Quality, e-Satisfaction, e-Trust and e-Loyalty.
2. This study uses a data base of customer reviews that are available in the context of American society to creating a product review in detail. However, in the context of Indonesian society, it seems difficult to obtain the similar data. It is necessary to change the research methodology. *Qualitative Diary Research* can be potentially to explore the e-Shopping customer experience.

**REFERENCES**

- [1] Xia, L.and Bechwati, N.N. Word of Mouse: The Role of Cognitive Personalization in Online Consumer Reviews. Journal of Interactive Advertising, 9 (1): 3-13, 2008.
- [2] Tuzovic, S. Frequent (flier) Frustration and the Dark Side of Word-of-Web: Exploring Online Dysfunctional Behavior in Online Feedback Forums. Journal of Services Marketing , 24 (6): 446-457, 2010.
- [3] Schweidel, D.A., Moe, W.W.and Boudreaux, C. Listening in on Online Conversations: Measuring Brand Sentiment with Social Media, 2011. Google search [socialmediagovernance.com/downloads/SSRN-id1874892.pdf](http://socialmediagovernance.com/downloads/SSRN-id1874892.pdf) access Januari 2012.
- [4] Kotler, P. and Keller, K.L. Marketing Management, Twelfth Edition. Pearson Prentice Hall. New Jersey, 2008.
- [5] Zeithaml, V.A., Parasuraman, A.and Malhotra, A. Service Quality Delivery Through Web Sites: A Critical Review of extant Knowledge. Journal of the Academy of Marketing Science 30 (4): 362-375, 2002.
- [6] Harridge-March, S. Electronic Marketing, the New Kid on the Block. Marketing Intelligence & Planning 22 (3): 297-309, 2004.
- [7] George, J.F. Influences on the Intent to Make Internet Purchases. Internet Research: Electronic Networking Applications and Policy 12 (2): 165-180, 2002.
- [8] Wang, M. Assessment of e-Service Quality via e-Satisfaction in e- Commerce Globalization. The Electronic Journal on

- Information Systems in Developing Countries 11 (10): 1-4, 2003.
- [9] Yang, Z. and Fang, X. Online Service Quality Dimensions and Their Relationships with Satisfaction: A Content Analysis of Customer Reviews of Securities Brokerage Services. *International Journal of Service Industry Management* 15 (3): 302-326, 2004.
- [10] Zeithaml *et al.*, Op. Cit., 362-375
- [11] Li, H. dan Suomi, R. A Proposed Scale for Measuring E-service Quality. *International Journal of u- and e-Service, Science and Technology* 2 (1): 1-10, 2009.
- [12] Li, H. dan Suomi, R., Op. Cit., 1-10
- [13] Zeithaml *et al.*, Op. Cit., 362-375
- [14] George, J.F., Op. Cit., 165-180
- [15] Wang, M., Op. Cit., 1-4
- [16] Sade-Beck, L. Internet Ethnography: Online and Offline. *International Journal of Qualitative Methods* 3(2): 1-14, 2004.
- [17] McQuarrie. Secondary Research. Google Search: [www.sagepub](http://www.sagepub)
- [18] Sade-Beck, L., Op. Cit., 1-14
- [19] Ahmed, J.U. Documentary Research Method: New Dimensions, *Indus Journal of Management & Social Sciences* 4(1):1-14, 2010.
- [20] Pollach, I. Electronic Word of Mouth: A Genre Analysis of Product Reviews on Consumer Opinion Web Sites. *Proceedings of the 39th International Conference on System Sciences Hawaii*. 1-10, 2006.
- [21] Xia, L. and Bechwati, N.N., Op. Cit., 3-13
- [22] Maeyer, P.D. and Estelami, H. Consumer Perceptions of Third Party Product Quality Ratings. *Journal of Business Research*, 64:1067-1073, 2011.
- [23] Mudambi, S.M. dan Schuff, D. What Makes a Helpful Online Review?: A Study of Customer Reviews on Amazon.Com. *MIS Quarterly* 34(1): 185-200, 2010
- [24] Sweeney, J.C., Soutar, G.N. and Mazzarol, T. Factors Influencing Word of Mouth Effectiveness: Receiver Perspectives. *European Journal of Marketing* 42 (3/4): 344-364, 2008.
- [25] Huang, Y.K. dan Yang, W.I. A study of Internet Book Reviews and Borrowing Intention. *Library Review* 59(7): 512-521, 2010.
- [26] Myers, M.D. *Qualitative Research in Business & Management*, First Published. SAGE Publications Ltd. London, 2009.
- [27] Goulding, C. Consumer Research, Interpretive paradigms and Methodological Ambiguities. *European Journal of Marketing* 33 (9/10): 859-873, 1999.
- [28] Kozinets, R.V. *Netnography: Doing Ethnographic Research Online*, Reprinted 2012. SAGE Publications Ltd, London, 2012.
- [29] Milliken, J. Qualitative Research and Marketing Management. *Management Decision* 39 (10): 71-77, 2001.
- [30] MAXQDA11 (Trial). Google search

# Estimation of Stress- Strength Reliability model using finite mixture of exponential distributions

K.Sandhya<sup>1</sup>, T.S.Umamaheswari<sup>2</sup>

<sup>1</sup>Department of Mathematics, Lal Bhadur college, P.G. Centre, Warangal

<sup>2</sup>Department of Mathematics, Kakatiya University, Warangal.

## ABSTRACT:

In this paper considered a situation where stress and strength follow finite mixture of exponential distributions to find the reliability of a system. It has been studied when stress follow exponential distribution and strength follow finite mixture of exponential distributions and both stress-strength follow the finite mixture of exponential distributions. The general expression for the reliability of a system is obtained. The reliability is computed numerically for different values of the stress and strength parameters. We estimate the parameters of the reliability stress-strength models by the method of maximum likelihood estimation. The role of finite mixture of exponential distributions is illustrated using a real life data on time to death of two groups of leukaemia patients.

**KEYWORDS:** Exponential distribution, Finite mixture of exponential distributions, Maximum Likelihood Estimation, Reliability, Stress-Strength model.

## 1. INTRODUCTION

Reliability of a system is the probability that a system will adequately perform its intended purpose for a given period of time under stated environmental conditions [1]. In some cases system failures occur due to certain type of stresses acting on them. Thus system composed of random strengths will have its strength as random variable and the stress applied on it will also be a random variable. A system fails whenever an applied stress exceeds strength of the system. In a finite mixture model, the distribution of random quantity of interest is modelled as a mixture of a finite number of component distributions in varying proportions [2]. The flexibility and high degree of accuracy of finite mixture models have been the main reason for their successful applications in a wide range of fields in the biological physical and social sciences. The estimation of reliability based on finite mixture of pareto and beta distributions was studied by Maya, T. Nair (2007)[3].

In reliability theory, the mixture distributions are used for the analysis of the failure times of a sample of items of coherent laser used in telecommunication network. In an experiment, one hundred and three laser devices were operated at a temperature of 70 degree Celsius until all had failed. The experiment was run longer than one year before all the devices had failed, because most of the devices were extremely reliable. The sample thus consists of two distinct populations, one with a very short mean life and one with a much longer mean life. This can be considered as an example of a mixture of two exponential distributions with probability density function of the form

$$f(x) = p\lambda_1 \exp(-\lambda_1 x) + (1-p)\lambda_2 \exp(-\lambda_2 x), \quad 0 \leq p \leq 1, \lambda_i > 0, i = 1, 2$$

The above model will be useful to predict how long all manufactured lasers should be life tested to assure that the final product contained no device from the infant mortality population.

In the present paper we discuss the statistical analysis of finite mixture of exponential distributions in the context of reliability theory. We give the definition and properties of the finite mixture of exponential distributions. We derive the reliability, when the strength X follows finite mixture of exponential and the stress Y takes exponential and finite mixture of exponential. We discuss estimation procedure for finite mixture of exponential distributions by the method of maximum likelihood estimation and also estimation of stress-strength reliability. We illustrate the method for a real data on survival times of leukaemia patients and finally give the conclusion.

**II. STATISTICAL MODEL:**

The assumptions taken in this model are

- (i) The random variables X and Y are independent.
- (ii) The values of stress and strength are non-negative.

If X denotes the strength of the component and Y is the stress imposed on it, then the reliability of the component is given by [1],

$$R = P(X > Y) = \int_0^\infty \left\{ \int_0^x g(y) dy \right\} f(x) dx \tag{1}$$

where f(x) and g(y) are probability density functions of strength and stress respectively.

A finite mixture of exponential distribution with k-components can be represented in the form

$$f(x) = p_1 f_1(x) + p_2 f_2(x) + \dots + p_k f_k(x) \tag{2}$$

$$\text{where } p_i > 0, i = 1, 2, \dots, k \quad \sum_{i=1}^k p_i = 1$$

The r<sup>th</sup> moment of the mixture of two exponential distributions

$$\begin{aligned} E(x^r) &= \int_0^\infty x^r \left[ p_1 \lambda_1 \exp(-\lambda_1 x) + (1 - p_1) \lambda_2 \exp(-\lambda_2 x) \right] dx \\ &= p_1 \lambda_1 \frac{(r+1)}{\lambda_1^{r+1}} + (1 - p_1) \lambda_2 \frac{(r+1)}{\lambda_2^{r+1}} \end{aligned}$$

When r = 1,  $E(x) = \frac{p_1}{\lambda_1} + \frac{1 - p_1}{\lambda_2} \quad 0 < p_1 < 1, \lambda_i > 0, i = 1, 2$

When r = 2,  $E(x^2) = \frac{2p_1}{\lambda_1^2} + \frac{2(1 - p_1)}{\lambda_2^2}$

Thus the variance is given by  $V(x) = \frac{p_1(2 - p_1)}{\lambda_1^2} + \frac{(1 - p_1)(2 - p_1)}{\lambda_2^2} - \frac{2p_1(1 - p_1)}{\lambda_1 \lambda_2}$

In this paper we are considering two cases. They are

- (1) Stress follows exponential distribution and strength follows finite mixture of exponential distributions.
- (2) Stress and strength follows finite mixture of exponential distributions.

**III. RELIABILITY COMPUTATIONS:**

Let X be the strength of the k-components with probability density functions f<sub>i</sub>(x); i=1,2,...,k. Strength X follows finite mixture of exponential distribution with pdf

$$f_i(x) = p_i \lambda_i \exp(-\lambda_i x), \quad \lambda_i > 0, x > 0, p_i > 0, i = 1, 2, \dots, k; \sum_{i=1}^k p_i = 1 \tag{3}$$

**3.1. Case(i) The stress Y follows exponential distribution:**

When the stress Y follows exponential with pdf

$$g(y) = \lambda \exp(-\lambda y), y > 0, \lambda > 0$$

As a special case of (3) with k = 2, we have

$$f(x) = p_1 \lambda_1 \exp(-\lambda_1 x) + (1 - p_1) \lambda_2 \exp(-\lambda_2 x), \lambda_i > 0, x > 0, (i = 1, 2)$$

And if X and Y are independent, then the reliability R from (1)

$$R_2 = \int_0^\infty \int_0^x (\lambda \exp(-\lambda y)) [p_1 \lambda_1 \exp(-\lambda_1 x) + (1 - p_1) \lambda_2 \exp(-\lambda_2 x)] dy dx$$

$$R_2 = 1 - p_1 \left( \frac{\lambda_1}{\lambda + \lambda_1} \right) - (1 - p_1) \left( \frac{\lambda_2}{\lambda + \lambda_2} \right) \tag{4}$$

As a special case of (3) with k = 3, we have

$$f(x) = p_1 \lambda_1 \exp(-\lambda_1 x) + p_2 \lambda_2 \exp(-\lambda_2 x) + p_3 \lambda_3 \exp(-\lambda_3 x), \lambda_i > 0, x > 0, (i = 1, 2, 3); \sum_{i=1}^3 p_i = 1$$

$$R_3 = \int_0^{\infty} \int_0^x (\lambda \exp(-\lambda y)) [p_1 \lambda_1 \exp(-\lambda_1 x) + p_2 \lambda_2 \exp(-\lambda_2 x) + p_3 \lambda_3 \exp(-\lambda_3 x)] dy dx$$

$$R_3 = 1 - p_1 \left( \frac{\lambda_1}{\lambda + \lambda_1} \right) - p_2 \left( \frac{\lambda_2}{\lambda + \lambda_2} \right) - p_3 \left( \frac{\lambda_3}{\lambda + \lambda_3} \right) \tag{5}$$

In general from (2),  $f(x) = p_1 f_1(x) + p_2 f_2(x) + \dots + p_k f_k(x)$

$$\text{where } p_i > 0, i = 1, 2, \dots, k \quad \sum_{i=1}^k p_i = 1$$

we get 
$$R_k = 1 - \sum_{i=1}^k p_i \frac{\lambda_i}{\lambda + \lambda_i} \tag{6}$$

From table 1 and table 2 and figs.1 and 2, it is observed that if stress parameter increases then the value of reliability increases, if strength parameter increases then the value of reliability decreases.

**3.2.Case (ii) The stress Y follows finite mixture of exponential distributions:**

For k = 2, we have

$$f(x) = p_1 \lambda_1 \exp(-\lambda_1 x) + (1 - p_1) \lambda_2 \exp(-\lambda_2 x), \lambda_1, \lambda_2 > 0$$

$$g(y) = p_3 \lambda_3 \exp(-\lambda_3 y) + (1 - p_3) \lambda_4 \exp(-\lambda_4 y), \lambda_3, \lambda_4 > 0$$

And if X and Y are independent, then the reliability R from (1)

$$R_2 = \int_0^{\infty} \int_0^x [p_3 \lambda_3 \exp(-\lambda_3 y) + (1 - p_3) \lambda_4 \exp(-\lambda_4 y)] [p_1 \lambda_1 \exp(-\lambda_1 x) + (1 - p_1) \lambda_2 \exp(-\lambda_2 x)] dy dx$$

$$= 1 - p_3 p_1 \frac{\lambda_1}{\lambda_1 + \lambda_3} - p_3 (1 - p_3) \frac{\lambda_2}{\lambda_2 + \lambda_3} - (1 - p_3) p_1 \frac{\lambda_1}{\lambda_1 + \lambda_4} - (1 - p_3) (1 - p_1) \frac{\lambda_2}{\lambda_2 + \lambda_4} \tag{7}$$

For k = 3, we have

$$f(x) = p_1 \lambda_1 \exp(-\lambda_1 x) + p_2 \lambda_2 \exp(-\lambda_2 x) + p_3 \lambda_3 \exp(-\lambda_3 x), \lambda_i > 0, x > 0, (i = 1, 2, 3); \sum_{i=1}^3 p_i = 1$$

Then

$$R_3 = \int_0^{\infty} \int_0^x [p_4 \lambda_4 \exp(-\lambda_4 y) + p_5 \lambda_5 \exp(-\lambda_5 y) + p_6 \lambda_6 \exp(-\lambda_6 y)] [p_1 \lambda_1 \exp(-\lambda_1 x) + p_2 \lambda_2 \exp(-\lambda_2 x) + p_3 \lambda_3 \exp(-\lambda_3 x)] dy dx$$

$$R_3 = 1 - p_4 p_1 \frac{\lambda_1}{\lambda_1 + \lambda_4} - p_4 p_2 \frac{\lambda_2}{\lambda_2 + \lambda_4} - p_4 p_3 \frac{\lambda_3}{\lambda_3 + \lambda_4}$$

$$\begin{aligned}
 & -p_5 p_1 \frac{\lambda_1}{\lambda_1 + \lambda_5} - p_5 p_2 \frac{\lambda_2}{\lambda_2 + \lambda_5} - p_5 p_3 \frac{\lambda_3}{\lambda_3 + \lambda_5} - p_6 p_1 \frac{\lambda_1}{\lambda_1 + \lambda_6} - p_6 p_2 \frac{\lambda_2}{\lambda_2 + \lambda_6} - p_6 p_3 \frac{\lambda_3}{\lambda_3 + \lambda_6} \\
 R_3 = & 1 - \sum_{j=i+3}^6 \sum_{i=1}^3 p_j p_i \frac{\lambda_i}{\lambda_i + \lambda_j}
 \end{aligned}
 \tag{8}$$

In general from (2),  $f(x) = p_1 f_1(x) + p_2 f_2(x) + \dots + p_k f_k(x)$

$$\text{where } p_i > 0, i = 1, 2, \dots, k \quad \sum_{i=1}^k p_i = 1$$

Then

$$R_k = 1 - \sum_{j=i+k}^{2k} \sum_{i=1}^k p_j p_i \frac{\lambda_i}{\lambda_i + \lambda_j}
 \tag{9}$$

From table 3 and table 4 and figs. 3 and 4, it is observed that if stress parameter increases then the value of reliability decreases, if strength parameter increases then the value of reliability increases.

### 3.3. Hazard Rate:

Let  $t$  denotes life time of a component with survival function  $S(t)$ . Then the survival function of the model is obtained as

$$S(t) = p_1 \lambda_1 \exp(-\lambda_1 t) + (1 - p_1) \lambda_2 \exp(-\lambda_2 t), \quad \lambda_i > 0, \quad t > 0, \quad 0 < p_1 < 1$$

For the model the hazard rate  $h(t)$  is given by

$$\begin{aligned}
 h(t) &= \frac{f(t)}{s(t)} \\
 &= \frac{p_1 \lambda_1 \exp(-\lambda_1 t) + (1 - p_1) \lambda_2 \exp(-\lambda_2 t)}{p_1 \exp(-\lambda_1 t) + (1 - p_1) \exp(-\lambda_2 t)}
 \end{aligned}
 \tag{10}$$

In general,

$$h(t) = \frac{\sum_{i=1}^k p_i \lambda_i \exp(-\lambda_i t)}{\sum_{i=1}^k p_i \exp(-\lambda_i t)}
 \tag{11}$$

Finite mixture of exponential possesses decreasing hazard rate and constant hazard rate depending upon the values of the parameters. Fig 5, show the behaviour of hazard rate at various time points.

## IV. ESTIMATION OF PARAMETERS:

We estimate the parameters of the models by the method of maximum likelihood estimation. Consider the situation when there are only two sub populations with mixing proportions  $p_1$  &  $(1-p_1)$  and  $f_1(x)$  and  $f_2(x)$  are exponential densities with parameters  $\lambda_1$  &  $\lambda_2$  respectively.

The likelihood function is given by

$$L(\lambda_1, \lambda_2, p_1 / \hat{y}) = \prod_{j=1}^n [ p_1 \lambda_1 \exp(-\lambda_1 y_j) + (1 - p_1) \lambda_2 \exp(-\lambda_2 y_j) ]
 \tag{12}$$

Where  $y_{ij}$  denoted the failure time of the  $j^{\text{th}}$  unit belonging to the  $i^{\text{th}}$  sub population  $j=1, 2, \dots, n_i$ ;  $i=1, 2$  and

$$\hat{y} = \{ y_{11}, y_{12}, \dots, y_{1n_1}; y_{21}, y_{22}, \dots, y_{2n_2} \}$$

Maximization of log likelihood function of (12) w.r.t the parameters yields the following equation

$$L = \frac{\underline{n}}{\underline{n}_1 \underline{n}_2} p_1^{n_1} (1 - p_1)^{n_2} \lambda_1^{n_1} \lambda_2^{n_2} \prod_{j=1}^{n_1} \exp(-\lambda_1 y_{1j}) \prod_{j=1}^{n_2} \exp(-\lambda_2 y_{2j})$$

$$L = c (\lambda_1 p_1)^{n_1} [(1-p_1)\lambda_2]^{n_2} \exp \left[ -\sum_{j=1}^{n_1} y_{1j} \lambda_1 - \sum_{j=1}^{n_2} y_{2j} \lambda_2 \right]$$

$$\log(L) = \log c + n_1 \log(p_1 \lambda_1) + n_2 \log(1-p_1) \lambda_2 - \lambda_1 \sum_{j=1}^{n_1} y_{1j} - \lambda_2 \sum_{j=1}^{n_2} y_{2j}$$

$$\frac{n_1}{\lambda_1} - \sum_{j=1}^{n_1} y_{1j} = 0, \quad \frac{n_2}{\lambda_2} - \sum_{j=1}^{n_2} y_{2j} = 0, \quad \frac{n_1}{p_1} - \frac{n_2}{(1-p_1)} = 0$$

$$\Rightarrow \hat{\lambda}_1 = \frac{n_1}{\sum_{j=1}^{n_1} y_{1j}} \tag{13}$$

$$\Rightarrow \hat{\lambda}_2 = \frac{n_2}{\sum_{j=1}^{n_2} y_{2j}} \tag{14}$$

$$\Rightarrow \hat{p}_1 = \frac{n_1}{n_1 + n_2} = \frac{n_1}{n} \quad \text{where } n = n_1 + n_2 \tag{15}$$

The above results can be generalized for any k, giving the following estimators

$$\hat{p}_1 = \frac{n_1}{n} \quad \& \quad n = \sum_{i=1}^k n_i \tag{16}$$

$$\Rightarrow \hat{\lambda}_i = \frac{n_i}{\sum_{j=1}^{n_i} y_{ij}} \tag{17}$$

**4.1. Estimation of Stress – Strength reliability:**

(i) When the strength X follows finite mixture of exponential distributions with parameters  $\lambda_i$  and  $p_i$  and the stress Y follows exponential distribution with parameter  $\lambda$ , then the M.L.E of R is given as

$$\hat{R}_k = 1 - \sum_{i=1}^k \hat{p}_i \frac{\hat{\lambda}_i}{\lambda + \hat{\lambda}_i} \tag{18}$$

(ii) When the strength X follows finite mixture of exponential distributions with parameters  $\lambda_i$  and  $p_i$  and the stress Y follows finite mixture of exponential distribution with parameter  $\lambda_j$  and  $p_j$  then the M.L.E of R is given as

$$\hat{R}_k = 1 - \sum_{j=i+k}^{2k} \sum_{i=1}^k \hat{p}_j \hat{p}_i \frac{\hat{\lambda}_i}{\hat{\lambda}_i + \hat{\lambda}_j} \tag{19}$$

**V. DATA ANALYSIS:**

We consider a data on time to death of two groups of leukaemia patients which is given in Table 5 (see Feigl and Zelen, 1965) to illustrate the procedure of estimation. We then estimate the parameters using M.L.E technique. Table 6 provides the values of the estimates by M.L.E method. Table 7 provides the maximum likelihood estimate of survival function at various time points. Table 8 provides the hazard rate function at various time points.

**Case (i) Stress has exponential distribution and Strength has mixture two of exponential distributions:**

Table 1

$P_1 = \lambda_1 = \lambda_2$	$\lambda$	R
0.1	0.1	0.5
0.1	0.2	0.666667
0.1	0.3	0.75
0.1	0.4	0.8
0.1	0.5	0.833333
0.1	0.6	0.857143
0.1	0.7	0.875
0.1	0.8	0.888889
0.1	0.9	0.9
0.1	1	0.909091

Table 2

$P_1$	$\lambda$	$\lambda_1 = \lambda_2$	R
0.1	0.7	0.1	0.875
0.1	0.7	0.2	0.777778
0.1	0.7	0.3	0.7
0.1	0.7	0.4	0.636364
0.1	0.7	0.5	0.583333
0.1	0.7	0.6	0.538462
0.1	0.7	0.7	0.5
0.1	0.7	0.8	0.466667
0.1	0.7	0.9	0.4375
0.1	0.7	1	0.411765

**Case(ii) Stress-Strength has mixture two of exponential distributions:**

Table 3

$P_1 = P_3$	$\lambda_1 = \lambda_2$	$\lambda_3 = \lambda_4$	R
0.1	0.1	0.7	0.875
0.1	0.2	0.7	0.777778
0.1	0.3	0.7	0.7
0.1	0.4	0.7	0.636364
0.1	0.5	0.7	0.583333
0.1	0.6	0.7	0.538462
0.1	0.7	0.7	0.5
0.1	0.8	0.7	0.466667
0.1	0.9	0.7	0.4375
0.1	1	0.7	0.411765

Table 4

$P_1 = P_3 = \lambda_1 = \lambda_2$	$\lambda_3 = \lambda_4$	R
0.1	0.1	0.5
0.1	0.2	0.666667
0.1	0.3	0.75
0.1	0.4	0.8
0.1	0.5	0.833333
0.1	0.6	0.857143
0.1	0.7	0.875
0.1	0.8	0.888889
0.1	0.9	0.9
0.1	1	0.909091

**Table 5**

Survival times of leukaemia patients

AG +ve	143	56	26	134	16	65	156	100	39	1	5	65	22	1	4	108	121
AG -ve	2	3	8	7	16	22	3	4	56	65	17	4	3	30	4	43	

**Table 6**

Estimates of parameters of survival times of leukaemia patients.

$\hat{\lambda}_1$	0.016
$\hat{\lambda}_2$	0.055
$\hat{p}_1$	0.515

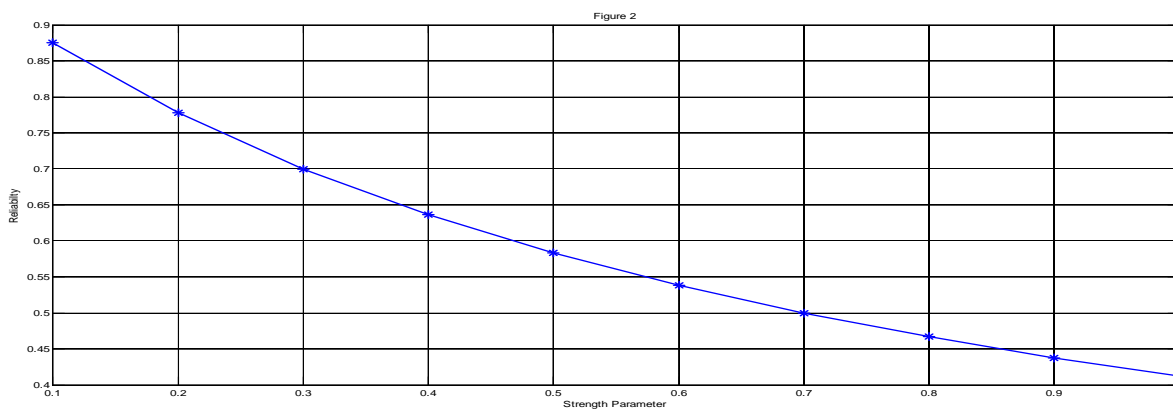
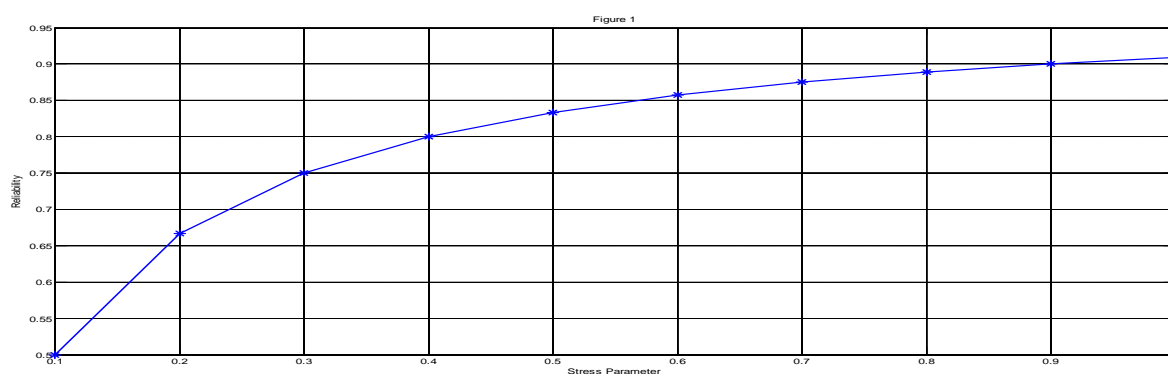
**Table 7**  
Maximum likelihood estimate of survival probability at various time points

T	1	10	50	75	100	120
$\hat{S}(t)$	0.9659	0.7187	0.2624	0.1630	0.1060	0.0762

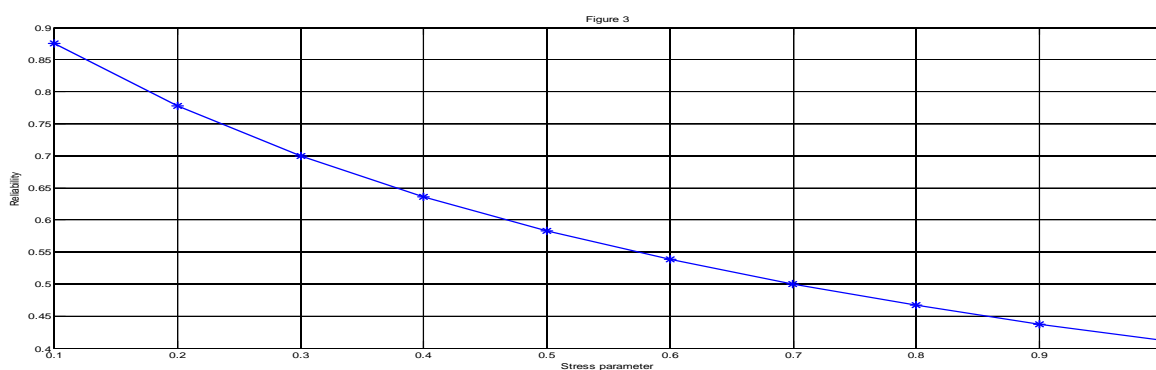
**Table 8**  
Hazard rate at various time points

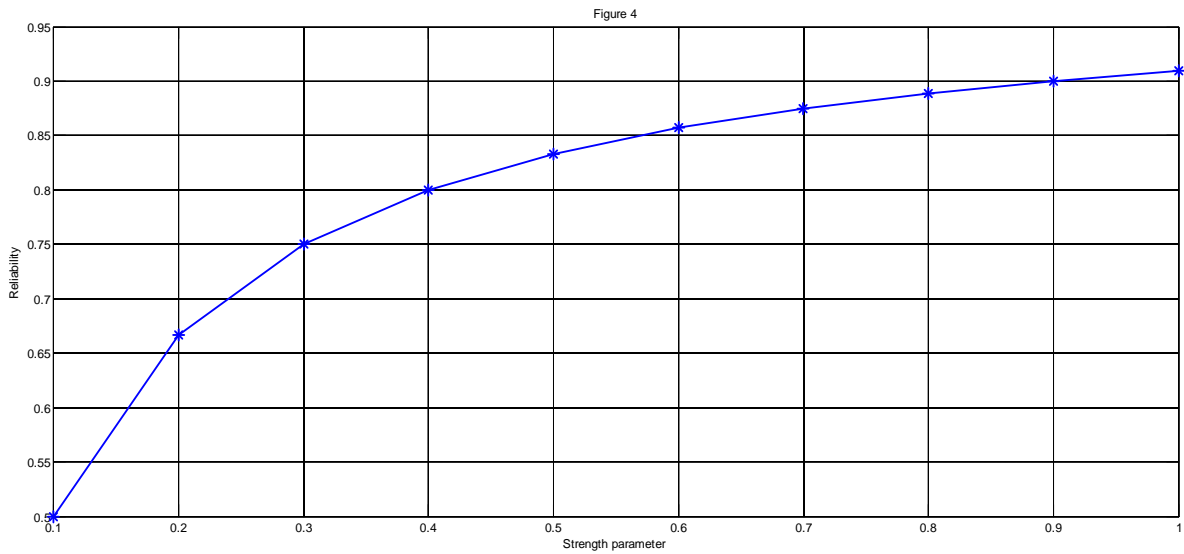
T	0.1	0.2	0.3	0.4	0.5	0.6	0.7	0.8	0.9	1
h(t)	0.5867	0.5501	0.5158	0.4836	0.4535	0.4252	0.3988	0.3740	0.3507	0.3289

**Case (i) Stress has exponential distribution and Strength has mixture two of exponential distributions:**

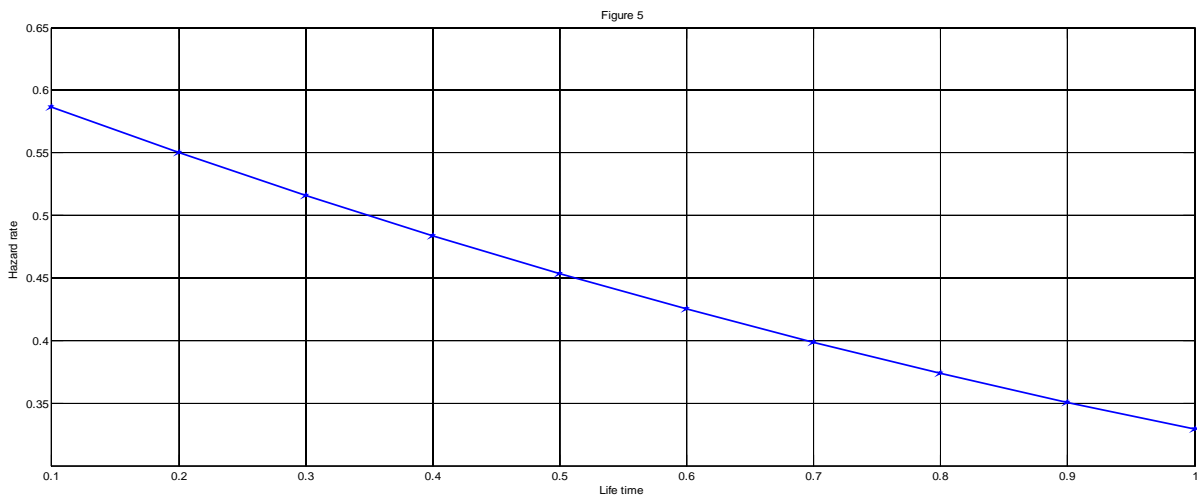


**Case(ii) Stress-Strength has mixture two of exponential distributions:**





**Hazard rate function:**



**VI. CONCLUSION:**

The role of finite mixture of exponential distributions in reliability analysis is studied. We derive the reliability, when the strength  $X$  follows finite mixture of exponential and the stress  $Y$  takes exponential and finite mixture of exponential. It has been observed by the computations and graphs, in case(i) if stress parameter increases then the value of reliability increases, if strength parameter increases then the value of reliability decreases. Where as in case(ii) if stress parameter increases then the value of reliability decreases, if strength parameter increases then the value of reliability increases. We developed estimates of parameters using Maximum likelihood estimation. The role of finite mixture of exponential distributions is illustrated using a real life data on time to death of two groups of leukaemia patients.

**REFERENCES:**

- [1] Kapur, K.C and Lamberson, L.R.: Reliability in Engineering Design, John Wiley and Sons, Inc., U.K. (1997).
- [2] Sinha, S.K. (1986). Reliability and Life Testing, Wiley Eastern Limited, New Delhi.
- [3] Maya, T.Nair (2007). On a finite mixture of Pareto and beta distributions. Ph.D Thesis submitted to Cochin University of Science and Technology, February 2007.
- [4] Feigal, P. and Zelen, M. (1965). Estimation of survival probabilities with concomitant information. Biometrics 21, 826-838.